# Vibration Analysis of Cantilever Beam With Two Inclined Cracks and Its Implementation in Fault Diagnosis


Biswajit Sahoo

# Vibration Analysis of Cantilever Beam With Two Inclined Cracks and Its Implementation in Fault Diagnosis

A thesis submitted to the Department of Mechanical Engineering, National Institute of Technology, Rourkela in partial fulfilment of the requirements for the award of the degree of

Master of Technology

In

Machine Design and Analysis

By

Biswajit Sahoo

Roll No. - 213ME1389

Under the supervision of

Prof. D.R. Parhi


National Institute of Technology, Rourkela

Odisha (India) - 769008

# DECLARATION

This thesis is the presentation of my original research work. Wherever contributions of others are involved, every effort is made to indicate this clearly, with due reference to the literature, and acknowledgement of collaborative research and discussions.

The work was done under the guidance of Professor D.R. Parhi, at National Institute of Technology, Rourkela.

Biswajit Sahoo

National Institute of Technology, Rourkela-
769008, Odisha, India

# CERTIFICATE

This is to certify that the thesis entitled "**Vibration Analysis of Cantilever Beam With Two Inclined Cracks and Its Implementation in Fault Diagnosis**" submitted by **Mr. Biswajit Sahoo** to the Department of Mechanical Engineering, National Institute of Technology, Rourkela, in partial fulfilment of the award of the degree of Master of Technology in Machine Design and Analysis, is an authentic work and is original. To the best of my knowledge, the work included in the thesis has not been submitted to any University/Institute for the award of and degree or diploma.

Prof. D.R. Parhi

Supervisor

Department of Mechanical Engineering,

National Institute of Technology, Rourkela

This work is dedicated to

My Parents

**Bidyadhar Sahoo** and **Renuprava Sahoo**

Who have given me unconditional freedom in everything. I don't know to what extent I have fulfilled their expectations, my personal assessment being marginal, but the freedom has remained uncompromised over the years (and I have enjoyed that).

And to

Prof. D.R. Parhi (Parhi Sir)

You are a dream supervisor to collaborate with.

## ACKNOWLEDGEMENT

I would like to thank Prof. Sunil Kumar Sarangi, Director, NIT, Rourkela, Prof. Siba Sankar Mohapatra, HOD, Mechanical Engineering, NIT, Rourkela, for providing a nice platform for doing research at this institute. I express my sincere thanks to all faculty members as well as all non-teaching staffs of Mechanical Engineering Department for being helpful every time the need arises.

I express my gratitude to Prof. Dayal Ramakrushna Parhi, my supervisor, for being always there with me at the time of need. Without his support, the journey wouldn't have been that enthralling, enriching and fulfilling. All research scholars, technical assistant and non-technical assistant of Robotics Lab deserve praise for being nice and helpful every time.

My heartiest thanks are to my batch mates and friends at NIT, Rourkela. The two years went like a breeze when you were around. You all will be missed.

Finally time for some technical acknowledgements. I have tried my best to present this thesis in a manner that is easily understandable as well as technically sound. But I strongly suspect – and others will agree with me after reading it – that it touches neither end completely. People more inclined towards technical sophistication might find it as a verbose piece of writing and a general reader – if she/he ever reads it – might find that it explains some portions and fails at many other occasions. So for both of the readership types my answer would be, by distorting Jack Kerouac's quote, that: One day I'll find the right words, and they will be both understandable and technically sound.

Despite my vigorous (late night) efforts to search the errors in the work, some would have managed to escape my attention, I doubt. So the responsibility for the occurrence of any error or any inadequacy is purely and surely my own.

## ABSTRACT

Cracks present in mechanical members reduce the service life of the member. The presence of a crack doesn't necessarily mean the worthlessness of the member rather it plainly indicates the reduction in full load application of the member. The natural frequencies are characteristics of a particular member, and they get modified with the introduction of crack. Modal analysis provides a mean to determine those vibration characteristics both for cracked and uncracked beam. The present research aims to determine the vibration response of a cantilever beam with two inclined cracks to both free and forced excitations when the inclination angle of the crack changes. Results obtained from ANSYS for free, and forced oscillation have been presented. Experimentally, free vibration analysis has been done, and natural frequencies have been obtained from Frequency Response plots, and it has been compared to the values obtained from ANSYS. Using both these vibration methods, both surface and internal cracks can be located and in some cases their magnitude can be estimated by only considering their response to vibration excitations. Three-dimensional surface plots of natural frequencies have been plotted to take into account all angle combinations for both cracks. Mode shapes of the uncracked beam and cracked beam with specific angle combination have been plotted that can be used for crack identification by comparing the values of total deformation. Fuzzy Logic has been applied to predict the expected location of the crack, its severity and its inclination. Percentage variation in relative natural frequencies of cracked beam to uncracked beam has been used as input in the Fuzzy system. Surface plots using Fuzzy Logic Designer of MATLAB have been generated to obtain the dependence of output on specific input parameters.

# Contents

DECLARATION ..... i
CERTIFICATE ..... ii
ACKNOWLEDGEMENT ..... iv
ABSTRACT ..... v
LIST OF TABLES ..... viii
LIST OF FIGURES ..... x
NOMENCLATURE ..... xv
1. INTRODUCTION ..... 1
1.1. MOTIVATION ..... 1
1.2. OBJECTIVE ..... 1
1.3. METHODOLOGY ADOPTED ..... 2
1.4. REVIEW OF LITERATURE ..... 2
1.5. THESIS LAYOUT ..... 7
2. MATHEMATICAL FORMULATION OF CRACKED BEAM VIBRATION ..... 9
2.1. Mathematical Formulation ..... 9
3. FINITE ELEMENT ANALYSIS OF CANTILEVER BEAM WITH DOUBLE INCLINED CRACK ..... 15
3.1. INTRODUCTION ..... 15
3.2. MODAL ANALYSIS USING ANSYS ..... 15
3.3. FINITE ELEMENT ANALYSIS OF UNCRACKED BEAM ..... 16
3.4. MODE SHAPES OF UNCRACKED BEAM ..... 17
3.5. FINITE ELEMENT ANALYSIS OF CRACKED BEAM ..... 20
3.5.1. For $\zeta 1$=0.409 and $\zeta 2$=0.636 (L1=45cm, L2=70cm, L=110cm) ..... 20
3.5.2 For $\zeta 1$=0.316 and $\zeta 2$=0.579 ($L_1$=30cm, $L_2$=55cm, L=95cm) ..... 22
3.5.3 For $\zeta 1$=0.1875 and $\zeta 2$=0.5 ($L_1$=15cm, $L_2$=40cm, L=80cm) ..... 23
3.6. MODE SHAPES OF CRACKED BEAM ..... 25
3.7. RESULTS AND DISCUSSION ..... 28
3.8. FORCED VIBRATION ANALYSIS OF DOUBLE INCLINED CRACK IN A CANTILEVER BEAM BY ANSYS ..... 51
4. EXPERIMENTAL INVESTIGATION ..... 54
4.1. THEORY ..... 54
4.2. EXPERIMENTAL SETUP AND COMPONENTS USED ..... 56
4.3. EXPERIMENTAL RESULTS ..... 58
4.4. COMPARISON OF RESULTS ..... 62

5. IMPLEMENTATION OF FUZZY LOGIC FOR FAULT DIAGNOSTIC .....65
5.1. INTRODUCTION.....65
5.2. THEORY OF FUZZY LOGIC .....66
5.3. ESTIMATION OF CRACK LOCATION USING FUZZY LOGIC.....69
5.3.1. RULES.....72
5.3.2. RESULTS.....73
5.4. ESTIMATION OF CRACK INCLINATION ANGLE USING FUZZY LOGIC.....78
5.4.1. RULES.....81
5.4.2. RESULTS.....82
5.5. ESTIMATION OF CRACK SEVERITY USING FUZZY LOGIC.....84
5.5.1. RULES.....86
5.5.2. RESULTS.....87
6. CONCLUSION AND SCOPE FOR FUTURE WORK.....90
6.1. SCOPE FOR FUTURE WORK:.....91

## LIST OF TABLES


| Table No. | Title | Page No. |
|---|---|---|
| 3.1 | Natural Frequency of uncracked beam obtained from ANSYS | 16 |
| 3.2 | Natural Frequency of uncracked beam obtained from Mathematical Analysis | 17 |
| 3.3 | 1st Natural Frequency For $\zeta_1$=0.409 and $\zeta_2$=0.636 (L1=45cm, L2=70cm, L=110cm) | 20 |
| 3.4 | 1st Relative Natural Frequency For $\zeta_1$=0.409 and $\zeta_2$=0.636 (L1=45cm, L2=70cm, L=110cm) | 20 |
| 3.5 | 2nd Natural Frequency For $\zeta_1$=0.409 and $\zeta_2$=0.636 (L1=45cm, L2=70cm, L=110cm) | 20 |
| 3.6 | 2nd Relative Natural Frequency For $\zeta_1$=0.409 and $\zeta_2$=0.636 (L1=45cm, L2=70cm, L=110cm) | 20 |
| 3.7 | 3rd Natural Frequency For $\zeta_1$=0.409 and $\zeta_2$=0.636 (L1=45cm, L2=70cm, L=110cm) | 21 |
| 3.8 | 3rd Relative Natural Frequency For $\zeta_1$=0.409 and $\zeta_2$=0.636 (L1=45cm, L2=70cm, L=110cm) | 21 |
| 3.9 | 4th Natural Frequency For $\zeta_1$=0.409 and $\zeta_2$=0.636 (L1=45cm, L2=70cm, L=110cm) | 21 |
| 3.10 | 4th Relative Natural Frequency For $\zeta_1$=0.409 and $\zeta_2$=0.636 (L1=45cm, L2=70cm, L=110cm) | 21 |
| 3.11 | 5th Natural Frequency For $\zeta_1$=0.409 and $\zeta_2$=0.636 (L1=45cm, L2=70cm, L=110cm) | 21 |
| 3.12 | 5th Relative Natural Frequency For $\boldsymbol{\zeta_1}$=0.409 and $\boldsymbol{\zeta_2}$=0.636 (L1=45cm, L2=70cm, L=110cm) | 21 |
| 3.13 | 1st Natural Frequency For $\zeta_1$=0.316 and $\zeta_2$=0.579 ($L_1$=30cm, $L_2$=55cm, L=95cm) | 22 |
| 3.14 | 1st Relative Natural Frequency For $\zeta_1$=0.316 and $\zeta_2$=0.579 ($L_1$=30cm, $L_2$=55cm, L=95cm) | 22 |
| 3.15 | 2nd Natural Frequency For $\zeta_1$=0.316 and $\zeta_2$=0.579 ($L_1$=30cm, $L_2$=55cm, L=95cm) | 22 |
| 3.16 | 2nd Relative Natural Frequency For $\zeta_1$=0.316 and $\zeta_2$=0.579 ($L_1$=30cm, $L_2$=55cm, L=95cm) | 22 |
| 3.17 | 3rd Natural Frequency For $\zeta_1$=0.316 and $\zeta_2$=0.579 ($L_1$=30cm, $L_2$=55cm, L=95cm) | 22 |
| .318 | 3rd Relative Natural Frequency For $\zeta_1$=0.316 and $\zeta_2$=0.579 ($L_1$=30cm, $L_2$=55cm, L=95cm) | 22 |
| 3.19 | 4th Natural Frequency For $\zeta_1$=0.316 and $\zeta_2$=0.579 ($L_1$=30cm, $L_2$=55cm, L=95cm) | 23 |
| 3.20 | 4th Relative Natural Frequency For $\zeta_1$=0.316 and $\zeta_2$=0.579 ($L_1$=30cm, $L_2$=55cm, L=95cm) | 23 |
| 3.21 | 5th Natural Frequency For $\zeta_1$=0.316 and $\zeta_2$=0.579 ($L_1$=30cm, $L_2$=55cm, L=95cm) | 23 |
| 3.22 | 5th Relative Natural Frequency For $\zeta_1$=0.316 and $\zeta_2$=0.579 ($L_1$=30cm, $L_2$=55cm, L=95cm) | 23 |
| 3.23 | 1st Natural Frequency For $\zeta_1$=0.1875 and $\zeta_2$=0.5 ($L_1$=15cm, $L_2$=40cm, L=80cm) | 23 |

| | | |
|---|---|---|
| 3.24 | 1st Relative Natural Frequency For $\zeta_1$=0.1875 and $\zeta_2$=0.5 ($L_1$=15cm, $L_2$=40cm, L=80cm) | 23 |
| 3.25 | 2nd Natural Frequency For $\zeta_1$=0.1875 and $\zeta_2$=0.5 ($L_1$=15cm, $L_2$=40cm, L=80cm) | 24 |
| 3.26 | 2nd Relative Natural Frequency For $\zeta_1$=0.1875 and $\zeta_2$=0.5 ($L_1$=15cm, $L_2$=40cm, L=80cm) | 24 |
| 3.27 | 3rd Natural Frequency For $\zeta_1$=0.1875 and $\zeta_2$=0.5 ($L_1$=15cm, $L_2$=40cm, L=80cm) | 24 |
| 3.28 | 3rd Relative Natural Frequency For $\zeta_1$=0.1875 and $\zeta_2$=0.5 ($L_1$=15cm, $L_2$=40cm, L=80cm) | 24 |
| 3.29 | 4th Natural Frequency For $\zeta_1$=0.1875 and $\zeta_2$=0.5 ($L_1$=15cm, $L_2$=40cm, L=80cm) | 24 |
| 3.30 | 4th Relative Natural Frequency For $\zeta_1$=0.1875 and $\zeta_2$=0.5 ($L_1$=15cm, $L_2$=40cm, L=80cm) | 24 |
| 3.31 | 5th Natural Frequency For $\zeta_1$=0.1875 and $\zeta_2$=0.5 ($L_1$=15cm, $L_2$=40cm, L=80cm) | 25 |
| 3.32 | 5th Relative Natural Frequency For $\zeta_1$=0.1875 and $\zeta_2$=0.5 ($L_1$=15cm, $L_2$=40cm, L=80cm) | 25 |
| 4.1 | Comparison of Natural Frequency for Uncracked Beam with L=1.1m, b=0.039m, h=0.005m, ρ=2750kg/m3, E=71GPa | 62 |
| 4.2 | Comparison of Natural Frequency for Uncracked Beam with L=0.95m, b=0.039m, h=0.005m, ρ=2750kg/m3, E=71GPa | 62 |
| 4.3 | Comparison of Natural Frequency for Uncracked Beam with L=0.8m, b=0.039m, h=0.005m, ρ=2750kg/m3, E=71GPa | 62 |
| 4.4 | Comparison of Natural Frequency for cracked beam (For $\zeta_1$=0.409 and $\zeta_2$=0.636) (L=1.1m, b=0.039m, h=0.005m, ρ=2750kg/m3, E=71GPa) | 63 |
| 4.5 | Comparison of Natural Frequency for cracked beam (For $\zeta_1$=0.316 and $\zeta_2$=0.579) (L=0.95m, b=0.039m, h=0.005m, ρ=2750kg/m3, E=71GPa) | 63 |
| 4.6 | Comparison of Natural Frequency for cracked beam (For $\zeta_1$=0.1875 and $\zeta_2$=0.5) ( L=0.8m, b=0.039m, h=0.005m, ρ=2750kg/m3, E=71GPa) | 64 |
| 5.1 | Fuzzy Rules for detection of Crack Location | 72 |
| 5.2 | Validation of Fuzzy Results with Results Obtained From ANSYS | 76 |
| 5.3 | Fuzzy Rules for detection of Crack Inclination Angle | 81 |
| 5.4 | Fuzzy Rules for detection of Crack Severity | 86 |

## LIST OF FIGURES


| Fig. No. | Title | Page No. |
|---|---|---|
| 2.1 | Three-dimensional view of double inclined cracked beam | 10 |
| 2.2 | Two-dimensional view of double inclined cracked beam | 11 |
| 3.1 | First Mode Shape of uncracked beam | 17 |
| 3.2 | Second Mode Shape of uncracked beam | 18 |
| 3.3 | First Torsional Mode Shape of uncracked beam | 18 |
| 3.4 | Third Transverse Mode Shape of uncracked beam | 19 |
| 3.5 | Fourth Transverse Mode Shape of uncracked beam | 19 |
| 3.6 | First Mode Shape of cracked beam | 25 |
| 3.7 | Second Mode Shape of cracked beam | 26 |
| 3.8 | First Torsional Mode Shape of cracked beam | 26 |
| 3.9 | Third Transverse Mode Shape of cracked beam | 27 |
| 3.10 | Fourth Transverse Mode Shape of cracked beam | 27 |
| 3.11 | Variation of FRNF w.r.t. Theta 2 for FRCL=0.409, SRCL=0.636 | 28 |
| 3.12 | Variation of FRNF w.r.t. Theta 1 for FRCL=0.409, SRCL=0.636 | 28 |
| 3.13 | Variation of FRNF w.r.t. Theta 2 for FRCL=0.361, SRCL=0.579 | 29 |
| 3.14 | Variation of FRNF w.r.t. Theta 1 for FRCL=0.361, SRCL=0.579 | 29 |
| 3.15 | Variation of FRNF w.r.t. Theta 2 for FRCL=0.1875, SRCL=0.5 | 29 |
| 3.16 | Variation of FRNF w.r.t. Theta 1 for FRCL=0.1875, SRCL=0.5 | 29 |
| 3.17 | Variation of SRNF w.r.t. Theta 2 for FRCL=0.409, SRCL=0.636 | 30 |
| 3.18 | Variation of SRNF w.r.t. Theta 1 for FRCL=0.409, SRCL=0.636 | 30 |
| 3.19 | Variation of SRNF w.r.t. Theta 2 for FRCL=0.361, SRCL=0.579 | 30 |
| 3.20 | Variation of SRNF w.r.t. Theta 1 for FRCL=0.361, SRCL=0.579 | 30 |
| 3.21 | Variation of SRNF w.r.t. Theta 2 for FRCL=0.1875, SRCL=0.5 | 31 |
| 3.22 | Variation of SRNF w.r.t. Theta 1 for FRCL=0.1875, SRCL=0.5 | 31 |
| 3.23 | Variation of 3rd RNF w.r.t. Theta 2 for FRCL=0.409, SRCL=0.636 | 31 |
| 3.24 | Variation of 3rd RNF w.r.t. Theta 1 for FRCL=0.409, SRCL=0.636 | 31 |
| 3.25 | Variation of 3rd RNF w.r.t. Theta 2 for FRCL=0.361, SRCL=0.579 | 32 |
| 3.26 | Variation of 3rd RNF w.r.t. Theta 1 for FRCL=0.361, SRCL=0.579 | 32 |
| 3.27 | Variation of 3rd RNF w.r.t. Theta 2 for FRCL=0.1875, SRCL=0.5 | 32 |
| 3.28 | Variation of 3rd RNF w.r.t. Theta 1 for FRCL=0.1875, SRCL=0.5 | 32 |
| 3.29 | Variation of 4th RNF w.r.t. Theta 2 for FRCL=0.409, SRCL=0.636 | 33 |
| 3.30 | Variation of 4th RNF w.r.t. Theta 1 for FRCL=0.409, SRCL=0.636 | 33 |
| 3.31 | Variation of 4th RNF w.r.t. Theta 2 for FRCL=0.361, SRCL=0.579 | 33 |
| 3.32 | Variation of 4th RNF w.r.t. Theta 1 for FRCL=0.361, SRCL=0.579 | 33 |
| 3.33 | Variation of 4th RNF w.r.t. Theta 2 for FRCL=0.1875, SRCL=0.5 | 34 |
| 3.34 | Variation of 4th RNF w.r.t. Theta 1 for FRCL=0.1875, SRCL=0.5 | 34 |
| 3.35 | Variation of 5th RNF w.r.t. Theta 2 for FRCL=0.409, SRCL=0.636 | 34 |
| 3.36 | Variation of 5th RNF w.r.t. Theta 1 for FRCL=0.409, SRCL=0.636 | 34 |
| 3.37 | Variation of 5th RNF w.r.t. Theta 2 for FRCL=0.361, SRCL=0.579 | 35 |
| 3.38 | Variation of 5th RNF w.r.t. Theta 1 for FRCL=0.361, SRCL=0.579 | 35 |
| 3.39 | Variation of 5th RNF w.r.t. Theta 2 for FRCL=0.1875, SRCL=0.5 | 35 |
| 3.40 | Variation of 5th RNF w.r.t. Theta 1 for FRCL=0.1875, SRCL=0.5 | 35 |
| 3.41 | Variation w.r.t. relative crack length for $\theta_1$=30 and $\theta_2$ varying for First Relative Natural Frequency | 36 |

| | | |
|---|---|---|
| 3.42 | Variation w.r.t. relative crack length for $\theta_2$=30 and $\theta_1$ varying for First Relative Natural Frequency | 36 |
| 3.43 | Variation w.r.t. relative crack length for $\theta_1$=60 and $\theta_2$ varying for First Relative Natural Frequency | 36 |
| 3.44 | Variation w.r.t. relative crack length for $\theta_2$=60 and $\theta_1$ varying for First Relative Natural Frequency | 36 |
| 3.45 | Variation w.r.t. relative crack length for $\theta_1$=90 and $\theta_2$ varying for First Relative Natural Frequency | 37 |
| 3.46 | Variation w.r.t. relative crack length for $\theta_2$=90 and $\theta_1$ varying for First Relative Natural Frequency | 37 |
| 3.47 | Variation w.r.t. relative crack length for $\theta_1$=120 and $\theta_2$ varying for First Relative Natural Frequency | 37 |
| 3.48 | Variation w.r.t. relative crack length for $\theta_2$=120 and $\theta_1$ varying for First Relative Natural Frequency | 37 |
| 3.49 | Variation w.r.t. relative crack length for $\theta_1$=150 and $\theta_2$ varying for First Relative Natural Frequency | 38 |
| 3.50 | Variation w.r.t. relative crack length for $\theta_2$=150 and $\theta_1$ varying for First Relative Natural Frequency | 38 |
| 3.51 | Variation w.r.t. relative crack length for $\theta_1$=30 and $\theta_2$ varying for Second Relative Natural Frequency | 38 |
| 3.52 | Variation w.r.t. relative crack length for $\theta_2$=30 and $\theta_1$ varying for Second Relative Natural Frequency | 38 |
| 3.53 | Variation w.r.t. relative crack length for $\theta_1$=60 and $\theta_2$ varying for Second Relative Natural Frequency | 39 |
| 3.54 | Variation w.r.t. relative crack length for $\theta_2$=60 and $\theta_1$ varying for Second Relative Natural Frequency | 39 |
| 3.55 | Variation w.r.t. relative crack length for $\theta_1$=90 and $\theta_2$ varying for Second Relative Natural Frequency | 39 |
| 3.56 | Variation w.r.t. relative crack length for $\theta_2$=90 and $\theta_1$ varying for Second Relative Natural Frequency | 39 |
| 3.57 | Variation w.r.t. relative crack length for $\theta_1$=120 and $\theta_2$ varying for Second Relative Natural Frequency | 40 |
| 3.58 | Variation w.r.t. relative crack length for $\theta_2$=120 and $\theta_1$ varying for Second Relative Natural Frequency | 40 |
| 3.59 | Variation w.r.t. relative crack length for $\theta_1$=150 and $\theta_2$ varying for Second Relative Natural Frequency | 40 |
| 3.60 | Variation w.r.t. relative crack length for $\theta_2$=150 and $\theta_1$ varying for Second Relative Natural Frequency | 40 |
| 3.61 | Variation w.r.t. relative crack length for $\theta_1$=30 and $\theta_2$ varying for Third Relative Natural Frequency | 41 |
| 3.62 | Variation w.r.t. relative crack length for $\theta_2$=30 and $\theta_1$ varying for Third Relative Natural Frequency | 41 |
| 3.63 | Variation w.r.t. relative crack length for $\theta_1$=60 and $\theta_2$ varying for Third Relative Natural Frequency | 41 |
| 3.64 | Variation w.r.t. relative crack length for $\theta_2$=60 and $\theta_1$ varying for Third Relative Natural Frequency | 41 |
| 3.65 | Variation w.r.t. relative crack length for $\theta_1$=90 and $\theta_2$ varying for Third Relative Natural Frequency | 42 |

| | | |
|---|---|---|
| 3.66 | Variation w.r.t. relative crack length for $\theta_2$=90 and $\theta_1$ varying for Third Relative Natural Frequency | 42 |
| 3.67 | Variation w.r.t. relative crack length for $\theta_1$=120 and $\theta_2$ varying for Third Relative Natural Frequency | 42 |
| 3.68 | Variation w.r.t. relative crack length for $\theta_2$=120 and $\theta_1$ varying for Third Relative Natural Frequency | 42 |
| 3.69 | Variation w.r.t. relative crack length for $\theta_1$=150 and $\theta_2$ varying for Third Relative Natural Frequency | 43 |
| 3.70 | Variation w.r.t. relative crack length for $\theta_2$=150 and $\theta_1$ varying for Third Relative Natural Frequency | 43 |
| 3.71 | Variation w.r.t. relative crack length for $\theta_1$=30 and $\theta_2$ varying for Fourth Relative Natural Frequency | 43 |
| 3.72 | Variation w.r.t. relative crack length for $\theta_2$=30 and $\theta_1$ varying for Fourth Relative Natural Frequency | 43 |
| 3.73 | Variation w.r.t. relative crack length for $\theta_1$=60 and $\theta_2$ varying for Fourth Relative Natural Frequency | 44 |
| 3.74 | Variation w.r.t. relative crack length for $\theta_2$=60 and $\theta_1$ varying for Fourth Relative Natural Frequency | 44 |
| 3.75 | Variation w.r.t. relative crack length for $\theta_1$=90 and $\theta_2$ varying for Fourth Relative Natural Frequency | 44 |
| 3.76 | Variation w.r.t. relative crack length for $\theta_2$=90 and $\theta_1$ varying for Fourth Relative Natural Frequency | 44 |
| 3.77 | Variation w.r.t. relative crack length for $\theta_1$=120 and $\theta_2$ varying for Fourth Relative Natural Frequency | 45 |
| 3.78 | Variation w.r.t. relative crack length for $\theta_2$=120 and $\theta_1$ varying for Fourth Relative Natural Frequency | 45 |
| 3.79 | Variation w.r.t. relative crack length for $\theta_1$=150 and $\theta_2$ varying for Fourth Relative Natural Frequency | 45 |
| 3.80 | Variation w.r.t. relative crack length for $\theta_2$=150 and $\theta_1$ varying for Fourth Relative Natural Frequency | 45 |
| 3.81 | Variation w.r.t. relative crack length for $\theta_1$=30 and $\theta_2$ varying for Fifth Relative Natural Frequency | 46 |
| 3.82 | Variation w.r.t. relative crack length for $\theta_2$=30 and $\theta_1$ varying for Fifth Relative Natural Frequency | 46 |
| 3.83 | Variation w.r.t. relative crack length for $\theta_1$=60 and $\theta_2$ varying for Fifth Relative Natural Frequency | 46 |
| 3.84 | Variation w.r.t. relative crack length for $\theta_2$=60 and $\theta_1$ varying for Fifth Relative Natural Frequency | 46 |
| 3.85 | Variation w.r.t. relative crack length for $\theta_1$=90 and $\theta_2$ varying for Fifth Relative Natural Frequency | 47 |
| 3.86 | Variation w.r.t. relative crack length for $\theta_2$=90 and $\theta_1$ varying for Fifth Relative Natural Frequency | 47 |
| 3.87 | Variation w.r.t. relative crack length for $\theta_1$=120 and $\theta_2$ varying for Fifth Relative Natural Frequency | 47 |
| 3.88 | Variation w.r.t. relative crack length for $\theta_2$=120 and $\theta_1$ varying for Fifth Relative Natural Frequency | 47 |
| 3.89 | Variation w.r.t. relative crack length for $\theta_1$=150 and $\theta_2$ varying for Fifth Relative Natural Frequency | 48 |

| | | |
|---|---|---|
| 3.90 | Variation w.r.t. relative crack length for $\theta_2$=150 and $\theta_1$ varying for Fifth Relative Natural Frequency | 48 |
| 3.91 | 3D Variation of First Relative Natural Frequency | 49 |
| 3.92 | 3D Variation of Second Relative Natural Frequency | 49 |
| 3.93 | 3D Variation of Third Relative Natural Frequency | 50 |
| 3.94 | 3D Variation of Fourth Relative Natural Frequency | 50 |
| 3.95 | 3D Variation of Fifth Relative Natural Frequency | 51 |
| 3.96 | Response when forced excitation is applied at the free end of the uncracked beam | 52 |
| 3.97 | Response when forced excitation is applied at the free end of the cracked beam | 52 |
| 3.98 | Response when forced excitation is applied between both the cracks | 53 |
| 3.99 | Response when forced excitation is applied between the fixed support and first crack | 53 |
| 4.1 | Accelerometer (Model 4513-001, Brüel & Kjær) | 56 |
| 4.2 | Impact Hammer Tip (Model 2302-5, Brüel & Kjær) | 56 |
| 4.3 | Data Acquisition System (3560-L, Brüel & Kjær) | 57 |
| 4.4 | Actual Setup with Accelerometer, Impact Hammer Tip and Data Acquisition System | 57 |
| 4.5 | Impulsive force applied by the Impact Hammer | 58 |
| 4.6 | Time Response | 59 |
| 4.7 | First Natural Frequency of Uncracked beam (L=110cm, b=3.9cm, h=0.5cm) | 59 |
| 4.8 | Second Natural Frequency of Uncracked beam (L=110cm, b=3.9cm, h=0.5cm) | 60 |
| 4.9 | Third Natural Frequency of Uncracked beam (L=110cm, b=3.9cm, h=0.5cm) | 60 |
| 4.10 | Fourth Natural Frequency of Uncracked beam (L=110cm, b=3.9cm, h=0.5cm) | 61 |
| 4.11 | Coherence plot | 61 |
| 5.1 | Triangular Membership Function | 66 |
| 5.2 | Trapezoidal Membership Function | 66 |
| 5.3 | Generalized Bell Membership Function | 67 |
| 5.4 | Gaussian Membership Function | 67 |
| 5.5 | Sigmoid Membership Function | 67 |
| 5.6 | S-Shaped Membership Function | 68 |
| 5.7 | Z-Shaped Membership Function | 68 |
| 5.8 | Hybrid Membership Function | 68 |
| 5.9 | Input Variable- Percentage variation in FRNF | 70 |
| 5.10 | Input Variable- Percentage variation in SRNF | 70 |
| 5.11 | Input Variable- Percentage variation in TRNF | 70 |
| 5.12 | Output Variable- Expected Crack Location | 71 |
| 5.13 | Application of Rules for FRNF=0.39, SRNF=1.04, TRNF=0.68 (Output=0.367) | 73 |
| 5.14 | Application of Rules for FRNF=0.42, SRNF=0.79, TRNF=0.71 (Output=0.229) | 74 |
| 5.15 | Application of Rules for FRNF=1.08, SRNF=0.65, TRNF=0.16 (Output=0.155) | 75 |

| | | |
|---|---|---|
| 5.16 | Surface plot of rules with FRNF and SRNF as input with crack location as output | 76 |
| 5.17 | Surface plot of rules with FRNF and TRNF as input with crack location as output | 77 |
| 5.18 | Surface plot of rules with TRNF and SRNF as input with crack location as output | 77 |
| 5.19 | Input Variable- Percentage variation in FRNF | 78 |
| 5.20 | Input Variable- Percentage variation in SRNF | 79 |
| 5.21 | Input Variable- Percentage variation in TRNF | 79 |
| 5.22 | Output Variable- Expected Crack Location | 79 |
| 5.23 | Application of Rules for FRNF=0.376, SRNF=0.7, TRNF=1.2 (Output=111) | 82 |
| 5.24 | Surface plot of rules with SRNF and FRNF as input with crack inclination angle as output | 83 |
| 5.25 | Surface plot of rules with TRNF and FRNF as input with crack inclination angle as output | 83 |
| 5.26 | Surface plot of rules with TRNF and SRNF as input with crack inclination angle as output | 84 |
| 5.27 | Input Variable- Percentage variation in FRNF | 85 |
| 5.28 | Input Variable- Percentage variation in SRNF | 85 |
| 5.29 | Input Variable- Percentage variation in TRNF | 85 |
| 5.30 | Output Variable- Expected Crack Location | 85 |
| 5.31 | Application of Rules for FRNF=1.2, SRNF=0.85, TRNF=0.75 (Severity = 1.04) | 87 |
| 5.32 | Application of Rules for FRNF=1.6, SRNF=1.7, TRNF=1.8 (Severity = 1.5) | 88 |
| 5.33 | Surface plot of rules with SRNF and FRNF as input for crack severity prediction | 89 |
| 5.34 | Surface plot of rules with TRNF and FRNF as input for crack severity prediction | 89 |

## NOMENCLATURE

| | |
|---|---|
| $L$ | = Length of the beam |
| $L_1$ | = Length of the first crack section from fixed end |
| $L_2$ | = Length of the second crack section from fixed end |
| $b$ | = Breadth of the beam |
| $h$ | = Total depth of the beam |
| $t$ | = Transverse depth of the crack tip |
| $\theta_1$ | = Angle of Inclination of first crack |
| $\theta_2$ | = Angle of Inclination of second crack |
| $P_i$ | = Applied load on $i^{th}$ direction |
| $u_i$ | = Displacement in the $i^{th}$ direction |
| $J$ | = Strain energy density |
| $K_{i\ (i=1, 2, 3)}$ | = Stress intensity factor for $i^{th}$ mode of fracture |
| $E$ | = Elastic modulus |
| $\vartheta$ | = Poisson's ratio |
| $c_{ij}$ | = Compliance coefficients |
| $\rho$ | = Density |
| $\zeta_1$ ($L_1/L$) | = First relative crack length |
| $\zeta_2$ ($L_2/L$) | = Second relative crack length |

# CHAPTER 1

## 1. INTRODUCTION

Structural health monitoring is one of the most used methods for fault detection. Much research has been put into this filed and currently many pieces of research are going on so as to develop efficient methods for precise detection of fault. Many traditional Non-Destructive Methods (NDT) have been used over the years. Visual Inspection, Ultrasonic method, X-ray method, Eddie current method and vibration methods are commonly used NDT methods. Out of these, vibration method is more popular as it is relatively cheap and reliable. This method can be used for complex structures. This research project is aimed at developing a comprehensive model for fault diagnosis using the study of cracked cantilever beam with two inclined cracks.

### 1.1. MOTIVATION

Much research has been previously done on cantilever beam with transverse through cracks, but that does not provide an exhaustive analysis. Ideally not all cracks are through transverse cracks and in many cases we encounter cases with inclined cracks. Some in the present research investigation of inclined cracks are carried out. This model is exhaustive in a sense that it makes other investigation on transverse cracks a special case of itself when a particular angle combination is chosen. Two inclined cracks are considered as this study can be easily extended to take into account both single crack and multiple cracks.

### 1.2. OBJECTIVE

The objective of this research is twofold. The first objective is to determine what changes occur in a beam due to the presence of crack. Considering the system to be undamped and linear, change in natural frequency, mode shapes and response of the system to forced

excitation is determined. A database of which is prepared for different inclination angles and different relative crack lengths.

The next objective is to use this database to predict the expected location of the crack, its inclination angle and its severity.

### 1.3. METHODOLOGY ADOPTED

The change that occurs in a beam due to crack is obtained by doing its Finite Element Analysis in ANSYS. Results are calculated by varying both crack angles independently and varying the relative position of crack with respect to the fixed end. Results have been obtained in non-dimensional form so that it is independent of the dimensions of the beam and can be extended to consider other cases. Non-dimensional lengths and non-dimensional frequencies are used.

After compiling the results by ANSYS, the next step is to check the validity of these results by comparing them with experimental results. Impact testing is done to find experimentally the results.

Finally to predict the expected crack location, its inclination angle and severity, Fuzzy Logic is used with a set of user-defined rules.

### 1.4. REVIEW OF LITERATURE

According to Rytter [1] the problem of damage diagnostic can be categorized into four different levels

Level 1: qualitative assessment of crack presence
Level 2: crack location identification
Level 3: crack severity assessment
Level 4: effect of all above on remaining service life of member

During vibration of a beam with a crack, the crack remains open for some part of the cycle, and it closes for remaining part of the period and this continues as long as vibration continues. Weight of the structural member and residuals loads (if any) impart a static deflection to the member and this, when combined with the vibration amplitude, may cause the crack to remain open, open and close intermittently and or always closed. If the magnitude of static deflection exceeds the vibration amplitude, the crack always remains open. For this case, the crack can be modelled as a linear model. But if the static deflection is small enough, depending upon the vibration amplitude the crack opens and regularly closes during its period. For the repeated opening and closing of the crack, the crack is modelled as a nonlinear system.

This repeated opening and closing of the crack can be modelled as a spring-mass system where the mass is acted upon by a spring force during half of its cycle and for the other half it is acted upon by a different spring force [2]. For a simple system having spring stiffness of $k_1$for half of the cycle and $k_1 + k_2$ for the other half, the natural frequencies for the first half and second half of the cycle becomes $\omega_1$and $\omega_2$ respectively where $\omega_1 = \sqrt{\frac{k_1}{m}}$ and $\omega_2 = \sqrt{\frac{k_1+k_2}{m}}$ and the bilinear frequency has been found to be

$$\omega_0 = \frac{2\omega_1 \omega_2}{\omega_1+\omega_2} \qquad (1)$$

The cracked beam has two different configurations. One is open crack, and other is closed crack. Each configuration can be modelled as a linear system, and each has its natural frequencies that can be solved by solving the eigenvalue problem. The two sets of natural frequencies or eigenvalues can be combined by using equation (1). The resultant frequency from equation (1) will be the effective natural frequency.

Cracked structures can be modelled broadly by three different techniques [3]. The first technique uses finite element method to represent the damage as a reduction in stiffness of a

particular element or group of elements. In the second technique, the cracked region and uncracked region are modelled separately. The crack free region is modelled by lumped mass or compliance matrix model. The third technique consists of continuous modelling. The basic idea of this method is to develop a first order differential equation using stationary variational principle also known as Hu-Washizu-Barr method [4]. The variational principle makes it possible to account for stress or strain concentrations.

Chatterjee et al. [5] have modelled the breathing crack as a contact problem using plane isoparametric element. They also assumed the problem to be frictionless with small displacement. To model a beam vibrating in its first mode, they have intuitively used a single degree of freedom oscillator with stiffness and mass that change abruptly.

Due to the presence of a crack, change in vibration response of beams has been studied by many. The reverse problem has also drawn the attention of many researchers i.e. given a vibration response; can we predict the presence of crack (if any)?

Nahvi et al. [6] have studied the problem of detecting cracks from vibration response. Using finite element methods (FEM), the beam has been discretized into different elements with the assumption that crack is present in each element. In each element, the crack depth is varied for each position of the crack. Modal analysis of crack in each element is done for various lengths and depths to obtain natural frequencies. Using these results, the authors plotted a class of three-dimensional plots of the frequency with respect to dimensionless crack location and depth for first three modes. The authors used normalized frequencies, which is the ratio of the natural frequency of cracked beam to the natural frequency of the uncracked beam.

The results obtained from [6] shows that the natural frequency of crack decreases as the location of crack moves towards the fixed end of the beam. Crack near the fixed end also

modifies the boundary constraint of the beam. Effect of nonlinearity has been ignored as the cracks are assumed to be always open during vibration.

Orhan [7] has suggested that the free vibration analysis is suitable for detecting single and double cracks. But forced vibration analysis is suitable only for single crack condition. The effect of changes in crack depth and location can be described better by dynamic response of forced vibration than free vibration.

Gudmundson [8] has modelled the cracks as sawing cuts in his experiments. He investigated an edge cracked beam with fatigue crack and studied the effect of crack closure on that beam. He observed that the eigen frequencies decreased at a slower rate as a function of crack length than in the case of an open crack. He introduced plastic deformation at the tip of the crack due to crack growth. These deformations try to close the crack as residual stresses appear in the beam. Thus for small vibration amplitudes, the crack remains closed. For longer cracks, a part of the crack remains open due to residual stresses, and it behaves as a shorter crack for small vibration amplitudes. The residual stresses act to close the crack. Thus for small vibration amplitudes, no change in eigen frequency is observed as the crack remains closed.

Narkis [9] modelled the crack as an equivalent spring connecting two parts of the beam. He observed that the only information necessary for identification of crack is the variation of first two natural frequencies with others information regarding the geometry of the beam or crack depth or beam material being unnecessary.

Khiem et al. [10] developed a transfer matrix method for frequency analysis of a multiple cracked beam based on rotational spring model of the crack. Their calculations revealed that an increase in number of cracks, in general, decreased the natural frequency of the beam irrespective of the boundary conditions at the end of the beam. The natural frequencies are

sensitive to elastic boundary conditions only for certain range of values of the spring constant and outside this range the number of cracks has no significant effect on natural frequencies.

Patil et al. [11] have modelled the transverse vibration through transfer matrix method and the cracks have been represented as rotational springs. The beam is divided into a number of segments, and each segment is assumed to carry a damage parameter. The procedure gives a linear relationship between natural frequency and damage parameter. The parameters are determined from the knowledge of the change in natural frequency. After obtaining them, each is used to pinpoint the location of crack and to determine its size.

Carneiro et al. [12] have developed a continuous model for transverse vibration of cracked beam including the shear deformations. The stress and strain concentrations introduced by the presence of a crack are represented by stress disturbance functions that modify the kinematic assumptions used in variational procedure.

The problem of opening and closing of crack is of piecewise interval nature in time domain. The closure and opening of the crack being the boundary of the sub-intervals over which linear equations govern the system. Abraham O.N.L. et al. [13] linearized the system using Fourier development of flexibility matrix. He introduced dry friction between crack faces to distinguish it from the uncracked beam case. The compatibility conditions at crack section are maintained using Lagrange multipliers to fulfil contact conditions and to construct a consistent stiffness matrix.

Pungo et al. [14] analyzed the vibration response of a cantilever beam subjected to harmonic force with cracks of different size and location. For the analysis, he used harmonic balance approach. If it is assumed that the structure behaves linearly, it may lead to incorrect conclusions about the state of damage. So for the inspection technique to be more generally applicable, it would be better to consider non-linear dynamic behavior of breathing cracks.

Lee Jinhee [15] has discussed the forward problem of identification of crack by using finite element methods. The crack has been modelled by a rotational spring without any mass. The node representing the crack has been assigned a degree of freedom value of three while other nodes have been assigned a degree of freedom value of two. The inverse problem has been solved by Newton-Raphson method for possible identification of crack locations and sizes.

Shifrin et al. [16] have investigated a beam with arbitrary number of cracks and calculated the natural frequencies applying a new approach. They used the model of a continuous beam and reduced the computation time for calculating natural frequencies as compared to other methods by decreasing the dimension of the matrix involved.

Kishen et al. [17] observed a decrease in critical load of the column due to the presence of crack using finite element method. Bouboulas et al. [18] used finite element analysis to model a crack that is not propagating for beam type elements. Reynders et al. [19] have developed a technique using which modal analysis can be done without using any parameter that is user specified. Kisa et al. [20] have done modal analysis of beams with multiple cracks and circular cross section. Zarfam et al. [21] have investigated beams subjected to moving mass and have obtained response spectrum when excitation is applied at the support. Staszewski et al. [22] have used wavelet theory to obtain frequency response for beams with parameters that vary with time. Civalek et al. [23] have used continuum mechanics to analyse bending and free vibration of cantilevered type micro-tubes. Zhao et al. [24] have investigated the dynamic behaviour of tapered cantilever type beams under the effect of moving mass.

### 1.5. THESIS LAYOUT

Chapter 1 is concerned with Introduction. In this chapter the motivation, objective and methodology adopted and review of literature has been discussed.

Chapter 2 tries to develop the governing equation of the cracked vibrating beam using mass and stiffness matrices. Linear and undamped conditions are assumed throughout the formulation.

Chapter 3 is concerned with the evaluation of results using ANSYS. Results have been tabulated by varying different parameters such as crack inclination angle, relative crack location and its response to forced excitation.

Chapter 4 validates the results obtained through ANSYS with that obtained from experimental testing. Errors have been calculated between them.

Chapter 5 uses Fuzzy Logic to predict the fault that is present in the structure. For this purpose, Fuzzy Rules have been formulated, and results obtained are compared to previously obtained values to check its correctness.

Chapter 6 discusses the conclusion and scope for future work.

# CHAPTER-2

## 2. MATHEMATICAL FORMULATION OF CRACKED BEAM VIBRATION

To mathematically determine the natural frequencies of a vibrating beam with inclined cracks, we need a governing equation that can satisfactorily model the problem. For the case of a continuous beam, for which the number of degrees of freedom is infinite, a simplified model can be obtained by considering a lumped parameter model for which the number of degrees of freedom is finite. In this chapter, an equation of motion is derived that can approximate the actual behaviour of cracked beam with double inclined crack.

### 2.1. Mathematical Formulation

For a finite degree of freedom system with no damping, the equation of motion involves a mass matrix, a stiffness matrix and an imposed excitation matrix or a null matrix depending upon the presence of an external excitation or not. To obtain the equation of motion for undamped vibration case, our main aim is to determine the stiffness matrix and the mass matrix of the cracked beam.

Presence of crack changes the stiffness of the beam. So accordingly, the stiffness matrix of the cracked beam differs from that of the uncracked beam. Instead of calculating the stiffness matrix directly, it is much more convenient to calculate the compliance matrix. The compliance coefficients are related to the strain energy of the cracked beam. The strain energy is further related to the stress intensity factors. The stress intensity factors can be referred from stress intensity factor handbooks [34]. The present case of cracked beam with double inclined crack is peculiar, for though stress intensity factors are exhaustively calculated for transverse cracks, it is a formidable task to calculate the stress intensity factors for inclined cracks for changing inclination angles. So the best way forward that seems feasible is to model the crack to be composed of several transverse cracks with varying depths so that the already developed stress

intensity factors for different loading conditions can be used for inclined cracks with reasonable accuracy.

For the case of general loading, the double inclined cracked beam can be represented as in Fig 2.1. The beam has a length L, width b and depth h. Its two-dimensional view is shown in Fig.2.2.

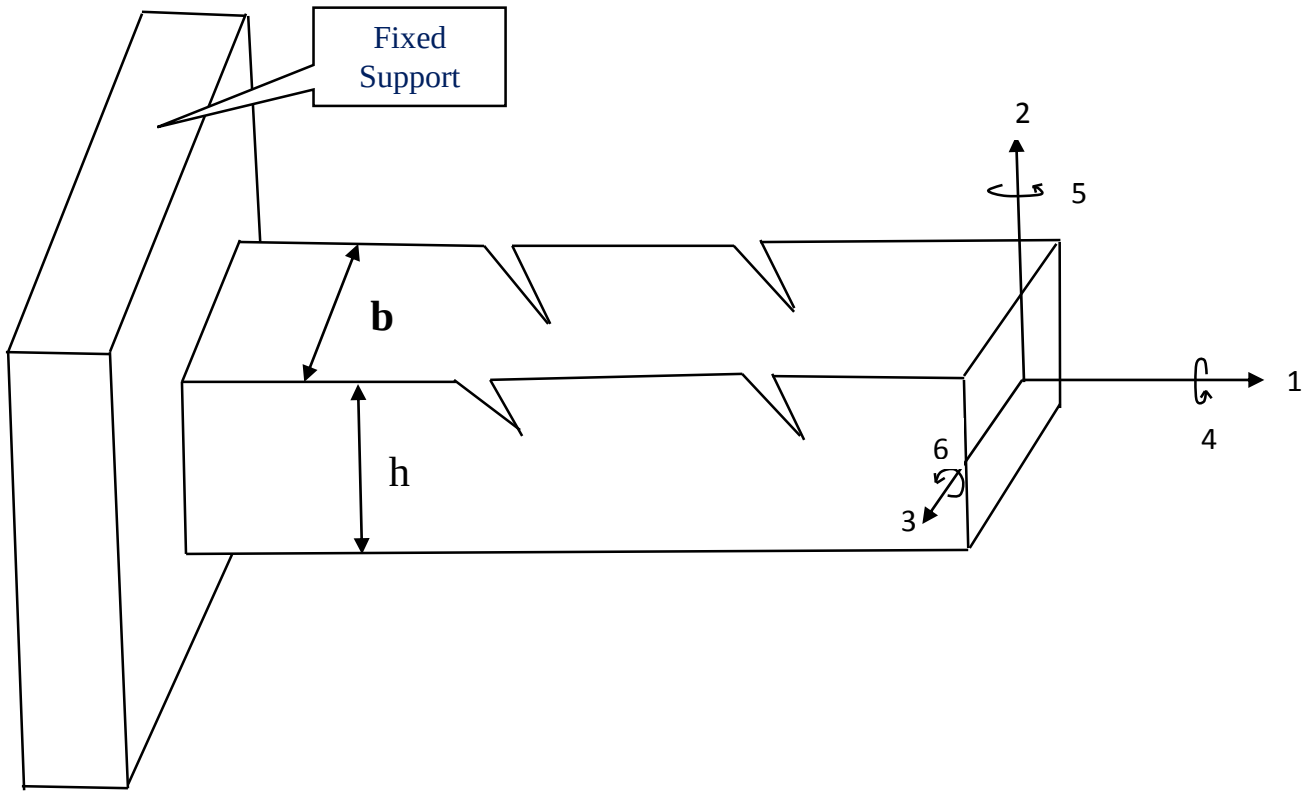


Fig. 2.1. Three-dimensional view of double inclined cracked beam

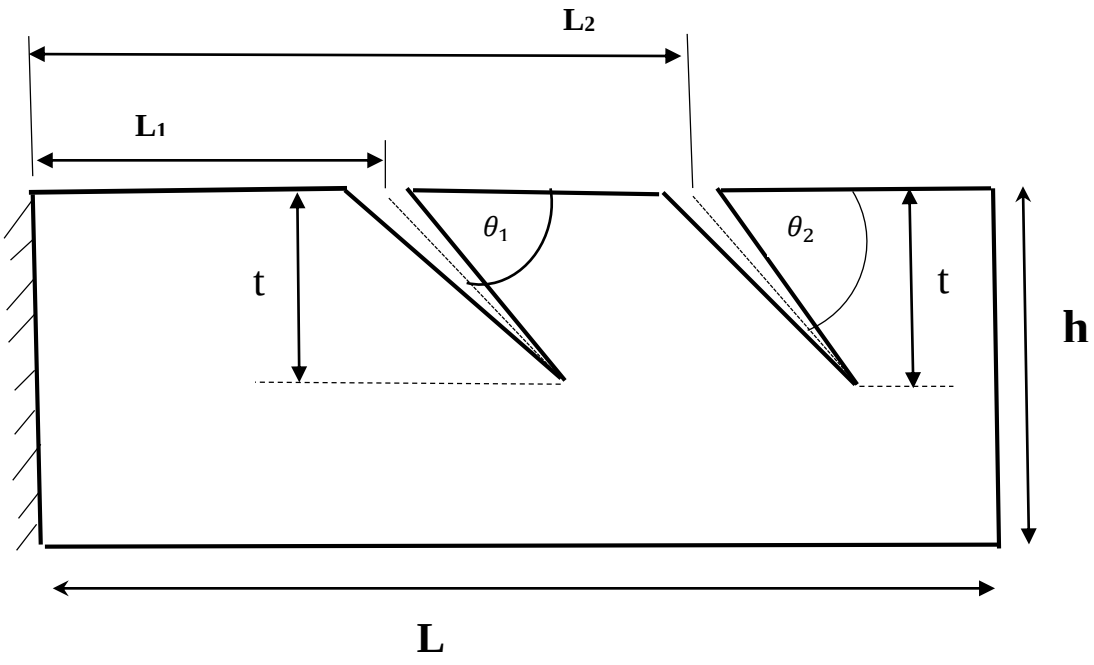


Fig. 2.2. Two-dimensional view of double inclined cracked beam

The strain energy of the beam changes due to the presence of crack. In the linear elastic range, flexibility coefficients can be expressed by stress intensity factors using Castigliano's theorem. The generalised displacement can be written as,

$$u_i = \frac{\partial}{\partial P_i} \int_0^a J(\xi) d\xi$$

Where J ($\xi$) is the strain energy density function.

$$J(\xi) = \frac{1}{E'} \left[ \left( \sum_{n=1}^{6} K_{In} \right)^2 + \left( \sum_{n=1}^{6} K_{IIn} \right)^2 + \frac{1}{1-\vartheta} \left( \sum_{n=1}^{6} K_{IIIn} \right)^2 \right]$$

Where, $E' = E/(1-\vartheta)$ for Plane Strain condition

E = Elasticity modulus

The additional flexibility introduced due to crack can be obtained from the generalized displacement equation and the definition of compliance

$$c_{in} = \frac{\partial u_i}{\partial P_n} = \frac{\partial^2}{\partial P_n \partial P_i} \int_0^a J(\xi) d\xi$$

The stress intensity factors necessary to evaluate the coefficients of flexibility matrix can be obtained from the literature [30], [31], [32].

The stress intensity factors are given as follows

$$K_{I1} = \frac{P_1 \sqrt{\pi \xi}}{hb} F_1(\bar{\xi})$$

$$K_{I2} = K_{I3} = K_{I4} = 0$$

$$K_{I5} = \frac{12 P_5 \sqrt{\pi \xi}}{hb^3} F_1(\bar{\xi})$$

$$K_{I6} = \frac{6 P_6 \sqrt{\pi \xi}}{h^2 b} F_2(\bar{\xi})$$

$$K_{II1} = 0$$

$$K_{II2} = \frac{\beta_z P_2 \sqrt{\pi \xi}}{hb} F_{II}(\bar{\xi})$$

$$K_{II3} = 0$$

$$K_{II4} = \frac{\varphi_y P_4 \sqrt{\pi \xi}}{hb} F_{II}(\bar{\xi})$$

$$K_{II5} = K_{II6} = 0$$

$$K_{III1} = K_{III2} = 0$$

$$K_{III3} = \frac{\beta_y P_3 \sqrt{\pi \xi}}{hb} F_{III}(\bar{\xi})$$

$$K_{III4} = \frac{\varphi_z P_4 \sqrt{\pi\bar{\xi}}}{hb} F_{III}(\bar{\xi})$$

$$K_{III5} = K_{III6} = 0$$

Where $\varphi_y$ and $\varphi_z$ are functions describing stress distribution during torsion and $\beta_y$ and $\beta_z$ are shear factors of the rectangular cross section.

$$F_1 = \frac{\sqrt{\frac{2}{\pi\bar{\xi}}\tan\left(\frac{\pi\bar{\xi}}{2}\right)}\left[0.752 + 2.02\bar{\xi} + 0.37\left(1 - \sin\left(\frac{\pi\bar{\xi}}{2}\right)\right)^3\right]}{\cos\left(\frac{\pi\bar{\xi}}{2}\right)}$$

$$F_2 = \frac{\sqrt{\frac{2}{\pi\bar{\xi}}\tan\left(\frac{\pi\bar{\xi}}{2}\right)}\left[0.923 + 0.199\left(1 - \sin\left(\frac{\pi\bar{\xi}}{2}\right)\right)^4\right]}{\cos\left(\frac{\pi\bar{\xi}}{2}\right)}$$

$$F_{II} = \frac{\left[1.30 - 0.65\bar{\xi} + 0.37\bar{\xi}^2 + 0.28\bar{\xi}^3\right]}{\sqrt{1 - \bar{\xi}}}$$

$$F_{III} = \sqrt{\frac{\pi\bar{\xi}}{\sin(\pi\bar{\xi})}}$$

Where, $\bar{\xi} = \frac{\xi}{h}$, $\bar{a} = \frac{a}{h}$ and $\bar{z} = \frac{z}{b}$

The shearing effect has been neglected in comparison to bending effects, as the length of the beam is very large as compared to its transverse dimensions.

$$c_{11} = \frac{2\pi}{E'b}\int_0^{\bar{a}} \bar{\xi} {F_1}^2(\bar{\xi}) d\bar{\xi} \int_{-1/2}^{1/2} d\bar{z}$$

$$c_{55} = \frac{288\pi}{E'b^3}\int_0^{\bar{a}} \bar{\xi} {F_2}^2(\bar{\xi}) d\bar{\xi} \int_{-1/2}^{1/2} d\bar{z}$$

$$c_{66} = \frac{77\pi}{E'bh^2}\int_0^{\bar{a}} \bar{\xi}{F_1}^2(\bar{\xi})d\bar{\xi}\int_{-1/2}^{1/2} d\bar{z}$$

$$c_{44} = \frac{2\pi}{E'b^2h}\left(\int_0^{\bar{a}} \bar{\xi}\left(\frac{1}{1-\vartheta}{\varphi_z}^2{F_{III}}^2(\bar{\xi}) + {\varphi_y}^2{F_{II}}^2(\bar{\xi})\right)d\bar{\xi}\int_{-1/2}^{1/2} d\bar{z}\right)$$

$$c_{15} = \frac{24\pi}{E'bh}\int_0^{\bar{a}} \bar{\xi}{F_1}^2(\bar{\xi})d\bar{\xi}\int_{-1/2}^{1/2} \bar{z}d\bar{z}$$

$$c_{56} = \frac{144\pi}{E'b^2h}\int_0^{\bar{a}} \bar{\xi}F_1(\bar{\xi})F_2(\bar{\xi})d\bar{\xi}\int_{-1/2}^{1/2} d\bar{z}$$

$$c_{16} = \frac{12\pi}{E'bh}\int_0^{\bar{a}} \bar{\xi}F_1(\bar{\xi})F_2(\bar{\xi})d\bar{\xi}\int_{-1/2}^{1/2} d\bar{z}$$

$$c_{22} = c_{33} = c_{24} = c_{34} = 0$$

So the additional flexibility matrix C for the cracked beam can be written as

$$C = \begin{bmatrix} c_{11} & 0 & 0 & 0 & c_{15} & c_{16} \\ 0 & 0 & 0 & 0 & 0 & 0 \\ 0 & 0 & 0 & 0 & 0 & 0 \\ 0 & 0 & 0 & c_{44} & 0 & 0 \\ c_{51} & 0 & 0 & 0 & c_{55} & c_{56} \\ c_{61} & 0 & 0 & 0 & c_{65} & c_{66} \end{bmatrix}$$

The stiffness matrix can be obtained from the flexibility matrix by taking its inverse. The mass matrix can be considered to be the same as that of the beam element as cracked node of the cracked element can be considered as of zero length and zero mass [33]. So the equation of motion for undamped forced vibration can be written as

$$[M]\{\ddot{u}\} + [K]\{u\} = \{F\}$$

For the free vibration case, the equation becomes

$$[M]\{\ddot{u}\} + [K]\{u\} = \mathbf{0}$$

Where **0** represents the null vector.

# CHAPTER 3

## 3. FINITE ELEMENT ANALYSIS OF CANTILEVER BEAM WITH DOUBLE INCLINED CRACK

The complexity involved in the determination of flexibility matrix and more importantly its dependence on inclination angle thwarts any attempt to solve the general equation of motion of vibrating beam with double inclined cracks for each and every value of inclination angles. So the next logical step seems to be that of determining the vibration characteristics by using various software that performs finite element analysis conveniently for complex cases. In this chapter finite element analysis of double cracked cantilever beam has been done by ANSYS 15.0 software and results have been obtained.

### 3.1. INTRODUCTION

Finite element method discretizes the structure into various parts called elements. The elements are connected to each other through nodes and boundary conditions at nodes are to be satisfied to get an approximate solution to any complex problem. The solution accuracy depends on the number of elements – higher the number of elements, better is the solution accuracy – and the shape of elements chosen, viz. triangular, quadrilateral, tetrahedral etc., depending on the problem requirement.

### 3.2. MODAL ANALYSIS USING ANSYS

Modal analysis– the so-called determination of mode shapes and corresponding natural frequencies – has been carried out in ANSYS. The material selected is an Aluminium Alloy with density 2750 kg/m$^3$. The dimensions of the beam – as per Fig.2.2 – are, L=110cm, b=3.9cm and h=0.5cm. Two dimensionless parameters are used which are defined as follows,

$$\zeta_1 = \frac{\text{Distance to the first crack from fixed support}(L_1)}{\text{Total length of the beam}(L)}$$

$$\zeta_2 = \frac{\text{Distance to the first crack from fixed support}(L_2)}{\text{Total length of the beam}(L)}$$

$$\text{Relative Natural Frequency} = \frac{\text{Natural frequency of cracked beam}}{\text{Natural Frequency of uncracked beam}}$$

The effect of crack and its position in the beam toward changing its dynamic characteristics have been studied using ANSYS, and it has been compared to that of the uncracked beam.

### 3.3. FINITE ELEMENT ANALYSIS OF UNCRACKED BEAM

By using the default mess settings of ANSYS 15.0, the first five natural frequencies obtained for various dimensions of the beam, for the same Aluminium Alloy having density 2750 kg/m$^3$, have been given in Table 3.1.

**Table 3.1.** Natural Frequency of uncracked beam obtained from ANSYS

| Mode | Natural Frequency(Hz) | Natural Frequency(Hz) | Natural Frequency(Hz) |
|---|---|---|---|
| | L=110cm | L=95cm | L=80cm |
| | b=3.9cm, h=0.5cm | b=3.9cm, h=0.5cm | b=3.9cm, h=0.5cm |
| 1 | 3.4049 | 4.5669 | 6.4434 |
| 2 | 21.336 | 28.616 | 40.372 |
| 3 | 26.453* | 35.458* | 49.982* |
| 4 | 59.74 | 80.122 | 113.03 |
| 5 | 117.07 | 157.01 | 221.51 |

(*- These are Torsional natural frequencies)

Out of these natural frequencies, the third natural frequency is due to torsional vibration, and the rest are due to transverse vibration of the beam. The mathematical calculation for obtaining the natural frequency of Euler- Bernoulli beams have been done centuries ago. For Aluminium Alloy beams with density 2750 kg/m3 and elastic modulus E=71GPa, values obtained from mathematical calculation of continuous beam are given in Table 3.2.

**Table 3.2.** Natural Frequency of uncracked beam obtained from Mathematical Analysis

| Mode | Natural Frequency(Hz) | Natural Frequency(Hz) | Natural Frequency(Hz) |
|---|---|---|---|
| | L=110cm | L=95cm | L=80cm |
| | b=3.9cm, h=0.5cm | b=3.9cm, h=0.5cm | b=3.9cm, h=0.5cm |
| 1 | 3.392 | 4.547 | 6.412 |
| 2 | 21.256 | 28.498 | 40.187 |
| 3 | 59.504 | 79.778 | 112.5 |
| 4 | 116.630 | 156.369 | 220.505 |

### 3.4. MODE SHAPES OF UNCRACKED BEAM

The mode shapes obtained from ansys is plotted for first five natural frequencies out of which one is torsional while others are transverse. Points of maximum and minimum deflection have been identified on the mode shapes.

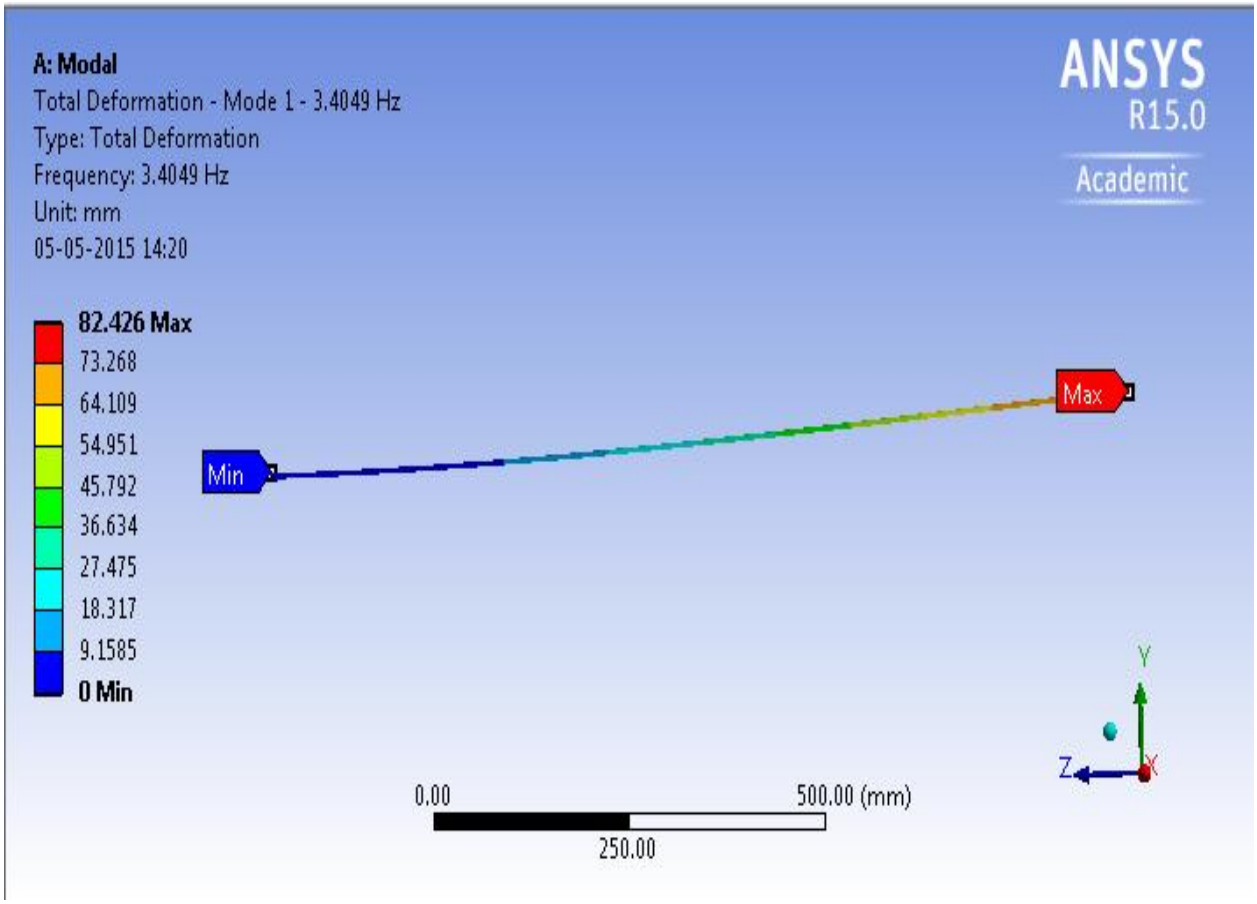


Fig.3.1. First Mode Shape of uncracked beam

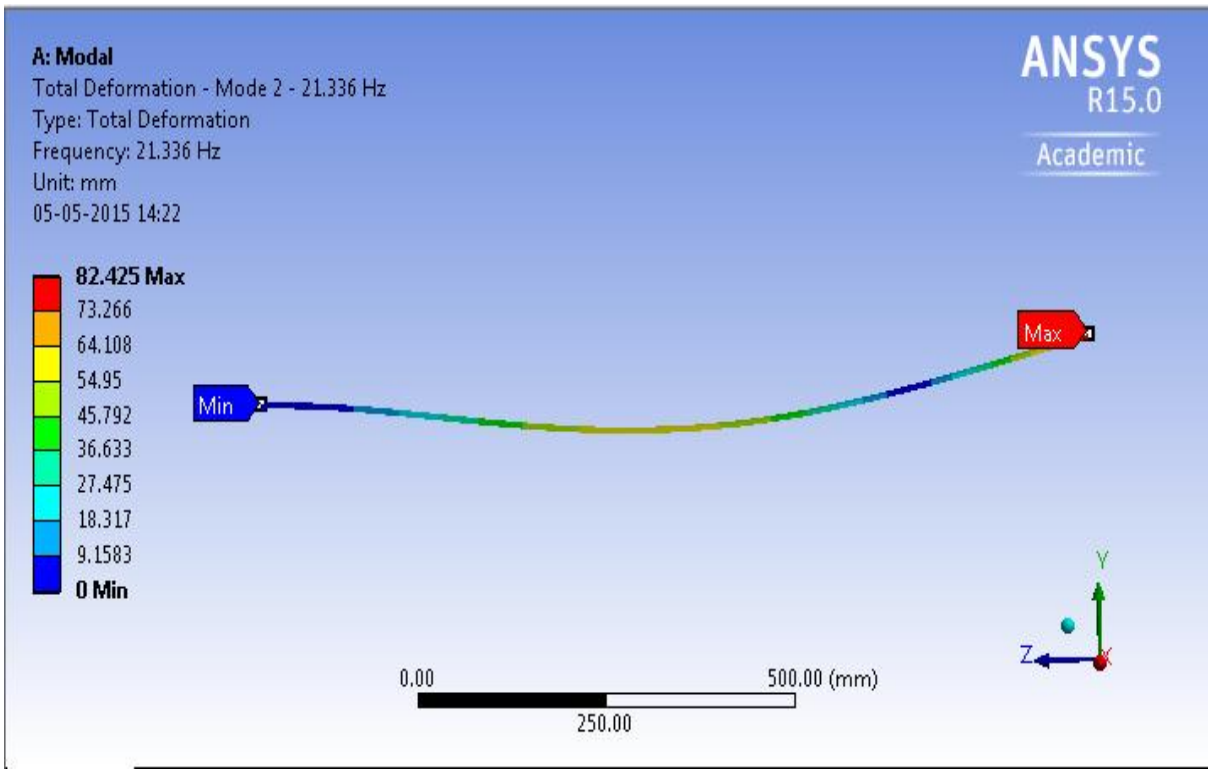


Fig.3.2. Second Mode Shape of uncracked beam

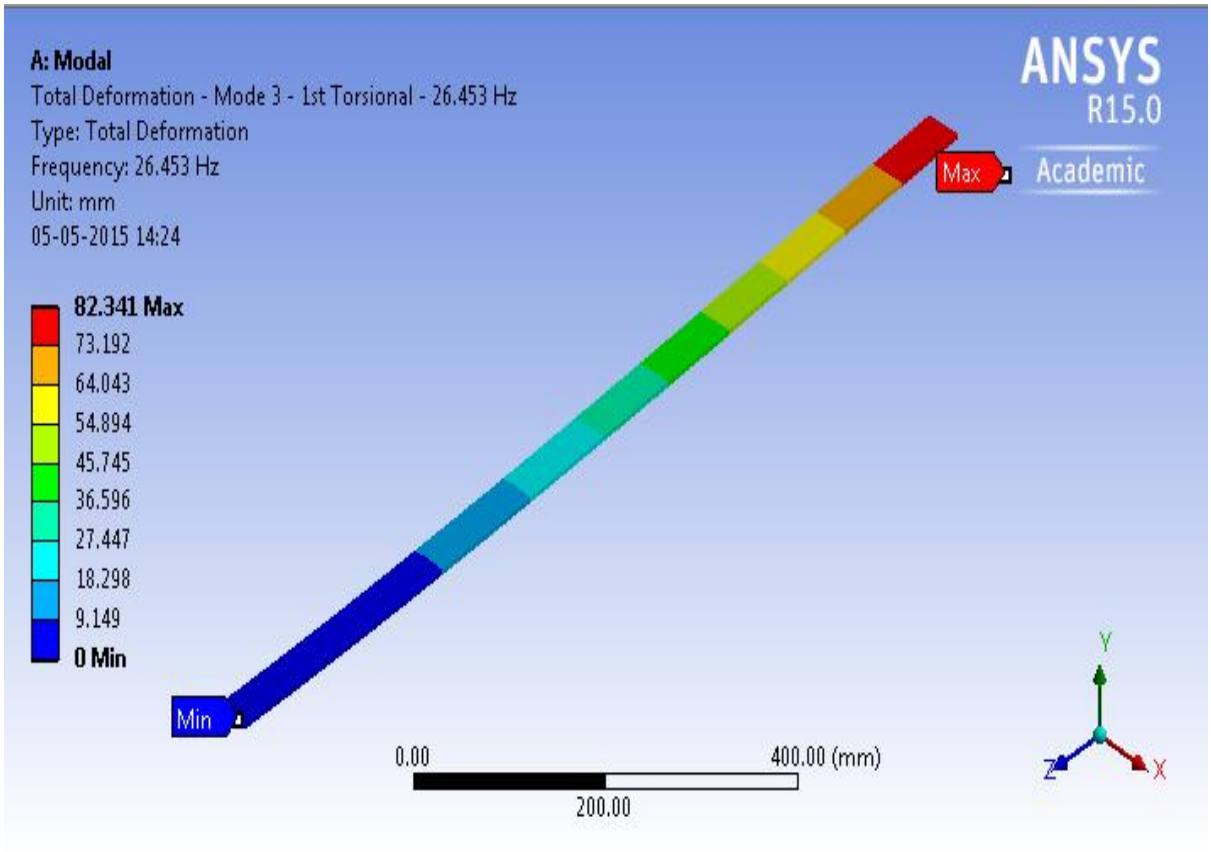


Fig.3.3. First Torsional Mode Shape of uncracked beam

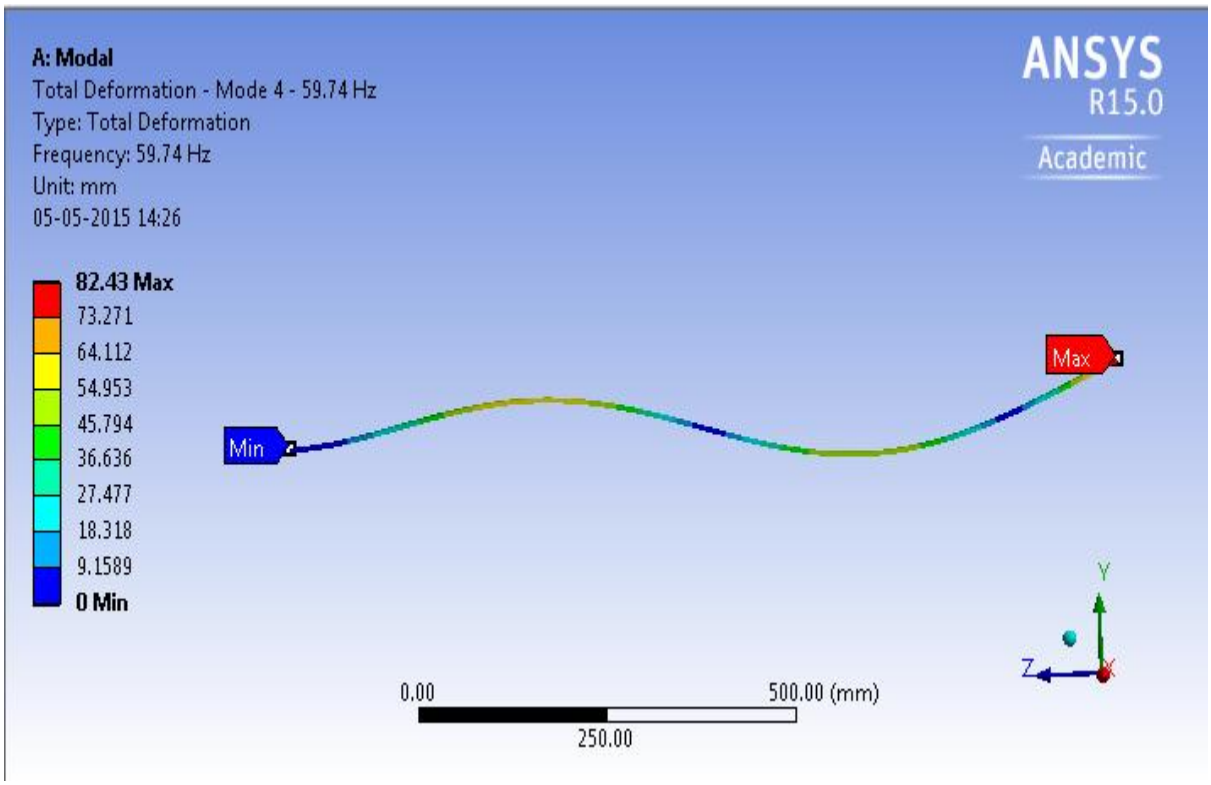


Fig.3.4. Third Transverse Mode Shape of uncracked beam

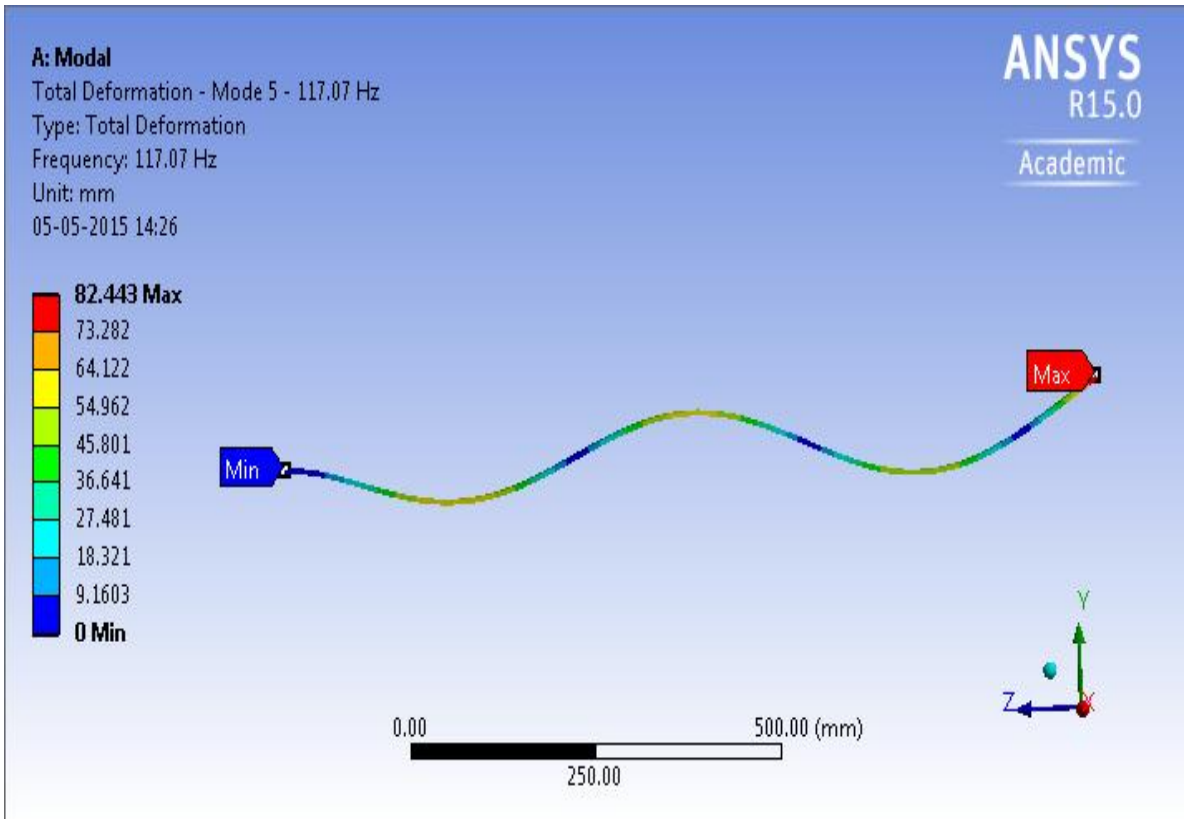


Fig.3.5. Fourth Transverse Mode Shape of uncracked beam

### 3.5. FINITE ELEMENT ANALYSIS OF CRACKED BEAM

Finite element analysis of cracked beam is done with two inclined cracks. The inclination angles of both cracks have been taken to be $30^0$, $60^0$, $90^0$, $120^0$ and $150^0$. Natural frequencies are obtained for three different relative lengths. Dimensionless relative natural frequencies have also been calculated.

#### 3.5.1. For $\zeta_1$=0.409 and $\zeta_2$=0.636 (L1=45cm, L2=70cm, L=110cm)

**Table 3.3.** 1st Natural Frequency

| $\theta_2$ ↓ | | $\theta_1$ → | | | | |
|---|---|---|---|---|---|---|
| | | 30 | 60 | 90 | 120 | 150 |
| | 30 | 3.3933 | 3.3935 | 3.3917 | 3.3937 | 3.3924 |
| | 60 | 3.3941 | 3.3936 | 3.3936 | 3.3937 | 3.3941 |
| | 90 | 3.3938 | 3.3934 | 3.3934 | 3.394 | 3.3933 |
| | 120 | 3.3934 | 3.3932 | 3.3936 | 3.393 | 3.3935 |
| | 150 | 3.3931 | 3.3932 | 3.393 | 3.3934 | 3.3927 |

**Table 3.4.** 1st Relative Natural Frequency

| $\theta_2$ ↓ | | $\theta_1$ → | | | | |
|---|---|---|---|---|---|---|
| | | 30 | 60 | 90 | 120 | 150 |
| | 30 | 0.9966 | 0.9967 | 0.9961 | 0.9967 | 0.9963 |
| | 60 | 0.9968 | 0.9967 | 0.9967 | 0.9967 | 0.9968 |
| | 90 | 0.9967 | 0.9966 | 0.9966 | 0.9968 | 0.9966 |
| | 120 | 0.9966 | 0.9966 | 0.9967 | 0.9965 | 0.9967 |
| | 150 | 0.9965 | 0.9966 | 0.9965 | 0.9966 | 0.9964 |

**Table 3.5.** 2nd Natural Frequency

| $\theta_2$ ↓ | | $\theta_1$ → | | | | |
|---|---|---|---|---|---|---|
| | | 30 | 60 | 90 | 120 | 150 |
| | 30 | 21.126 | 21.139 | 21.128 | 21.153 | 21.121 |
| | 60 | 21.137 | 21.14 | 21.14 | 21.147 | 21.143 |
| | 90 | 21.14 | 21.151 | 21.141 | 21.151 | 21.115 |
| | 120 | 21.131 | 21.137 | 21.142 | 21.144 | 21.137 |
| | 150 | 21.13 | 21.141 | 21.148 | 21.156 | 21.109 |

**Table 3.6.** 2nd Relative Natural Frequency

| $\theta_2$ ↓ | | $\theta_1$ → | | | | |
|---|---|---|---|---|---|---|
| | | 30 | 60 | 90 | 120 | 150 |
| | 30 | 0.9902 | 0.9908 | 0.9903 | 0.9914 | 0.9899 |
| | 60 | 0.9907 | 0.9908 | 0.9908 | 0.9911 | 0.991 |
| | 90 | 0.9908 | 0.9913 | 0.9909 | 0.9913 | 0.9896 |
| | 120 | 0.9904 | 0.9907 | 0.9909 | 0.991 | 0.9907 |
| | 150 | 0.9903 | 0.9909 | 0.9912 | 0.9916 | 0.9894 |

**Table 3.7.** 3rd Natural Frequency

| $\theta_2$ ↓ | | $\theta_1$ → | | | | |
|---|---|---|---|---|---|---|
| | | 30 | 60 | 90 | 120 | 150 |
| | 30 | 26.415 | 26.416 | 26.411 | 26.416 | 26.413 |
| | 60 | 26.419 | 26.417 | 26.417 | 26.417 | 26.419 |
| | 90 | 26.418 | 26.416 | 26.417 | 26.419 | 26.416 |
| | 120 | 26.416 | 26.415 | 26.416 | 26.415 | 26.416 |
| | 150 | 26.414 | 26.415 | 26.415 | 26.415 | 26.413 |

**Table 3.8.** 3rd Relative Natural Frequency

| $\theta_2$ ↓ | | $\theta_1$ → | | | | |
|---|---|---|---|---|---|---|
| | | 30 | 60 | 90 | 120 | 150 |
| | 30 | 0.9986 | 0.9986 | 0.9984 | 0.9986 | 0.9985 |
| | 60 | 0.9987 | 0.9986 | 0.9986 | 0.9986 | 0.9987 |
| | 90 | 0.9987 | 0.9986 | 0.9986 | 0.9987 | 0.9986 |
| | 120 | 0.9986 | 0.9986 | 0.9986 | 0.9986 | 0.9986 |
| | 150 | 0.9985 | 0.9986 | 0.9986 | 0.9986 | 0.9985 |

**Table 3.9.** 4th Natural Frequency

| $\theta_2$ ↓ | | $\theta_1$ → | | | | |
|---|---|---|---|---|---|---|
| | | 30 | 60 | 90 | 120 | 150 |
| | 30 | 59.254 | 59.298 | 59.301 | 59.346 | 59.273 |
| | 60 | 59.265 | 59.289 | 59.294 | 59.318 | 59.301 |
| | 90 | 59.274 | 59.325 | 59.295 | 59.322 | 59.226 |
| | 120 | 59.251 | 59.279 | 59.29 | 59.307 | 59.287 |
| | 150 | 59.246 | 59.286 | 59.312 | 59.335 | 59.207 |

**Table 3.10.** 4th Relative Natural Frequency

| $\theta_2$ ↓ | | $\theta_1$ → | | | | |
|---|---|---|---|---|---|---|
| | | 30 | 60 | 90 | 120 | 150 |
| | 30 | 0.9919 | 0.9926 | 0.9927 | 0.9934 | 0.9922 |
| | 60 | 0.992 | 0.9925 | 0.9925 | 0.9929 | 0.9927 |
| | 90 | 0.9922 | 0.9931 | 0.9926 | 0.993 | 0.9914 |
| | 120 | 0.9918 | 0.9923 | 0.9925 | 0.9928 | 0.9924 |
| | 150 | 0.9917 | 0.9924 | 0.9928 | 0.9932 | 0.9911 |

**Table 3.11.** 5th Natural Frequency

| $\theta_2$ ↓ | | $\theta_1$ → | | | | |
|---|---|---|---|---|---|---|
| | | 30 | 60 | 90 | 120 | 150 |
| | 30 | 116.78 | 116.77 | 116.72 | 116.77 | 116.75 |
| | 60 | 116.81 | 116.8 | 116.8 | 116.79 | 116.8 |
| | 90 | 116.81 | 116.79 | 116.8 | 116.81 | 116.8 |
| | 120 | 116.81 | 116.8 | 116.81 | 116.8 | 116.8 |
| | 150 | 116.81 | 116.81 | 116.8 | 116.81 | 116.8 |

**Table 3.12.** 5th Relative Natural Frequency

| $\theta_2$ ↓ | | $\theta_1$ → | | | | |
|---|---|---|---|---|---|---|
| | | 30 | 60 | 90 | 120 | 150 |
| | 30 | 0.9975 | 0.9974 | 0.997 | 0.9974 | 0.9973 |
| | 60 | 0.9978 | 0.9977 | 0.9977 | 0.9976 | 0.9977 |
| | 90 | 0.9978 | 0.9976 | 0.9977 | 0.9978 | 0.9977 |
| | 120 | 0.9978 | 0.9977 | 0.9978 | 0.9977 | 0.9977 |
| | 150 | 0.9978 | 0.9978 | 0.9977 | 0.9978 | 0.9977 |

### 3.5.2 For $\zeta_1$=0.316 and $\zeta_2$=0.579 ($L_1$=30cm, $L_2$=55cm, L=95cm)

**Table 3.13.** 1st Natural Frequency

| $\theta_2$ ↓ | | $\theta_1$ → | | | | |
|---|---|---|---|---|---|---|
| | | 30 | 60 | 90 | 120 | 150 |
| | 30 | 4.5413 | 4.5414 | 4.546 | 4.5441 | 4.5411 |
| | 60 | 4.5453 | 4.5476 | 4.547 | 4.5478 | 4.5447 |
| | 90 | 4.5459 | 4.5442 | 4.5436 | 4.5444 | 4.545 |
| | 120 | 4.5489 | 4.5475 | 4.5438 | 4.5446 | 4.5469 |
| | 150 | 4.5407 | 4.5386 | 4.5413 | 4.5413 | 4.5399 |

**Table 3.14.** 1st Relative Natural Frequency

| $\theta_2$ ↓ | | $\theta_1$ → | | | | |
|---|---|---|---|---|---|---|
| | | 30 | 60 | 90 | 120 | 150 |
| | 30 | 0.9944 | 0.9944 | 0.9954 | 0.995 | 0.9944 |
| | 60 | 0.9953 | 0.9958 | 0.9956 | 0.9958 | 0.9951 |
| | 90 | 0.9954 | 0.995 | 0.9949 | 0.9951 | 0.9952 |
| | 120 | 0.9961 | 0.9958 | 0.9949 | 0.9951 | 0.9956 |
| | 150 | 0.9943 | 0.9938 | 0.9944 | 0.9944 | 0.9941 |

**Table 3.15.** 2nd Natural Frequency

| $\theta_2$ ↓ | | $\theta_1$ → | | | | |
|---|---|---|---|---|---|---|
| | | 30 | 60 | 90 | 120 | 150 |
| | 30 | 28.358 | 28.375 | 28.411 | 28.389 | 28.358 |
| | 60 | 28.37 | 28.418 | 28.391 | 28.431 | 28.35 |
| | 90 | 28.372 | 28.411 | 28.384 | 28.423 | 28.339 |
| | 120 | 28.382 | 28.398 | 28.386 | 28.426 | 28.357 |
| | 150 | 28.375 | 28.407 | 28.387 | 28.386 | 28.345 |

**Table 3.16.** 2nd Relative Natural Frequency

| $\theta_2$ ↓ | | $\theta_1$ → | | | | |
|---|---|---|---|---|---|---|
| | | 30 | 60 | 90 | 120 | 150 |
| | 30 | 0.991 | 0.9916 | 0.9928 | 0.9921 | 0.991 |
| | 60 | 0.9914 | 0.9931 | 0.9921 | 0.9935 | 0.9907 |
| | 90 | 0.9915 | 0.9928 | 0.9919 | 0.9933 | 0.9903 |
| | 120 | 0.9918 | 0.9924 | 0.992 | 0.9934 | 0.9909 |
| | 150 | 0.9916 | 0.9927 | 0.992 | 0.992 | 0.9905 |

**Table 3.17.** 3rd Natural Frequency

| $\theta_2$ ↓ | | $\theta_1$ → | | | | |
|---|---|---|---|---|---|---|
| | | 30 | 60 | 90 | 120 | 150 |
| | 30 | 35.358 | 35.359 | 35.363 | 35.367 | 35.357 |
| | 60 | 35.374 | 35.379 | 35.377 | 35.38 | 35.372 |
| | 90 | 35.377 | 35.369 | 35.367 | 35.37 | 35.374 |
| | 120 | 35.38 | 35.379 | 35.37 | 35.373 | 35.377 |
| | 150 | 35.357 | 35.352 | 35.36 | 35.36 | 35.356 |

**Table 3.18.** 3rd Relative Natural Frequency

| $\theta_2$ ↓ | | $\theta_1$ → | | | | |
|---|---|---|---|---|---|---|
| | | 30 | 60 | 90 | 120 | 150 |
| | 30 | 0.9972 | 0.9972 | 0.9973 | 0.9974 | 0.9972 |
| | 60 | 0.9976 | 0.9978 | 0.9977 | 0.9978 | 0.9976 |
| | 90 | 0.9977 | 0.9975 | 0.9974 | 0.9975 | 0.9976 |
| | 120 | 0.9978 | 0.9978 | 0.9975 | 0.9976 | 0.9977 |
| | 150 | 0.9972 | 0.997 | 0.9972 | 0.9972 | 0.9971 |

**Table 3.19.** 4th Natural Frequency

| $\theta_2$ ↓ | | $\theta_1$ → | | | | |
|---|---|---|---|---|---|---|
| | | 30 | 60 | 90 | 120 | 150 |
| | 30 | 79.391 | 79.417 | 79.546 | 79.495 | 79.423 |
| | 60 | 79.489 | 79.578 | 79.552 | 79.599 | 79.501 |
| | 90 | 79.504 | 79.501 | 79.476 | 79.523 | 79.503 |
| | 120 | 79.577 | 79.566 | 79.485 | 79.532 | 79.555 |
| | 150 | 79.4 | 79.385 | 79.436 | 79.439 | 79.399 |

**Table 3.20.** 4th Relative Natural Frequency

| $\theta_2$ ↓ | | $\theta_1$ → | | | | |
|---|---|---|---|---|---|---|
| | | 30 | 60 | 90 | 120 | 150 |
| | 30 | 0.9909 | 0.9912 | 0.9928 | 0.9922 | 0.9913 |
| | 60 | 0.9921 | 0.9932 | 0.9929 | 0.9935 | 0.9922 |
| | 90 | 0.9923 | 0.9922 | 0.9919 | 0.9925 | 0.9923 |
| | 120 | 0.9932 | 0.9931 | 0.992 | 0.9926 | 0.9929 |
| | 150 | 0.991 | 0.9908 | 0.9914 | 0.9915 | 0.991 |

**Table 3.21.** 5th Natural Frequency

| $\theta_2$ ↓ | | $\theta_1$ → | | | | |
|---|---|---|---|---|---|---|
| | | 30 | 60 | 90 | 120 | 150 |
| | 30 | 156.37 | 156.4 | 156.48 | 156.42 | 156.29 |
| | 60 | 156.41 | 156.51 | 156.43 | 156.51 | 156.28 |
| | 90 | 156.41 | 156.47 | 156.39 | 156.47 | 156.25 |
| | 120 | 156.42 | 156.47 | 156.39 | 156.47 | 156.29 |
| | 150 | 156.35 | 156.45 | 156.35 | 156.34 | 156.21 |

**Table 3.22.** 5th Relative Natural Frequency

| $\theta_2$ ↓ | | $\theta_1$ → | | | | |
|---|---|---|---|---|---|---|
| | | 30 | 60 | 90 | 120 | 150 |
| | 30 | 0.9959 | 0.9961 | 0.9966 | 0.9962 | 0.9954 |
| | 60 | 0.9962 | 0.9968 | 0.9963 | 0.9968 | 0.9954 |
| | 90 | 0.9962 | 0.9966 | 0.9961 | 0.9966 | 0.9952 |
| | 120 | 0.9962 | 0.9966 | 0.9961 | 0.9966 | 0.9954 |
| | 150 | 0.9958 | 0.9964 | 0.9958 | 0.9957 | 0.9949 |

### 3.5.3 For $\zeta_1$=0.1875 and $\zeta_2$=0.5 ($L_1$=15cm, $L_2$=40cm, L=80cm)

**Table 3.23.** 1st Natural Frequency

| $\theta_2$ ↓ | | $\theta_1$ → | | | | |
|---|---|---|---|---|---|---|
| | | 30 | 60 | 90 | 120 | 150 |
| | 30 | 6.3737 | 6.3832 | 6.3818 | 6.3808 | 6.3806 |
| | 60 | 6.3838 | 6.3873 | 6.3925 | 6.3895 | 6.3839 |
| | 90 | 6.3797 | 6.3872 | 6.3898 | 6.3795 | 6.3807 |
| | 120 | 6.3759 | 6.3849 | 6.3766 | 6.3871 | 6.3885 |
| | 150 | 6.368 | 6.3694 | 6.3686 | 6.3716 | 6.3658 |

**Table 3.24.** 1st Relative Natural Frequency

| $\theta_2$ ↓ | | $\theta_1$ → | | | | |
|---|---|---|---|---|---|---|
| | | 30 | 60 | 90 | 120 | 150 |
| | 30 | 0.9892 | 0.9907 | 0.9904 | 0.9903 | 0.9903 |
| | 60 | 0.9908 | 0.9913 | 0.9921 | 0.9916 | 0.9908 |
| | 90 | 0.9901 | 0.9913 | 0.9917 | 0.9901 | 0.9903 |
| | 120 | 0.9895 | 0.9909 | 0.9896 | 0.9913 | 0.9915 |
| | 150 | 0.9883 | 0.9885 | 0.9884 | 0.9889 | 0.988 |

**Table 3.25.** 2nd Natural Frequency

| $\theta_2$ ↓ | | $\theta_1$ → | | | | |
|---|---|---|---|---|---|---|
| | | 30 | 60 | 90 | 120 | 150 |
| | 30 | 40.036 | 40.098 | 40.06 | 40.036 | 40.038 |
| | 60 | 40.037 | 40.048 | 40.11 | 40.116 | 40.055 |
| | 90 | 40.035 | 40.036 | 40.109 | 40.116 | 40.037 |
| | 120 | 40.033 | 40.039 | 40.037 | 40.103 | 40.055 |
| | 150 | 39.998 | 40.044 | 40.025 | 40.11 | 39.961 |

**Table 3.26.** 2nd Relative Natural Frequency

| $\theta_2$ ↓ | | $\theta_1$ → | | | | |
|---|---|---|---|---|---|---|
| | | 30 | 60 | 90 | 120 | 150 |
| | 30 | 0.9917 | 0.9932 | 0.9923 | 0.9917 | 0.9917 |
| | 60 | 0.9917 | 0.992 | 0.9935 | 0.9937 | 0.9921 |
| | 90 | 0.9917 | 0.9917 | 0.9935 | 0.9937 | 0.9917 |
| | 120 | 0.9916 | 0.9918 | 0.9917 | 0.9933 | 0.9921 |
| | 150 | 0.9907 | 0.9919 | 0.9914 | 0.9935 | 0.9898 |

**Table 3.27.** 3rd Natural Frequency

| $\theta_2$ ↓ | | $\theta_1$ → | | | | |
|---|---|---|---|---|---|---|
| | | 30 | 60 | 90 | 120 | 150 |
| | 30 | 49.712 | 49.749 | 49.745 | 49.741 | 49.739 |
| | 60 | 49.747 | 49.754 | 49.772 | 49.76 | 49.748 |
| | 90 | 49.73 | 49.76 | 49.766 | 49.728 | 49.73 |
| | 120 | 49.715 | 49.746 | 49.72 | 49.752 | 49.756 |
| | 150 | 49.69 | 49.694 | 49.691 | 49.7 | 49.681 |

**Table 3.28.** 3rd Relative Natural Frequency

| $\theta_2$ ↓ | | $\theta_1$ → | | | | |
|---|---|---|---|---|---|---|
| | | 30 | 60 | 90 | 120 | 150 |
| | 30 | 0.9946 | 0.9953 | 0.9953 | 0.9952 | 0.9951 |
| | 60 | 0.9953 | 0.9954 | 0.9958 | 0.9956 | 0.9953 |
| | 90 | 0.995 | 0.9956 | 0.9957 | 0.9949 | 0.995 |
| | 120 | 0.9947 | 0.9953 | 0.9948 | 0.9954 | 0.9955 |
| | 150 | 0.9942 | 0.9942 | 0.9942 | 0.9944 | 0.994 |

**Table 3.29.** 4th Natural Frequency

| $\theta_2$ ↓ | | $\theta_1$ → | | | | |
|---|---|---|---|---|---|---|
| | | 30 | 60 | 90 | 120 | 150 |
| | 30 | 112.82 | 112.85 | 112.85 | 112.85 | 112.85 |
| | 60 | 112.87 | 112.88 | 112.89 | 112.88 | 112.87 |
| | 90 | 112.86 | 112.88 | 112.89 | 112.85 | 112.87 |
| | 120 | 112.86 | 112.88 | 112.85 | 112.88 | 112.9 |
| | 150 | 112.85 | 112.85 | 112.85 | 112.85 | 112.85 |

**Table 3.30.** 4th Relative Natural Frequency

| $\theta_2$ ↓ | | $\theta_1$ → | | | | |
|---|---|---|---|---|---|---|
| | | 30 | 60 | 90 | 120 | 150 |
| | 30 | 0.9981 | 0.9984 | 0.9984 | 0.9984 | 0.9984 |
| | 60 | 0.9986 | 0.9987 | 0.9988 | 0.9987 | 0.9986 |
| | 90 | 0.9985 | 0.9987 | 0.9988 | 0.9984 | 0.9986 |
| | 120 | 0.9985 | 0.9987 | 0.9984 | 0.9987 | 0.9988 |
| | 150 | 0.9984 | 0.9984 | 0.9984 | 0.9984 | 0.9984 |

**Table 3.31.** 5th Natural Frequency

| $\theta_2$ ↓ | | $\theta_1$ → | | | | |
|---|---|---|---|---|---|---|
| | | 30 | 60 | 90 | 120 | 150 |
| | 30 | 218.43 | 218.92 | 218.72 | 218.59 | 218.6 |
| | 60 | 218.7 | 218.81 | 219.21 | 219.16 | 218.78 |
| | 90 | 218.63 | 218.79 | 219.16 | 218.97 | 218.66 |
| | 120 | 218.56 | 218.76 | 218.57 | 219.08 | 218.91 |
| | 150 | 218.29 | 218.52 | 218.42 | 218.85 | 218.08 |

**Table 3.32.** 5th Relative Natural Frequency

| $\theta_2$ ↓ | | $\theta_1$ → | | | | |
|---|---|---|---|---|---|---|
| | | 30 | 60 | 90 | 120 | 150 |
| | 30 | 0.9861 | 0.9883 | 0.9874 | 0.9868 | 0.9869 |
| | 60 | 0.9873 | 0.9878 | 0.9896 | 0.9894 | 0.9877 |
| | 90 | 0.987 | 0.9877 | 0.9894 | 0.9885 | 0.9871 |
| | 120 | 0.9867 | 0.9876 | 0.9867 | 0.989 | 0.9883 |
| | 150 | 0.9855 | 0.9865 | 0.9861 | 0.988 | 0.9845 |

### 3.6. MODE SHAPES OF CRACKED BEAM

Mode shapes of the cracked beam are similar to that of the uncracked beam – the only difference being the slight change in total deflection, natural frequency and the change in position of nodes [35]. For the sake of completeness, mode shapes have been shown only for one set of relative crack lengths with both the inclination angles remaining the same.

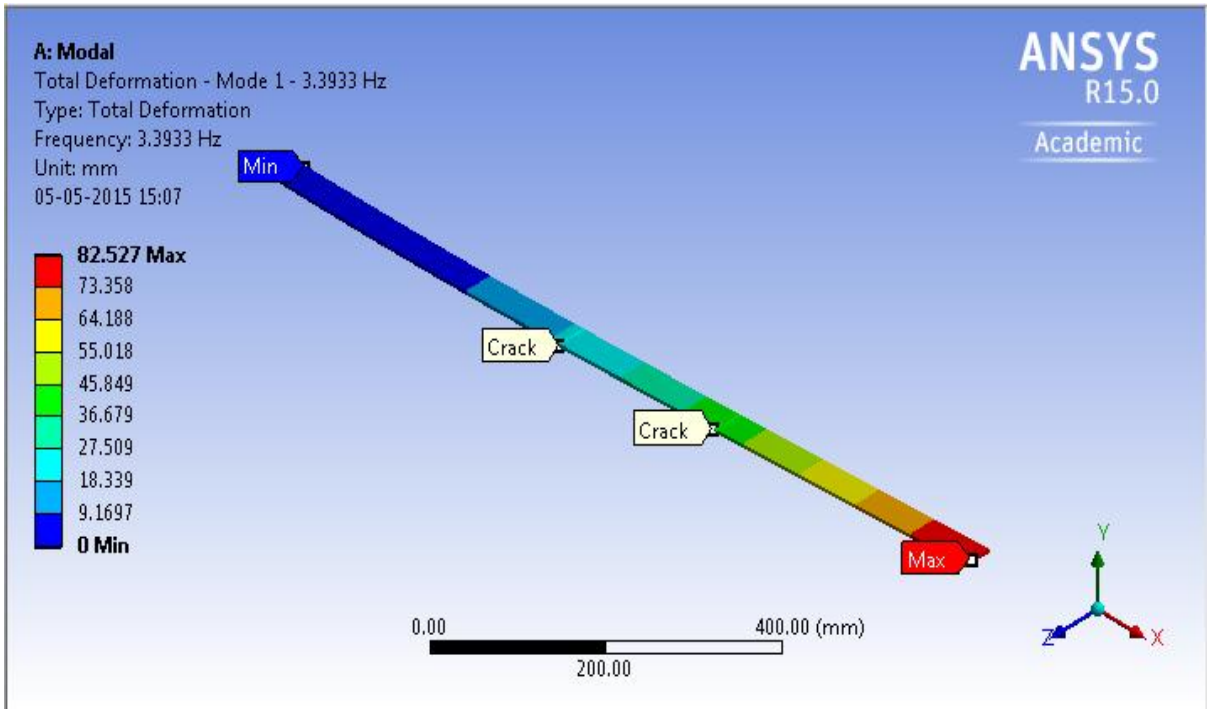


Fig. 3.6. First Mode Shape of cracked beam

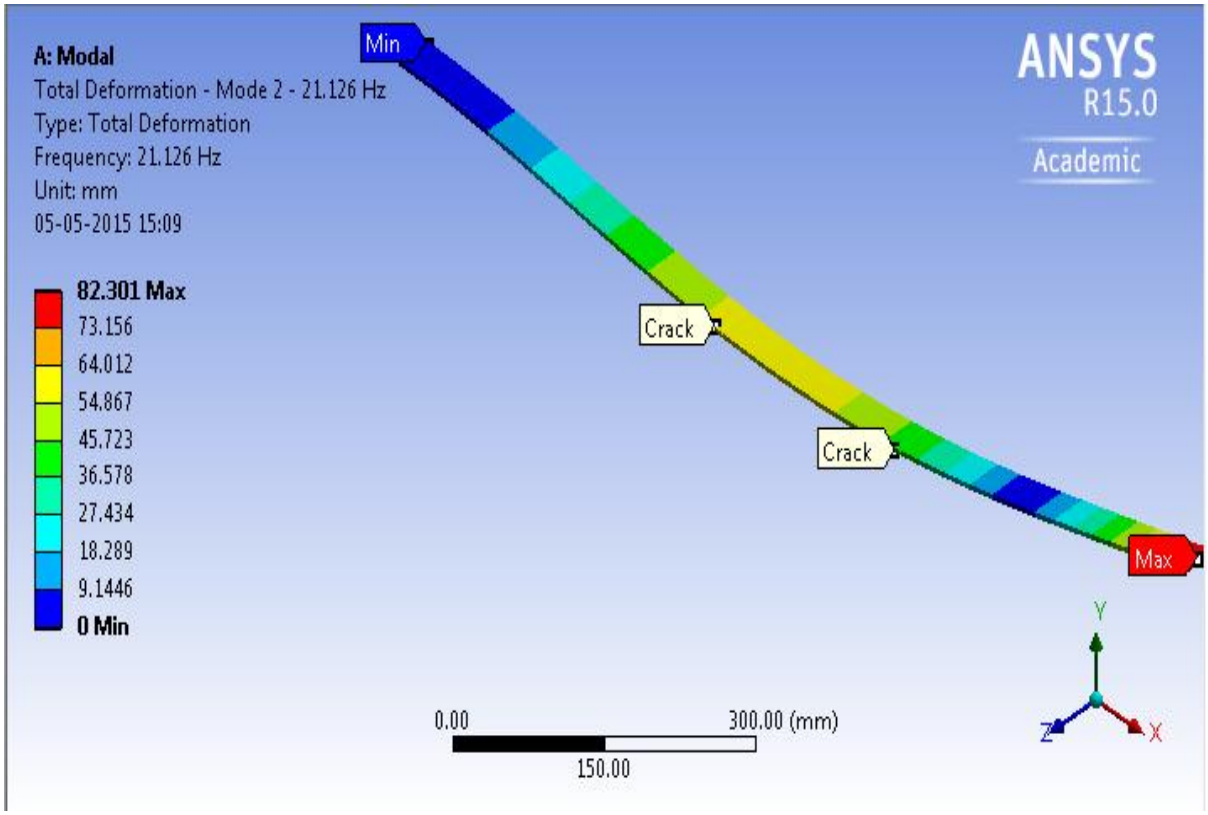


Fig. 3.7. Second Mode Shape of cracked beam

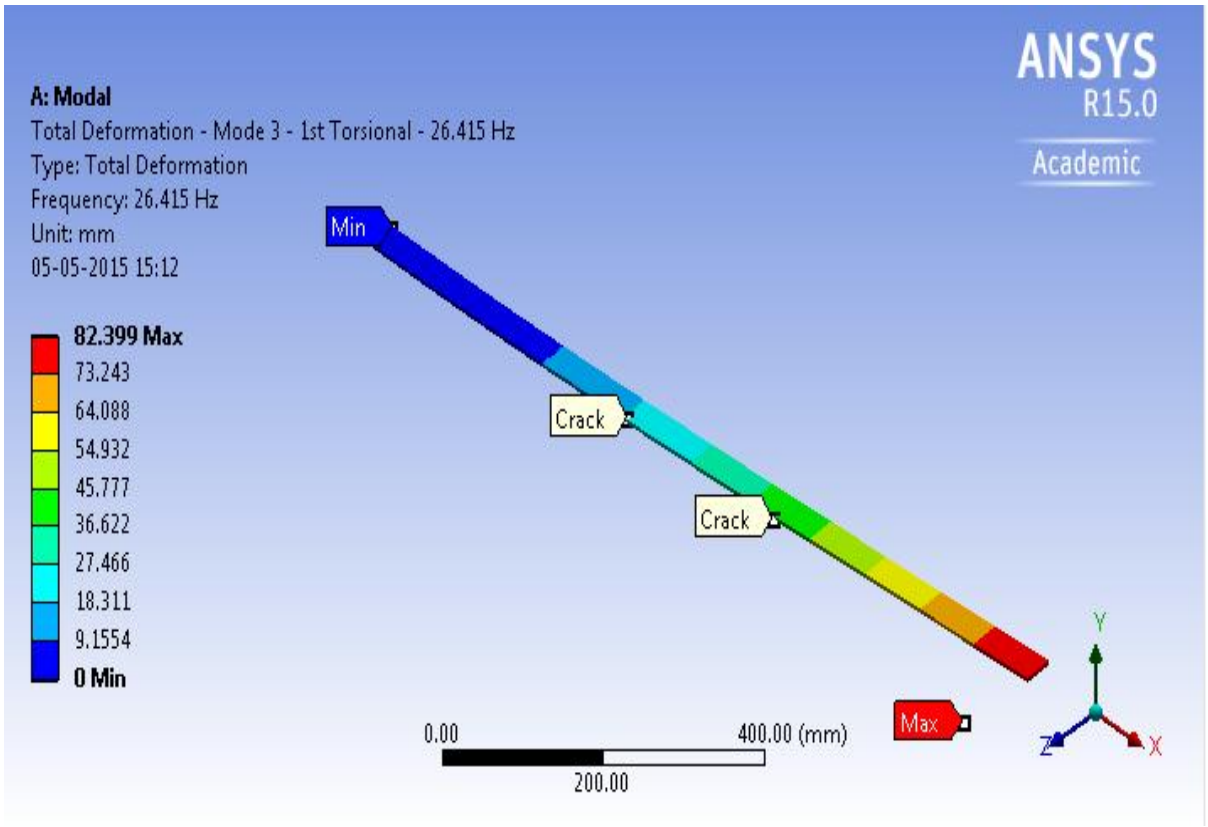


Fig. 3.8. First Torsional Mode Shape of cracked beam

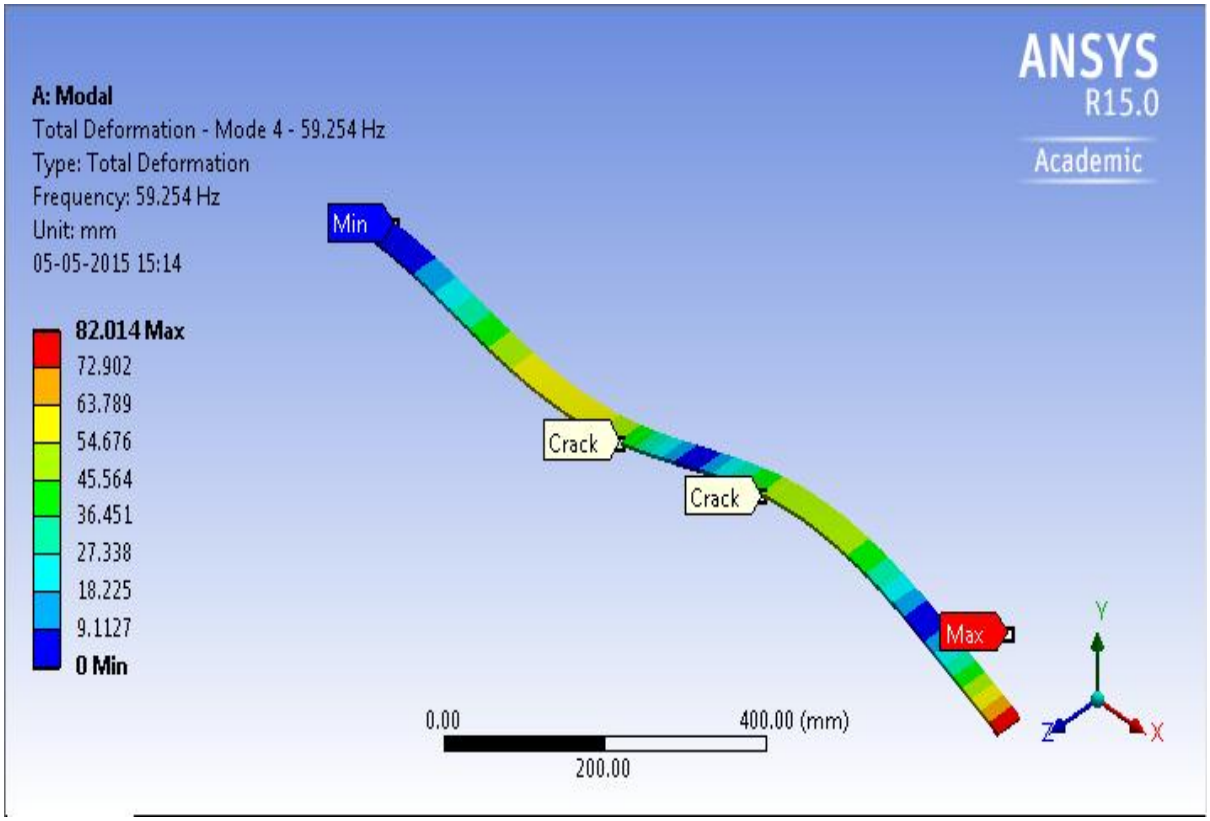


Fig. 3.9. Third Transverse Mode Shape of cracked beam

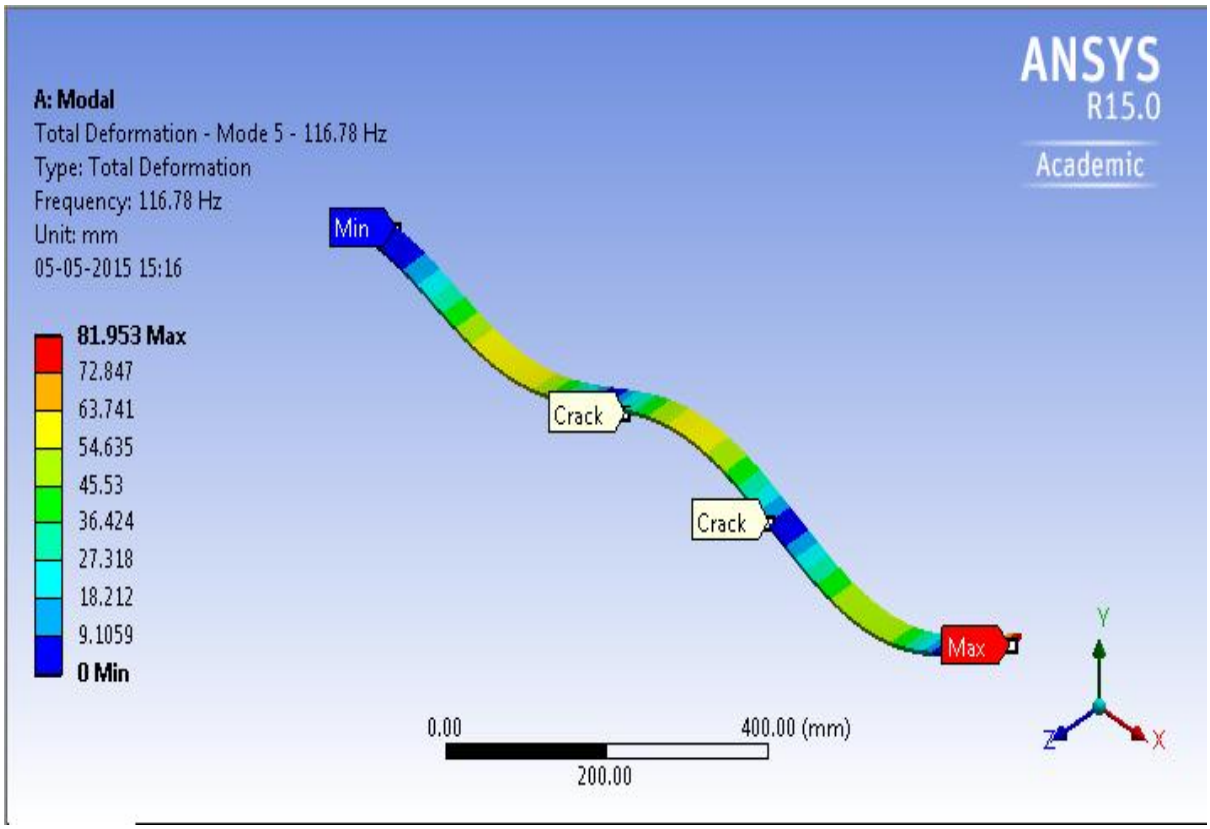


Fig. 3.10. Fourth Transverse Mode Shape of cracked beam

### 3.7. RESULTS AND DISCUSSION

For different relative crack lengths, variation in natural frequency for different values of $\theta_1$ with respect to $\theta_2$ and variation in natural frequency for different values of $\theta_2$ with respect to $\theta_1$ have been considered. At first it might seem redundant to consider both the cases but both variations have been plotted to determine which of the angle is more critical to the variation of natural frequency than other. In the following figures, FRCL and SRCL have been used to denote the first relative crack length and second relative crack length respectively.

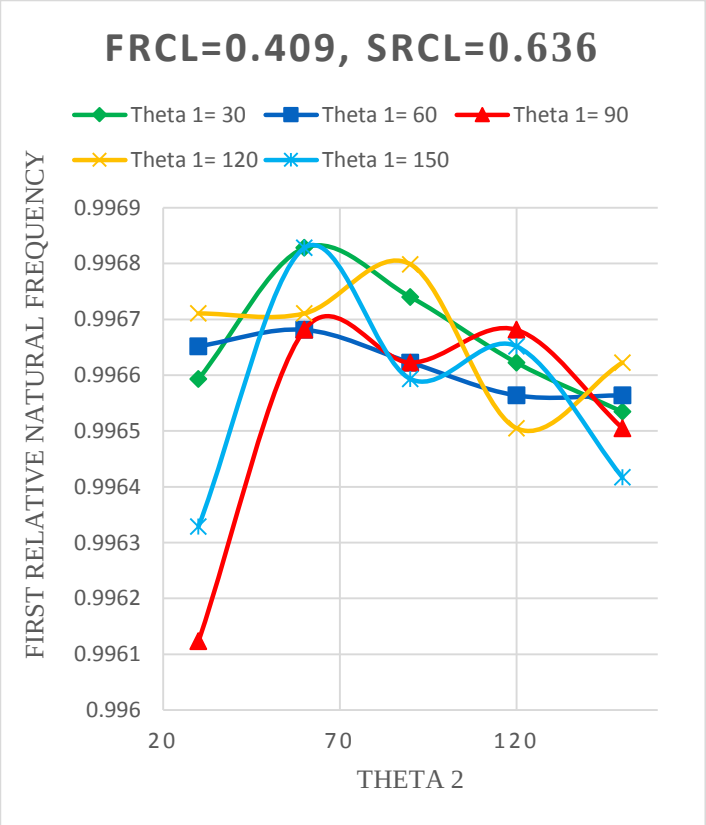


Fig.3.11. Variation of FRNF w.r.t. Theta 2

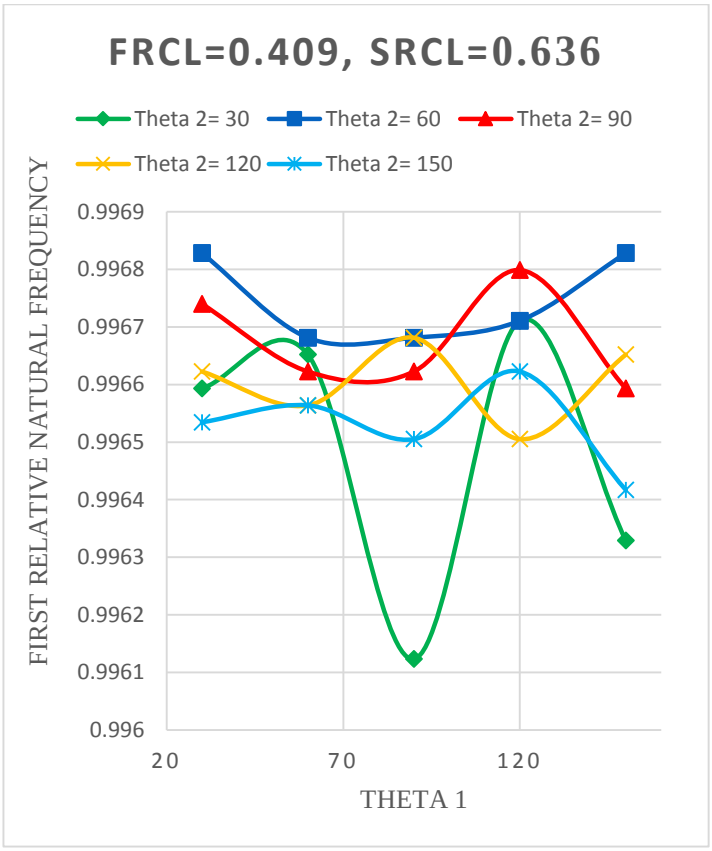


Fig.3.12. Variation of FRNF w.r.t. Theta 1

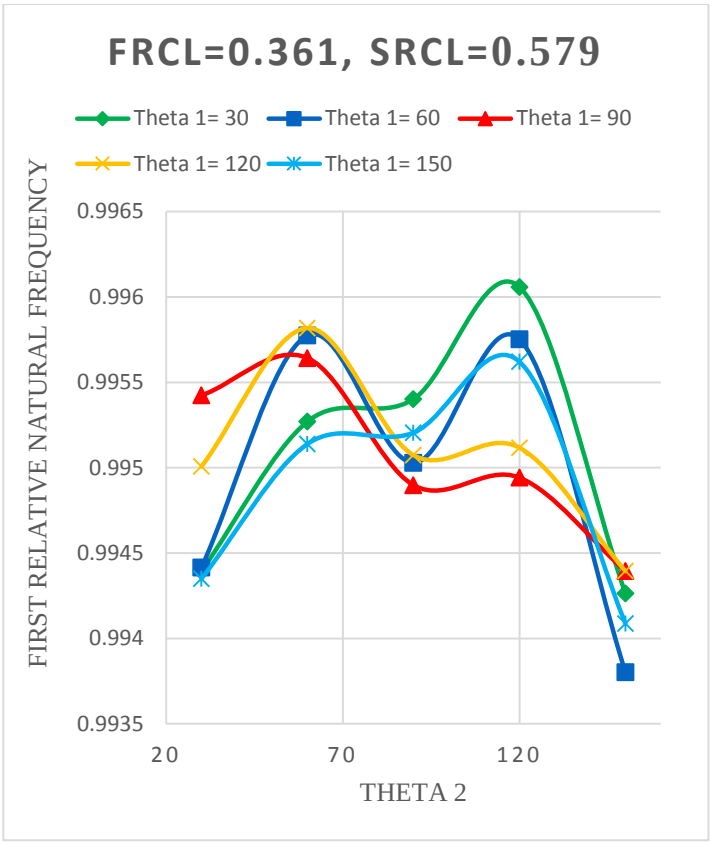


Fig.3.13. Variation of FRNF w.r.t. Theta 2

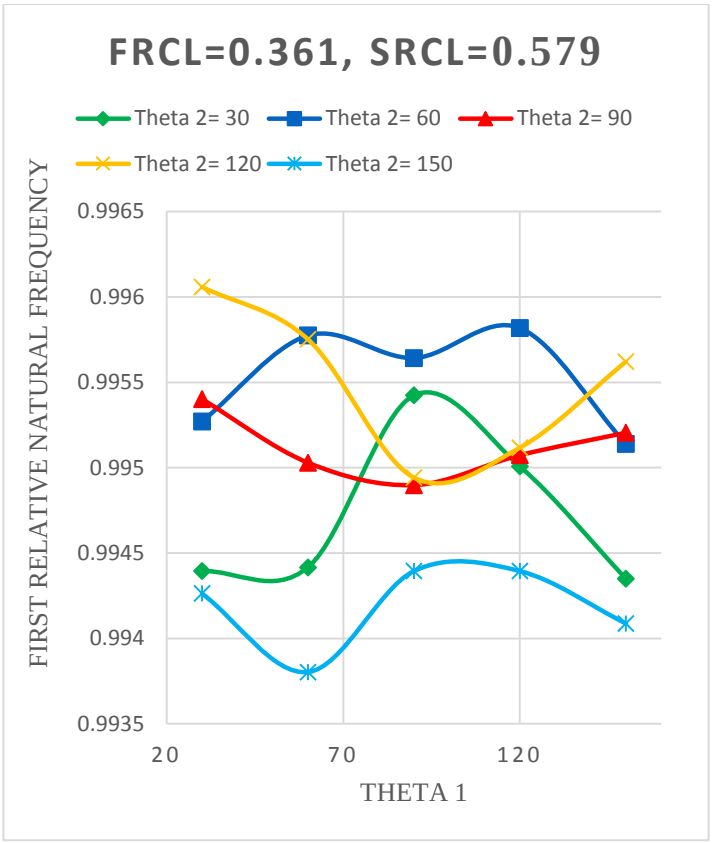


Fig.3.14. Variation of FRNF w.r.t. Theta 1

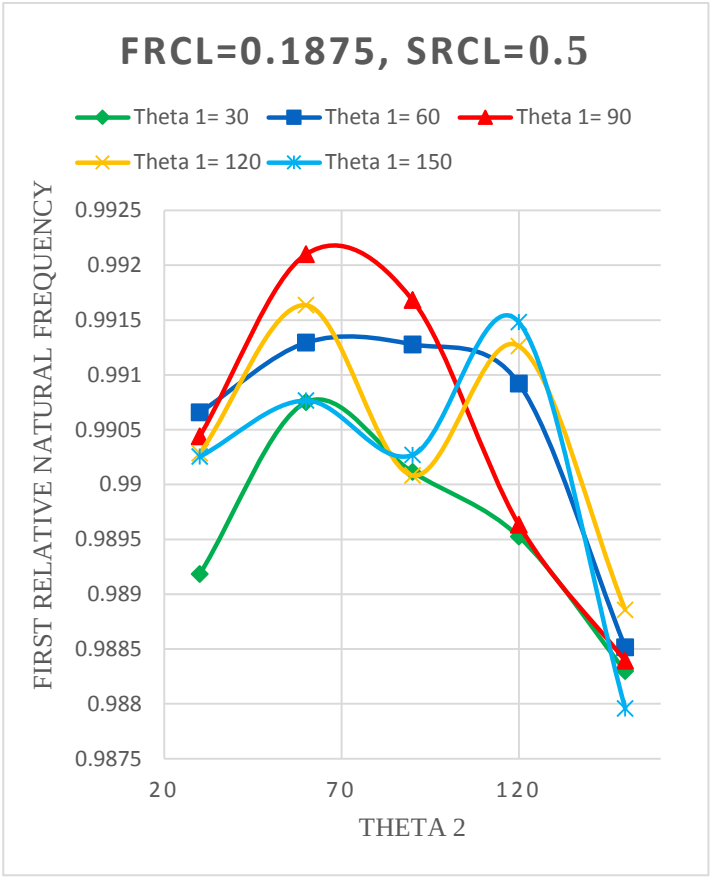


Fig.3.15. Variation of FRNF w.r.t. Theta 2

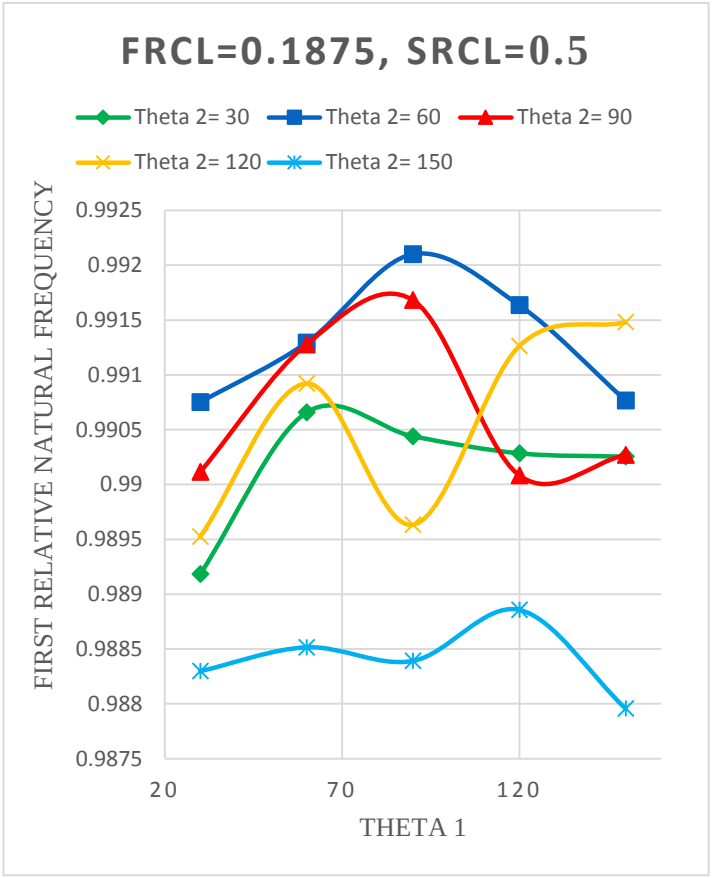


Fig.3.16. Variation of FRNF w.r.t. Theta 1

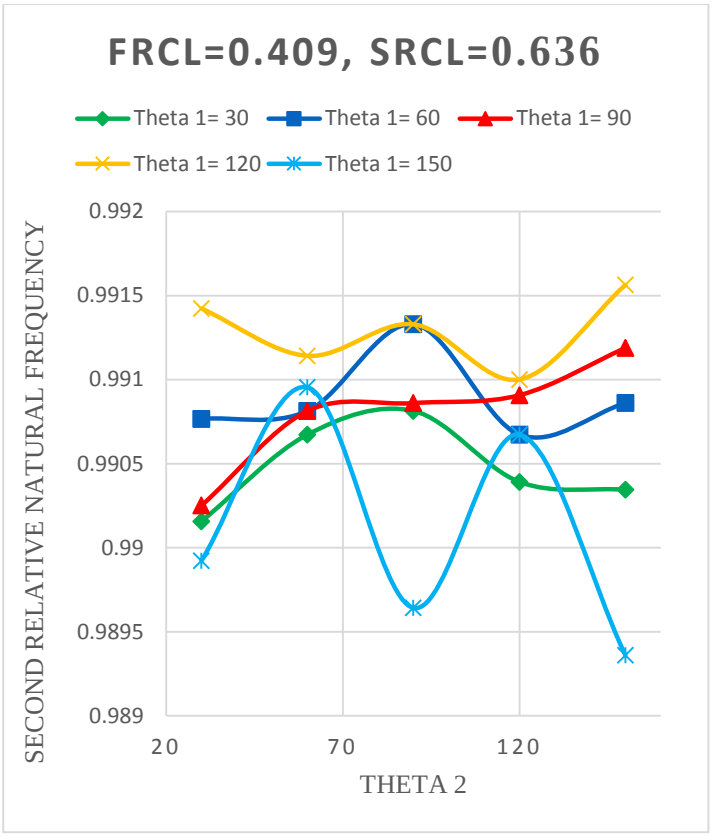


Fig.3.17. Variation of 2nd RNF w.r.t. Theta 2

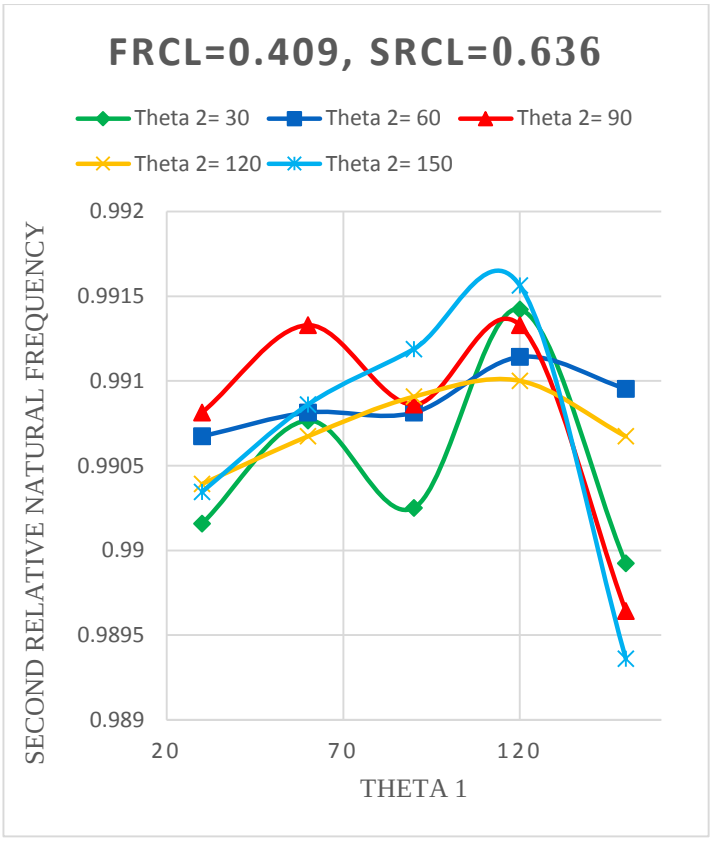


Fig.3.18. Variation of 2nd RNF w.r.t. Theta 1

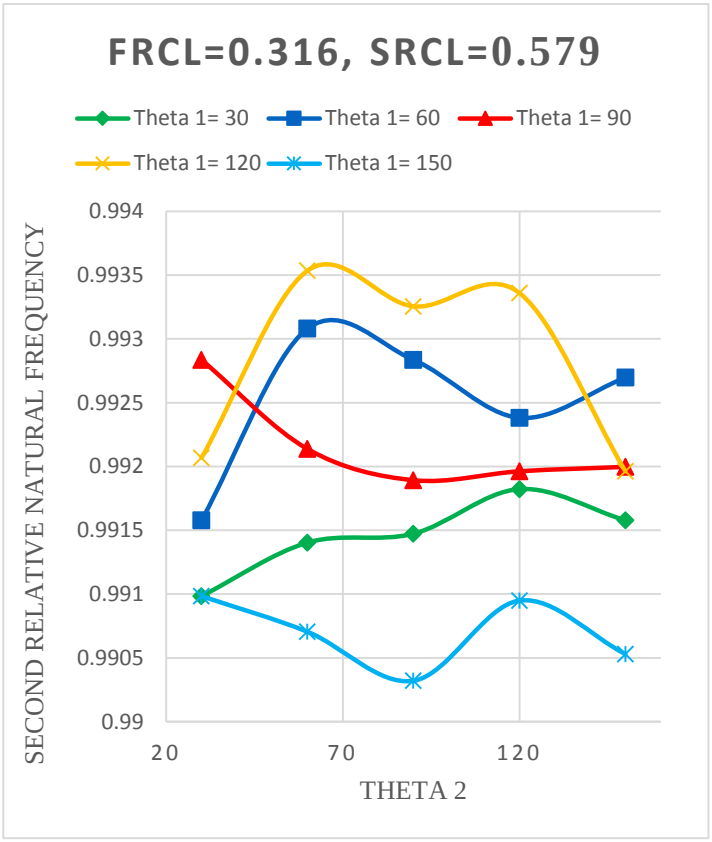


Fig.3.19. Variation of 2nd RNF w.r.t. Theta 2

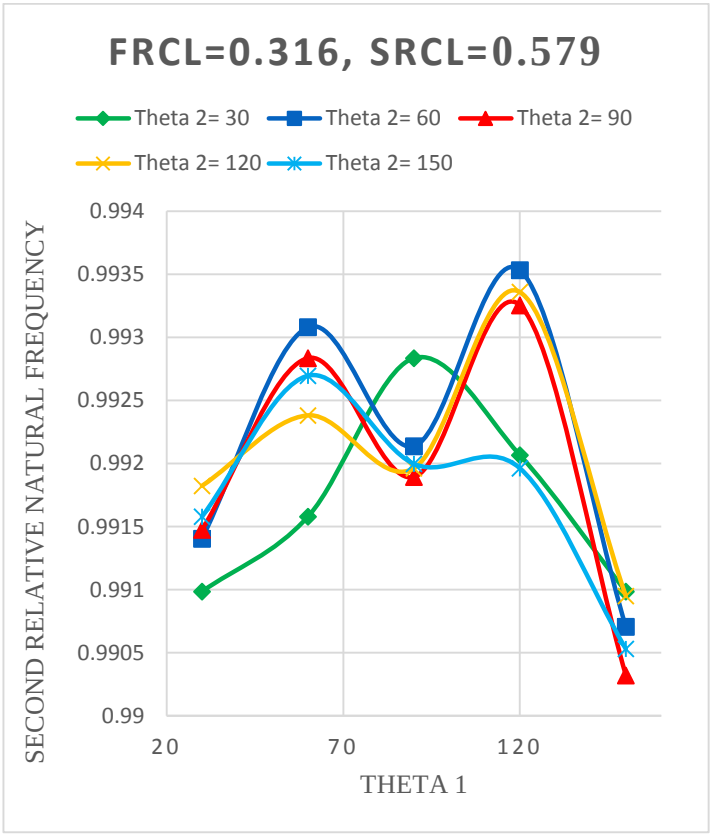


Fig.3.20. Variation of 2nd RNF w.r.t. Theta 1

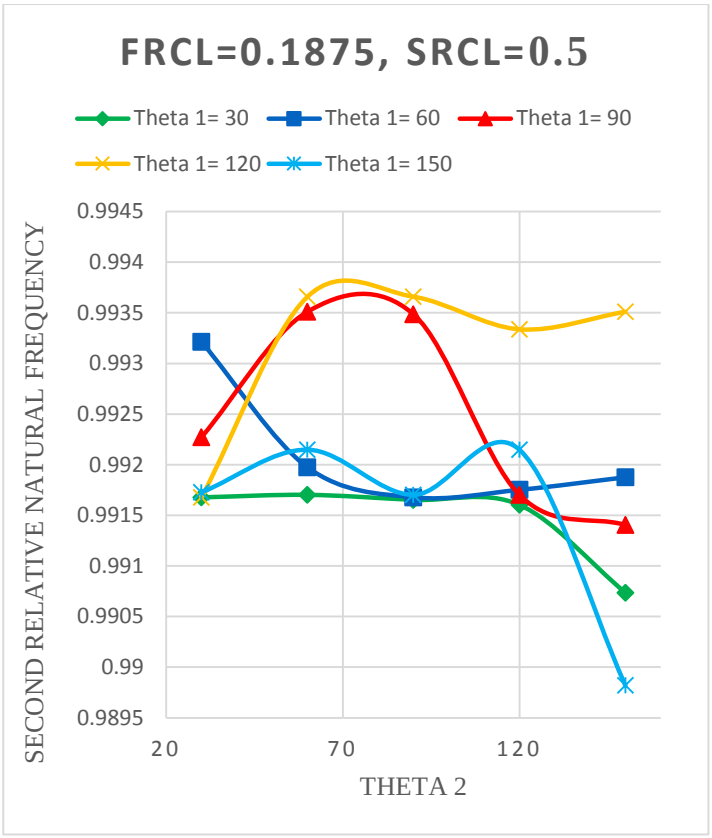


Fig.3.21. Variation of 2nd RNF w.r.t. Theta 2

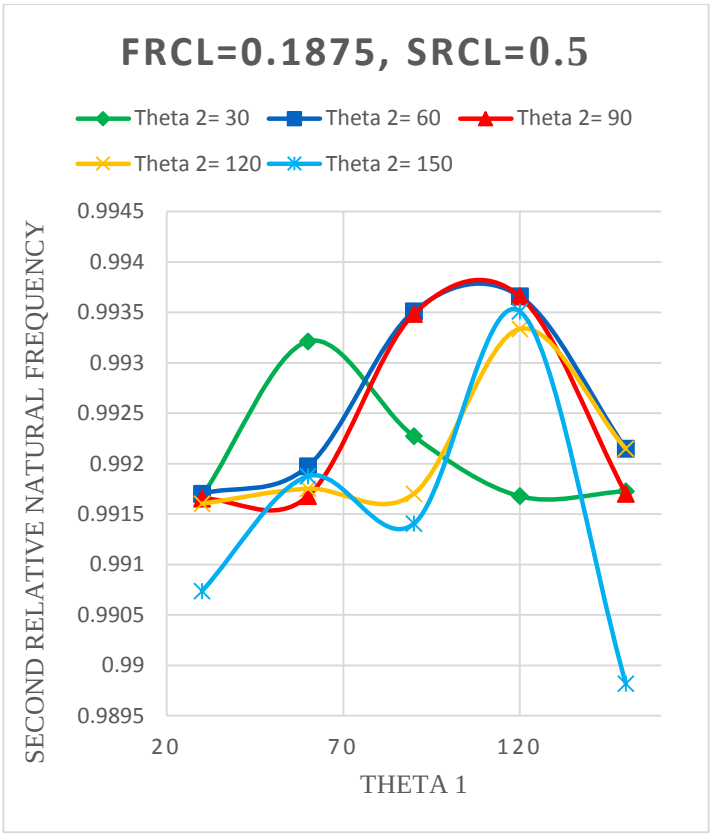


Fig.3.22. Variation of 2nd RNF w.r.t. Theta 1

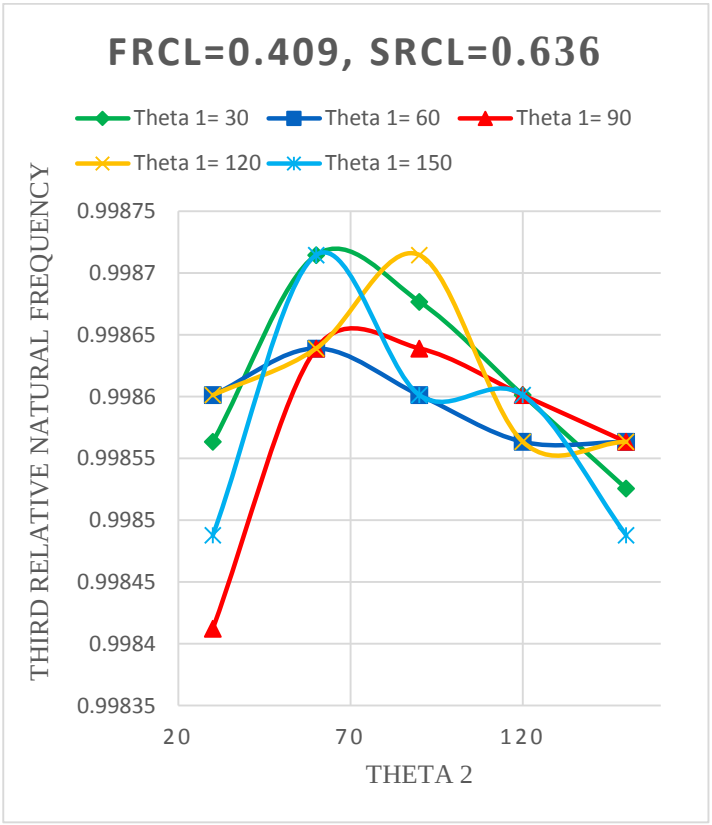


Fig.3.23. Variation of 3rd RNF w.r.t. Theta 2

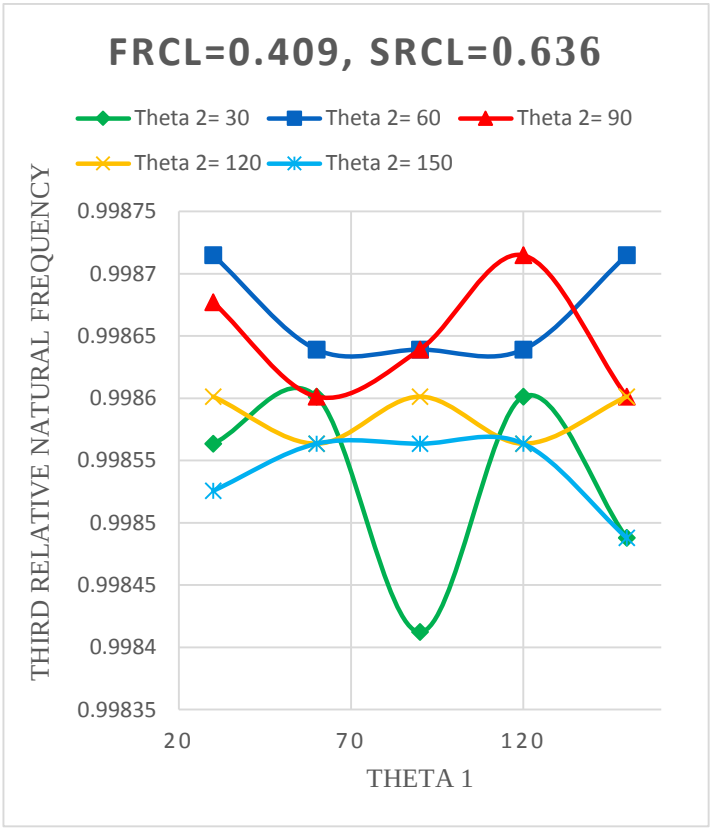


Fig.3.24. Variation of 3rd RNF w.r.t. Theta 1

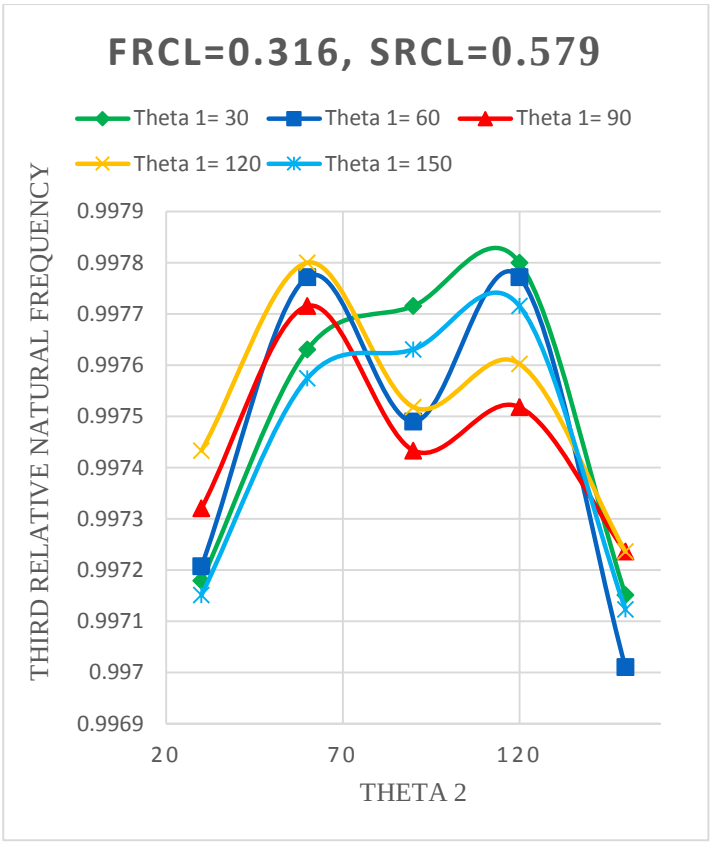


Fig.3.25. Variation of 3rd RNF w.r.t. Theta 2

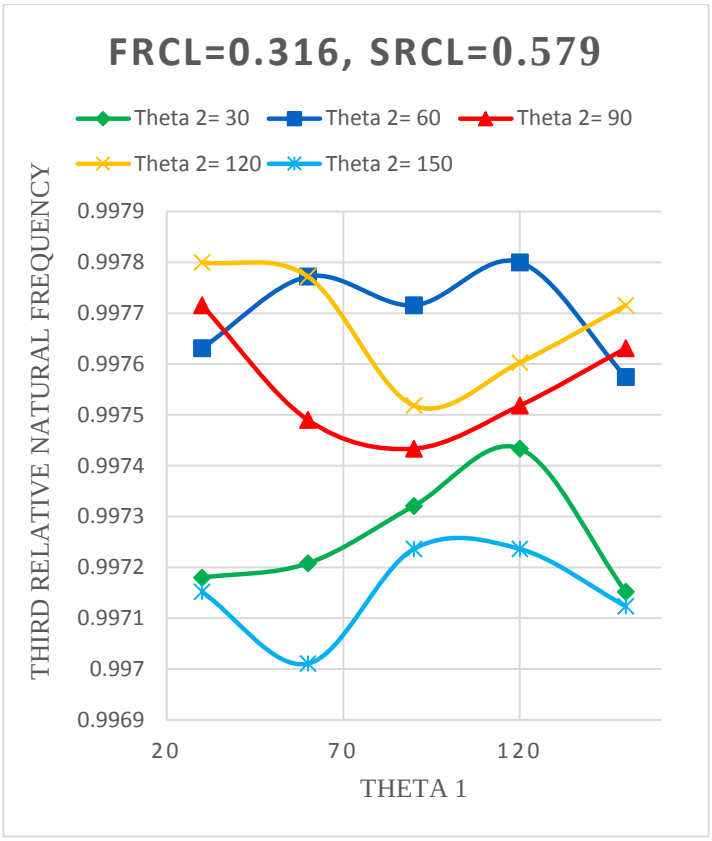


Fig.3.26. Variation of 3rd RNF w.r.t. Theta 1

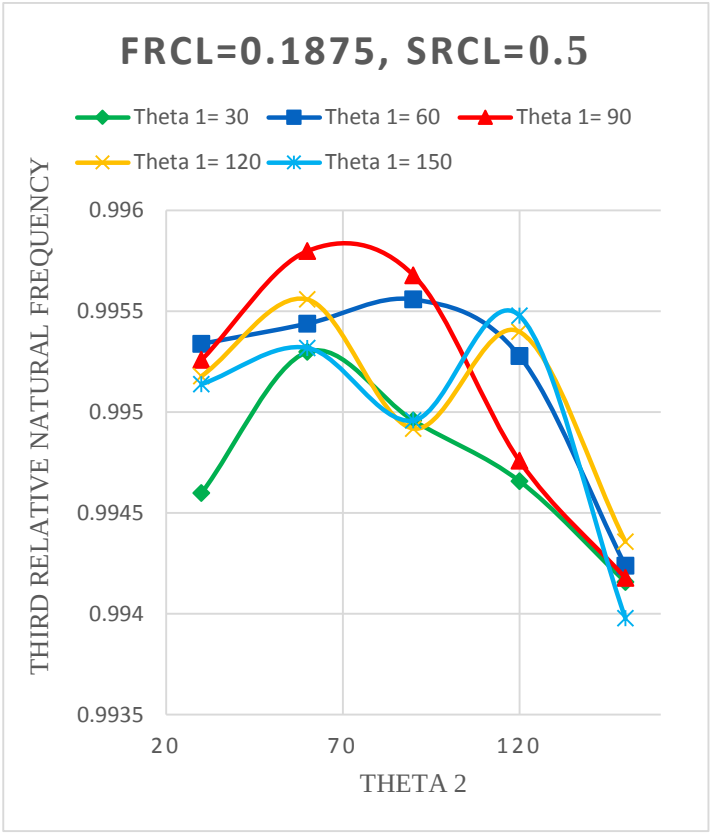


Fig.3.27. Variation of 3rd RNF w.r.t. Theta 2

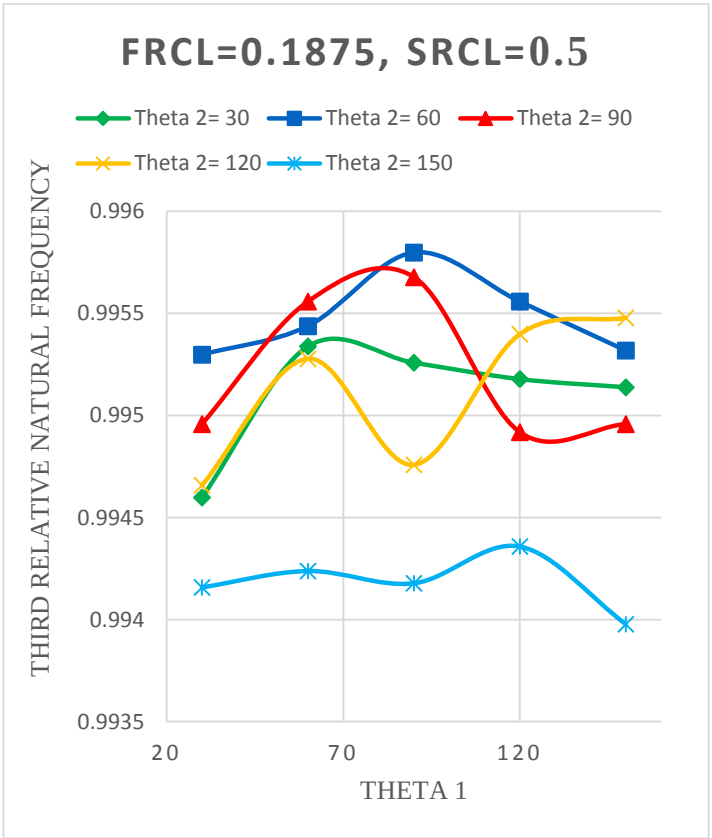


Fig.3.28. Variation of 3rd RNF w.r.t. Theta 1

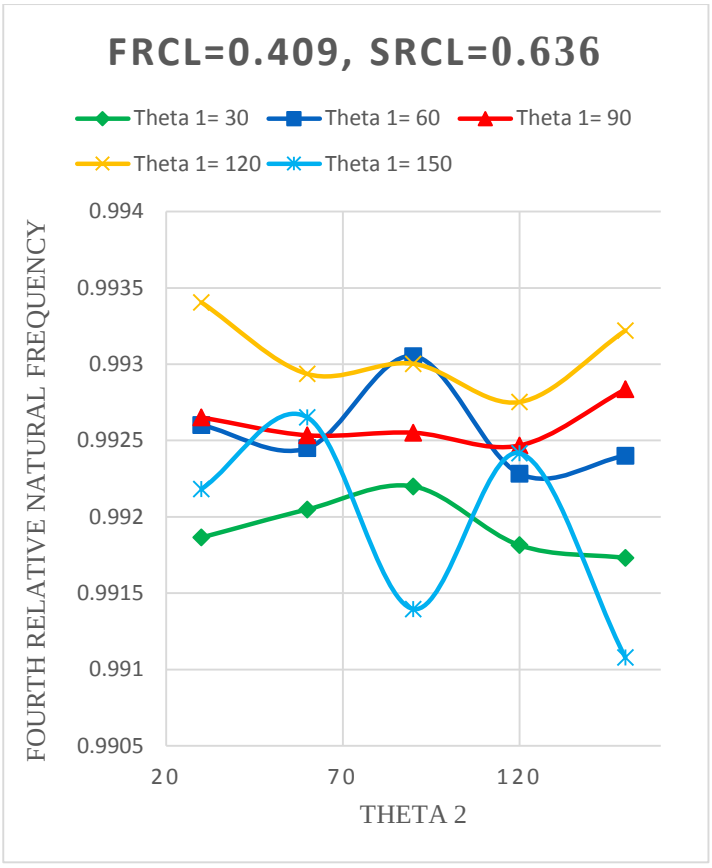


Fig.3.29. Variation of 4th RNF w.r.t. Theta 2

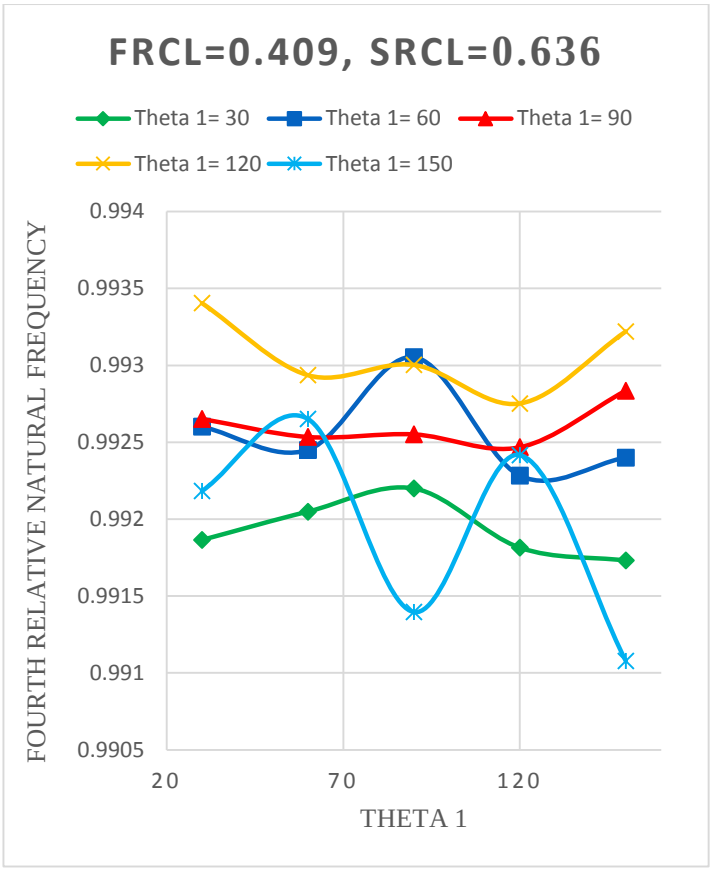


Fig.3.30. Variation of 4th RNF w.r.t. Theta 1

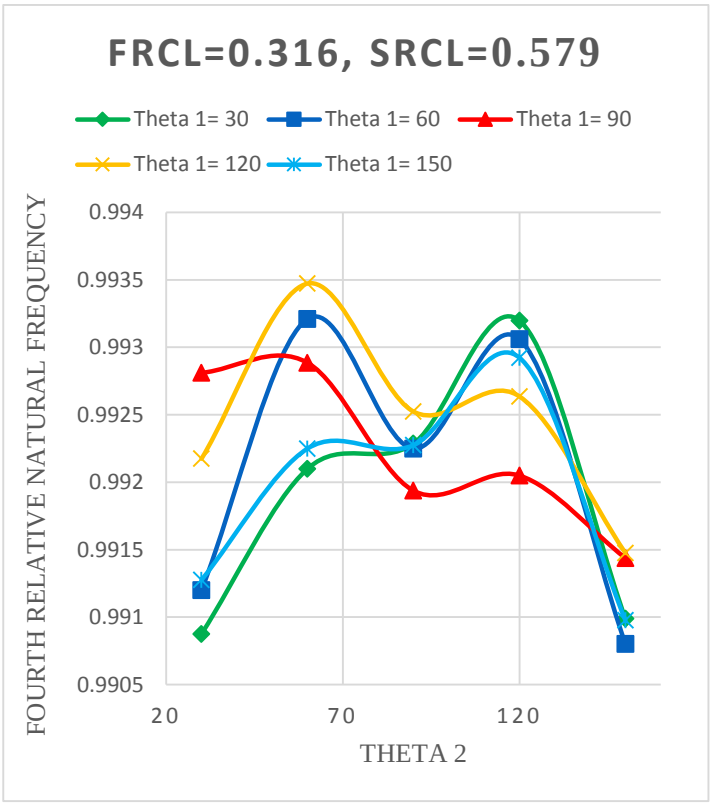


Fig.3.31. Variation of 4th RNF w.r.t. Theta 2

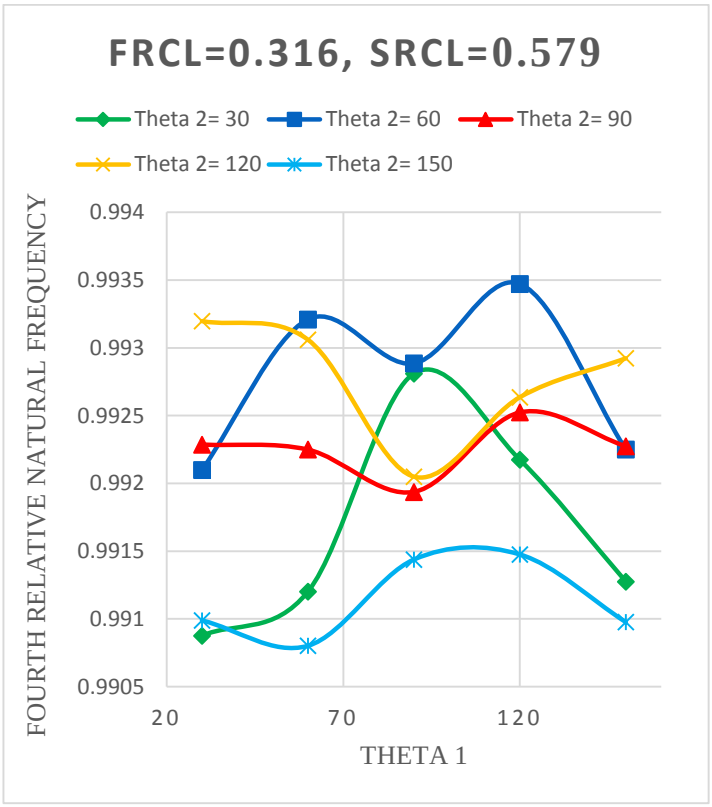


Fig.3.32. Variation of 4th RNF w.r.t. Theta 1

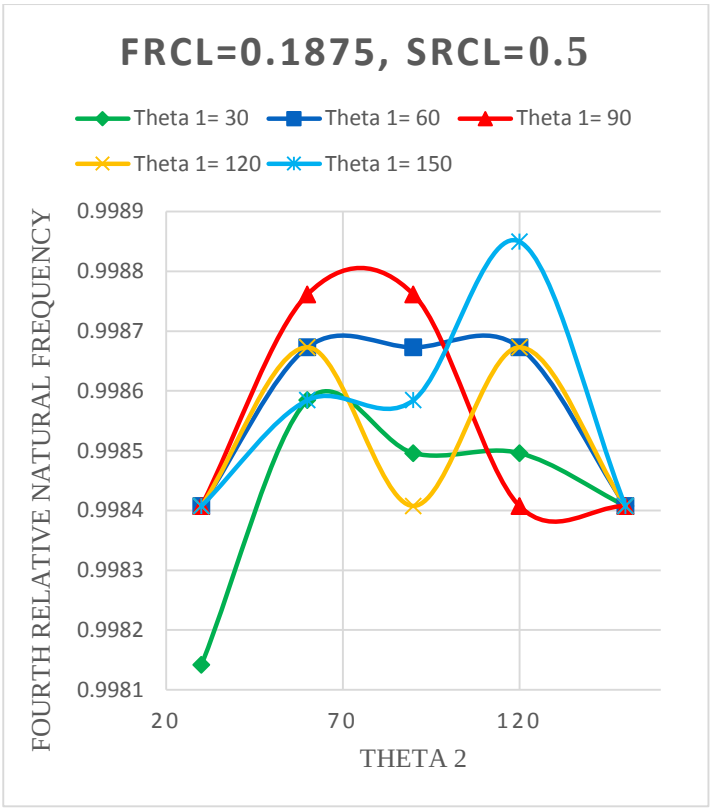


Fig.3.33. Variation of 4th RNF w.r.t. Theta 2

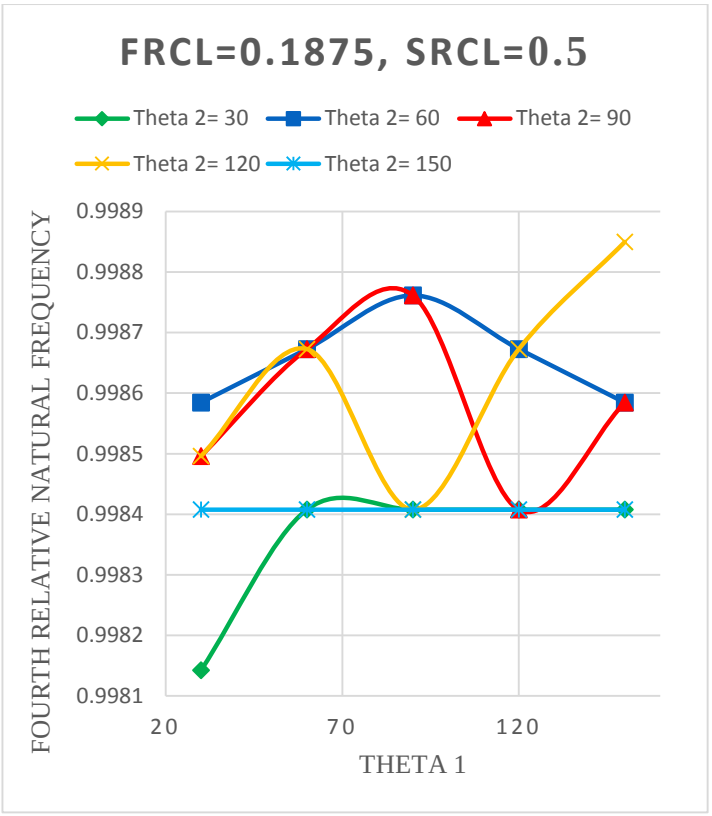


Fig.3.34. Variation of 4th RNF w.r.t. Theta 1

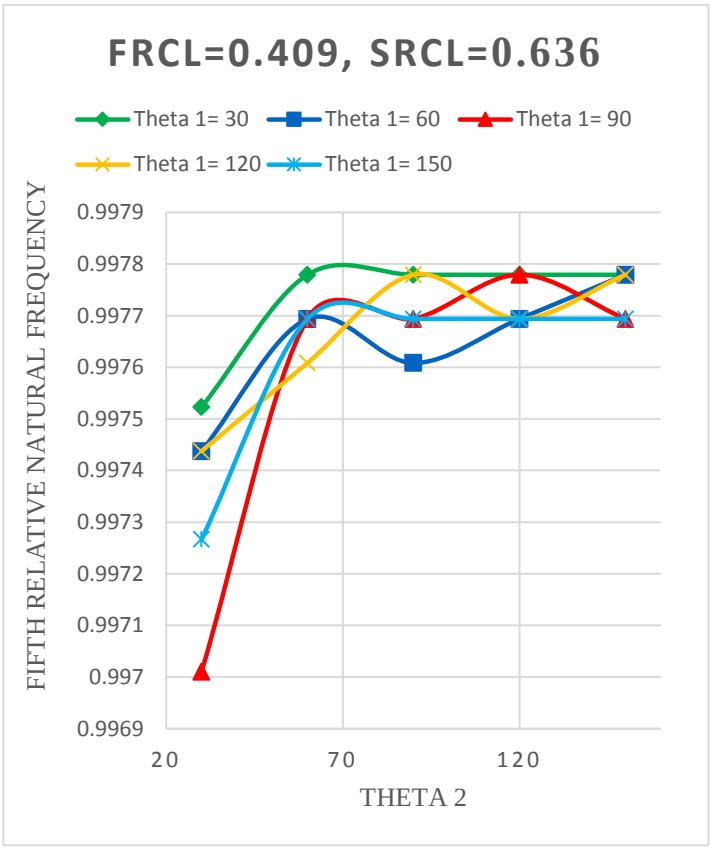


Fig.3.35. Variation of 5th RNF w.r.t. Theta 2

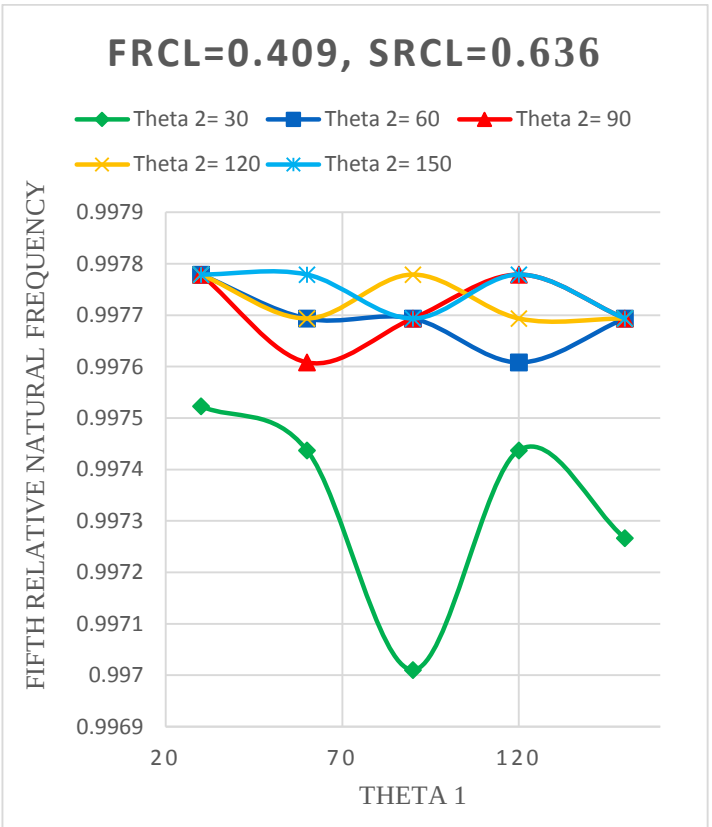


Fig.3.36. Variation of 5th RNF w.r.t. Theta 1

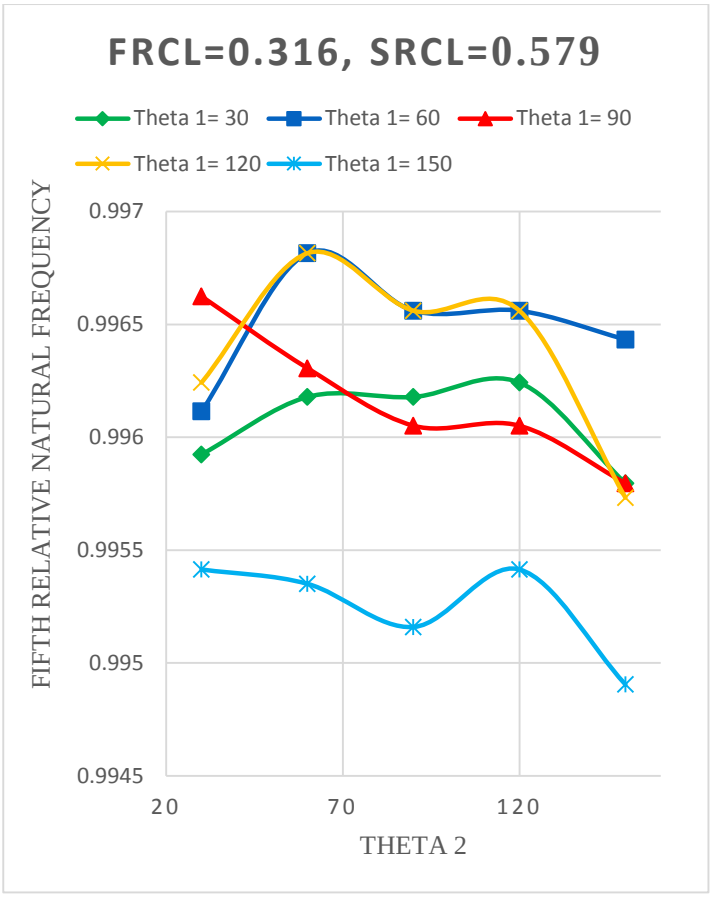


Fig.3.37. Variation of 5th RNF w.r.t. Theta 2

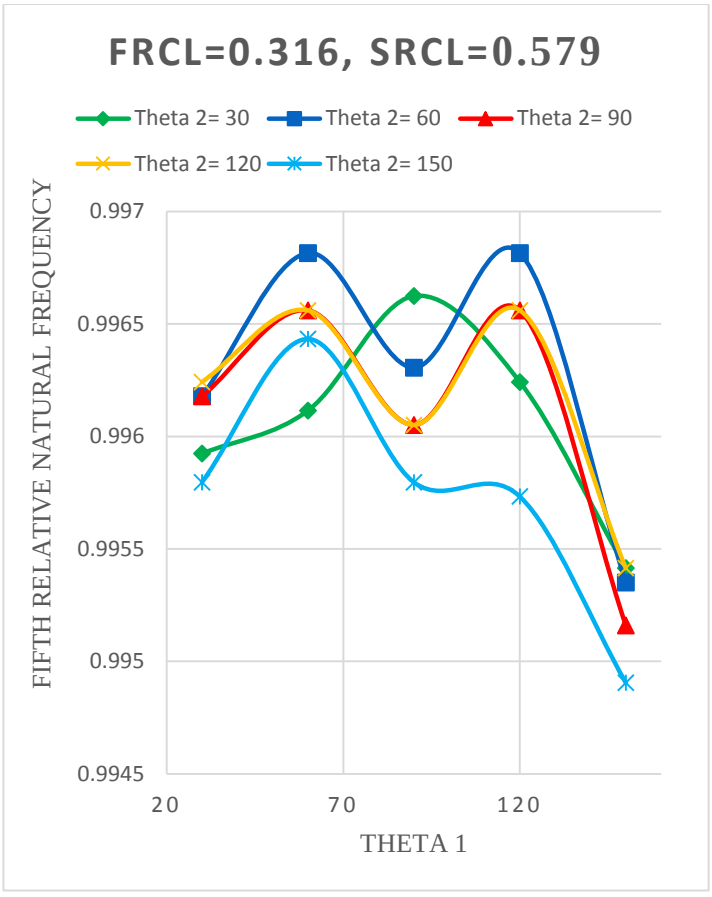


Fig.3.38. Variation of 5th RNF w.r.t. Theta 1

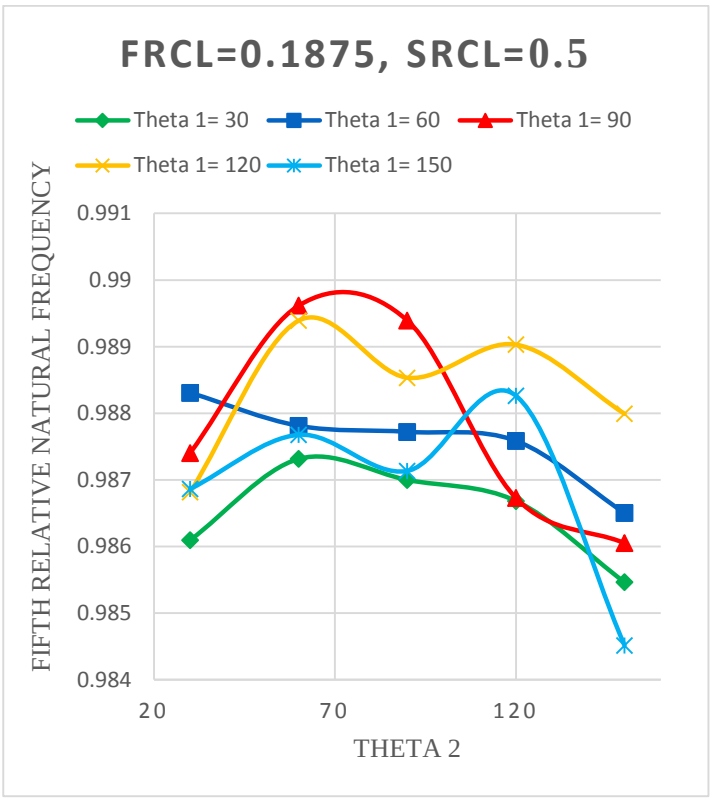


Fig.3.39. Variation of 5th RNF w.r.t. Theta 2

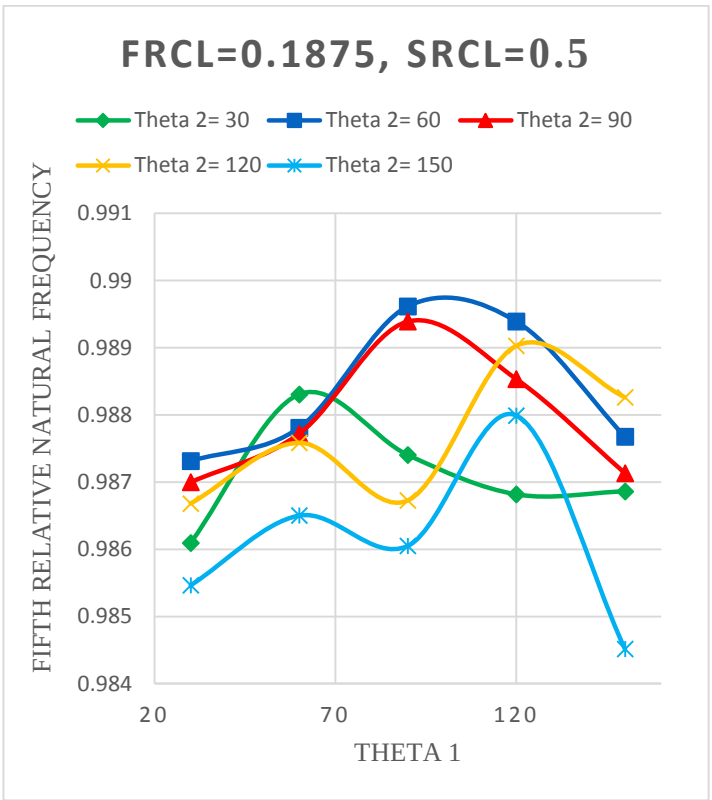


Fig.3.40. Variation of 5th RNF w.r.t. Theta 1

From the above plots, it is possible to extract variation in relative natural frequency with respect to different relative crack lengths. These plots would mean extracting one plot at a time from each relative crack length and plotting them in a single curve. Plots showing the variation of relative natural frequency with relative crack location have been shown below.

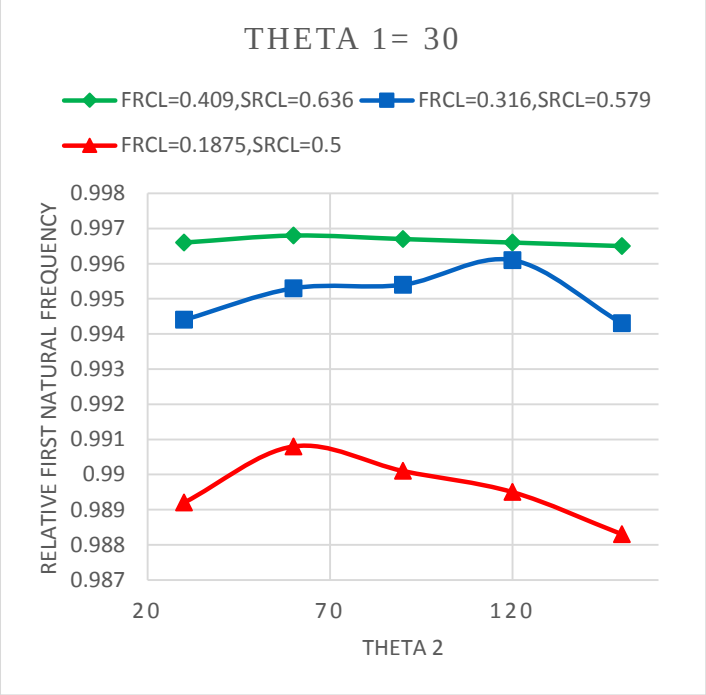


Fig.3.41. Variation w.r.t. relative crack length

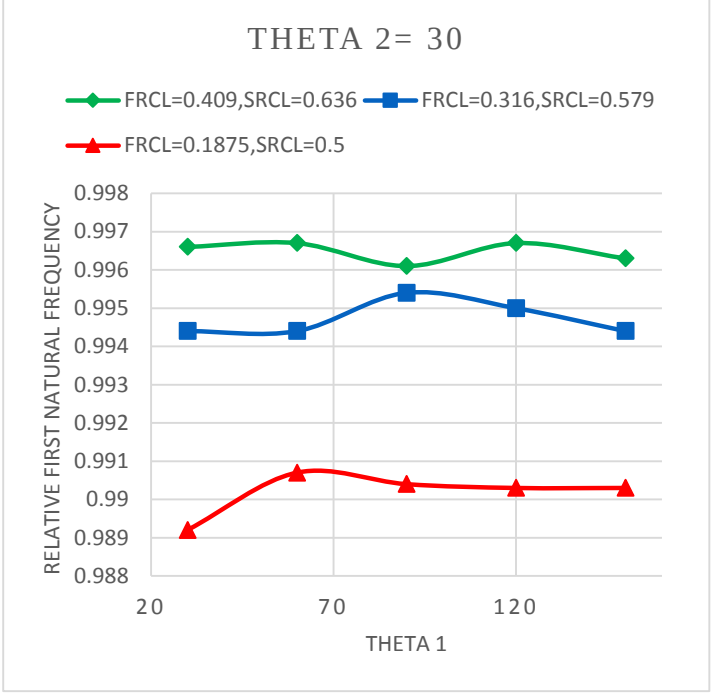


Fig.3.42. Variation w.r.t. relative crack length

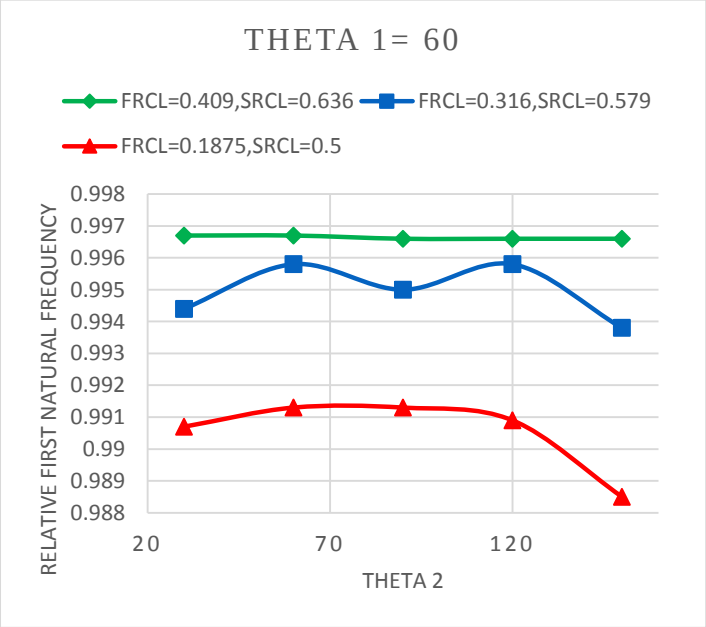


Fig.3.43. Variation w.r.t. relative crack length

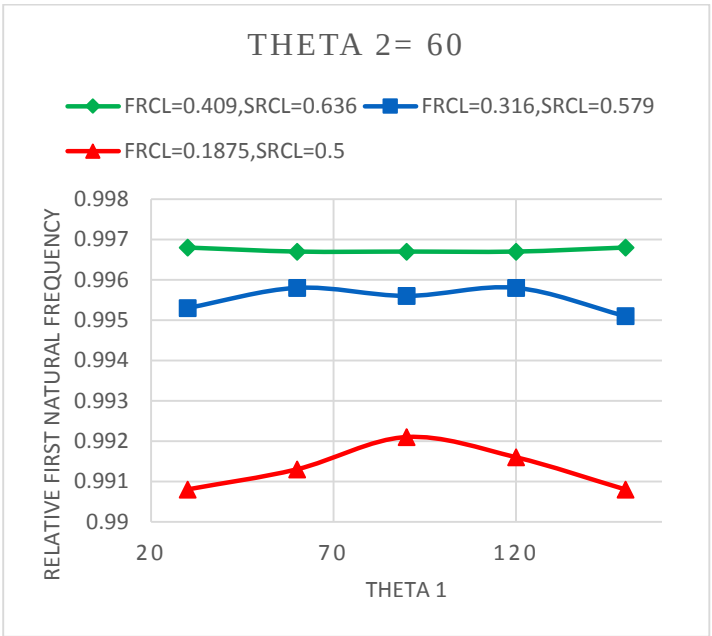


Fig.3.44. Variation w.r.t. relative crack length

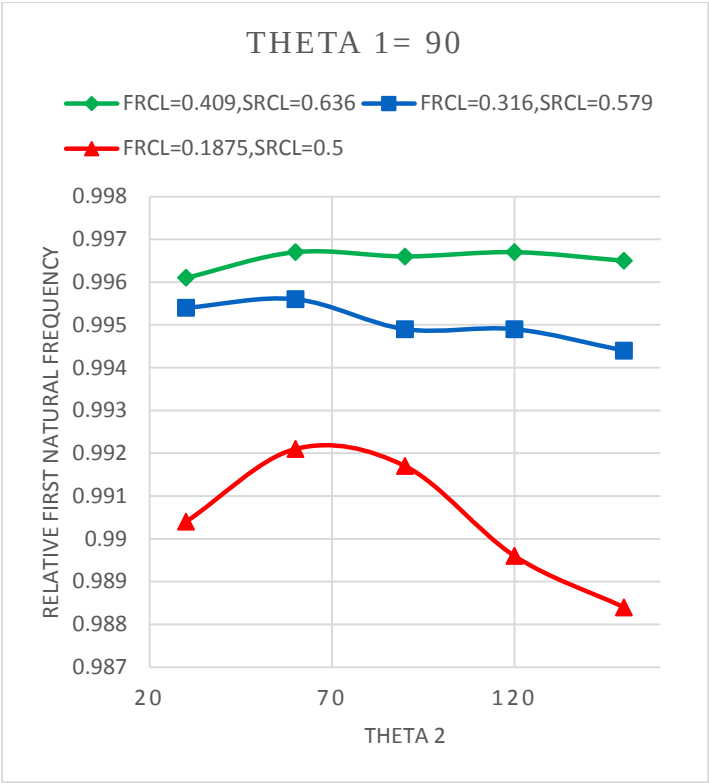


Fig.3.45. Variation w.r.t. relative crack length

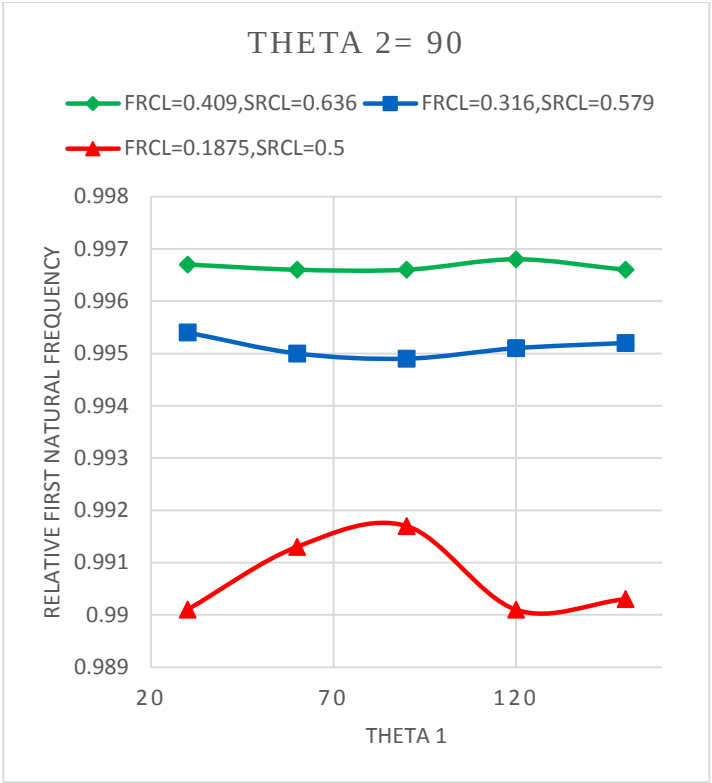


Fig.3.46. Variation w.r.t. relative crack length

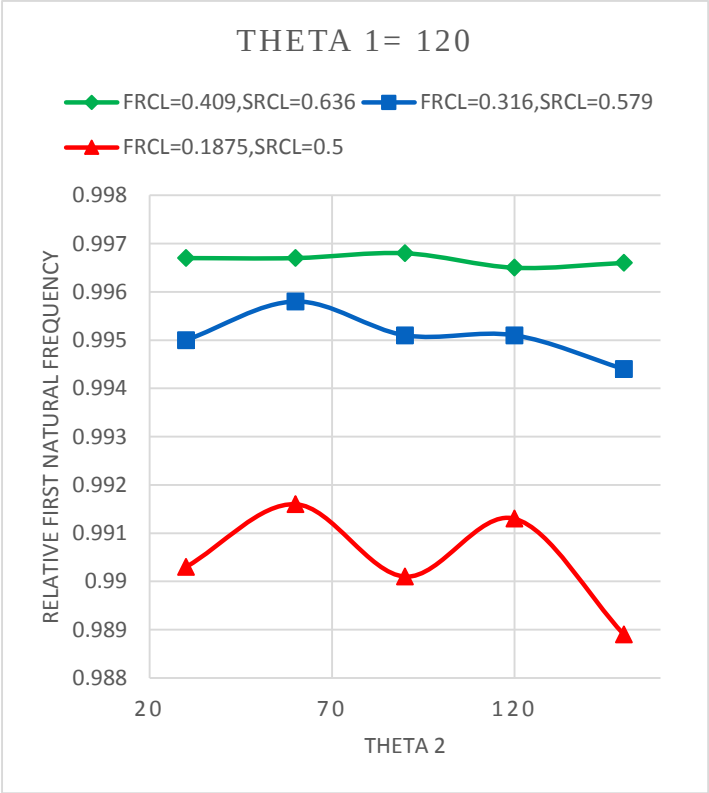


Fig.3.47. Variation w.r.t. relative crack length

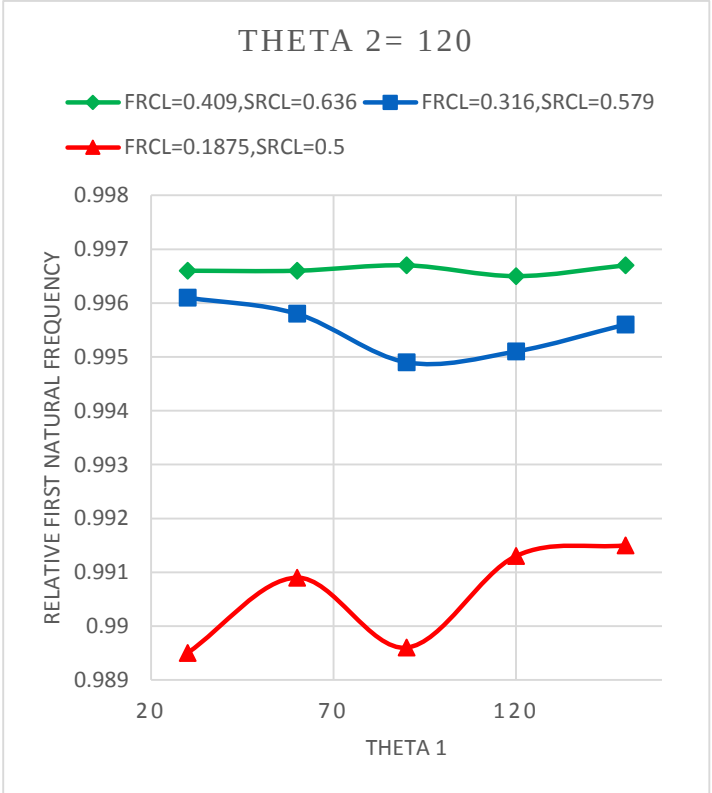


Fig.3.48. Variation w.r.t. relative crack length

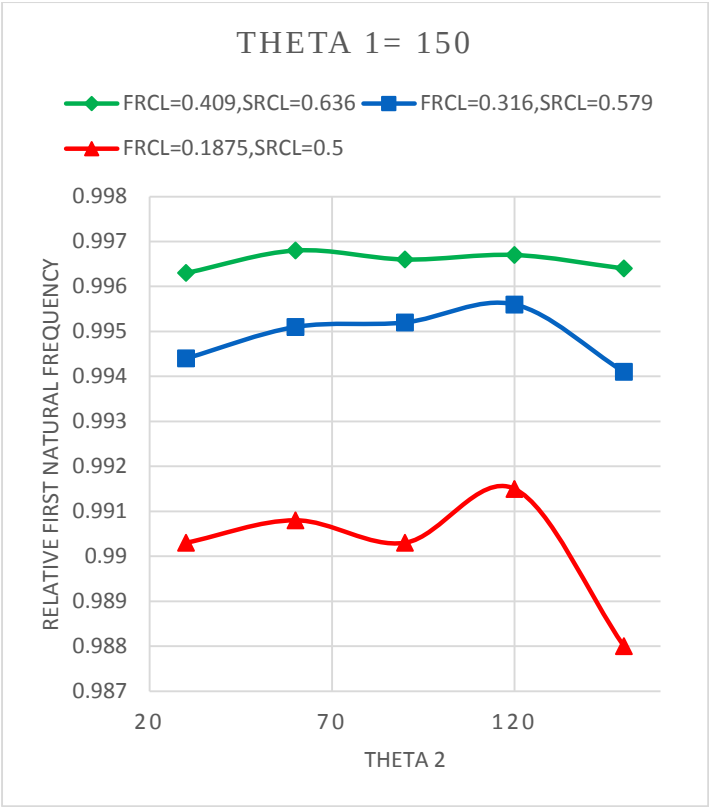


Fig.3.49. Variation w.r.t. relative crack length

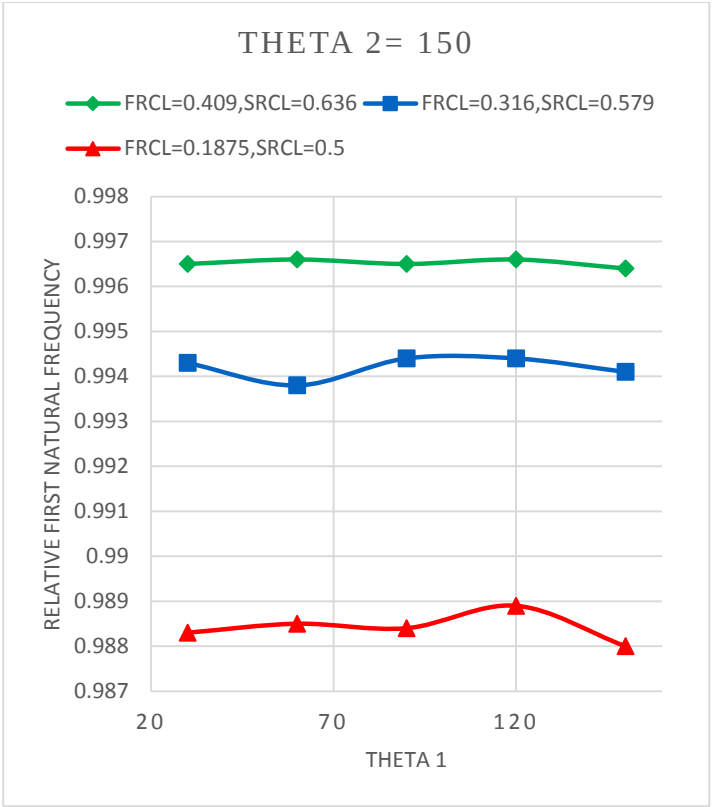


Fig.3.50. Variation w.r.t. relative crack length

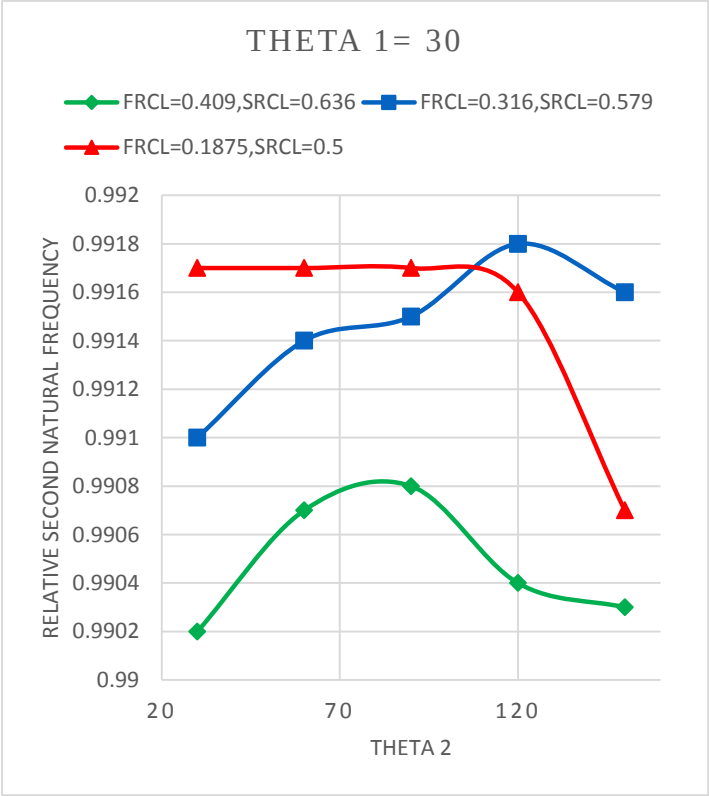


Fig.3.51. Variation w.r.t. relative crack length

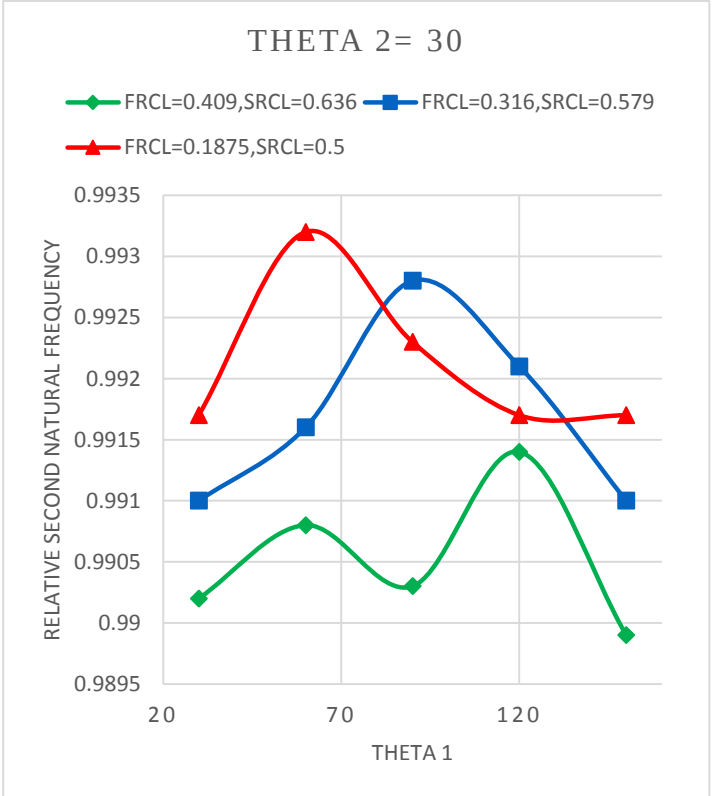


Fig.3.52. Variation w.r.t. relative crack length

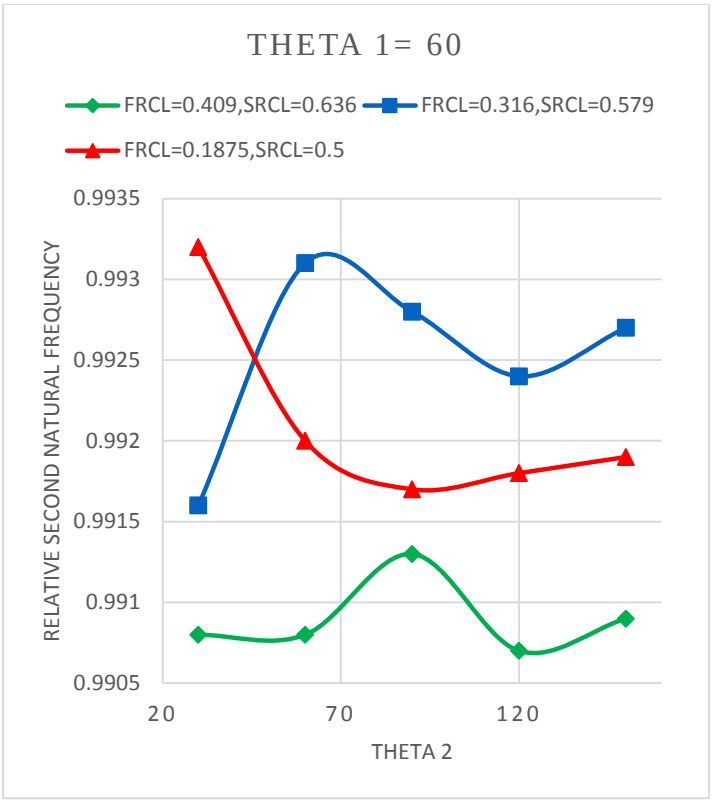


Fig.3.53. Variation w.r.t. relative crack length

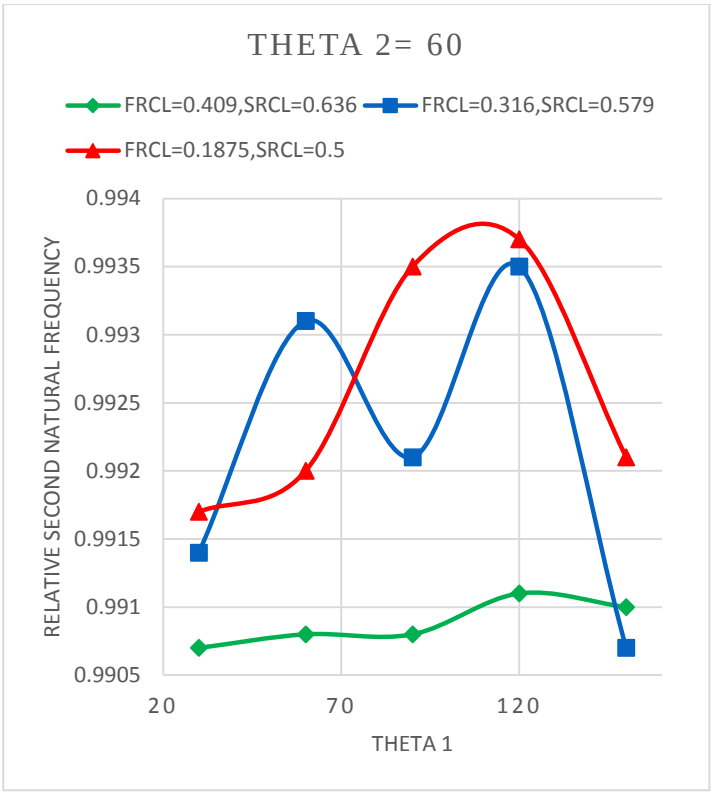


Fig.3.54. Variation w.r.t. relative crack length

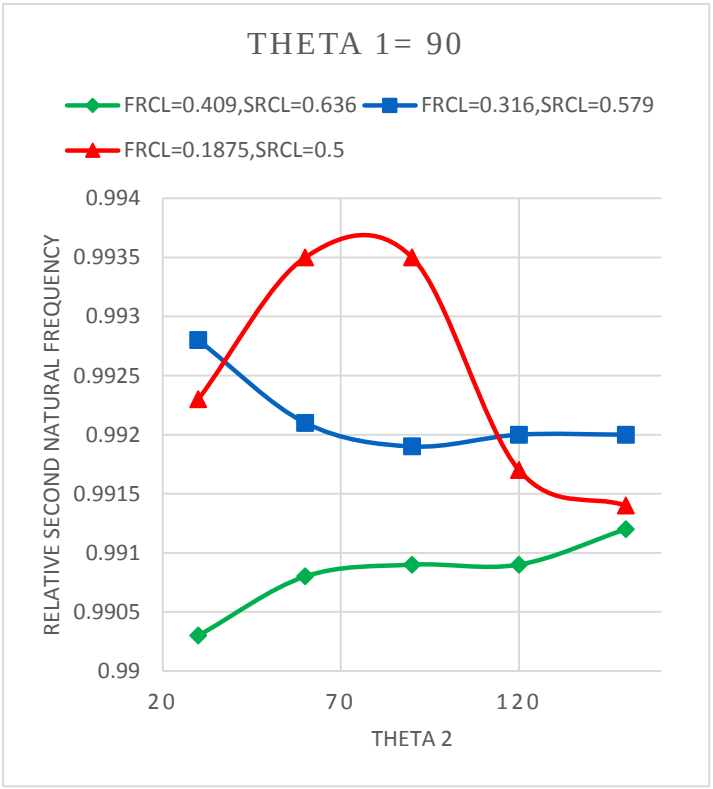


Fig.3.55. Variation w.r.t. relative crack length

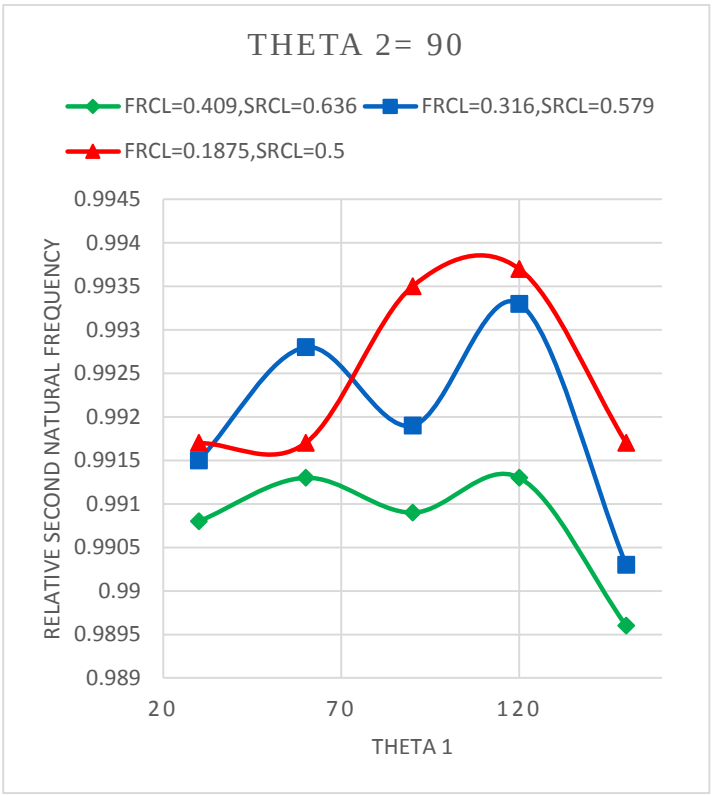


Fig.3.56. Variation w.r.t. relative crack length

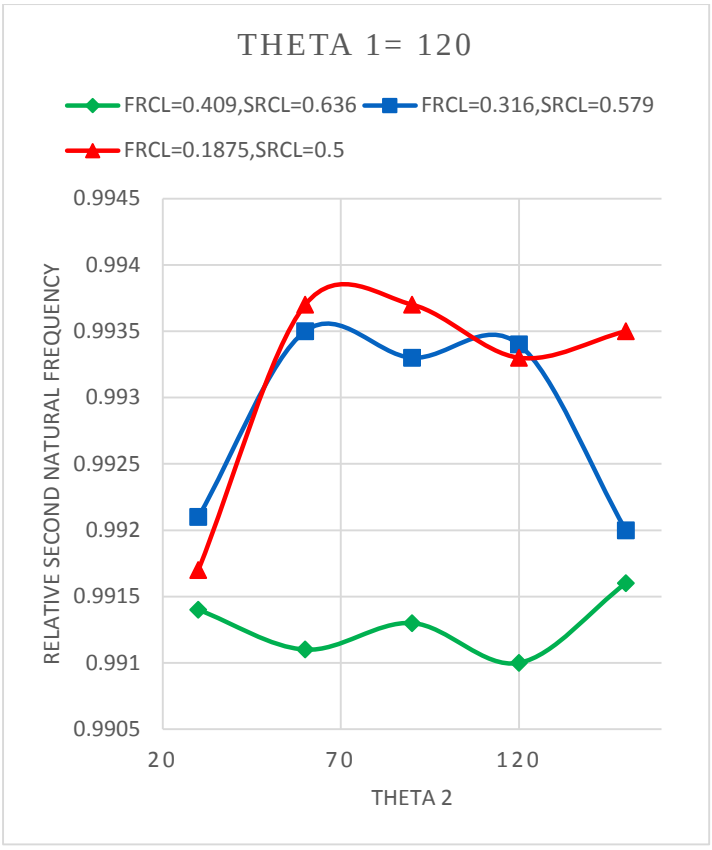


Fig.3.57. Variation w.r.t. relative crack length

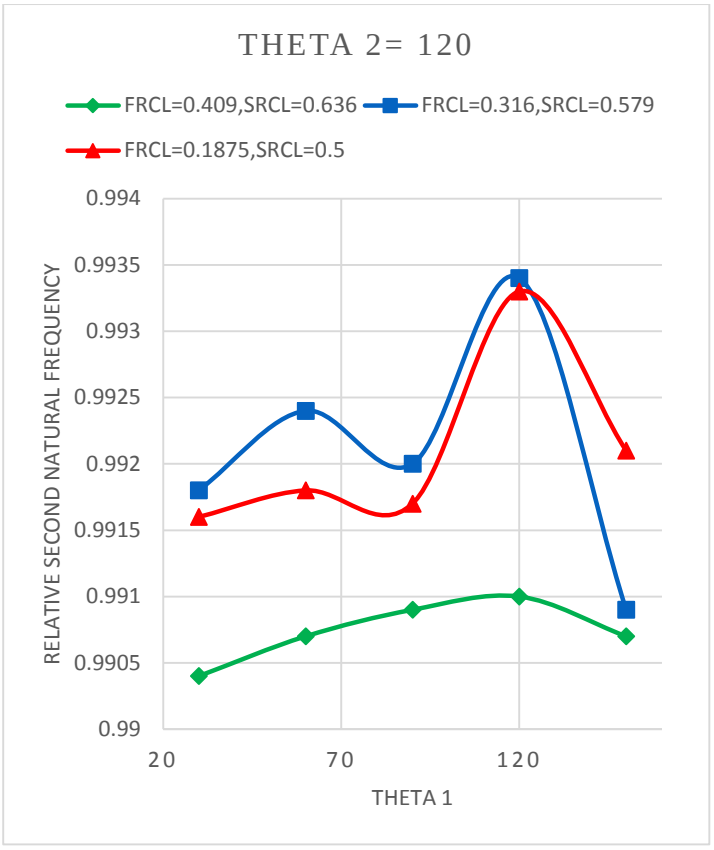


Fig.3.58. Variation w.r.t. relative crack length

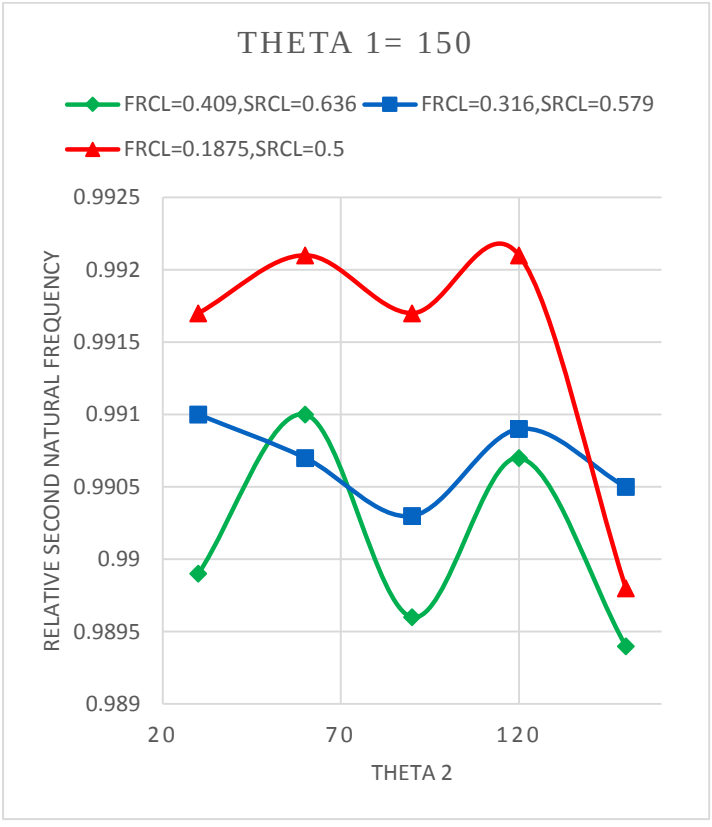


Fig.3.59. Variation w.r.t. relative crack length

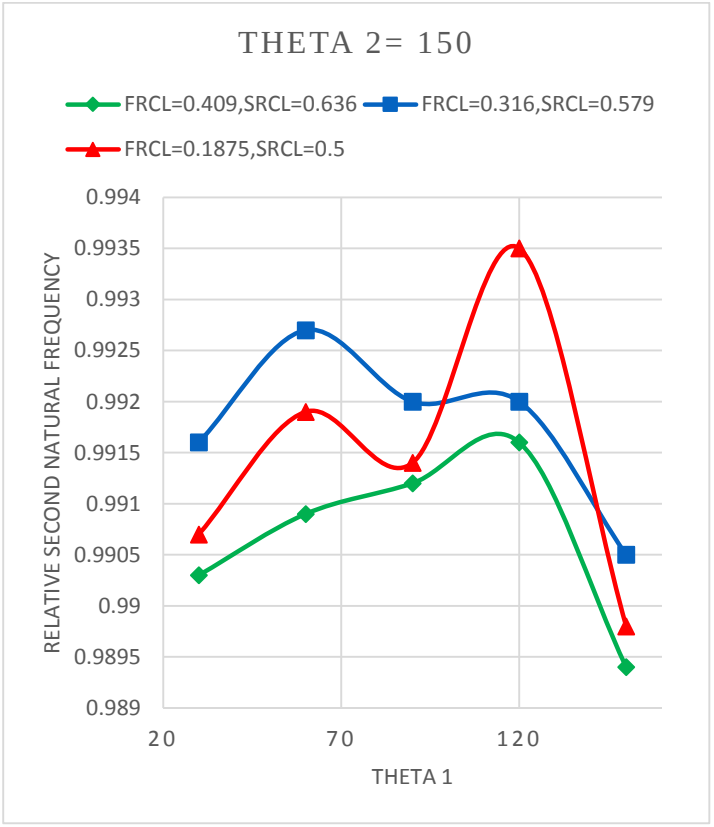


Fig.3.60. Variation w.r.t. relative crack length

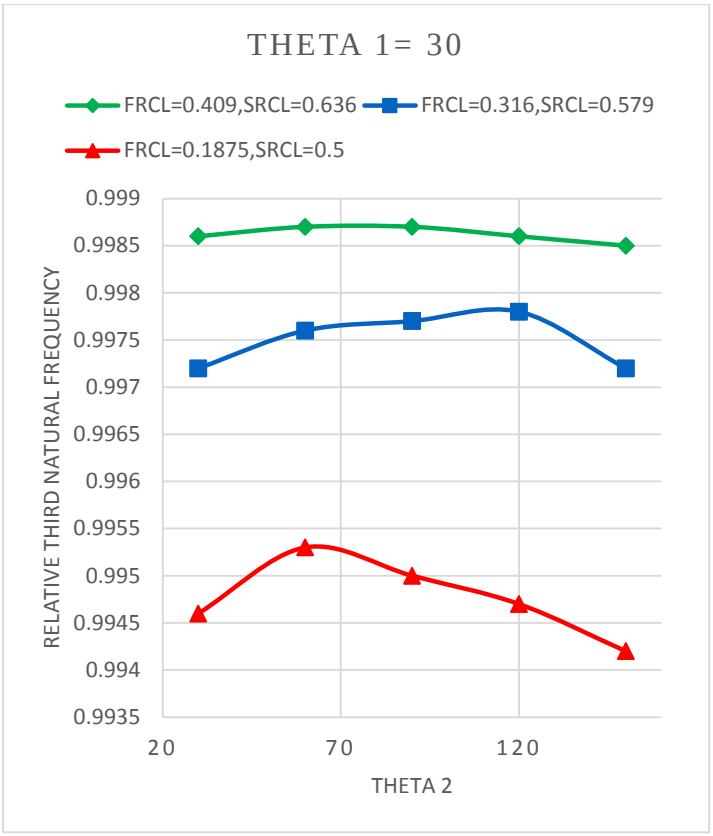


Fig.3.61. Variation w.r.t. relative crack length

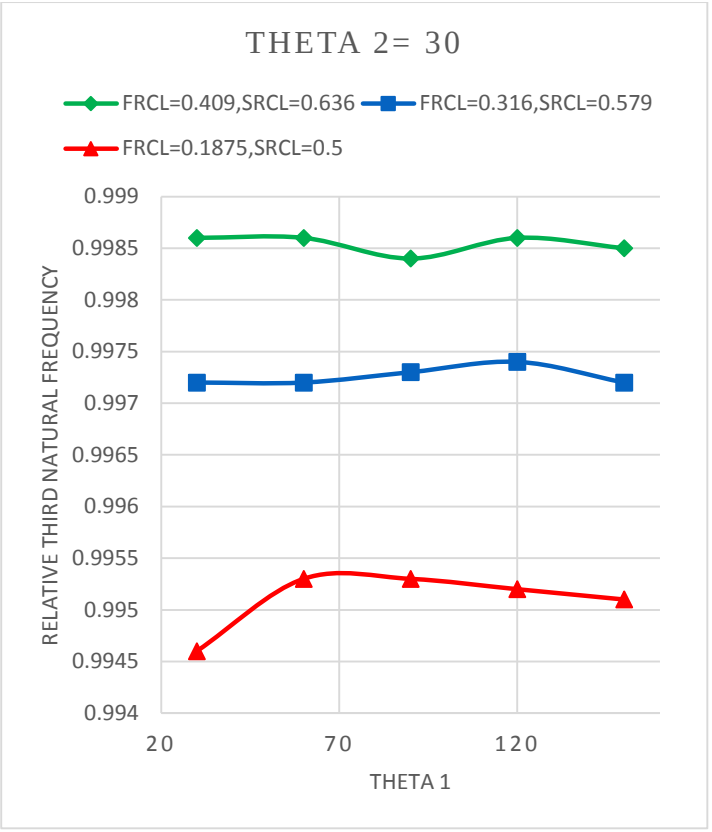


Fig.3.62. Variation w.r.t. relative crack length

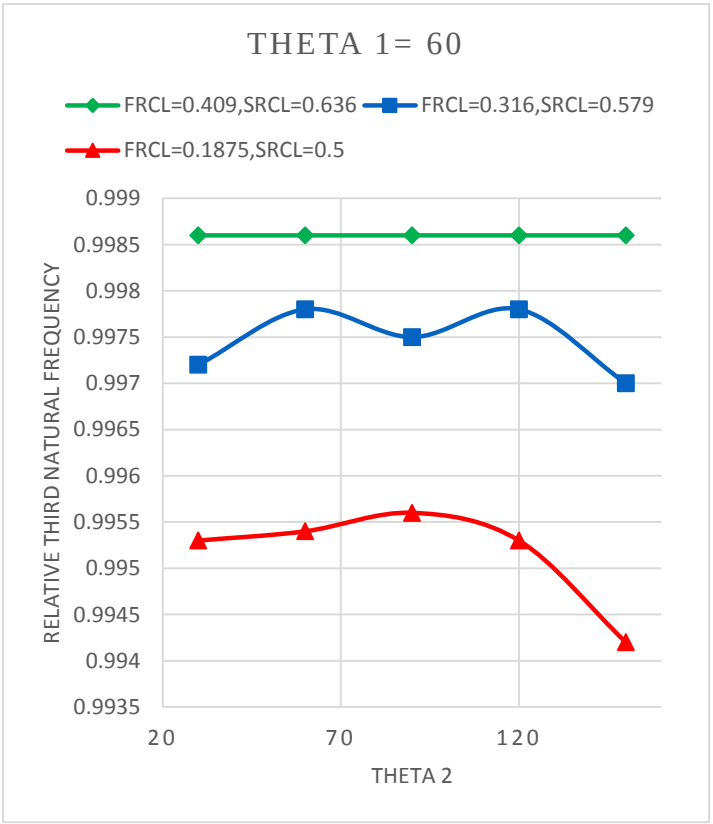


Fig.3.63. Variation w.r.t. relative crack length

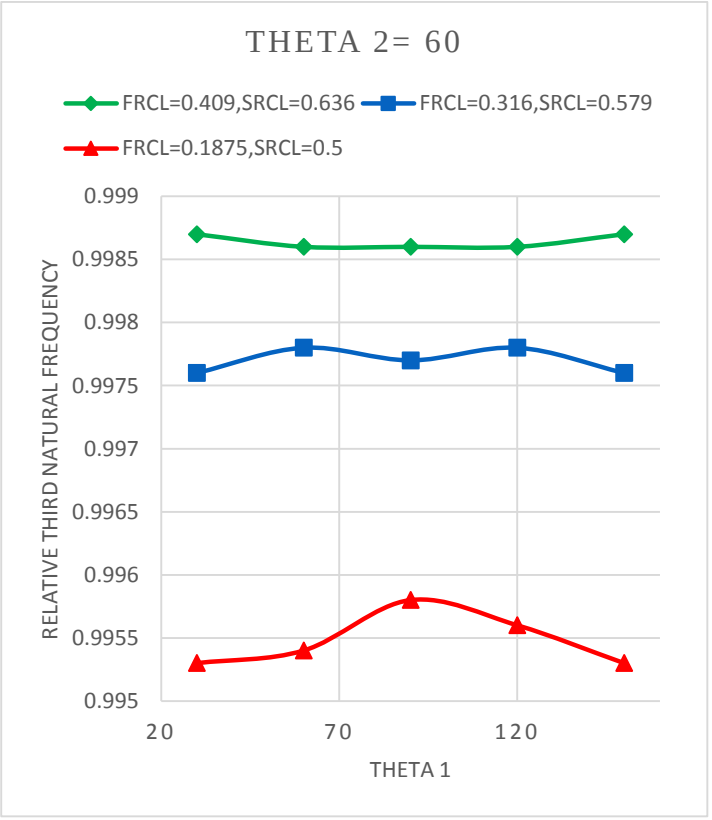


Fig.3.64. Variation w.r.t. relative crack length

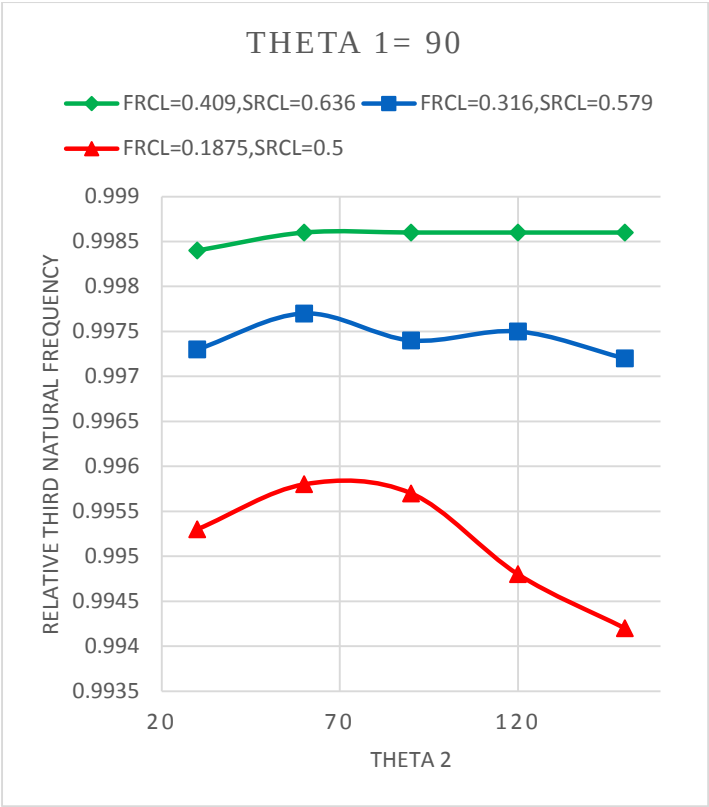


Fig.3.65. Variation w.r.t. relative crack length

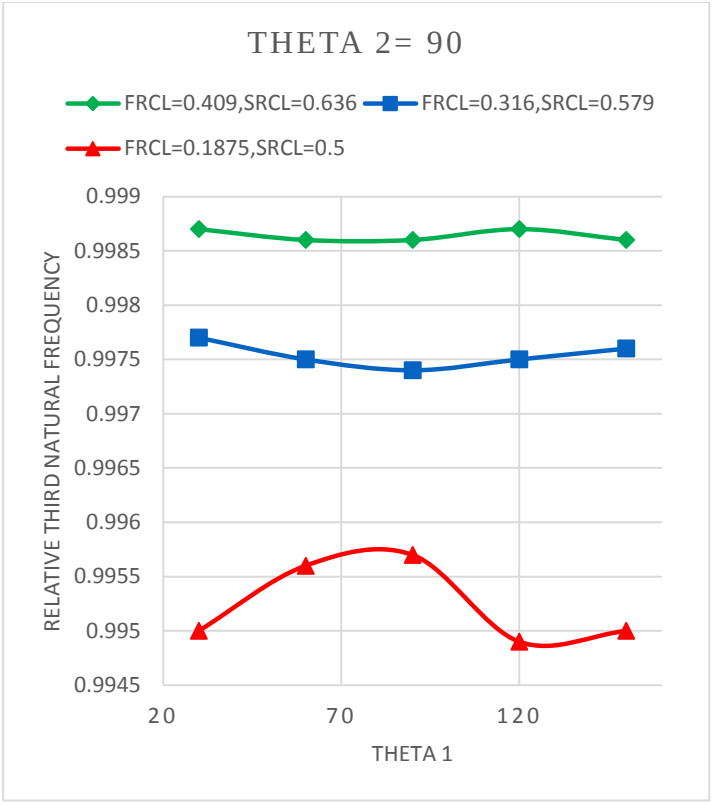


Fig.3.66. Variation w.r.t. relative crack length

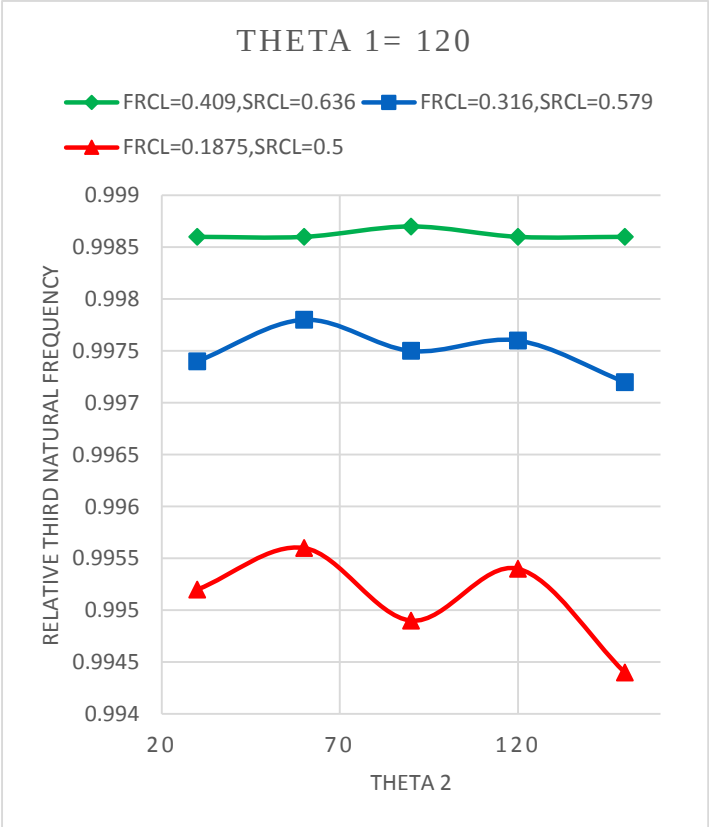


Fig.3.67. Variation w.r.t. relative crack length

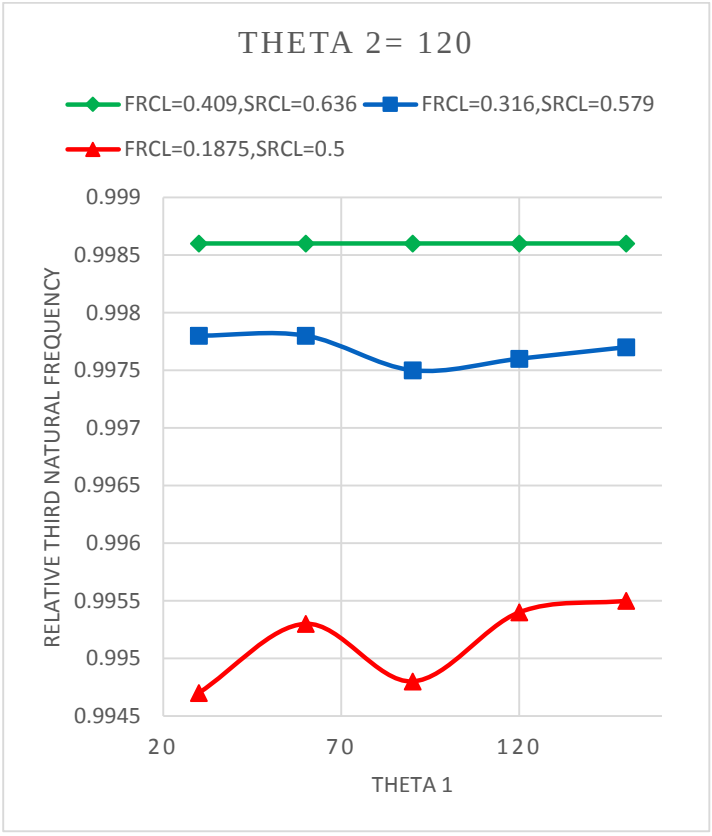


Fig.3.68. Variation w.r.t. relative crack length

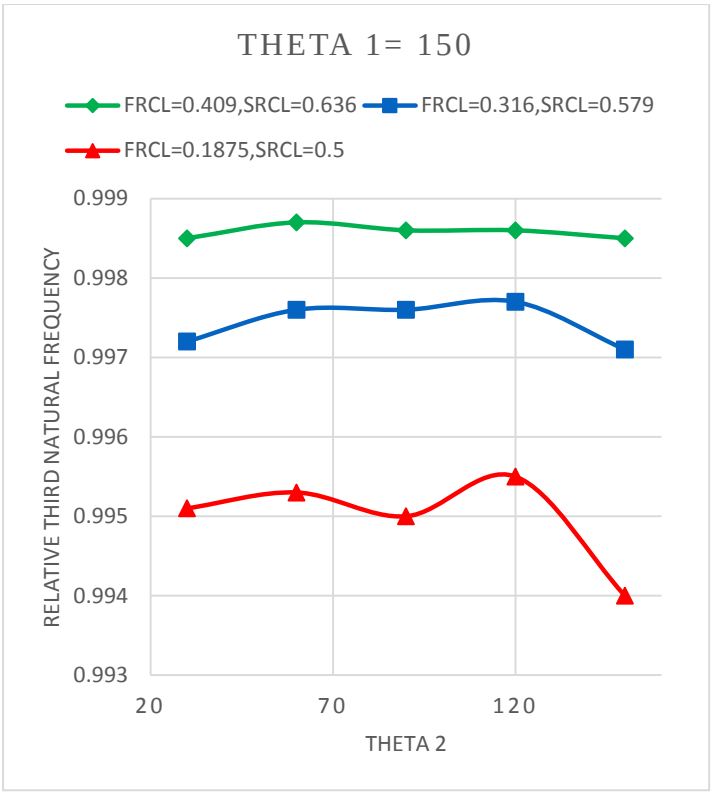


Fig.3.69. Variation w.r.t. relative crack length

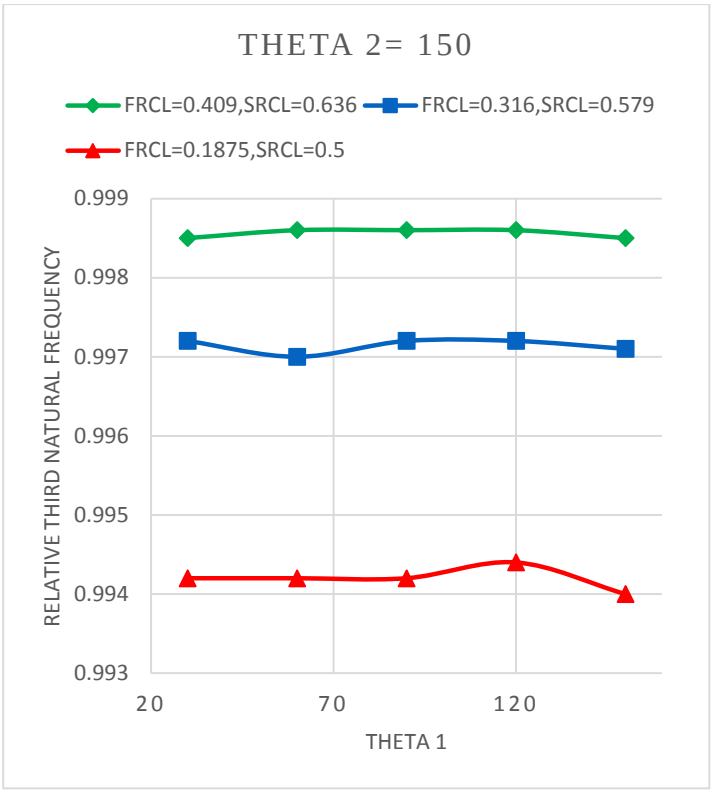


Fig.3.70. Variation w.r.t. relative crack length

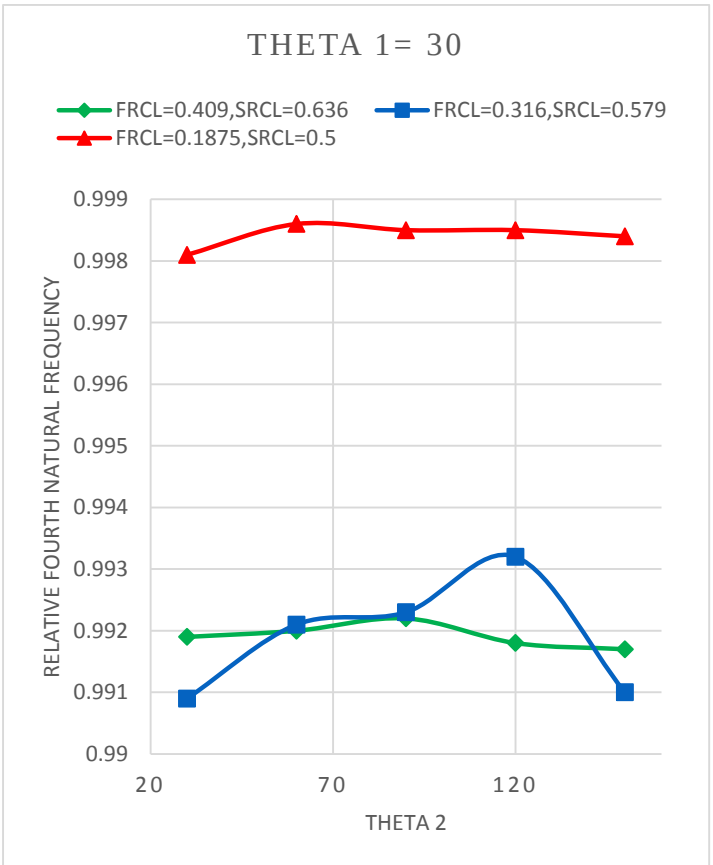


Fig.3.71. Variation w.r.t. relative crack length

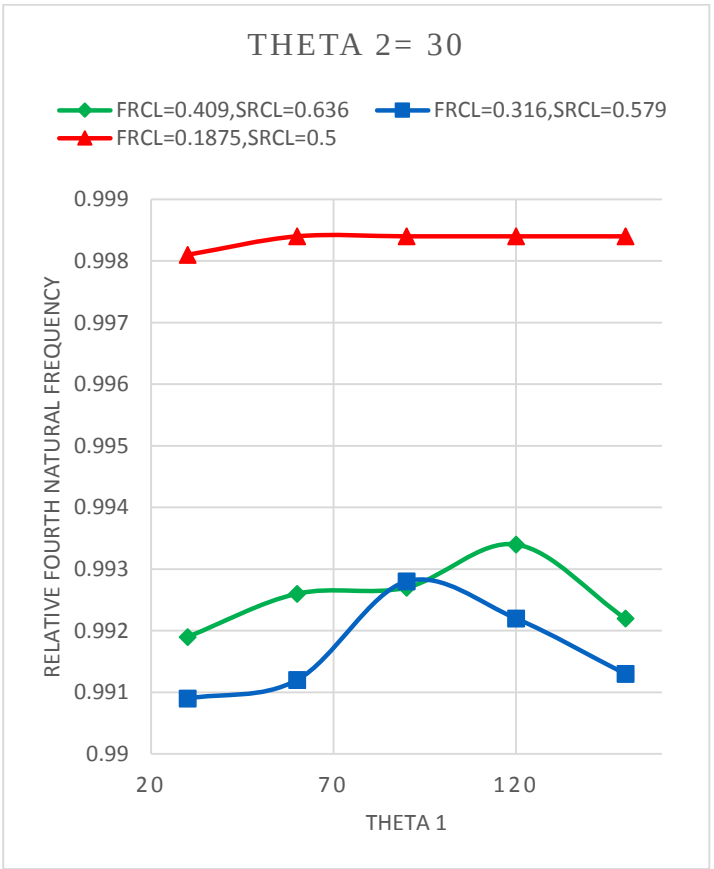


Fig.3.72. Variation w.r.t. relative crack length

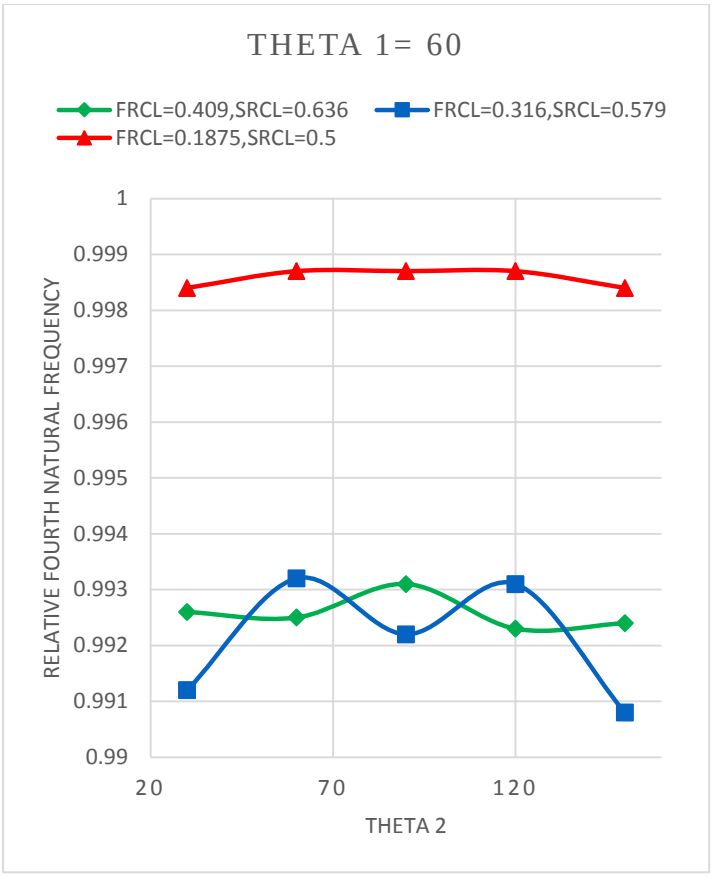


Fig.3.73. Variation w.r.t. relative crack length

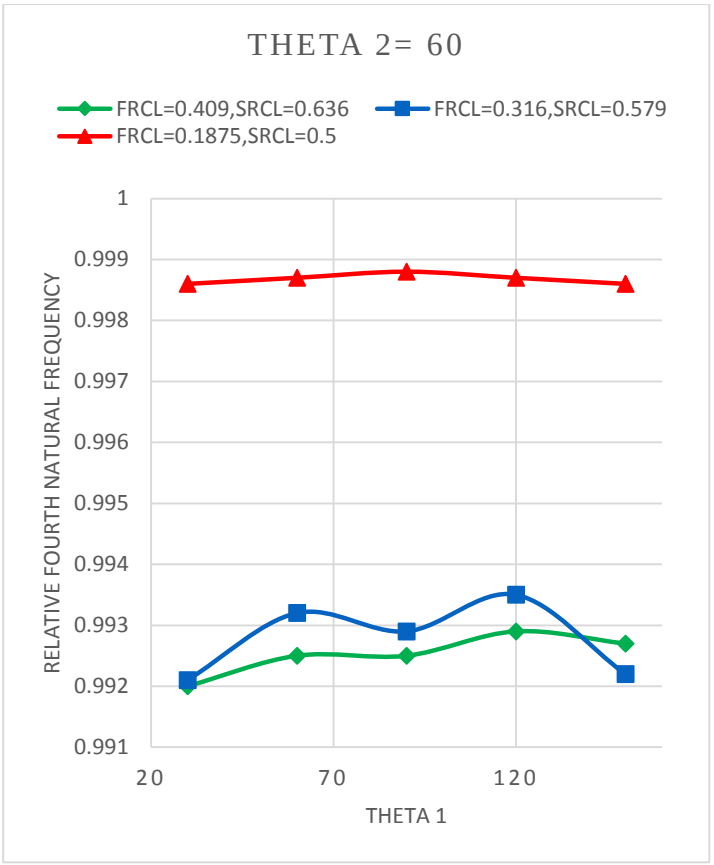


Fig.3.74. Variation w.r.t. relative crack length

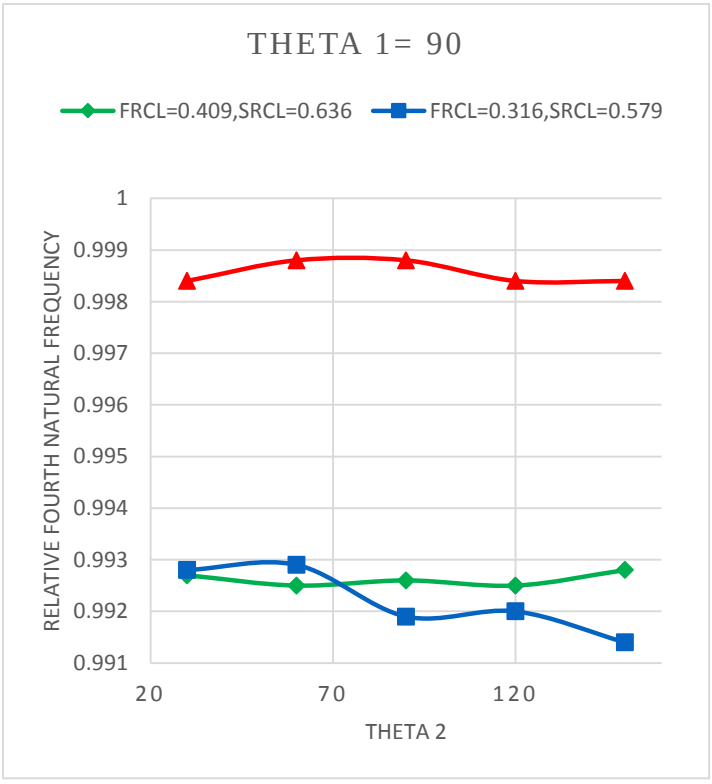


Fig.3.75. Variation w.r.t. relative crack length

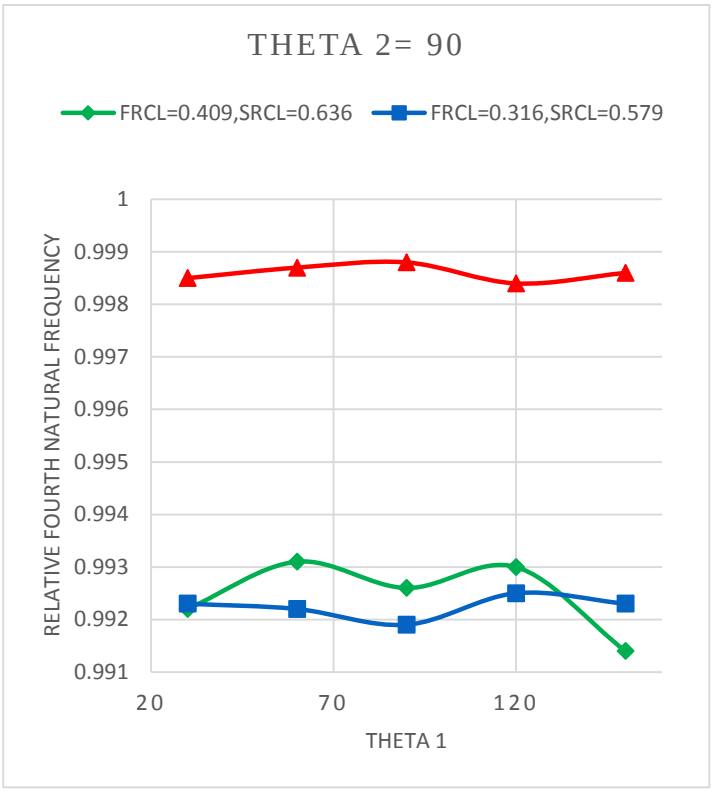


Fig.3.76. Variation w.r.t. relative crack length

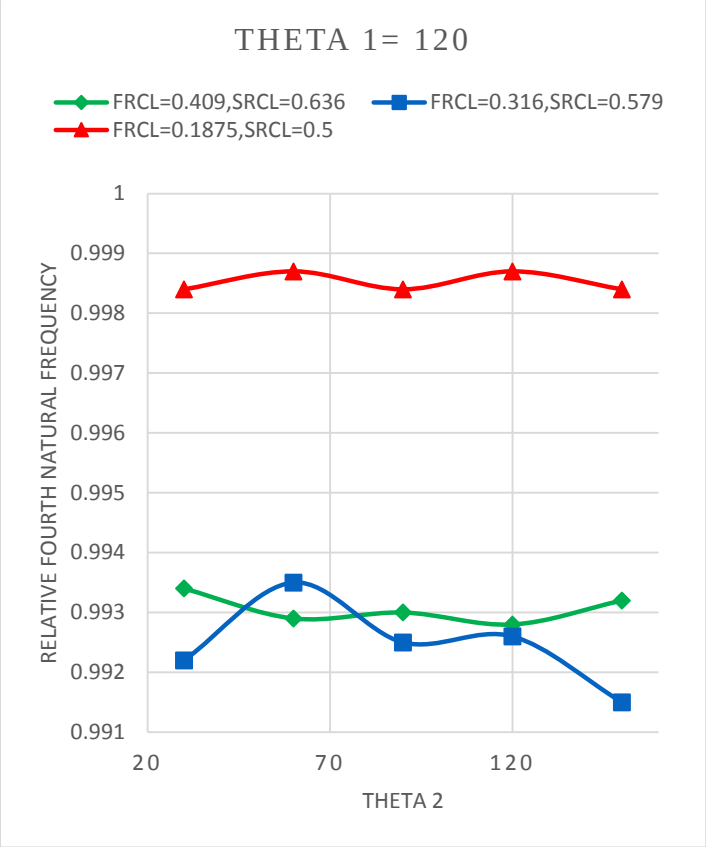


Fig.3.77. Variation w.r.t. relative crack length

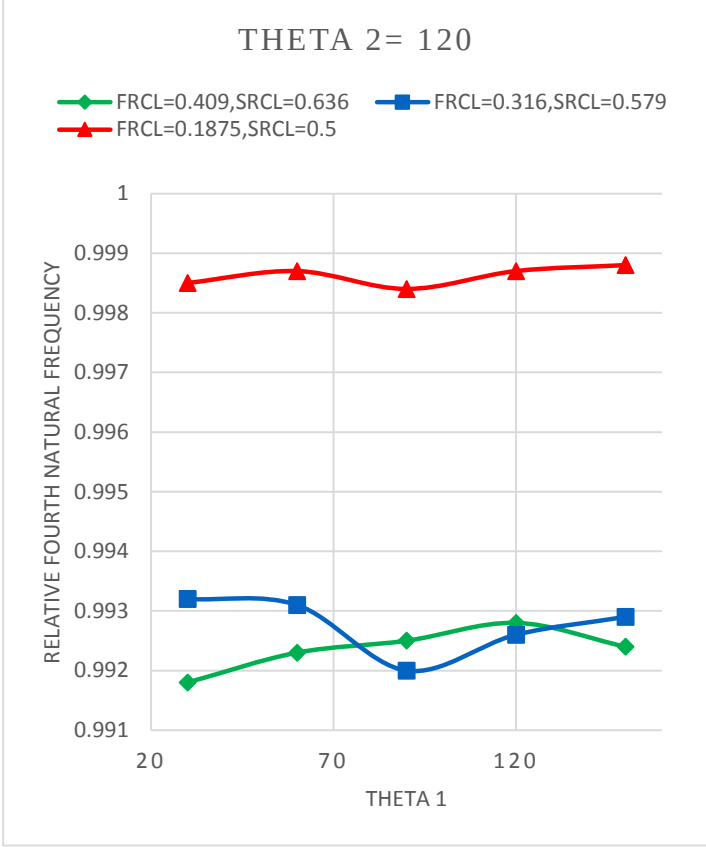


Fig.3.78. Variation w.r.t. relative crack length

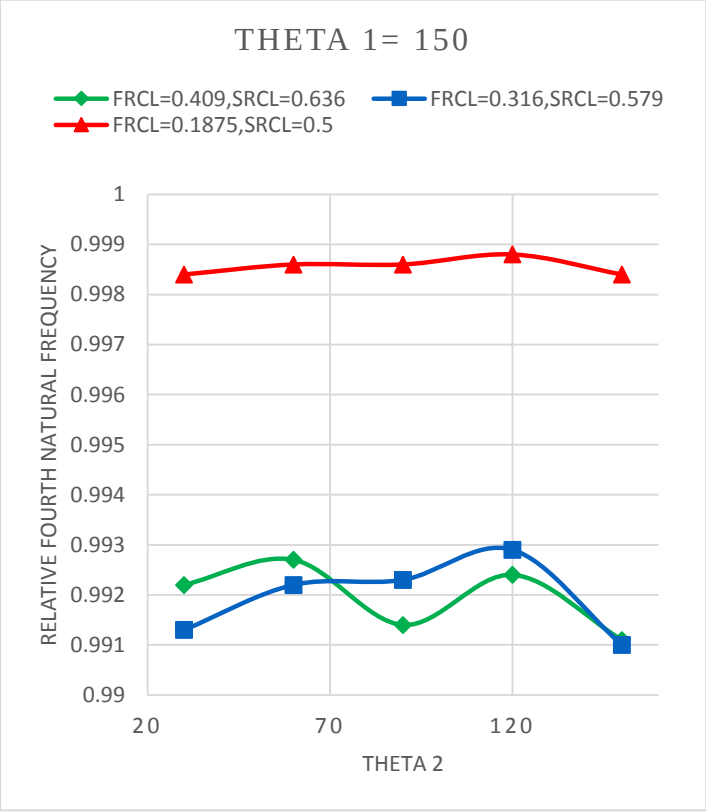


Fig.3.79. Variation w.r.t. relative crack length

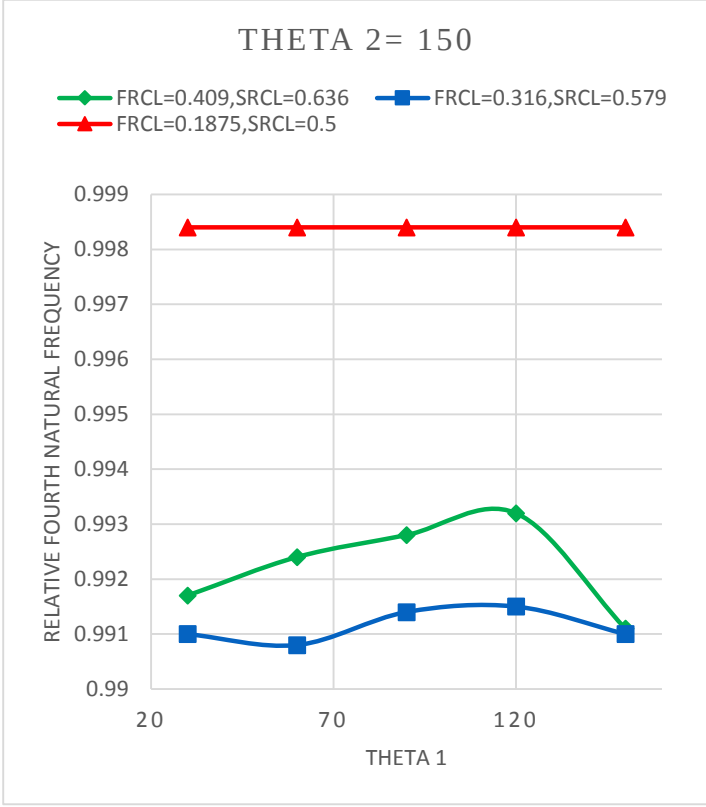


Fig.3.80. Variation w.r.t. relative crack length

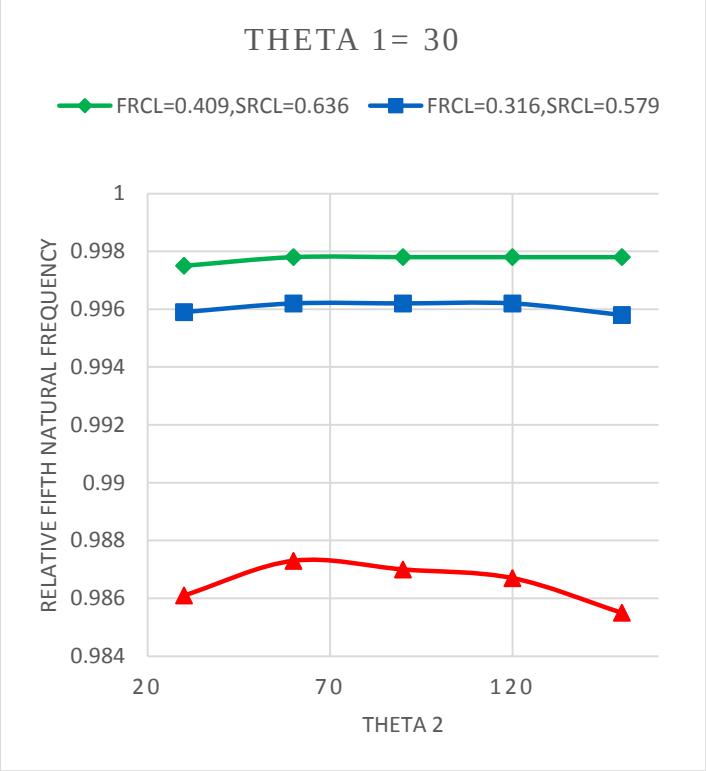


Fig.3.81. Variation w.r.t. relative crack length

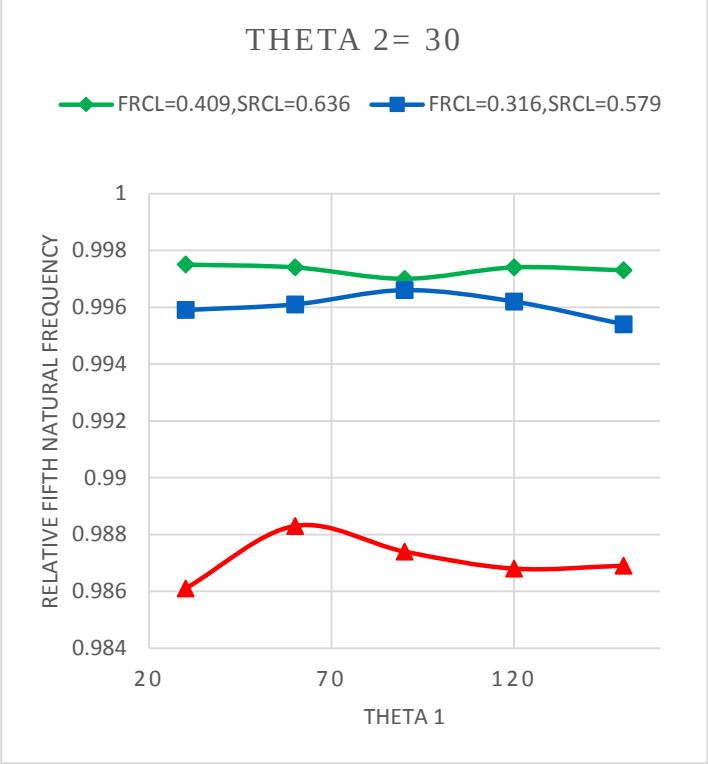


Fig.3.82. Variation w.r.t. relative crack length

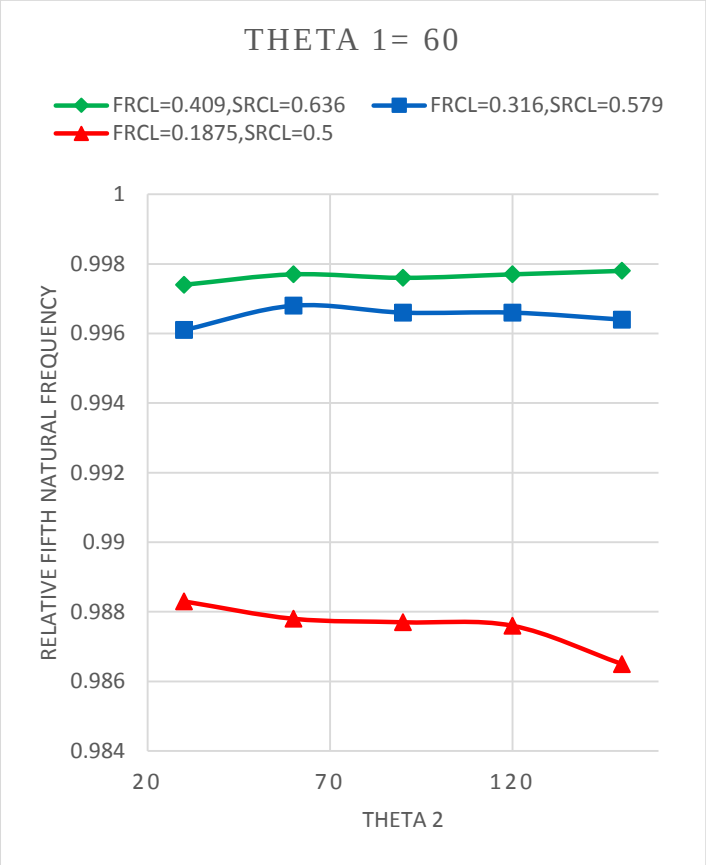


Fig.3.83. Variation w.r.t. relative crack length

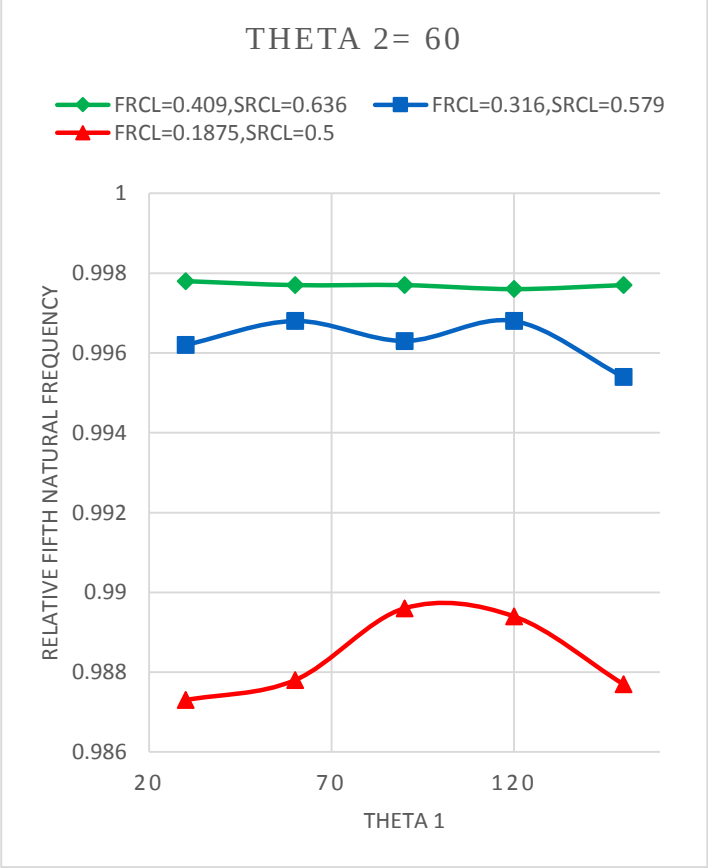


Fig.3.84. Variation w.r.t. relative crack length

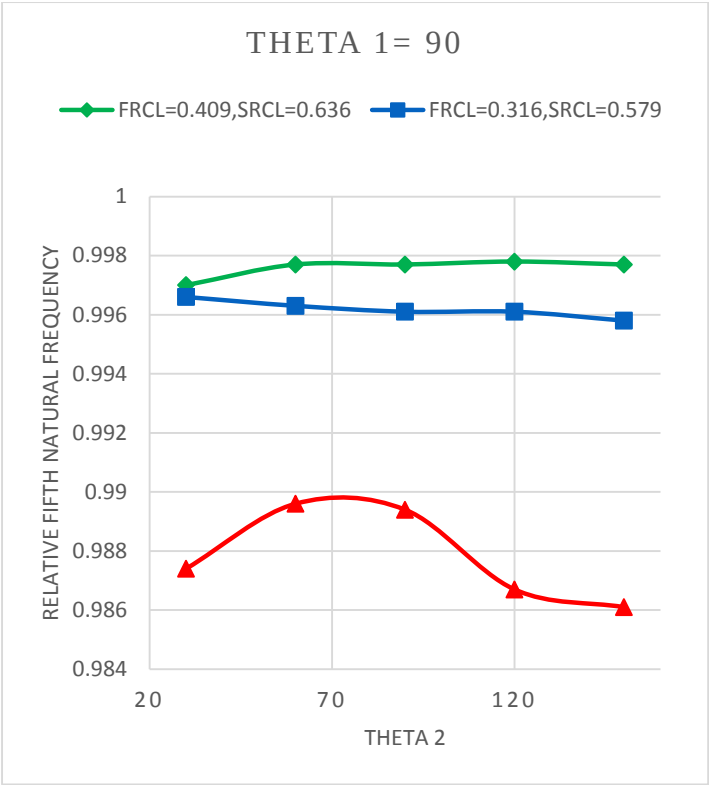


Fig.3.85. Variation w.r.t. relative crack length

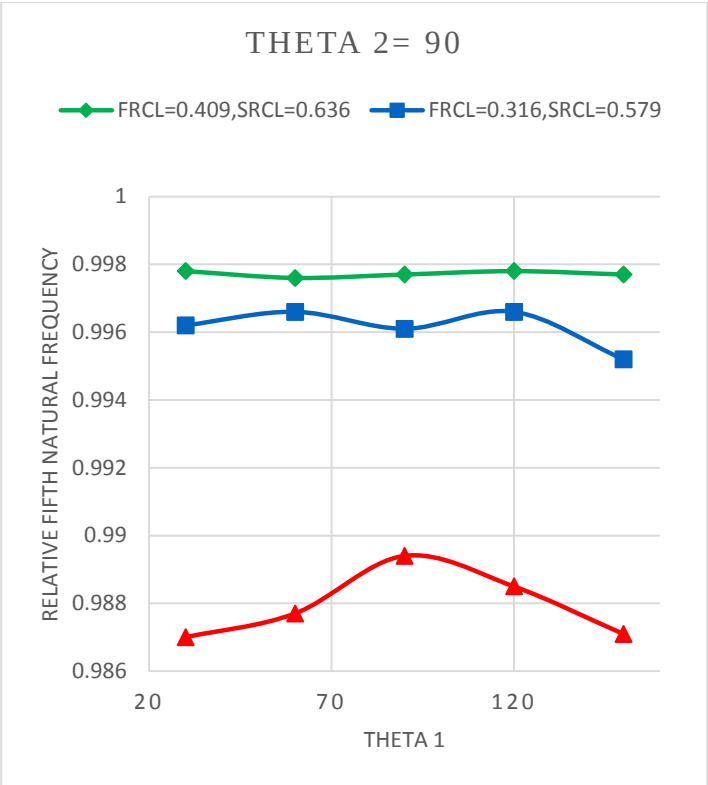


Fig.3.86. Variation w.r.t. relative crack length

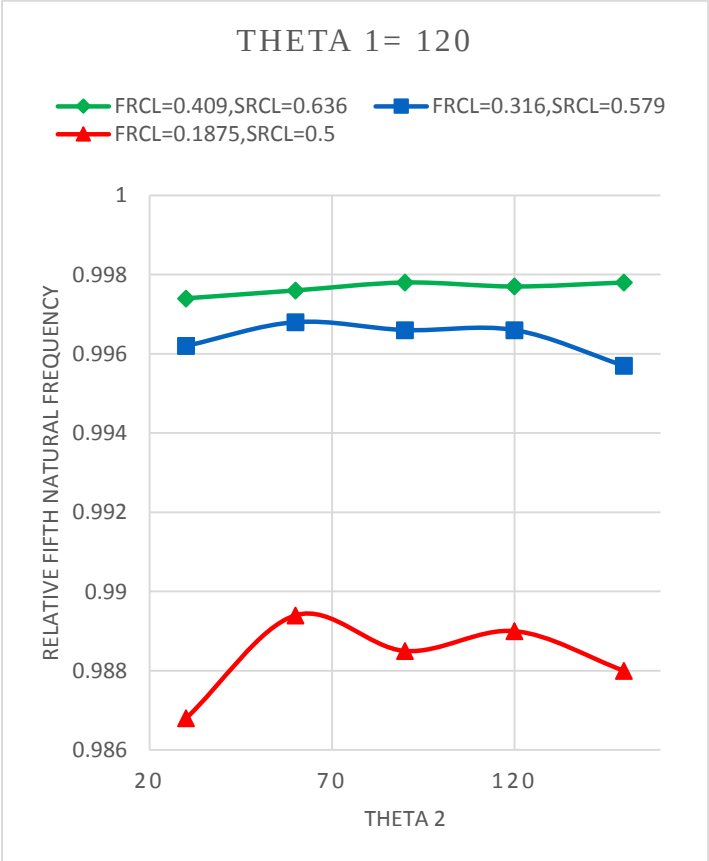


Fig.3.87. Variation w.r.t. relative crack length

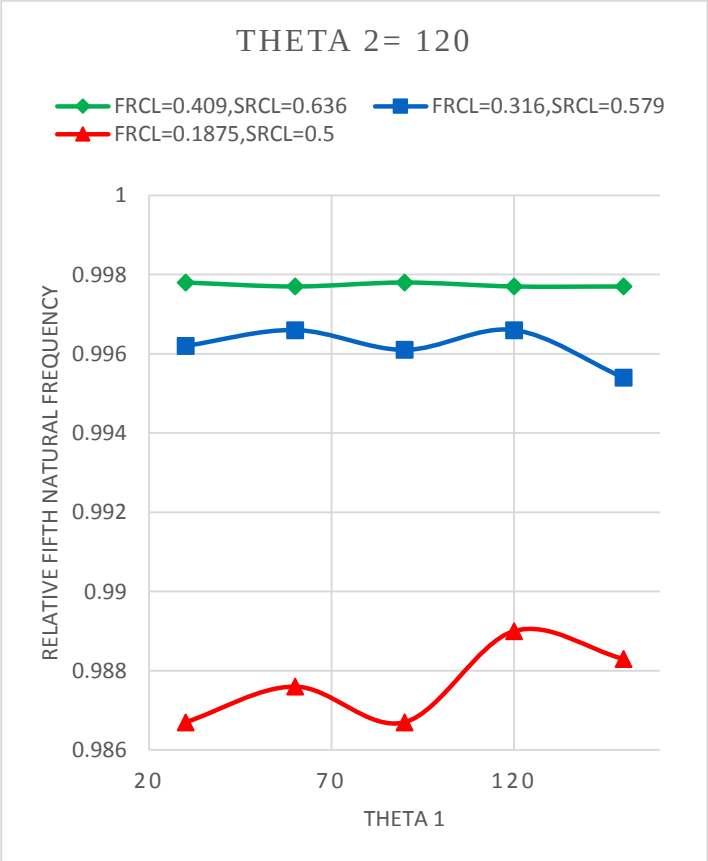


Fig.3.88. Variation w.r.t. relative crack length

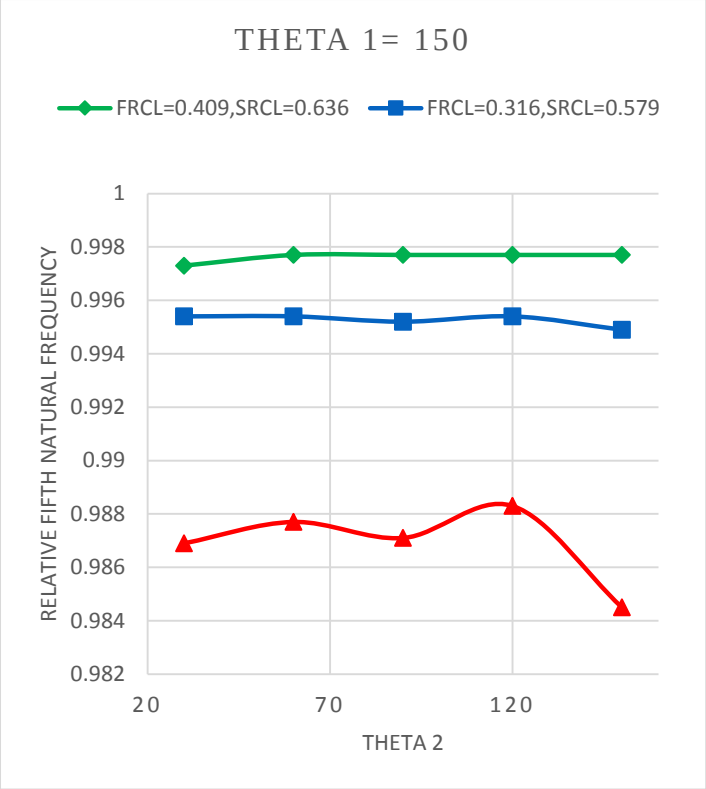


Fig.3.89. Variation w.r.t. relative crack length

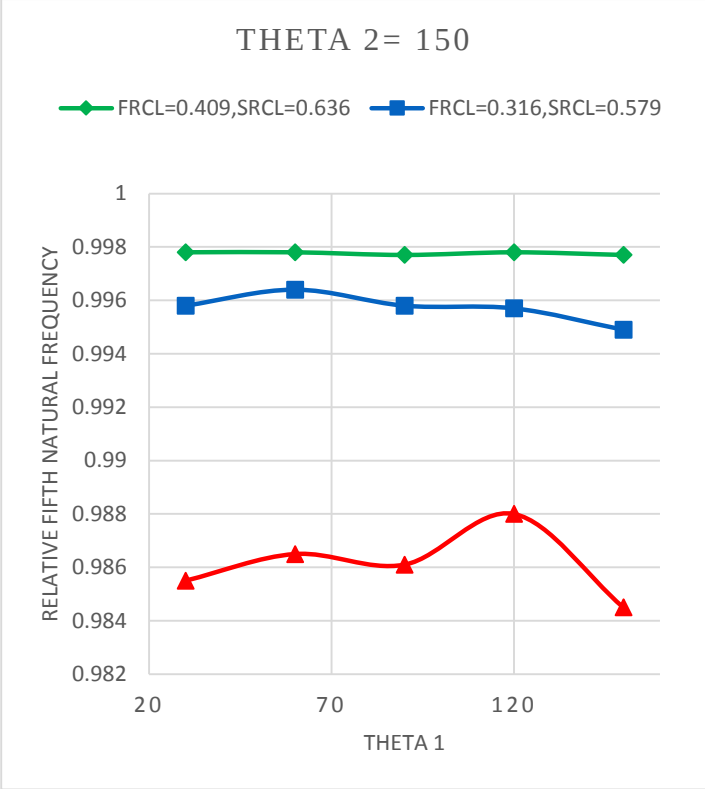


Fig.3.90. Variation w.r.t. relative crack length

From the above plots, it can be seen that with decrease in relative crack length, relative first natural frequency decreases all the time. But no specific trend can be observed for second relative natural frequency. Third relative natural frequency (i.e. first torsional natural frequency) behaves like the first relative natural frequency and decreases as relative crack length decreases. For fourth relative natural frequency, as the relative length becomes much smaller, relative natural frequency increases. Fifth relative natural frequency decreases with decrease in relative crack location. Variation of relative natural frequencies can be plotted in three-dimensional plots so that when the angle of inclination becomes arbitrary, these plots can act as reference.

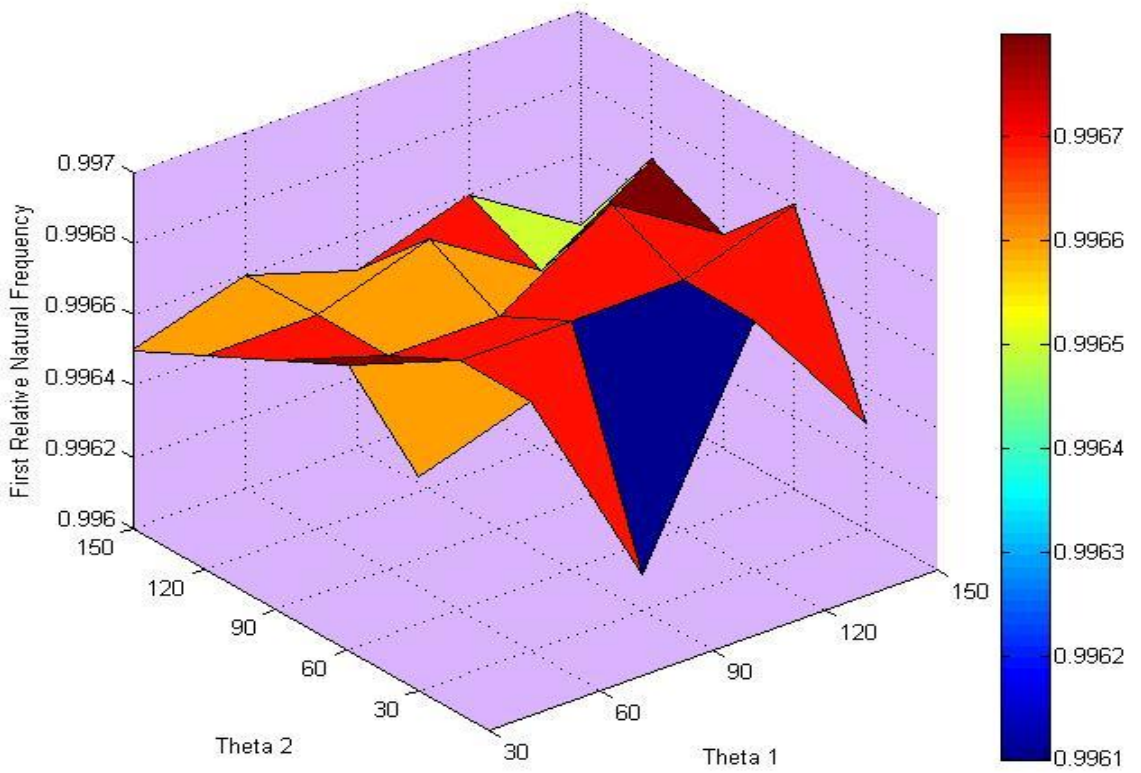


Fig.3.91. 3D Variation of First Relative Natural Frequency

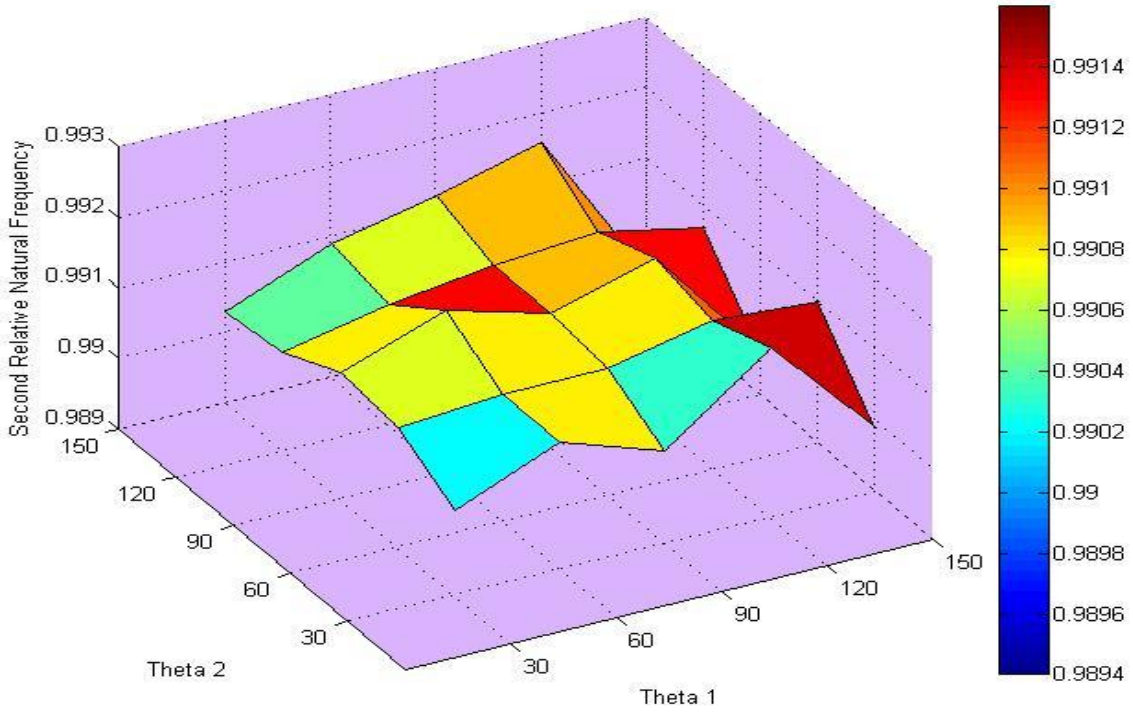


Fig.3.92. 3D Variation of First Relative Natural Frequency

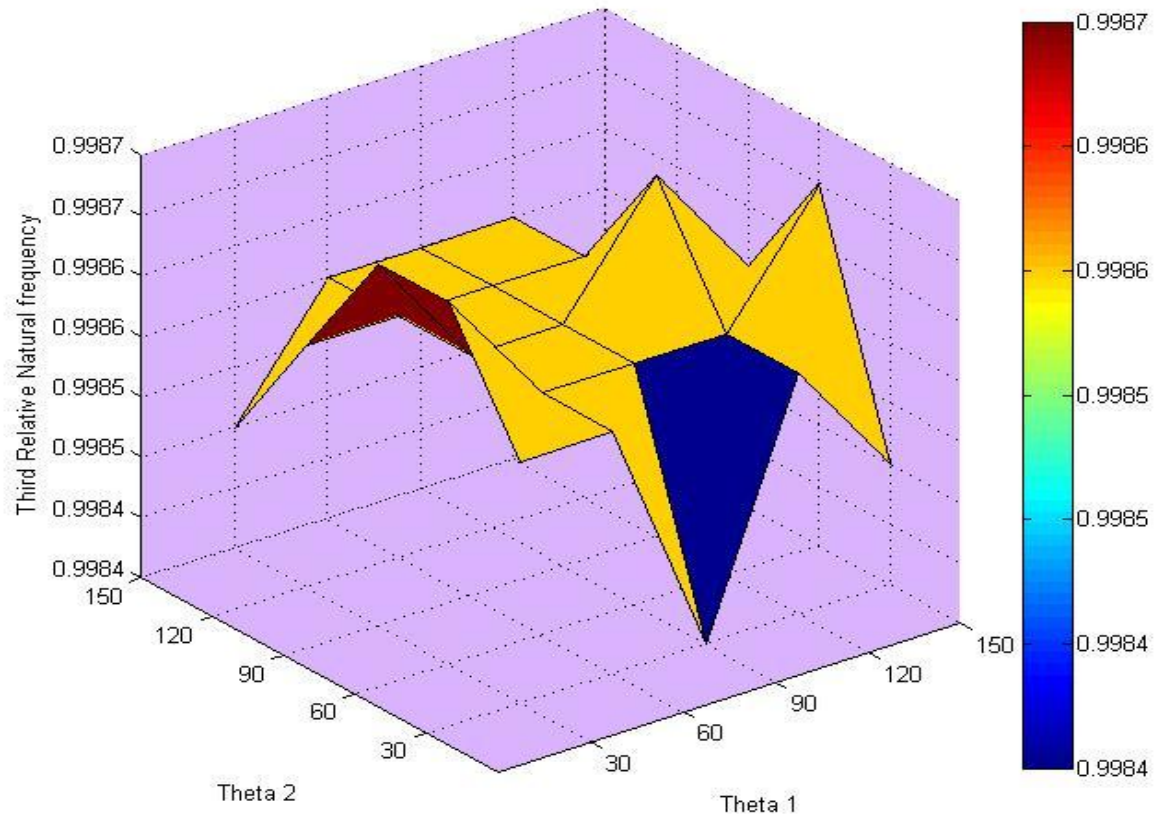


Fig.3.93. 3D Variation of First Relative Natural Frequency

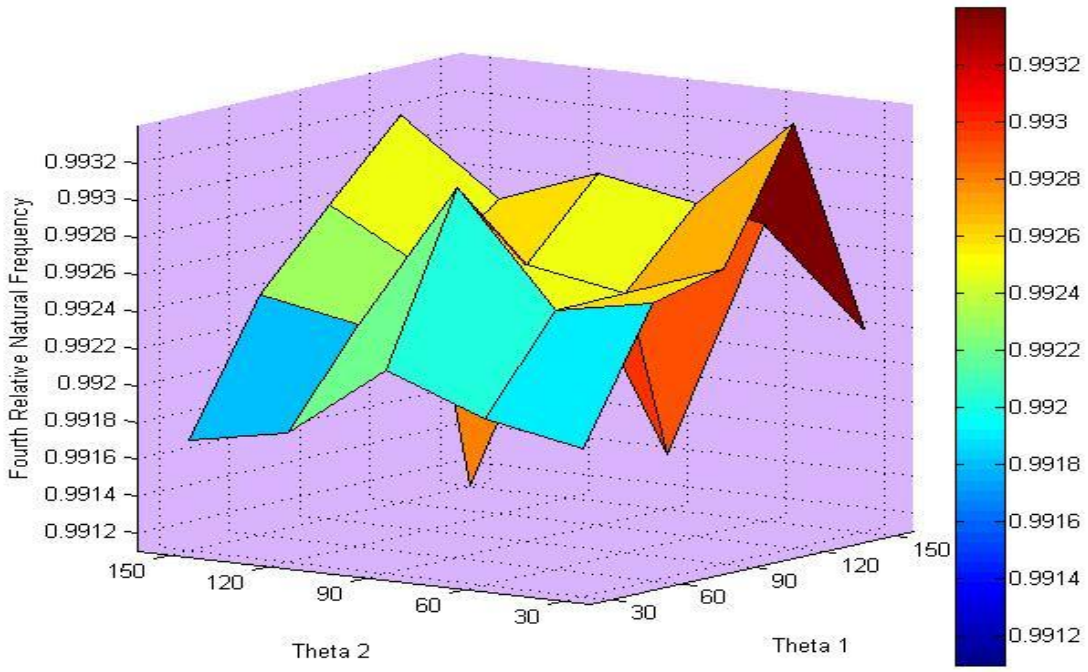


Fig.3.94. 3D Variation of First Relative Natural Frequency

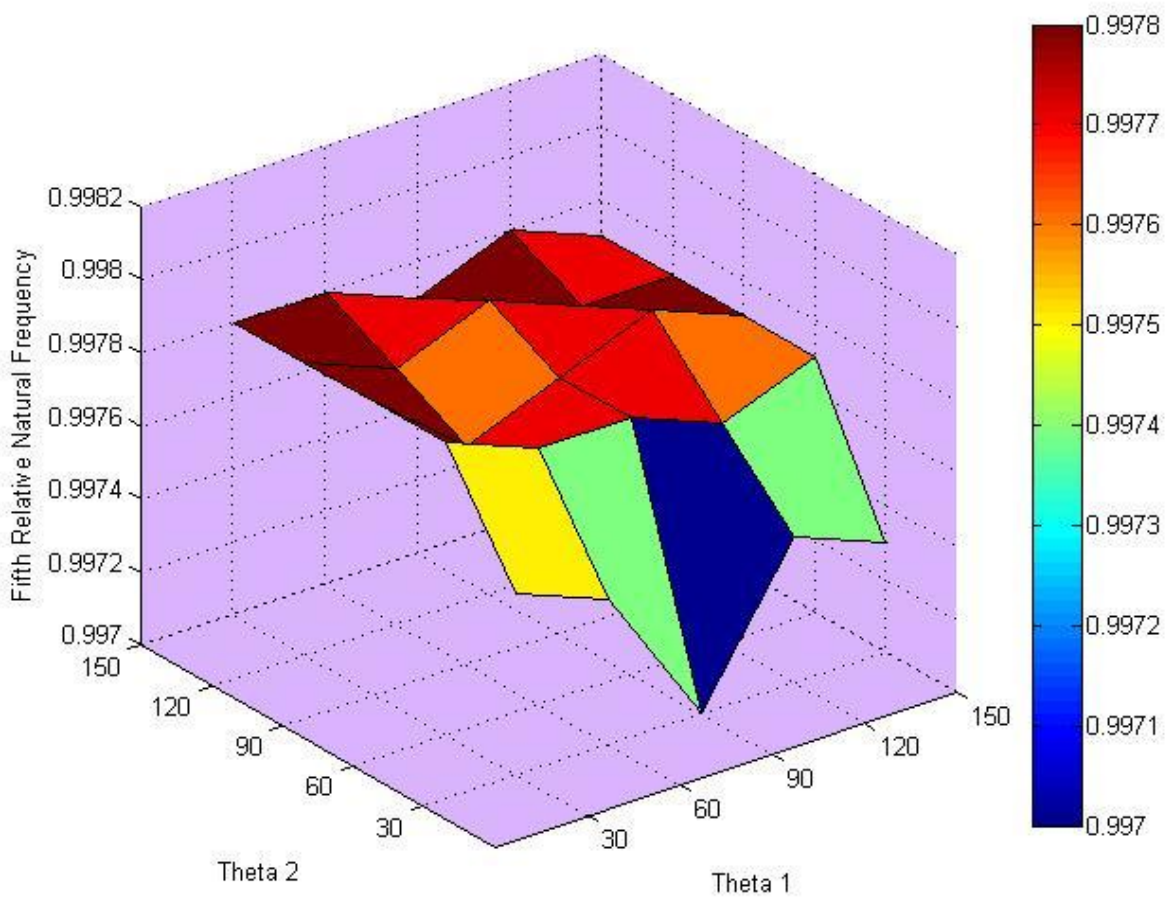


Fig.3.95. 3D Variation of First Relative Natural Frequency

### 3.8. FORCED VIBRATION ANALYSIS OF DOUBLE INCLINED CRACK IN A CANTILEVER BEAM BY ANSYS

This analysis has been done in ANSYS Harmonic Response. Three different loading conditions and their effect on displacement and acceleration analysis has been considered. First the harmonic load is applied at the free end of the beam then it is applied in between the two cracks and finally it is applied between the fixed end and initial crack. For uncracked beam when the harmonic load is applied at the free end, the displacement and acceleration response look like Fig.3.96.

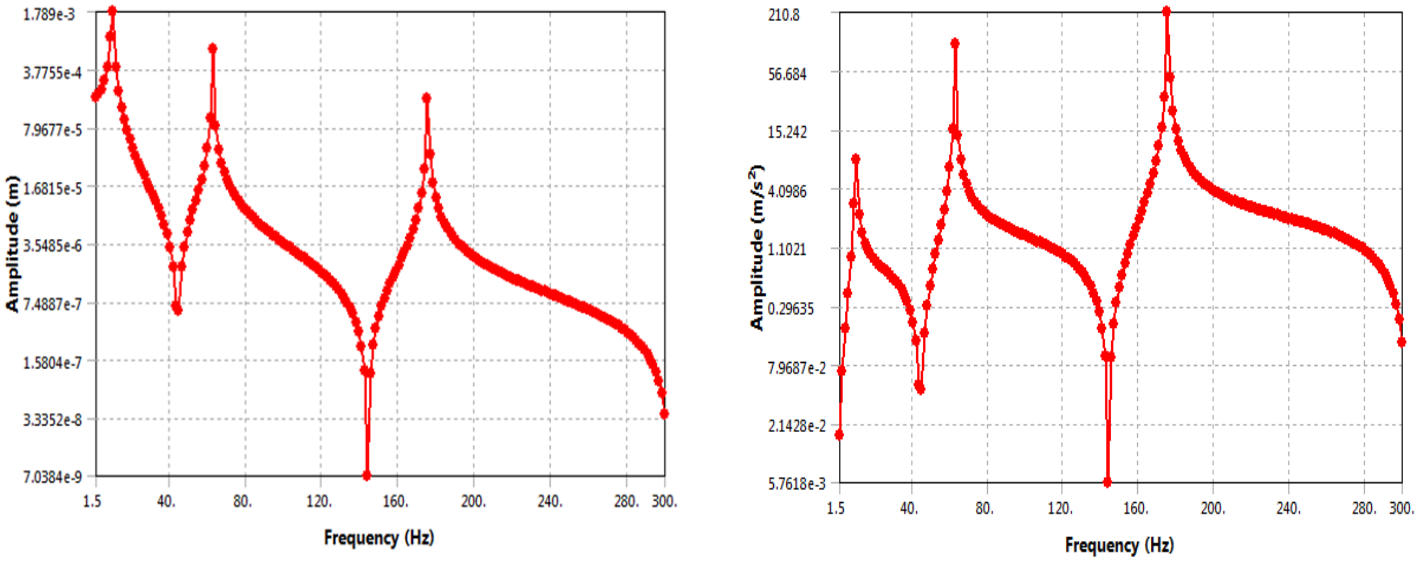


Fig.3.96. Response when forced excitation is applied at the free end of the uncracked beam

All the analysis is done for the crack angle of $60^0$ for both inclined cracks. For cracked beam with end load application, the response looks like Fig.3.97.

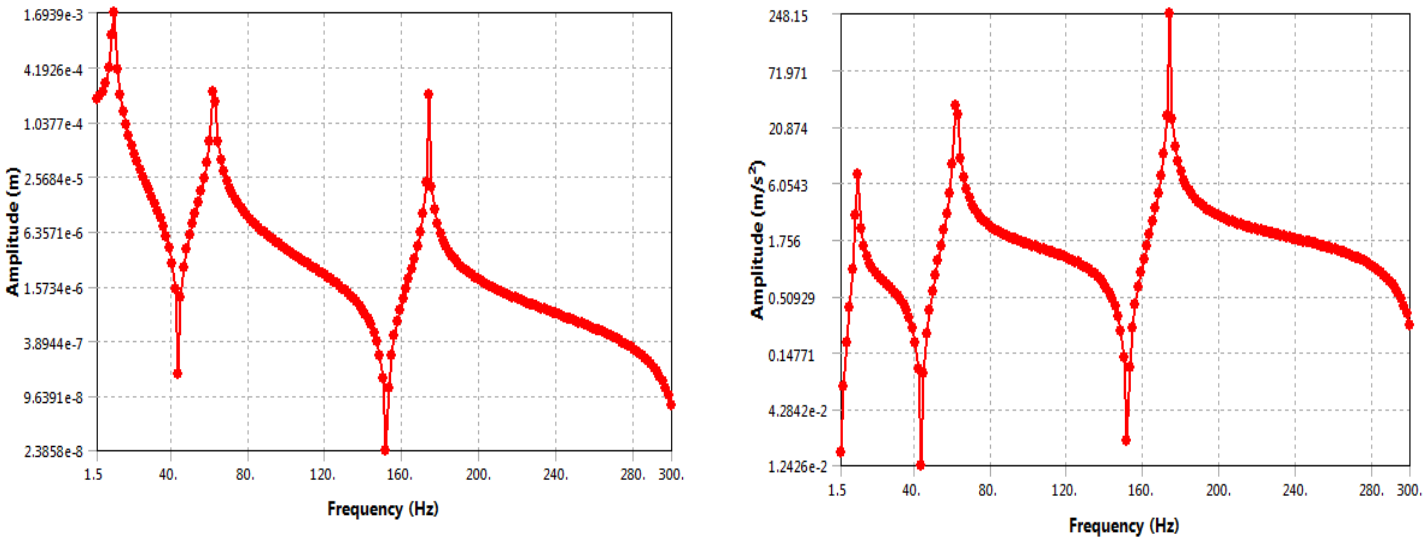


Fig.3.97. Response when forced excitation is applied at the free end of the cracked beam

For the load application point in between both the cracks the response look like Fig.3.98.

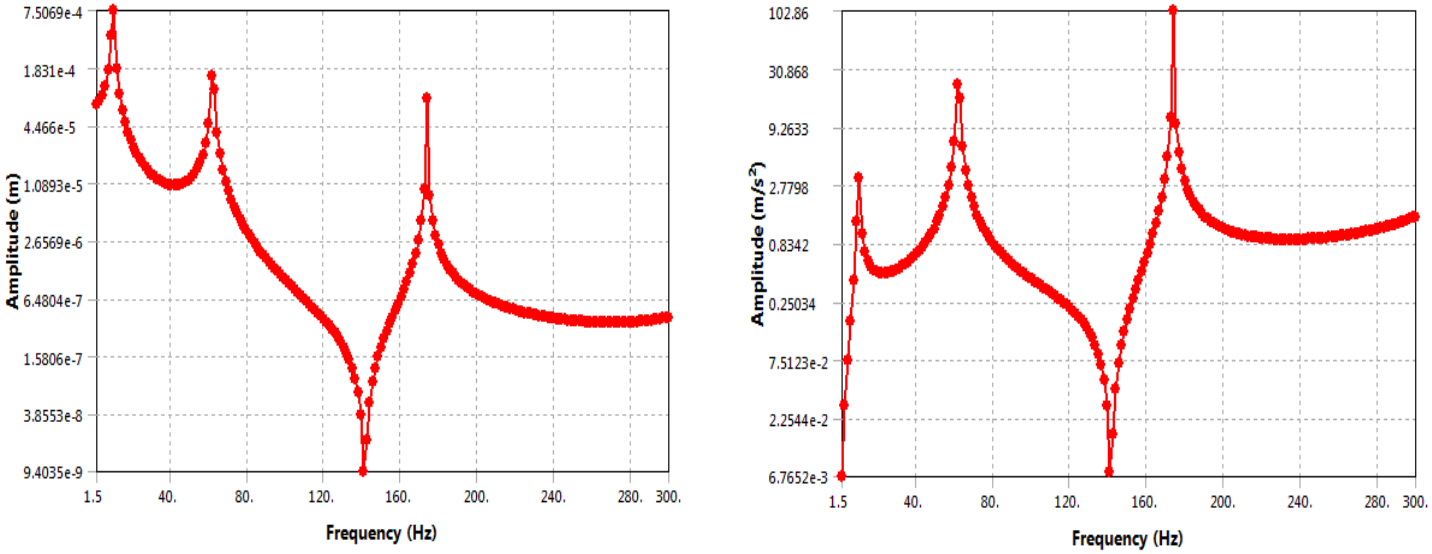


Fig.3.98. Response when forced excitation is applied between both the cracks

When the load is applied between the fixed end and first crack location, the response appears as Fig.3.99.

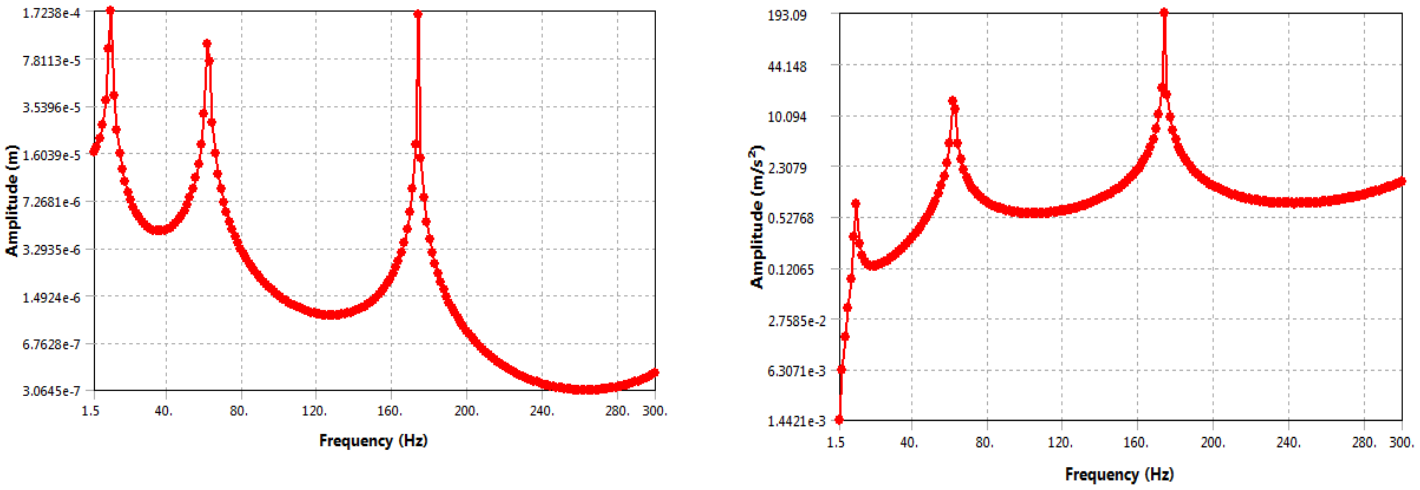


Fig.3.99. Response when forced excitation is applied between the fixed support and first crack

The above forced vibration analysis can be performed for other angle combinations and can be compared to forced vibration responses of test specimens to detect cracks.

# CHAPTER 4

## 4. EXPERIMENTAL INVESTIGATION

Values obtained from ANSYS should be checked for their accuracy in the actual physical system. For that purpose, we need to check how much deviation occurs in the values obtained in ANSYS to actual ones. In this chapter free vibration analysis of the uncracked beam and cracked beam has been done using Impact Hammer test. Percentage errors have been calculated for actual values obtained from Impact Testing to that obtained from ANSYS. Instead of testing all cases that were investigated in ANSYS, only uncracked beam, cracked beam with both inclinations angles $90^0$, $30^0$ and $150^0$, have been considered.

### 4.1. THEORY

When a signal is represented with respect to time, it's called a time domain signal. The time domain signal can be continuous as well as discrete. When the signal value is known for all real values of time, it's called continuous signal, and when the signal value is known for various separate instances, the signal is called discrete.

All real life signals are not composed of single frequency rather they contain a mixture of different frequencies. A time domain plot of various signal can be obtained by using transducers that convert the mechanical response into electrical signals and after proper modulation we get the required plot with respect to time. But at times we require the frequencies of which the time domain signal is composed of and the time domain plot is of no help in that regard.

To get the information about frequencies we need Fast Fourier Transform, which extracts frequencies from time domain plot. The signal thus obtained from Fast Fourier Transform is plotted against frequency, and the plot is called a frequency domain plot. The frequency domain function can be converted back to time domain function by Inverse Fourier Transform.

Experimental determination of natural frequency comes broadly under signal analysis. For free vibration analysis, we need one accelerometer, one impact hammer and data acquisition system. Accelerometer is mounted on the beam, and when the beam is excited, it measures the acceleration with respect to time.

When the beam is hit by the hammer tip, some initial excitation is provided to the beam. This excitation excites not one but more than one modes simultaneously. The number of modes that are excited depends on the hardness of the hammer tip. Harder the tip, higher the frequencies that are excited. So after hitting the beam, what we get by the accelerometer is a (time) signal that is composed of sinusoidal waves of more than one frequency along with some inevitable noise that makes the signal look more complicated though it is sinusoidal in nature. Our main aim is then to decipher the frequencies that made up the signal we obtained from the accelerometer. A convenient way to get those frequencies is to transform the time domain signal into the frequency domain signal. In the frequency domain, we only get the frequencies that were responsible for the original signal.

The data acquisition system does the necessary FFT analysis to transform the time domain signal into frequency domain signal. To obtain FFT of the continuous time signal, we first need to convert the continuous time domain signal into a discrete signal by choosing specific samples. The sampling rate should be large enough to avoid aliasing, and it should also satisfy Nyquist theorem. The sampling rate should not be too high as too high sampling rate might introduce error. In frequency domain plot, the frequencies appear as peaks. The relative heights of the peaks are a measure of the contribution of that particular mode towards the total time response. If noise is present in the system, instead of getting sharp peaks, we get blunted peaks. Mathematical details of Signal Processing and Frequency Analysis can be referred from any standard textbook such as [25].

## 4.2. EXPERIMENTAL SETUP AND COMPONENTS USED

Fig.4.1. Accelerometer (Model 4513-001, Brüel & Kjær)

Fig.4.2. Impact Hammer Tip (Model 2302-5, Brüel & Kjær)


Fig.4.3. Data Acquisition System (3560-L, Brüel & Kjær)

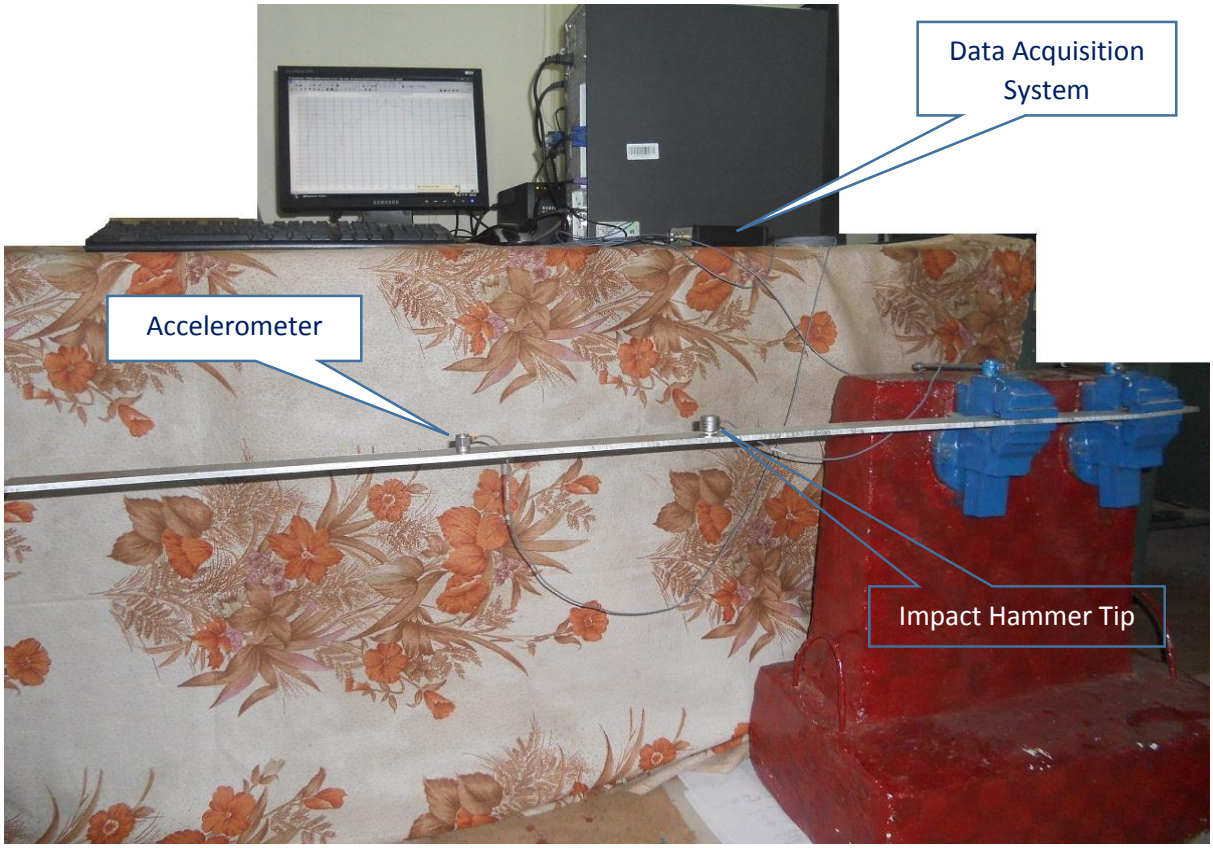


Fig.4.4. Actual Setup with Accelerometer, Impact Hammer Tip and Data Acquisition System

### 4.3. EXPERIMENTAL RESULTS

The beam is first hit by the impact hammer once. The accelerometer thus produces a time domain plot of the oscillation. Both the force and the acceleration have been shown in Fig.4.6 and Fig.4.7 respectively. The time response is then sent to an analyser that is incorporated in the data acquisition system, and FFT analysis of the signal is done to obtain Frequency Response Plots.

In Frequency Response plots, the peaks correspond to natural frequencies. Fig.4.8, 4.9, 4.10 and 4.11 show four natural frequencies on the same frequency response plot. The peaks would have been sharp had there not been any noise present in the system. Due to the presence of noise the peaks are blunted in the frequency response figures shown. Coherence that is a measure of noise present in the system is plotted in Fig.4.12. For no noise case, coherence value is always one but it deviates from one due to the inevitable presence of noise in the system as shown in the coherence plot.

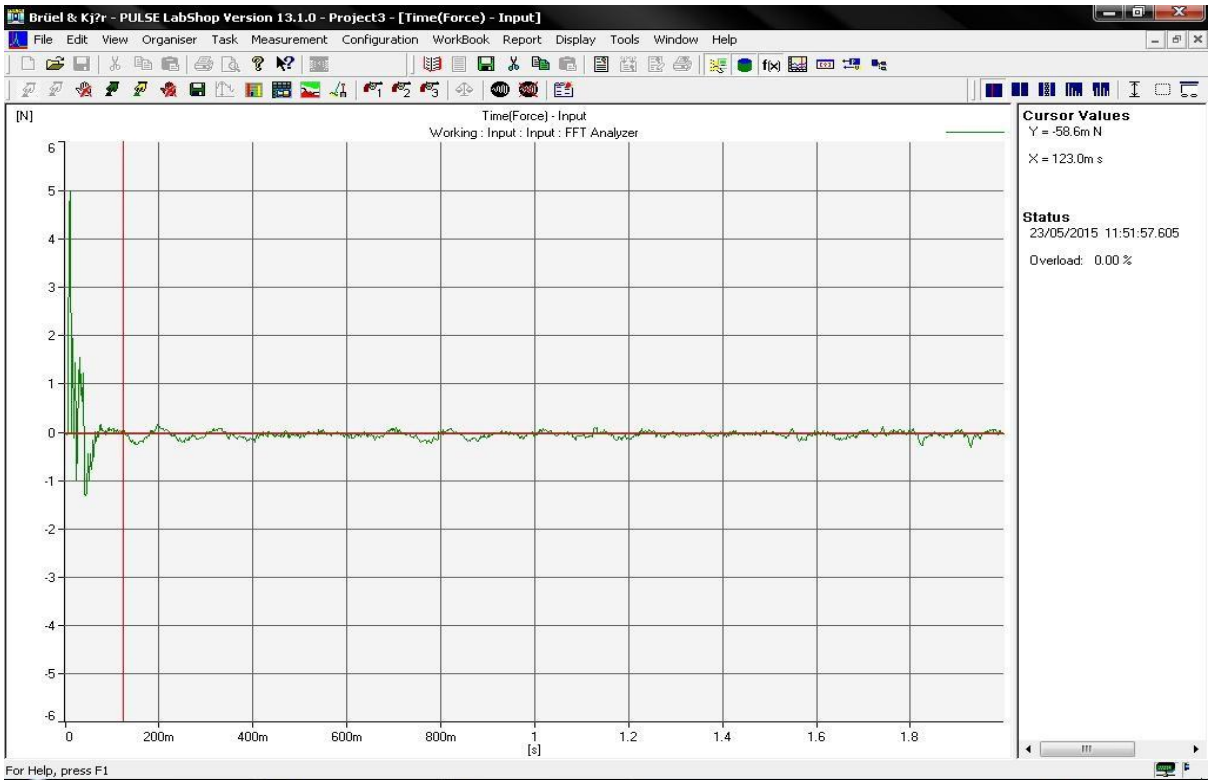


Fig.4.5. Impulsive force applied by the Impact Hammer

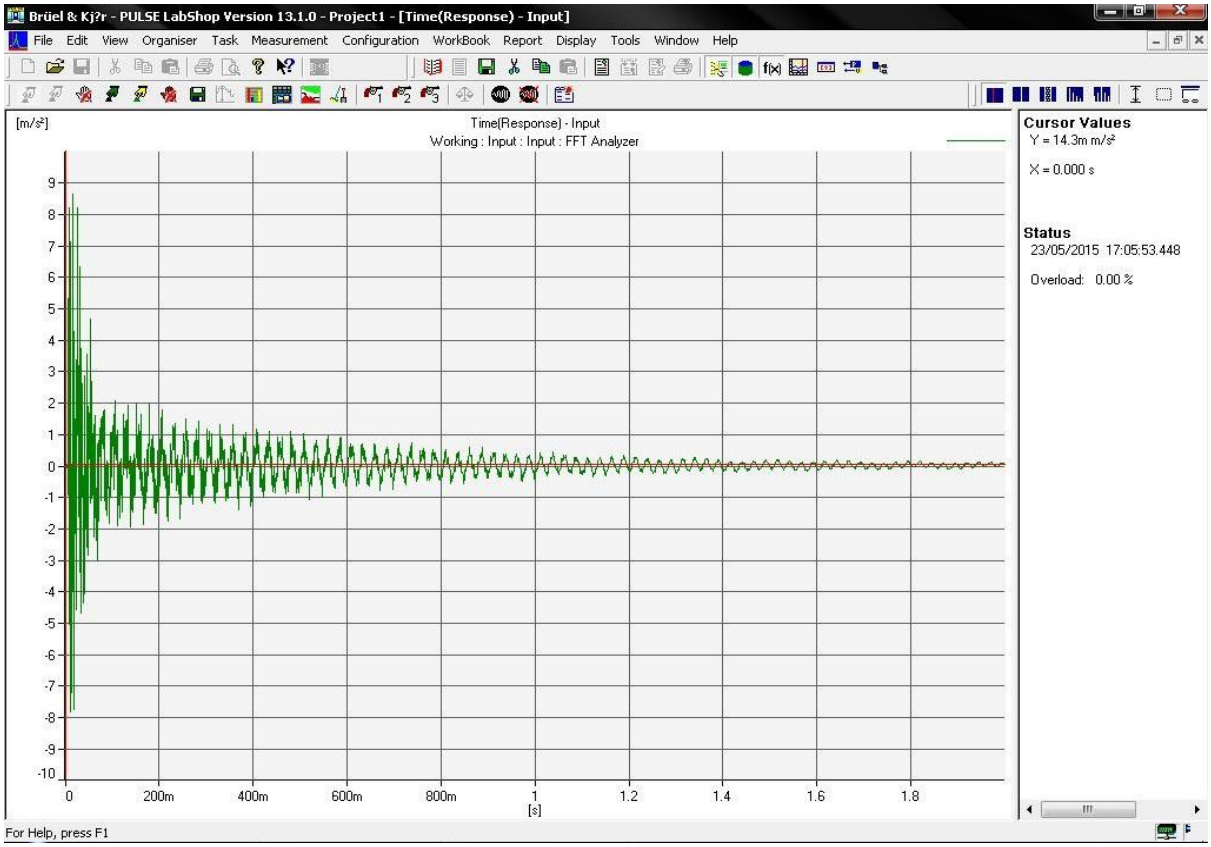


Fig.4.6. Time Response

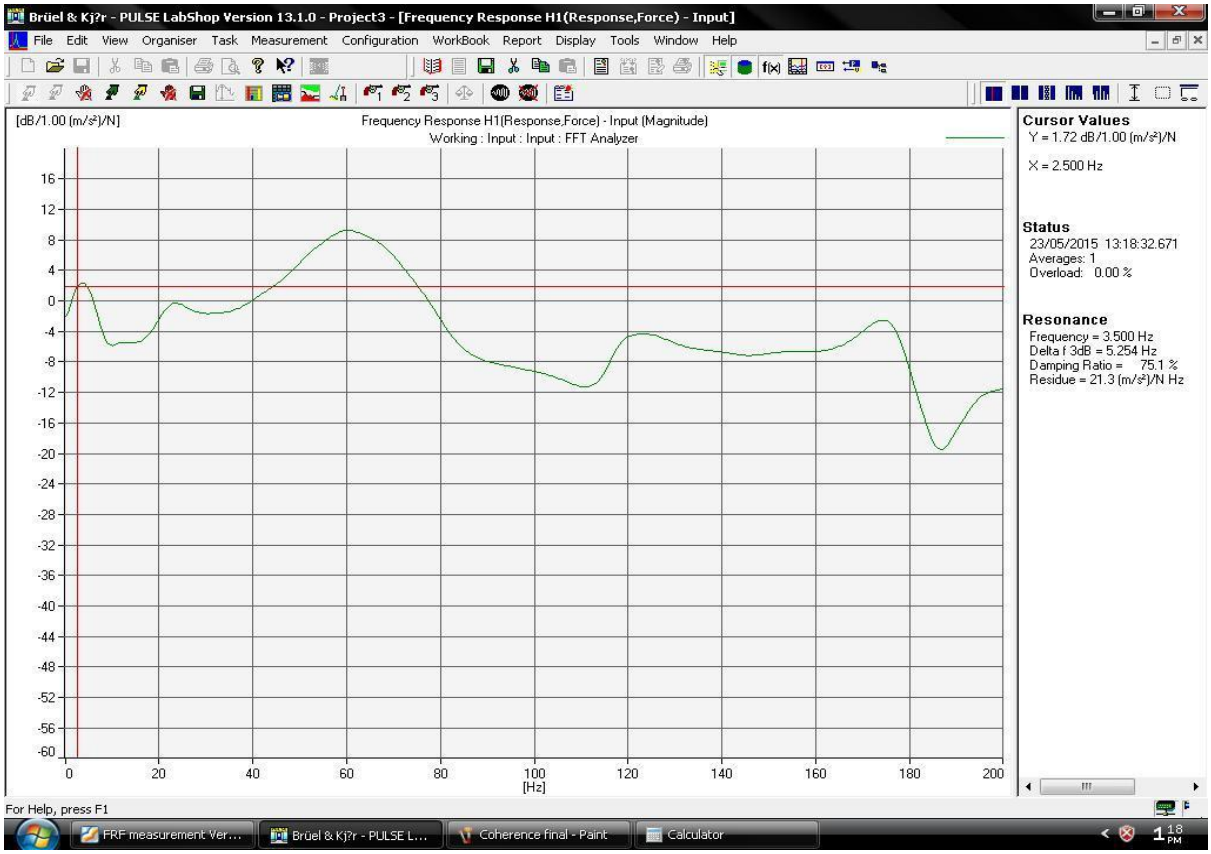


Fig.4.7. First Natural Frequency of Uncracked beam (L=110cm, b=3.9cm, h=0.5cm)

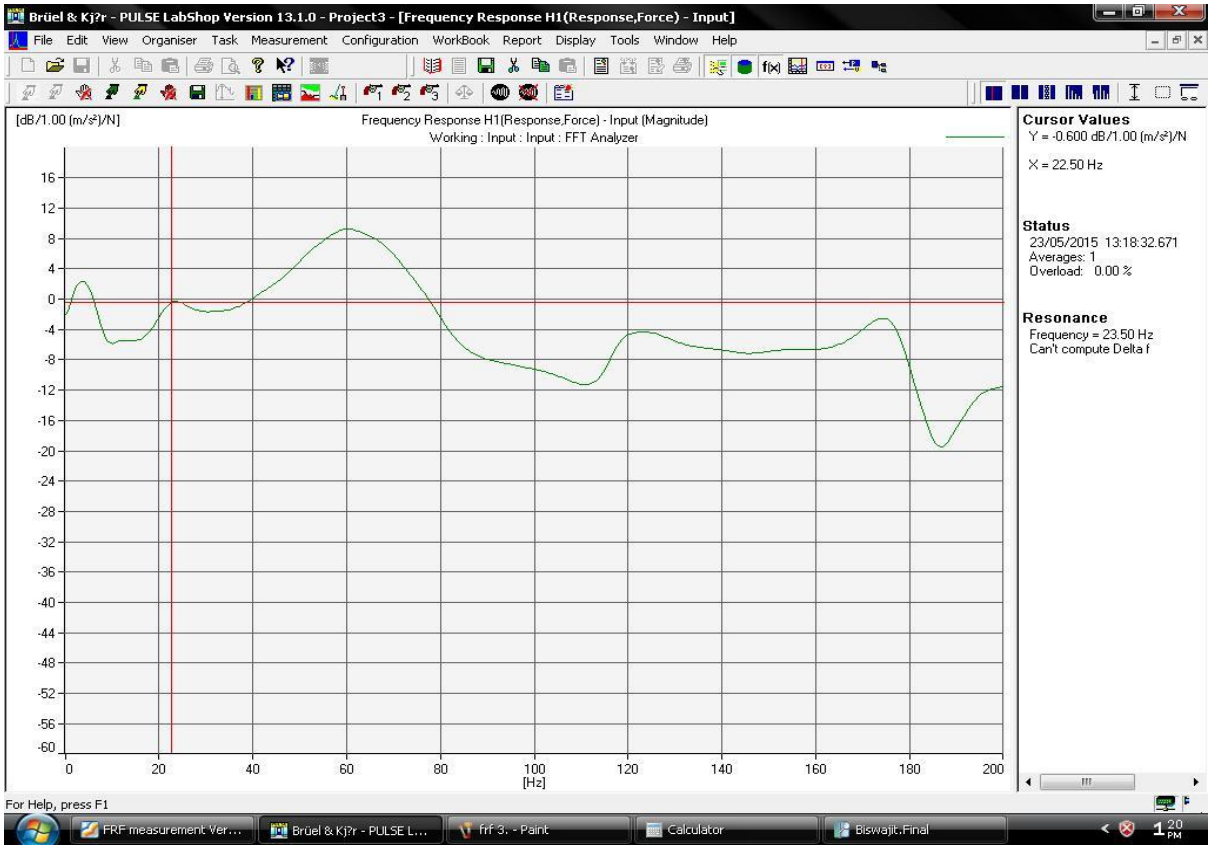


Fig.4.8. Second Natural Frequency of Uncracked beam (L=110cm, b=3.9cm, h=0.5cm)

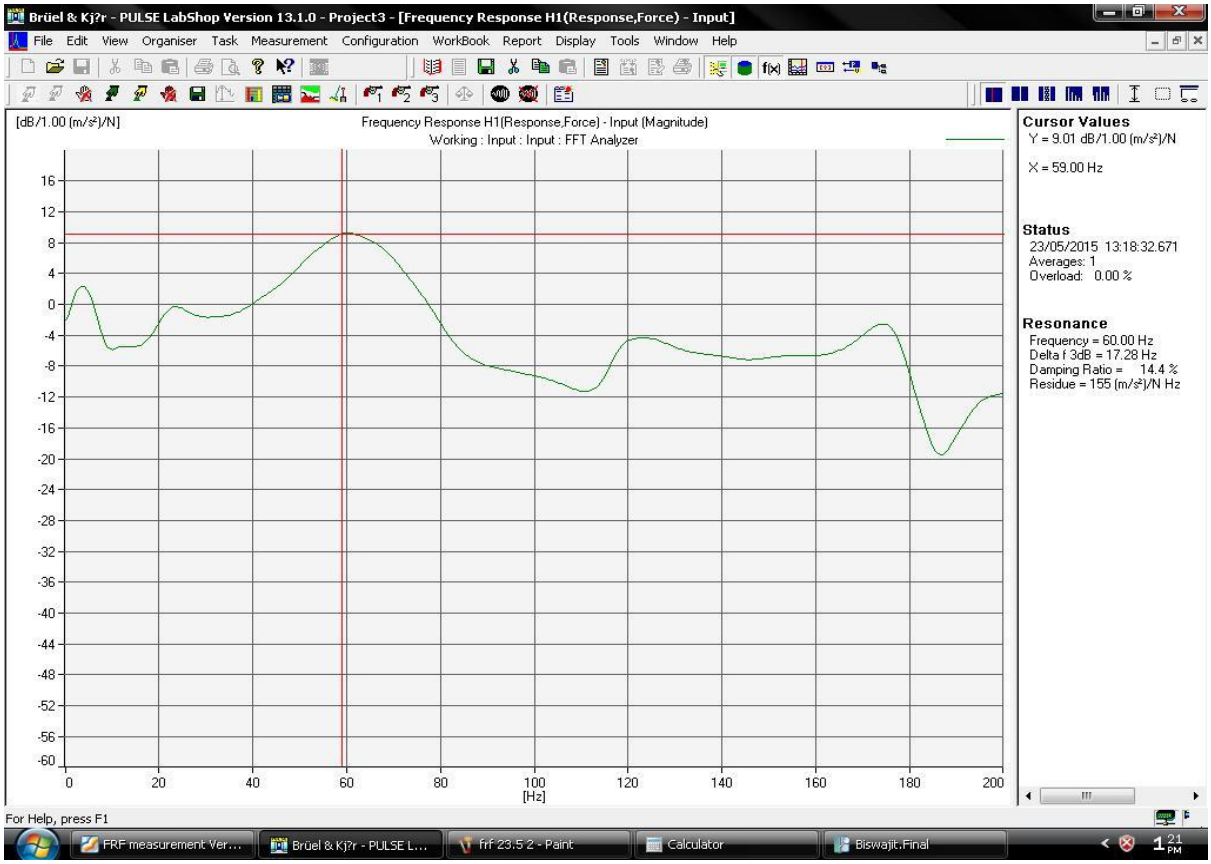


Fig.4.9. Third Natural Frequency of Uncracked beam (L=110cm, b=3.9cm, h=0.5cm)

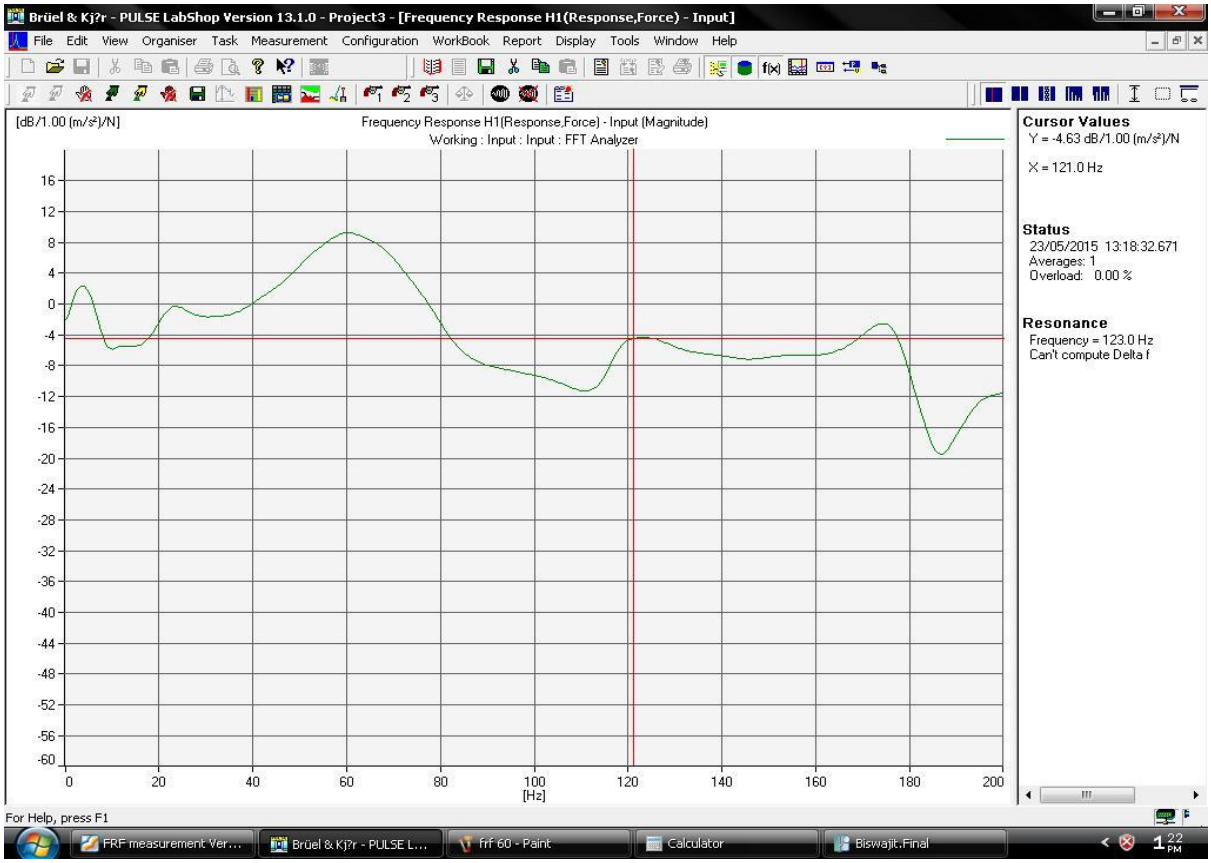


Fig.4.10. Fourth Natural Frequency of Uncracked beam (L=110cm, b=3.9cm, h=0.5cm)

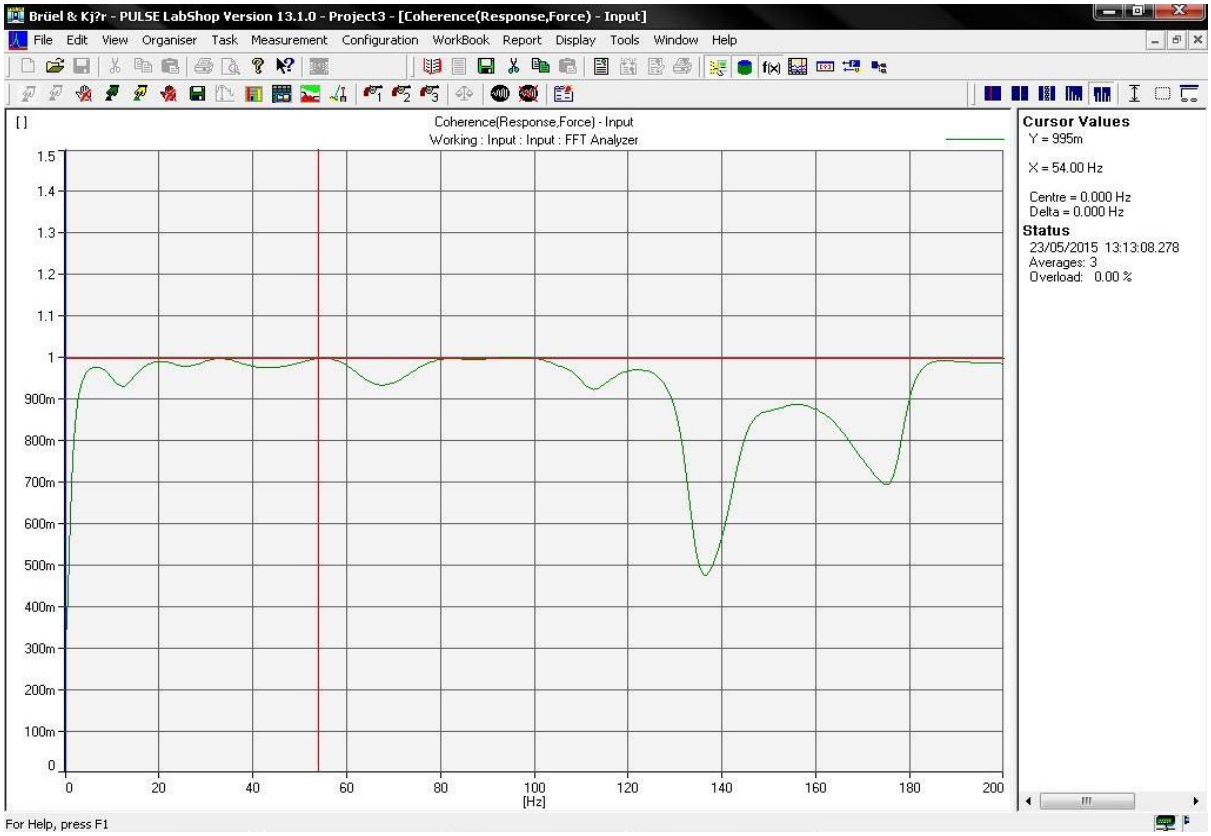


Fig.4.11. Coherence plot

The test was conducted many times, and average values were taken. It is found that the values obtained from ANSYS are within acceptable error limits.

### 4.4. COMPARISON OF RESULTS

**Table 4.1.** Comparison of Natural Frequency for Uncrcaked Beam with L=1.1m, b=0.039m, h=0.005m, ρ=2750kg/m3, E=71GPa

| Mode | Theoretical | ANSYS | Experimental | % error (between Theoretical and Experimental) | % error (between ANSYS and Experimental) | % error (between Theoretical and ANSYS) |
|---|---|---|---|---|---|---|
| 1 | 3.392 | 3.4049 | 3.5 | 3.2% | 2.79% | 0.38% |
| 2 | 21.256 | 21.336 | 23 | 8.2% | 7.8% | 0.37% |
| 3 | 59.504 | 59.74 | 60 | 0.83% | 0.44% | 0.4% |
| 4 | 116.630 | 117.07 | 123 | 5.46% | 5.06% | 0.38% |

**Table 4.2.** Comparison of Natural Frequency for Uncrcaked Beam with L=0.95m, b=0.039m, h=0.005m, ρ=2750kg/m3, E=71GPa

| Mode | Theoretical | ANSYS | Experimental | % error (between Theoretical and Experimental) | % error (between ANSYS and Experimental) | % error (between Theoretical and ANSYS) |
|---|---|---|---|---|---|---|
| 2 | 28.498 | 28.616 | 30 | 5.27% | 4.8% | 0.04% |
| 3 | 79.778 | 80.122 | 80 | 0.28% | 0.15% | 0.04% |
| 4 | 156.369 | 157.01 | 160 | 2.32% | 1.9% | 0.04% |

**Table 4.3.** Comparison of Natural Frequency for Uncrcaked Beam with L=0.8m, b=0.039m, h=0.005m, ρ=2750kg/m3, E=71GPa

| Mode | Theoretical | ANSYS | Experimental | % error (between Theoretical and Experimental) | % error (between ANSYS and Experimental) | % error (between Theoretical and ANSYS) |
|---|---|---|---|---|---|---|
| 2 | 40.178 | 40.372 | 43 | 7.02% | 6.51% | 0.05% |
| 3 | 112.5 | 113.03 | 115 | 2.22% | 1.74% | 0.05% |
| 4 | 220.505 | 221.51 | 230 | 4.31% | 3.83% | 0.05% |

**Table 4.4.** Comparison of Natural Frequency for cracked beam (For $\zeta_1$=0.409 and $\zeta_2$=0.636) (L=1.1m, b=0.039m, h=0.005m, ρ=2750kg/m3, E=71GPa)

| Angle | Mode (Transverse) | ANSYS | Experimental (Cracked) | Error (ANSYS and Experimental) |
|---|---|---|---|---|
| $\theta_1 = 30^0, \theta_2 = 30^0$ | 2 | 21.126 | 22 | 4.14% |
| | 3 | 59.254 | 59 | 0.43% |
| | 4 | 116.78 | 120 | 2.76% |
| $\theta_1 = 90^0, \theta_2 = 90^0$ | 2 | 21.141 | 21 | 0.67% |
| | 3 | 59.295 | 58 | 2.18% |
| | 4 | 116.8 | 119 | 1.88% |
| $\theta_1 = 150^0, \theta_2 = 150^0$ | 2 | 21.109 | 22.5 | 6.59% |
| | 3 | 59.207 | 58.5 | 1.19% |
| | 4 | 116.8 | 117 | 0.17% |

**Table 4.5.** Comparison of Natural Frequency for cracked beam (For $\zeta_1$=0.316 and $\zeta_2$=0.579) (L=0.95m, b=0.039m, h=0.005m, ρ=2750kg/m3, E=71GPa)

| Angle | Mode (Transverse) | ANSYS | Experimental (Cracked) | Error (ANSYS and Experimental) |
|---|---|---|---|---|
| $\theta_1 = 30^0, \theta_2 = 30^0$ | 2 | 28.358 | 29 | 2.2% |
| | 3 | 79.391 | 78 | 1.7% |
| | 4 | 156.37 | 158 | 1.04% |
| $\theta_1 = 90^0, \theta_2 = 90^0$ | 2 | 28.384 | 28 | 1.35% |
| | 3 | 79.476 | 76.5 | 3.74% |
| | 4 | 156.39 | 156 | 0.25% |
| $\theta_1 = 150^0, \theta_2 = 150^0$ | 2 | 28.345 | 28.5 | 0.55% |
| | 3 | 79.399 | 77 | 3.02% |
| | 4 | 156.21 | 157 | 0.51% |

**Table 4.6.** Comparison of Natural Frequency for cracked beam (For $\zeta_1$=0.1875 and $\zeta_2$=0.5) ( L=0.8m, b=0.039m, h=0.005m, ρ=2750kg/m3, E=71GPa)

| Angle | Mode (Transverse) | ANSYS | Experimental (Cracked) | Error (ANSYS and Experimental) |
|---|---|---|---|---|
| $\theta_1 = 30^0, \theta_2 = 30^0$ | 2 | 40.036 | 41 | 2.41% |
| | 3 | 112.82 | 113 | 0.16% |
| | 4 | 218.43 | 220 | 0.72% |
| $\theta_1 = 90^0, \theta_2 = 90^0$ | 2 | 40.109 | 37 | 7.75% |
| | 3 | 112.89 | 110 | 2.56% |
| | 4 | 219.16 | 215 | 1.9% |
| $\theta_1 = 150^0, \theta_2 = 150^0$ | 2 | 39.961 | 42 | 5.1% |
| | 3 | 112.85 | 113 | 0.13% |
| | 4 | 218.08 | 217 | 0.5% |

In the above cases first relative natural frequencies are not considered except the first case. For the cases studied here, the value of first relative frequencies is quite small, and noise becomes a dominant factor. So the percentage error obtained particularly in the first relative natural frequency is quite higher than the error obtained in all other natural frequencies for this particular test specimen. All the above values are averages that are obtained after repeated experiments. The percentage of error is found to be within acceptable limits. So the values obtained from ANSYS can be used for prediction purpose with some consideration for error. Thus, in the next chapter where Fuzzy Logic is used for prediction purpose, values obtained from ANSYS have been used as they were found to be deviating from actual values by small percentages.

# CHAPTER 5

## 5. IMPLEMENTATION OF FUZZY LOGIC FOR FAULT DIAGNOSTIC

Unavailability of previously tabulated data for each and every case of cracked beam requires one to predict or guess in some cases the possible outcomes. For the case of a cantilever beam with two inclined cracks, there are a total of infinite times infinite possibilities that can be considered to detect any change in vibration characteristics of the beam to that of uncracked beam as the inclination of each angle can take infinite possible values from $0^0$-$180^0$. So for all practical purposes some convenient angular inclinations have been taken for each of $\theta_1$ and $\theta_2$, and experimental values have been obtained. But in real life, all cracks are not supposed to fall within one of those values for which experimental data have been obtained. For the cases for which experimental data is not readily available, we have to rely on some other technique(s) to judiciously predict the vibration characteristics. Fuzzy logic is one such technique that can be used for this purpose. Use of fuzzy logic for the prediction of crack location, its severity and inclination is explained in the following sections.

### 5.1. INTRODUCTION

Our understanding of the physical world involves the use of qualitative terms like low, medium, high, etc. in various contexts. These qualitative terms define the physical system rather vaguely but as we the human beings use sophisticated high-level languages for our communication, these vaguely defined terms don't possess a serious problem before us. Rather we arrive at a conclusion effortlessly and quickly.

But the situation changes dramatically when it comes down to the computers to handle complex real-life problems involving vaguely defined terms. Computers use low-level binary language for all purposes. So we have to convert somehow the linguistic variables to some numerical form that can be understood by the computer. After this conversion, the computer

performs the decision-making job more efficiently than human beings. Fuzzy logic uses this technique for various real life decision making.

### 5.2. THEORY OF FUZZY LOGIC

Fuzzy logic uses different membership functions to convert the linguistic variables to its numerical counterpart. Each membership function, over a range, assigns a probability or degree of truthfulness of the linguistic variable for a particular value. The degree of membership varies between 0 and 1. Fuzzy logic uses various type of membership functions like Triangular, Trapezoidal, Gaussian, Generalized Bell, Sigmoid, S- Shaped, and Z- Shaped, etc. to name some. The choice of a particular membership function depends on the problem at hand and a mixture of membership functions, known as Hybrid Membership Function, can be used if the need arises for the same. Following figures show various membership functions.

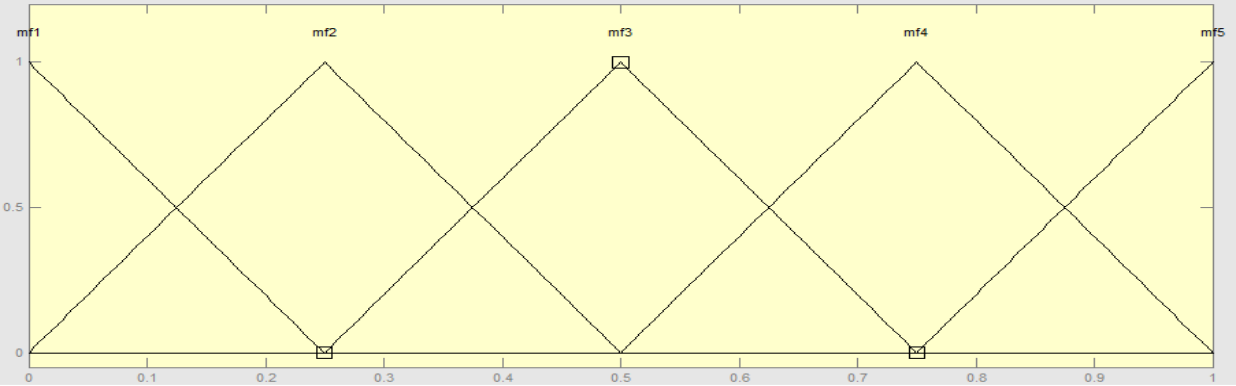


**Fig.5.1.** Triangular Membership Function

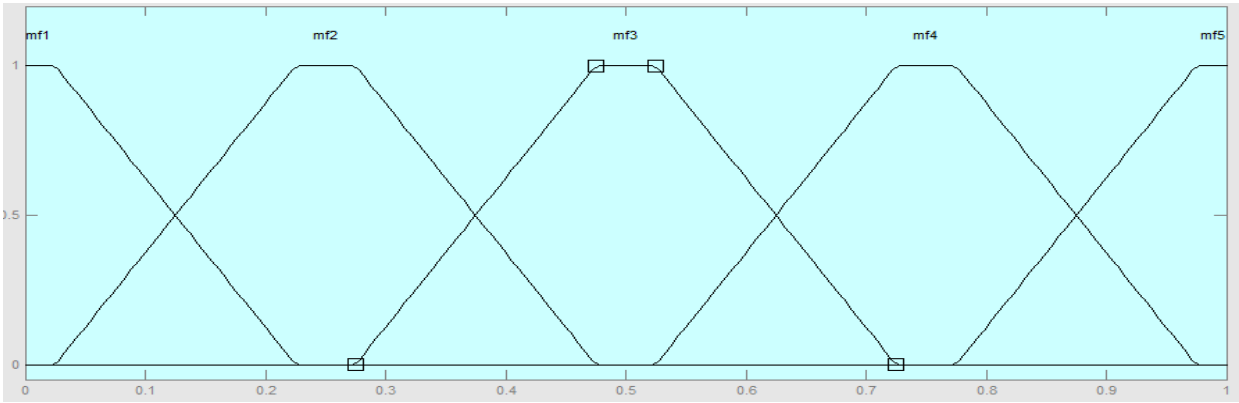


**Fig.5.2.** Trapezoidal Membership Function

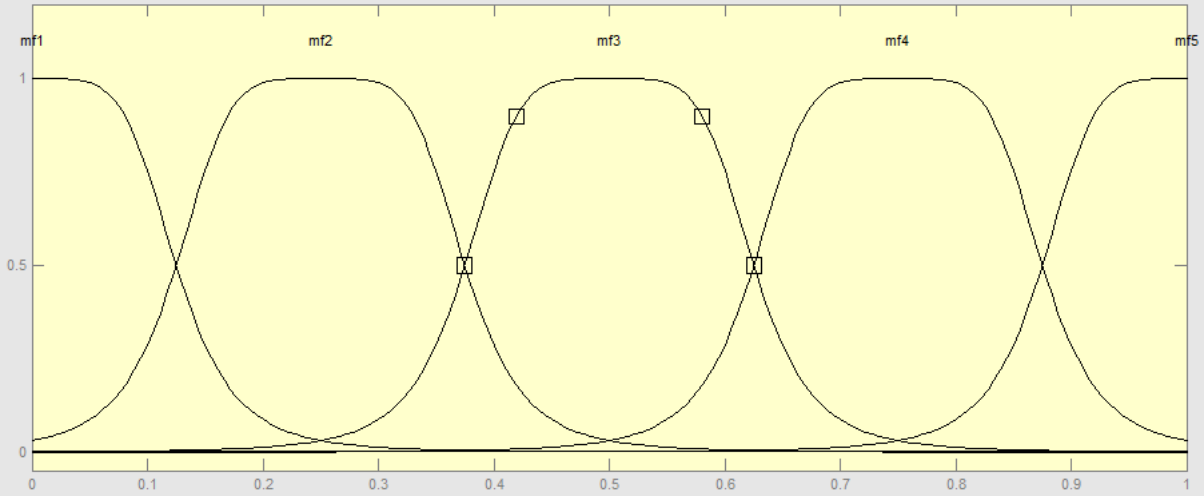


Fig.5.3. Generalized Bell Membership Function

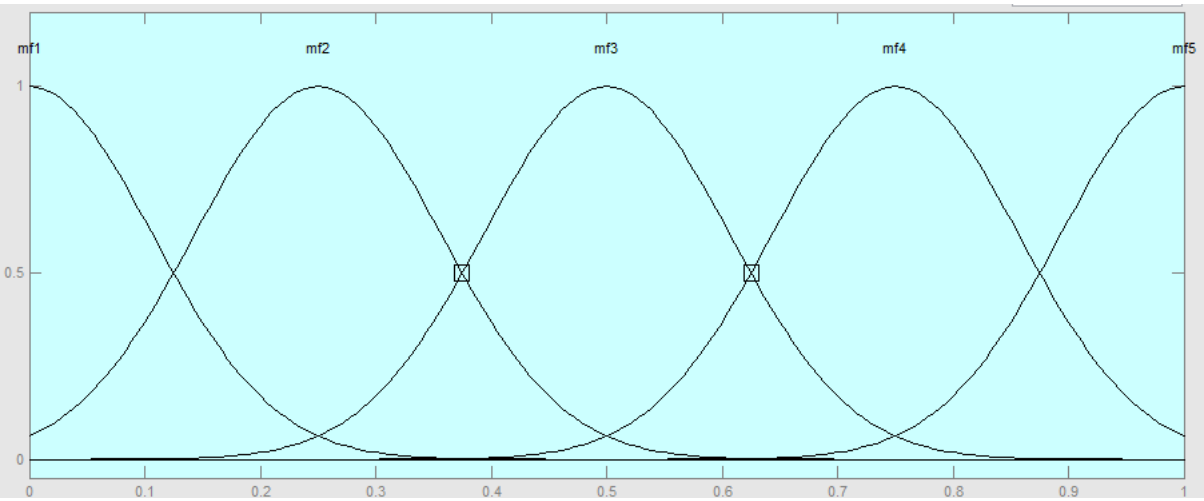


Fig.5.4. Gaussian Membership Function

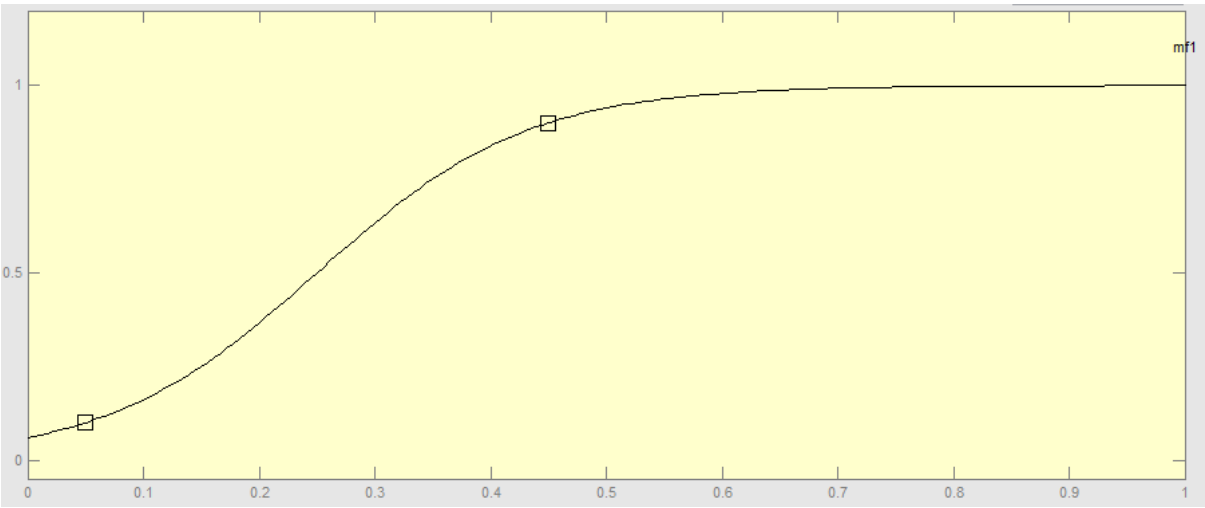


Fig.5.5. Sigmoid Membership Function

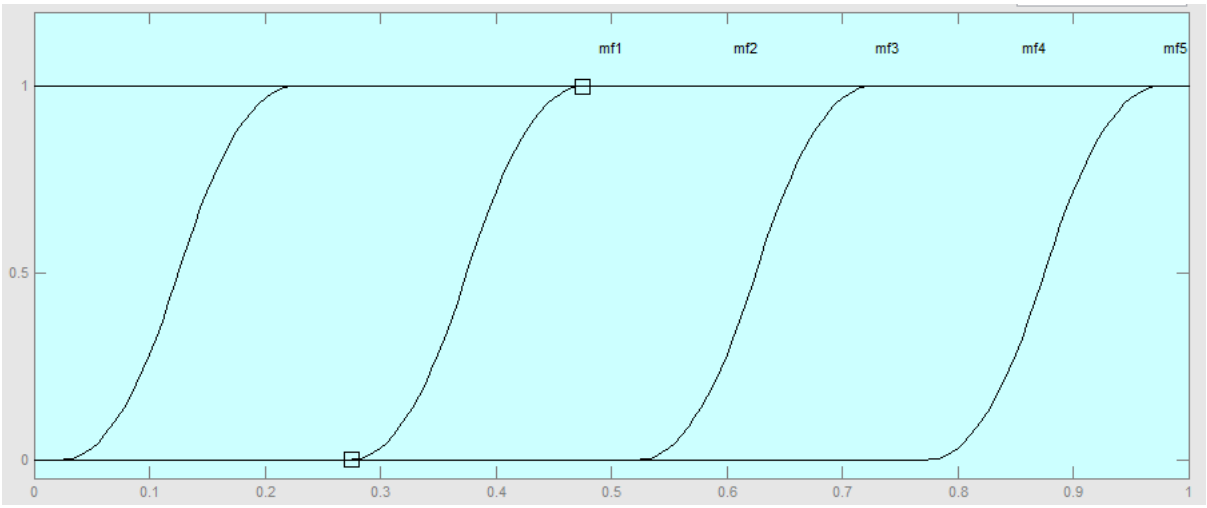


Fig.5.6. S-Shaped Membership Function

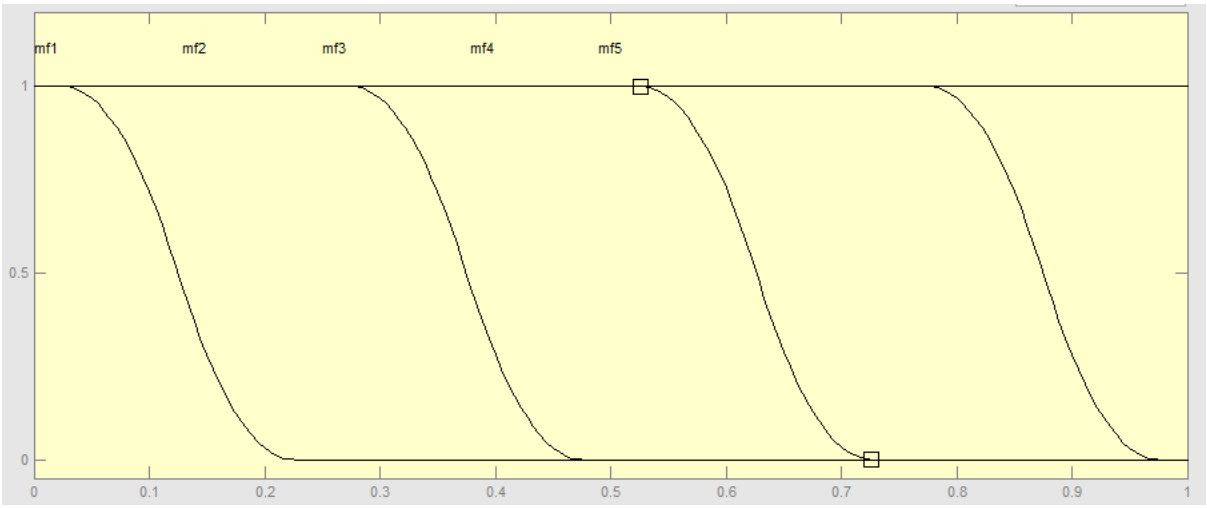


Fig.5.7. Z-Shaped Membership Function

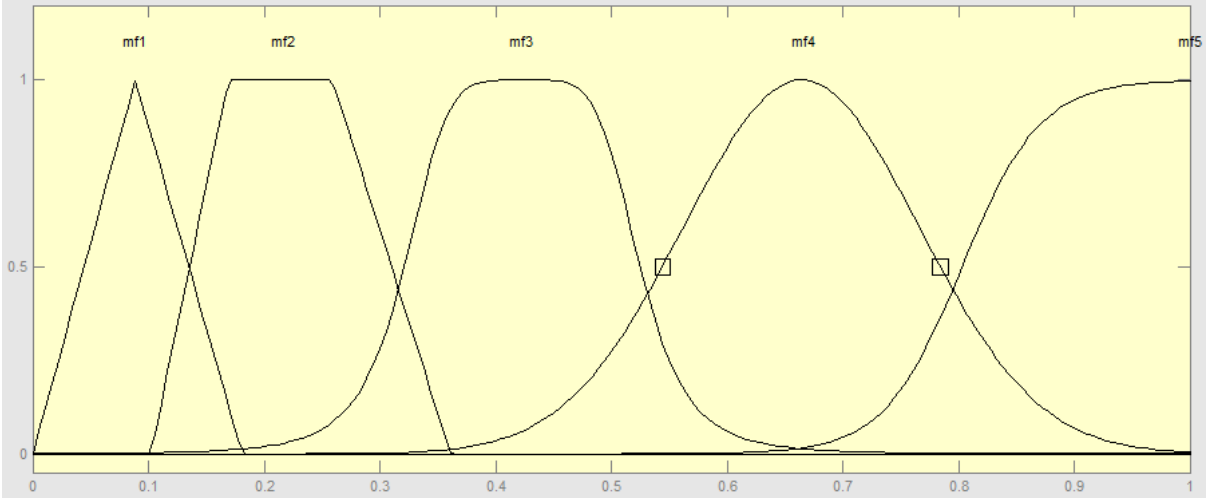


Fig.5.8. Hybrid Membership Function

After selecting a membership function, rules are formulated depending on the problem requirement. Conclusions are extracted from the execution of different rules that are activated depending on the inputs. An output is obtained for each rule, and the weighted average of all outputs is taken for the final output. This type of fuzzy systems is called Mamdani Type inference system. In the next sections, Mamdani type fuzzy systems are used to evaluate the expected crack location, crack severity and crack inclination angle.

### 5.3. ESTIMATION OF CRACK LOCATION USING FUZZY LOGIC

In this section, the expected location of crack will be determined using fuzzy logic using the percentage variation of first, second and third relative natural frequencies. Percentage variation in relative natural frequencies for the first three frequencies will be used as inputs. Total 27 rules have been formulated. The rules are given in Table 5.1. However, it must be remembered that these rules are not universal neither in number of rules nor in its formulation. Reasonable formulation of rules depends on experience and personal expertise in dealing with a particular type of problem. Similarly, the number of rules might vary from person to person along with the membership functions.

Here I have used triangular membership functions. The input being the percentage change in relative natural frequency. For each input, three triangular membership functions have been used. The input range for each membership function is decided from previously calculated data.

The input and output membership functions are shown in the following figures.

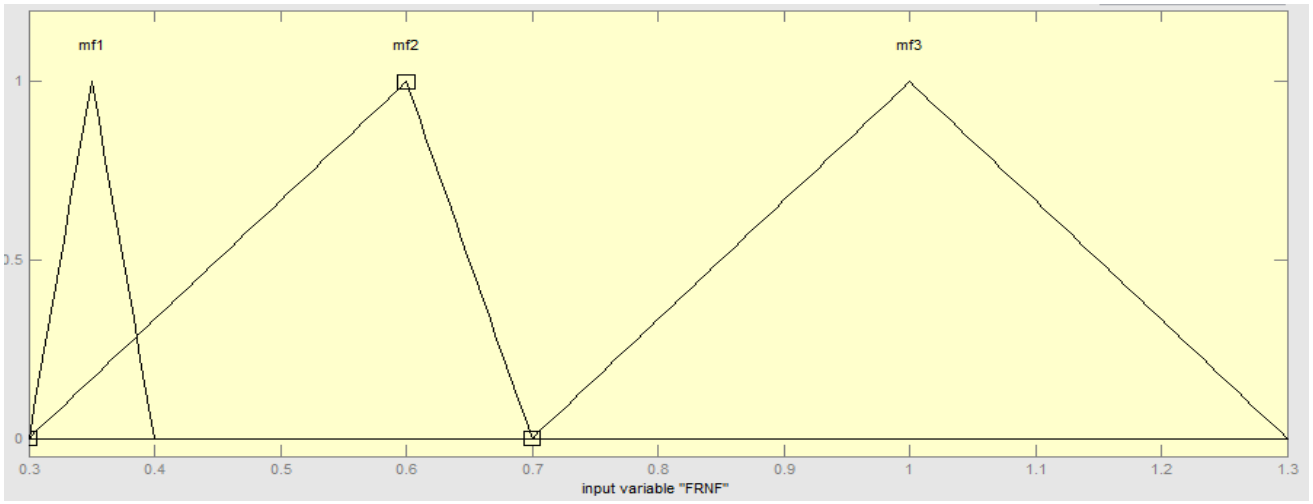


Fig.5.9. Input Variable- Percentage variation in FRNF

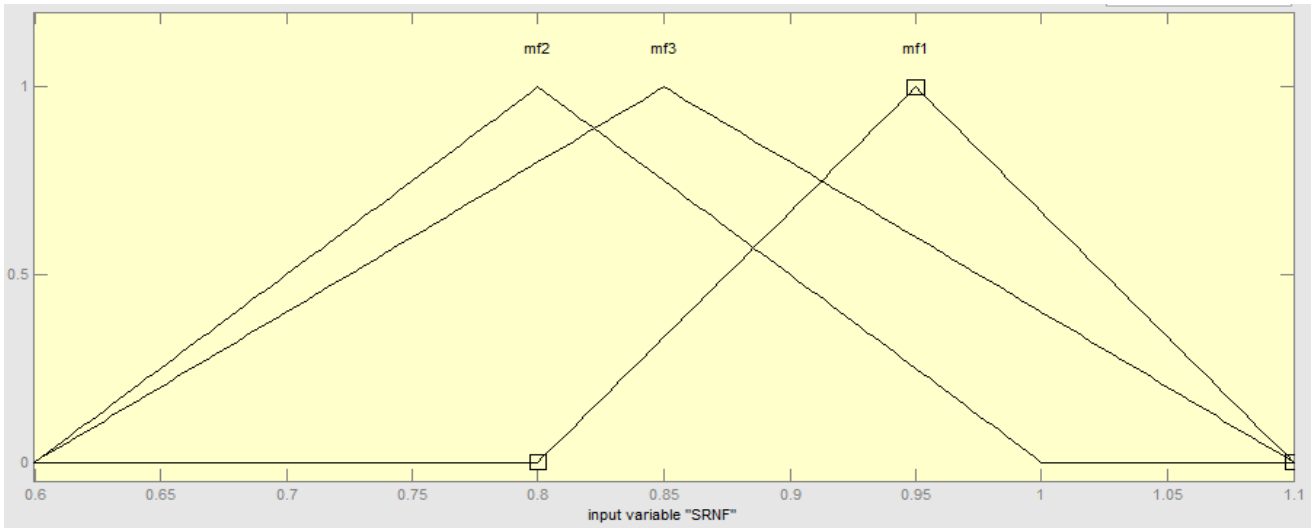


Fig.5.10. Input Variable- Percentage variation in SRNF

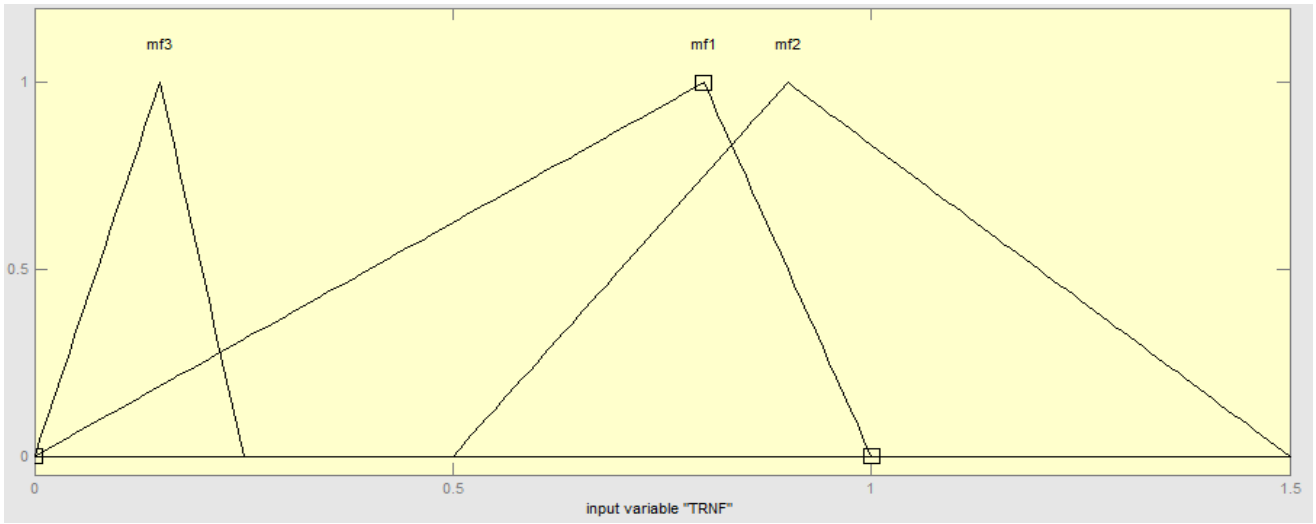


Fig.5.11. Input Variable- Percentage variation in TRNF

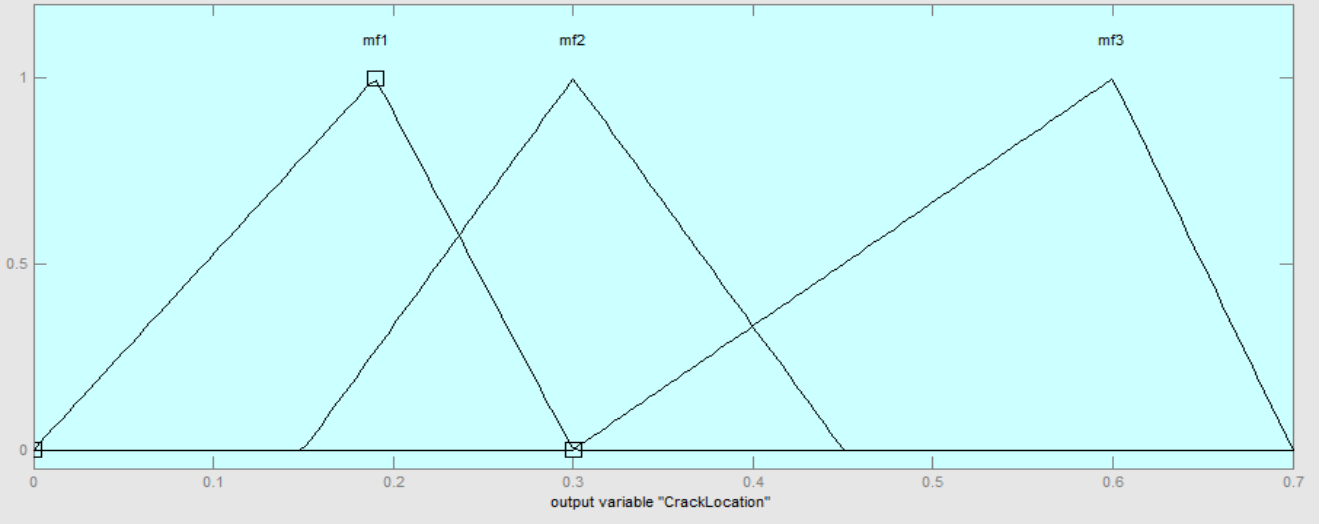


Fig.5.12. Output Variable- Expected Crack Location

Parameters of first Input Variable- Percentage variation in FRNF:

mf1= [0.3 0.35 0.4]

mf2= [0.3 0.6 0.7]

mf3= [0.7 1 1.3]

Parameters of second Input Variable- Percentage variation in SRNF:

mf1= [0.8 0.95 1.1]

mf2= [0.6 0.8 1]

mf3= [0.6 0.85 1.1]

Parameters of third Input Variable- Percentage variation in TRNF (Transverse, i.e. $4^{th}$ RNF as TRNF obtained from ANSYS is a Torsional one):

mf1= [0 0.8 1]

mf2= [0.5 0.9 1.5]

mf3= [0 0.15 0.25]

Parameters of Output Variable- Expected Crack Location:

mf1= [0 0.15 0.3]

mf2= [0.15 0.3 0.45]

mf3= [0.3 0.6 0.7]

### 5.3.1. RULES

**Table 5.1.** Fuzzy Rules for detection of Crack Location

| Sl. No. | FRNF | SRNF | TRNF | Output |
|---|---|---|---|---|
| 1 | mf1 | mf1 | mf1 | mf3 |
| 2 | mf1 | mf1 | mf2 | mf2 |
| 3 | mf1 | mf1 | mf3 | mf3 |
| 4 | mf1 | mf2 | mf1 | mf3 |
| 5 | mf1 | mf2 | mf2 | mf2 |
| 6 | mf1 | mf2 | mf3 | mf2 |
| 7 | mf1 | mf3 | mf1 | mf1 |
| 8 | mf1 | mf3 | mf2 | mf2 |
| 9 | mf1 | mf3 | mf3 | mf1 |
| 10 | mf2 | mf1 | mf1 | mf3 |
| 11 | mf2 | mf1 | mf2 | mf2 |
| 12 | mf2 | mf1 | mf3 | mf3 |
| 13 | mf2 | mf2 | mf1 | mf2 |
| 14 | mf2 | mf2 | mf2 | mf2 |
| 15 | mf2 | mf2 | mf3 | mf2 |
| 16 | mf2 | mf3 | mf1 | mf1 |
| 17 | mf2 | mf3 | mf2 | mf2 |
| 18 | mf2 | mf3 | mf3 | mf2 |
| 19 | mf3 | mf1 | mf1 | mf1 |
| 20 | mf3 | mf1 | mf2 | mf1 |
| 21 | mf3 | mf1 | mf3 | mf3 |
| 22 | mf3 | mf2 | mf1 | mf1 |
| 23 | mf3 | mf2 | mf2 | mf1 |
| 24 | mf3 | mf2 | mf3 | mf1 |
| 25 | mf3 | mf3 | mf1 | mf1 |
| 26 | mf3 | mf3 | mf2 | mf1 |
| 27 | mf3 | mf3 | mf3 | mf1 |

All rules are If-Then type rules connected by AND operator.

### 5.3.2. RESULTS

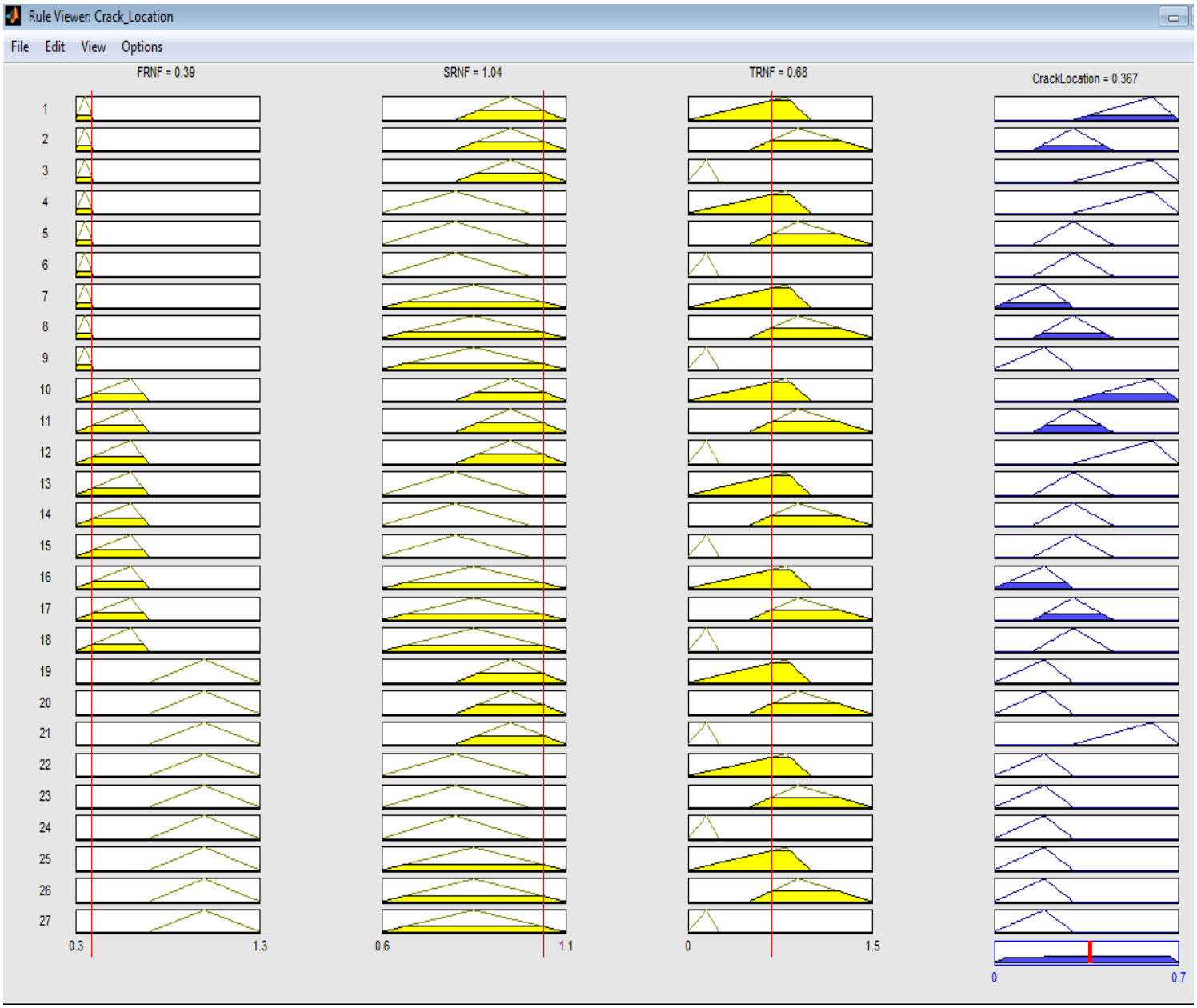


Fig.5.13. Application of Rules for FRNF=0.39, SRNF=1.04, TRNF=0.68 (Output=0.367)

When values of percentage variation of FRNF, SRNF and TRNF were chosen randomly from tabulated data that were obtained for $\zeta_1$=0.409 and $\zeta_2$=0.636, the fuzzy rules (Table 5.1.) predicted the expected relative location to be 0.367 which is greater than $\zeta_1$=0.316 and $\zeta_1$=0.1875 and in close agreement with $\zeta_1$=0.409. The application of rule the has been shown in Fig.5.12 which has been obtained in MATLAB.

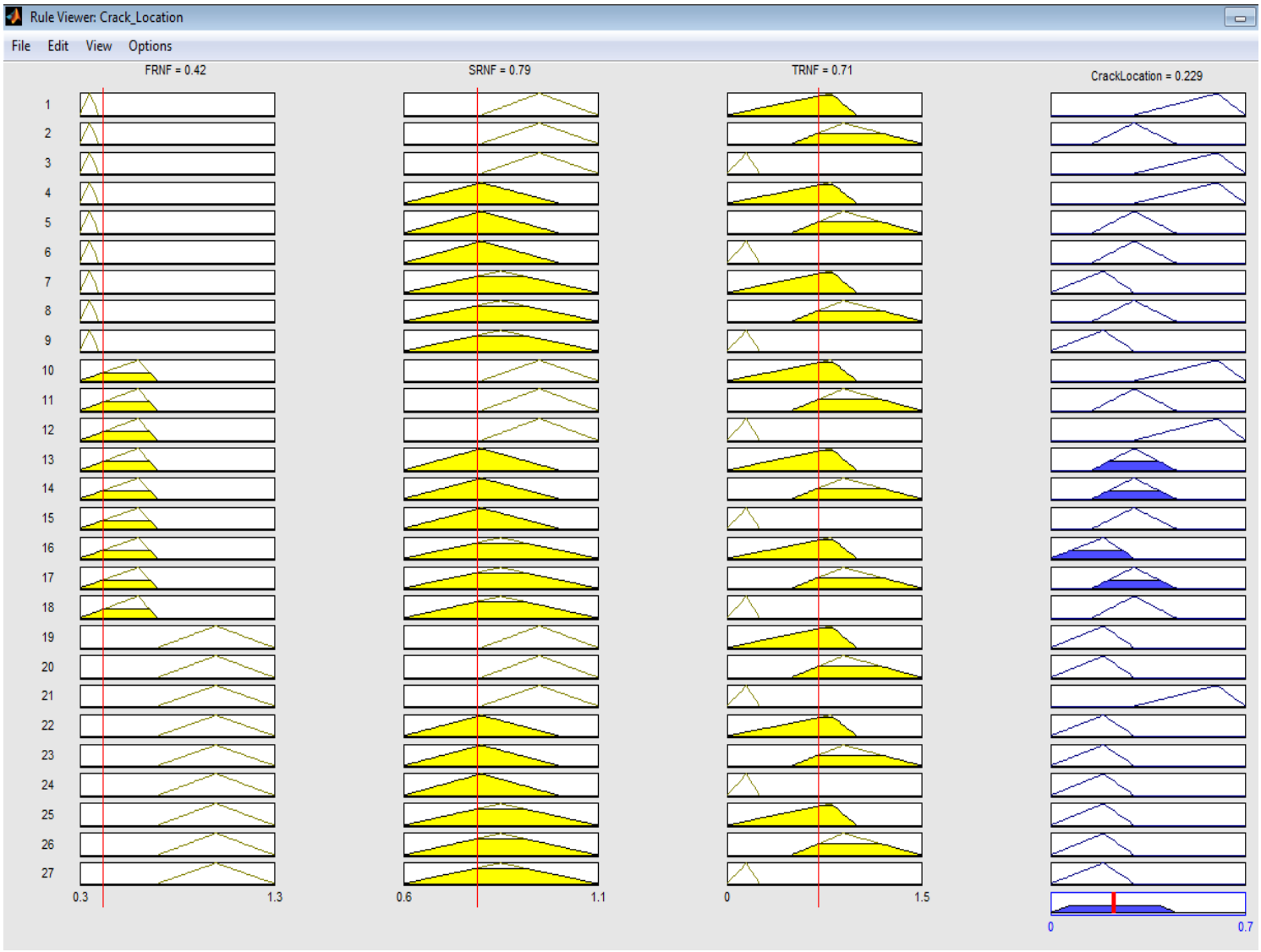


Fig.5.14. Application of Rules for FRNF=0.42, SRNF=0.79, TRNF=0.71 (Output=0.229)

When values of percentage variation of FRNF, SRNF and TRNF were chosen randomly from tabulated data that were obtained for $\zeta_1$=0.316 and $\zeta_2$=0.579, the fuzzy rules (Table 5.1.) predicted the expected relative location to be 0.229 which is greater than $\zeta_1$=0.1875 but smaller than $\zeta_1$=0.409. It is in reasonable agreement with $\zeta_1$=0.316. The application of rule the has been shown in Fig.5.13 which has been obtained in MATLAB.

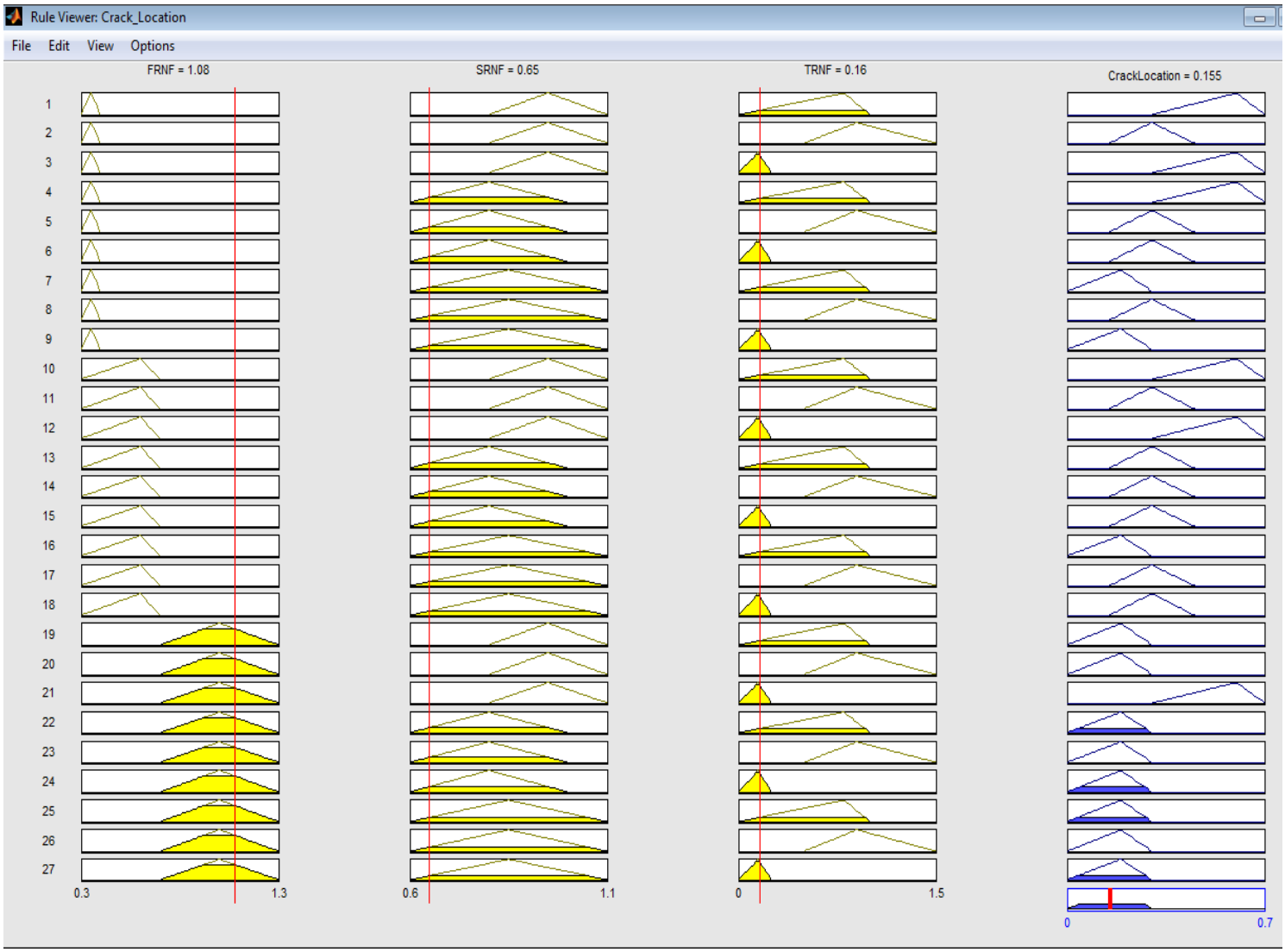


Fig.5.15. Application of Rules for FRNF=1.08, SRNF=0.65, TRNF=0.16 (Output=0.155)

When values of percentage variation of FRNF, SRNF and TRNF were chosen randomly from tabulated data that were obtained for $\zeta_1$=0.1875 and $\zeta_2$=0.5, the fuzzy rules (Table 5.1.) predicted the expected relative location to be 0.155 which is smaller than $\zeta_1$=0.1875 and is in close agreement with $\zeta_1$=0.316. The application of rule has been shown in Fig.5.14 which has been obtained in MATLAB. The surface plots of rules for various input parameters have been shown in Fig.5.15, 5.16 and 5.17.

**Table 5.2. Validation of Fuzzy Results with Results Obtained From ANSYS**

| Relative Crack length | % Variation in FRNF | % Variation in SRNF | % Variation in TRNF | Fuzzy Logic Result | % error |
|---|---|---|---|---|---|
| $\zeta_1$=0.409 and $\zeta_2$=0.636 | 0.39 | 1.04 | 0.68 | 0.367 | 10.3% |
| | 0.32 | 0.98 | 0.82 | 0.359 | 12.2% |
| $\zeta_1$=0.316 and $\zeta_2$=0.579 | 0.42 | 0.79 | 0.71 | 0.229 | 27.5% |
| | 0.44 | 0.69 | 0.9 | 0.236 | 25.3% |
| $\zeta_1$=0.1875 and $\zeta_2$=0.80 | 1.08 | 0.65 | 0.16 | 0.155 | 17.3% |
| | 1.15 | 0.8 | 0.12 | 0.159 | 15.2% |

The above table indicates that when randomly chosen values were taken from known relative lengths, the Fuzzy Result was found to be close to the previously known relative lengths. For instance, 0.3, 1.04 and 0.68 are randomly chosen percentage change in FRNF, SRNF and TRNF when $\zeta_1$=0.409 and $\zeta_2$=0.636 (known). When these three inputs were given to the Fuzzy System the result i.e. expected relative crack location was found to be 0.367.

### 5.3.3. SURFACE PLOTS

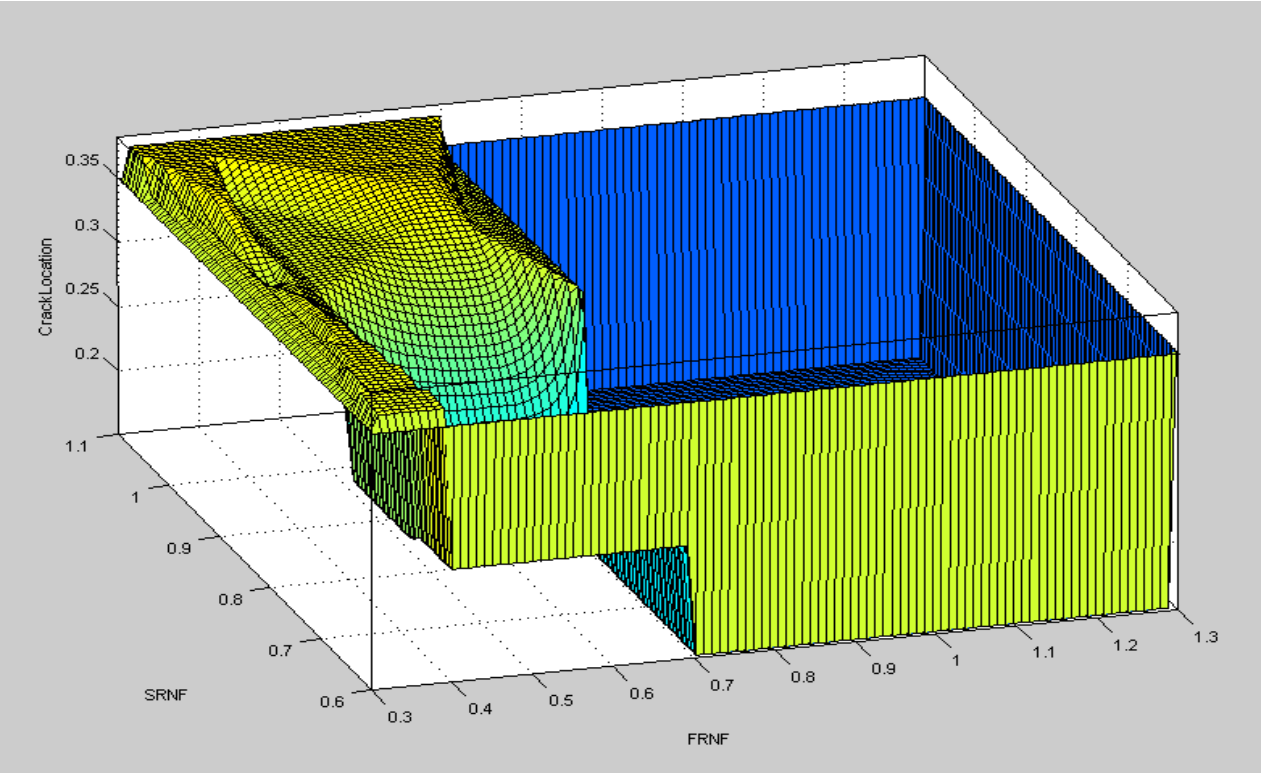


Fig.5.16. Surface plot of rules with FRNF and SRNF as input with crack location as output

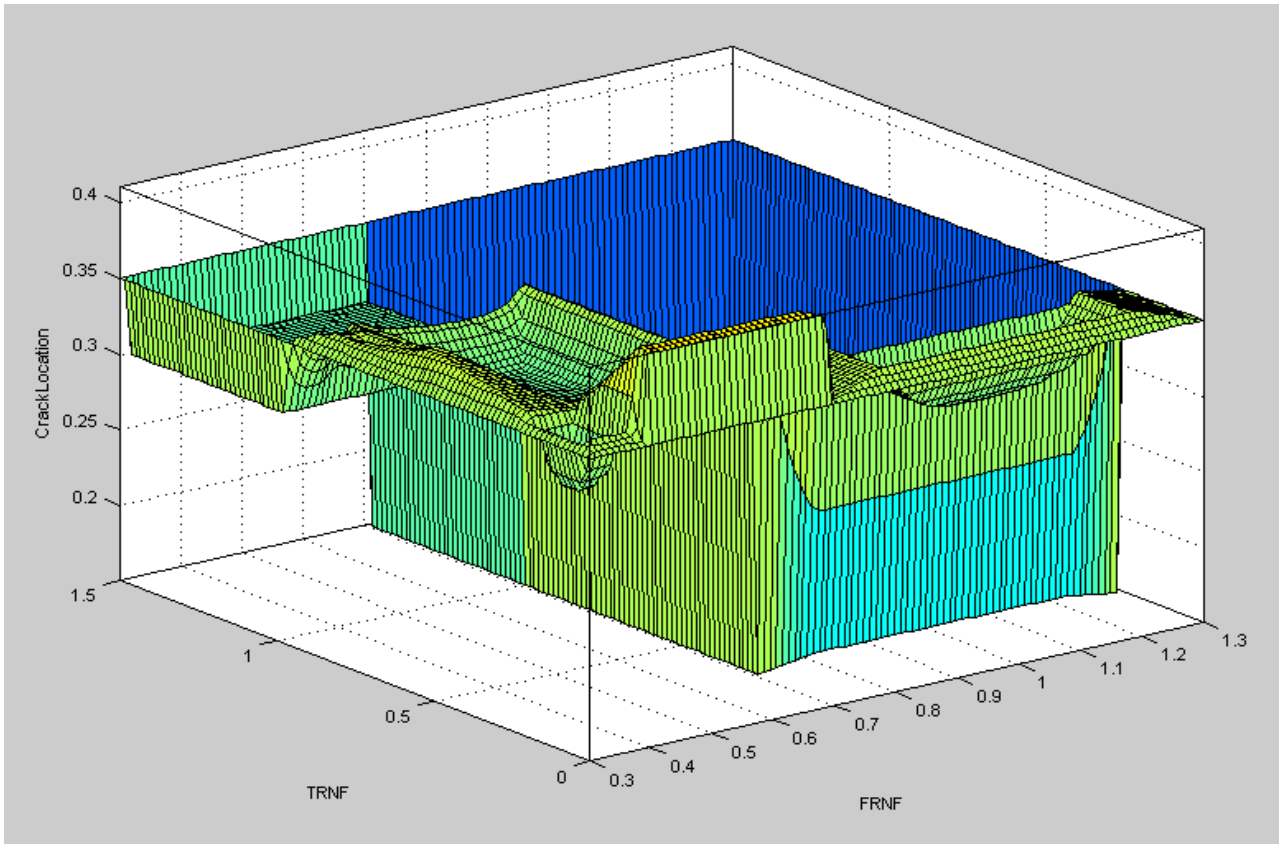


Fig.5.17. Surface plot of rules with FRNF and TRNF as input with crack location as output

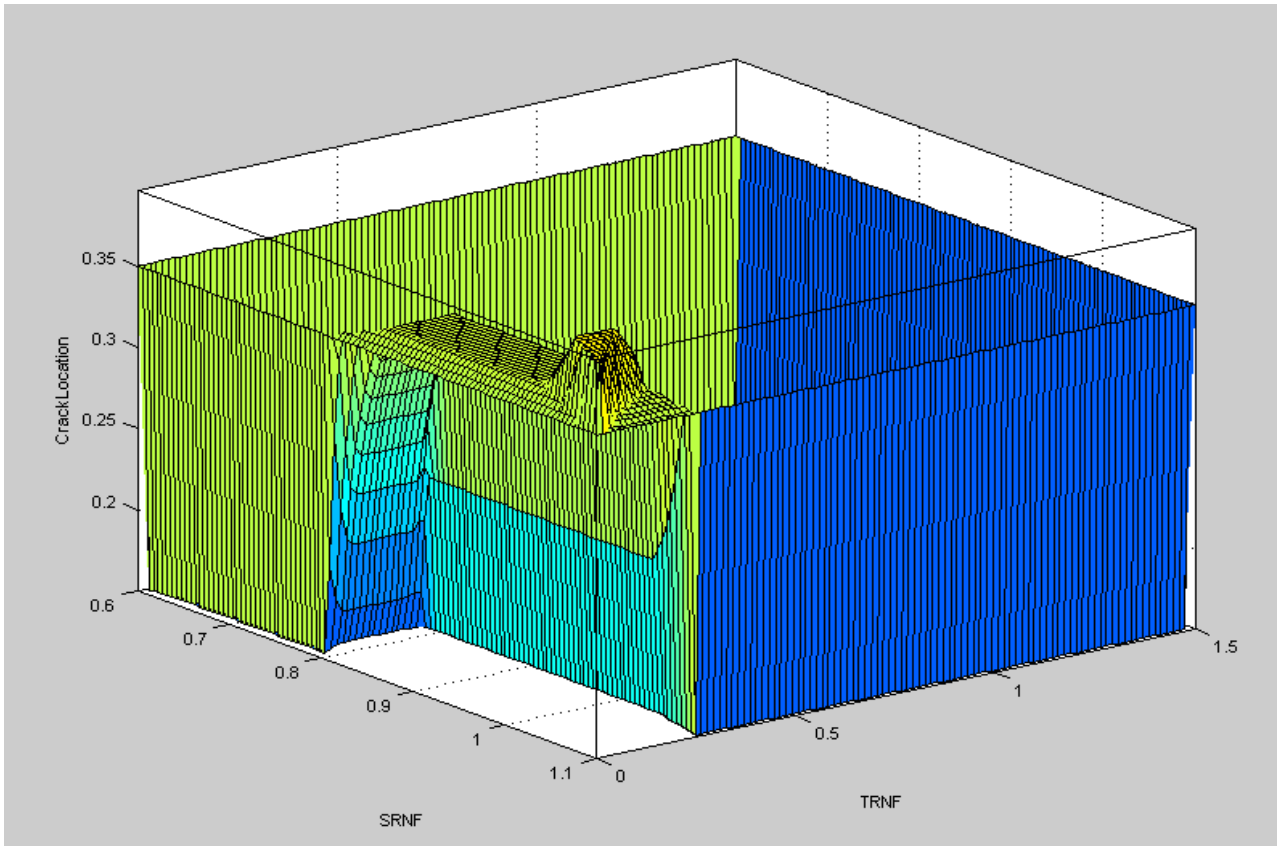


Fig.5.18. Surface plot of rules with TRNF and SRNF as input with crack location as output

## 5.4. ESTIMATION OF CRACK INCLINATION ANGLE USING FUZZY LOGIC

In this section, the expected crack inclination angle will be determined using fuzzy logic using the percentage variation of first, second and third relative natural frequencies. Percentage variation in relative natural frequencies for the first three frequencies will be used as inputs. Total 27 rules have been formulated. The rules are given in Table 5.2. However, it must be remembered that these rules are not universal neither in number of rules nor in its formulation. Reasonable formulation of rules depends on experience and personal expertise in dealing with a particular type of problem. Similarly, the number of rules might vary from person to person along with the membership functions.

Here I have used triangular membership functions. The input being the percentage change in relative natural frequency. For each input, three triangular membership functions have been used. The input range for each membership function is decided from previously calculated data.

The input and output membership functions are shown in the following figures.

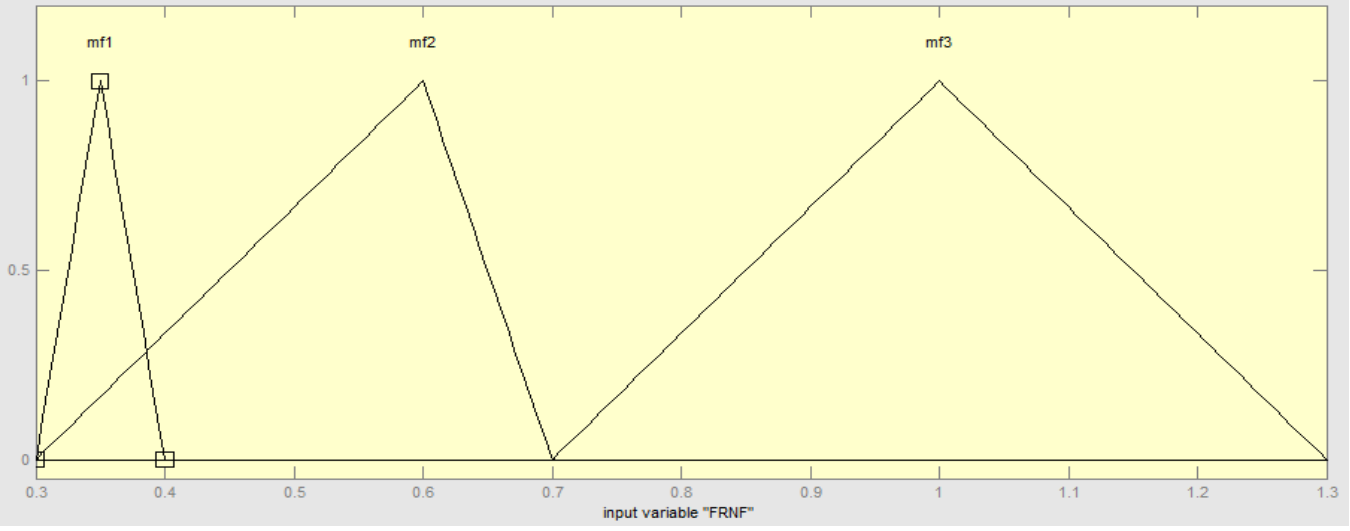


Fig.5.19. Input Variable- Percentage variation in FRNF

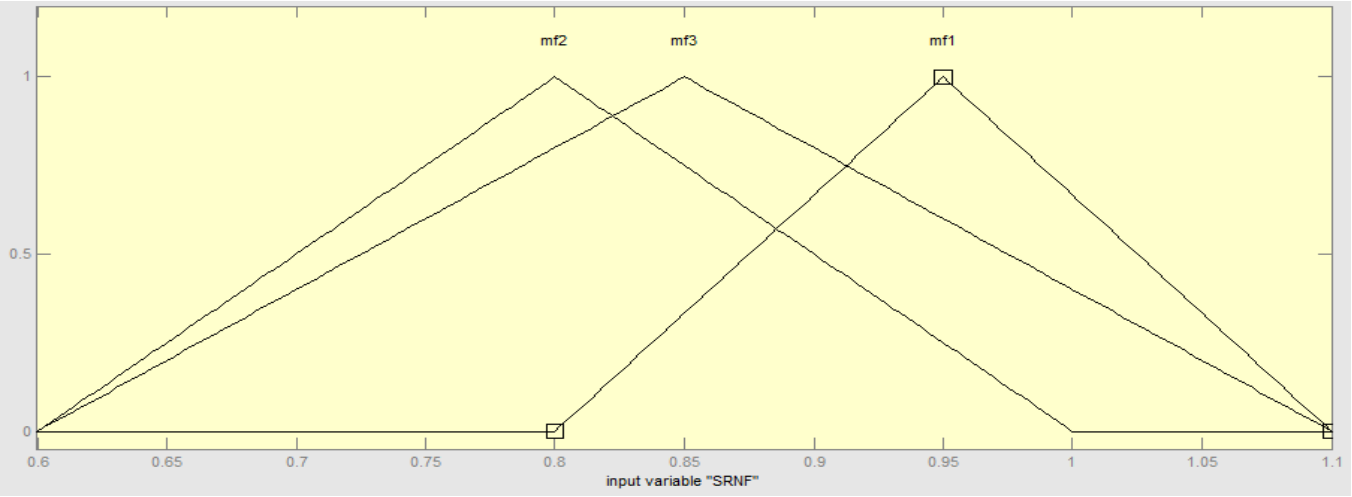


Fig.5.20. Input Variable- Percentage variation in SRNF

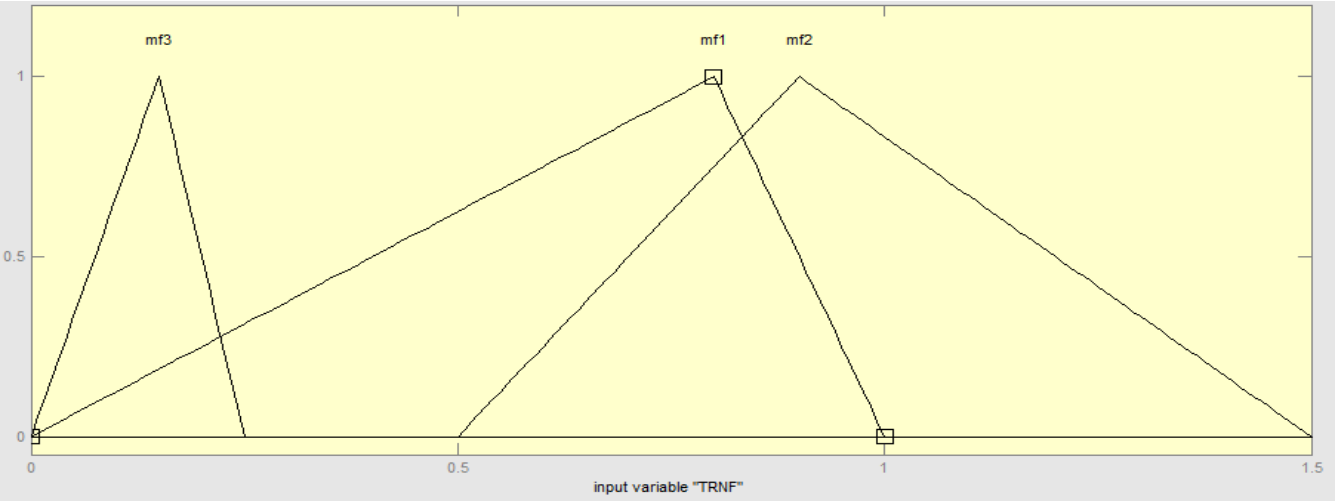


Fig.5.21. Input Variable- Percentage variation in TRNF

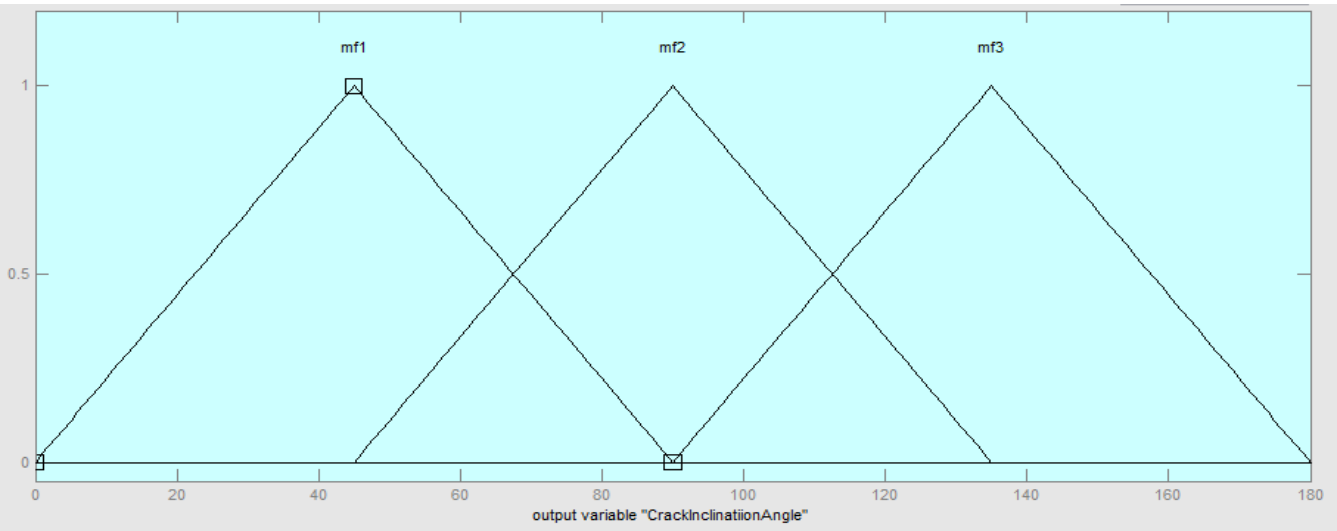


Fig.5.22. Output Variable- Expected Crack Location

Parameters of first Input Variable- Percentage variation in FRNF:

mf1= [0.3 0.35 0.4]

mf2= [0.3 0.6 0.7]

mf3= [0.7 1 1.3]

Parameters of second Input Variable- Percentage variation in SRNF:

mf1= [0.8 0.95 1.1]

mf2= [0.6 0.8 1]

mf3= [0.6 0.85 1.1]

Parameters of third Input Variable- Percentage variation in TRNF (Transverse):

mf1= [0 0.8 1]

mf2= [0.5 0.9 1.5]

mf3= [0 0.15 0.25]

Parameters of Output Variable- Expected Crack Inclination Angle:

mf1= [0 45 90]

mf2= [45 90 135]

mf3= [90 135 180]

### 5.4.1. RULES

**Table 5.3.** Fuzzy Rules for detection of Crack Inclination Angle

| Sl. No. | FRNF | SRNF | TRNF | Output |
|---|---|---|---|---|
| 1 | mf1 | mf1 | mf1 | mf3 |
| 2 | mf1 | mf1 | mf2 | mf1 |
| 3 | mf1 | mf1 | mf3 | mf3 |
| 4 | mf1 | mf2 | mf1 | mf2 |
| 5 | mf1 | mf2 | mf2 | mf2 |
| 6 | mf1 | mf2 | mf3 | mf3 |
| 7 | mf1 | mf3 | mf1 | mf1 |
| 8 | mf1 | mf3 | mf2 | mf3 |
| 9 | mf1 | mf3 | mf3 | mf1 |
| 10 | mf2 | mf1 | mf1 | mf1 |
| 11 | mf2 | mf1 | mf2 | mf1 |
| 12 | mf2 | mf1 | mf3 | mf3 |
| 13 | mf2 | mf2 | mf1 | mf2 |
| 14 | mf2 | mf2 | mf2 | mf2 |
| 15 | mf2 | mf2 | mf3 | mf3 |
| 16 | mf2 | mf3 | mf1 | mf1 |
| 17 | mf2 | mf3 | mf2 | mf2 |
| 18 | mf2 | mf3 | mf3 | mf3 |
| 19 | mf3 | mf1 | mf1 | mf2 |
| 20 | mf3 | mf1 | mf2 | mf2 |
| 21 | mf3 | mf1 | mf3 | mf1 |
| 22 | mf3 | mf2 | mf1 | mf2 |
| 23 | mf3 | mf2 | mf2 | mf3 |
| 24 | mf3 | mf2 | mf3 | mf2 |
| 25 | mf3 | mf3 | mf1 | mf2 |
| 26 | mf3 | mf3 | mf2 | mf1 |
| 27 | mf3 | mf3 | mf3 | mf1 |

All rules are If-Then type rules connected by AND operator.

### 5.4.2. RESULTS

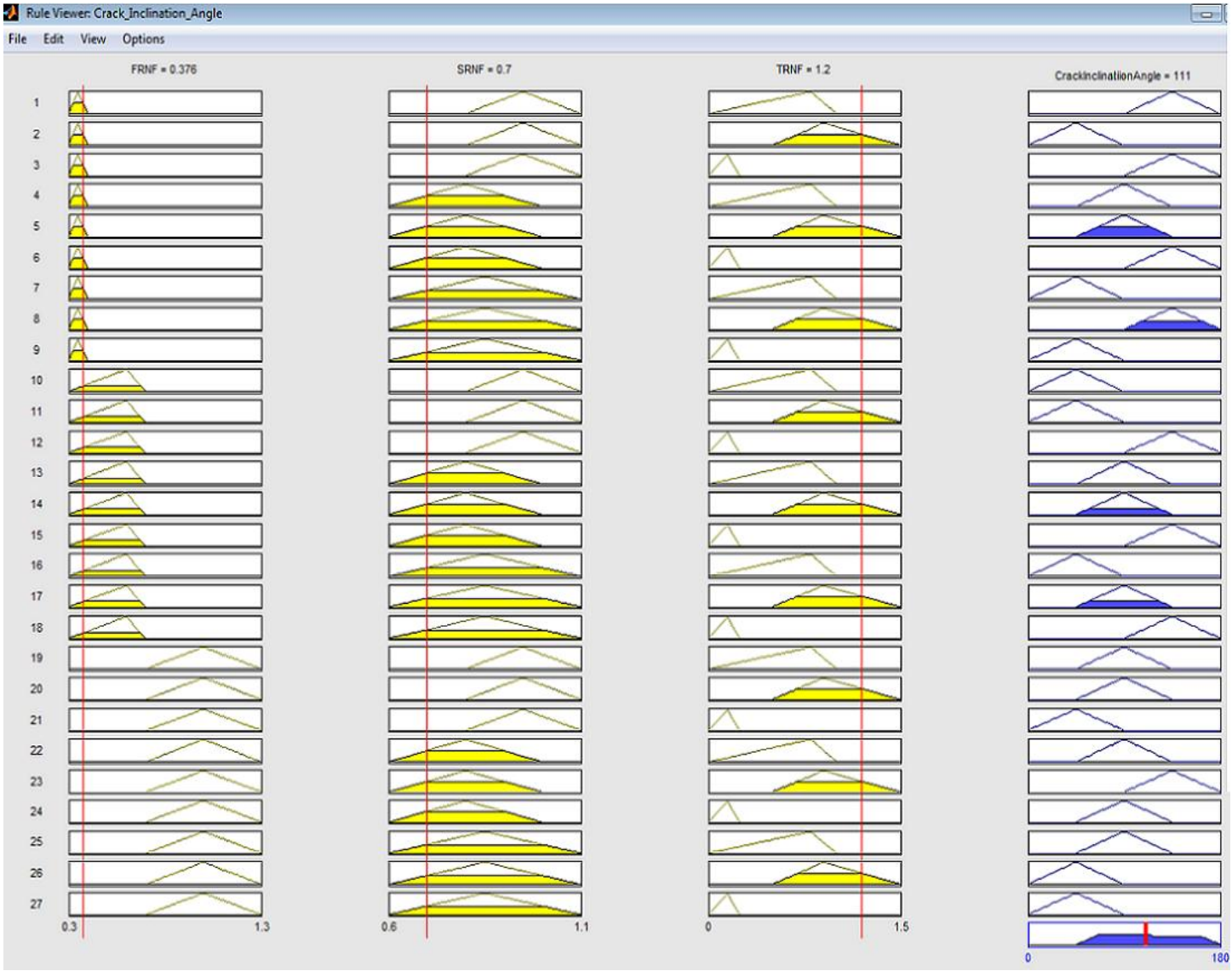


Fig.5.23. Application of Rules for FRNF=0.376, SRNF=0.7, TRNF=1.2 (Output=111)

When values of percentage variation of FRNF, SRNF and TRNF were chosen to be 0.376, 0.7 and 1.2 respectively, the output inclination angle was found to be $111^0$. The application of the rule has been shown in Fig.5.22, which has been obtained in MATLAB. The Fuzzy System gave excellent answers for $90^0$ inclination angle. Better result for other angles can be obtained by modifying the membership functions as well as formulating more number of rules. The surface plots of rules for various input parameters have been shown in Fig.5.23, 5.24 and 5.25.

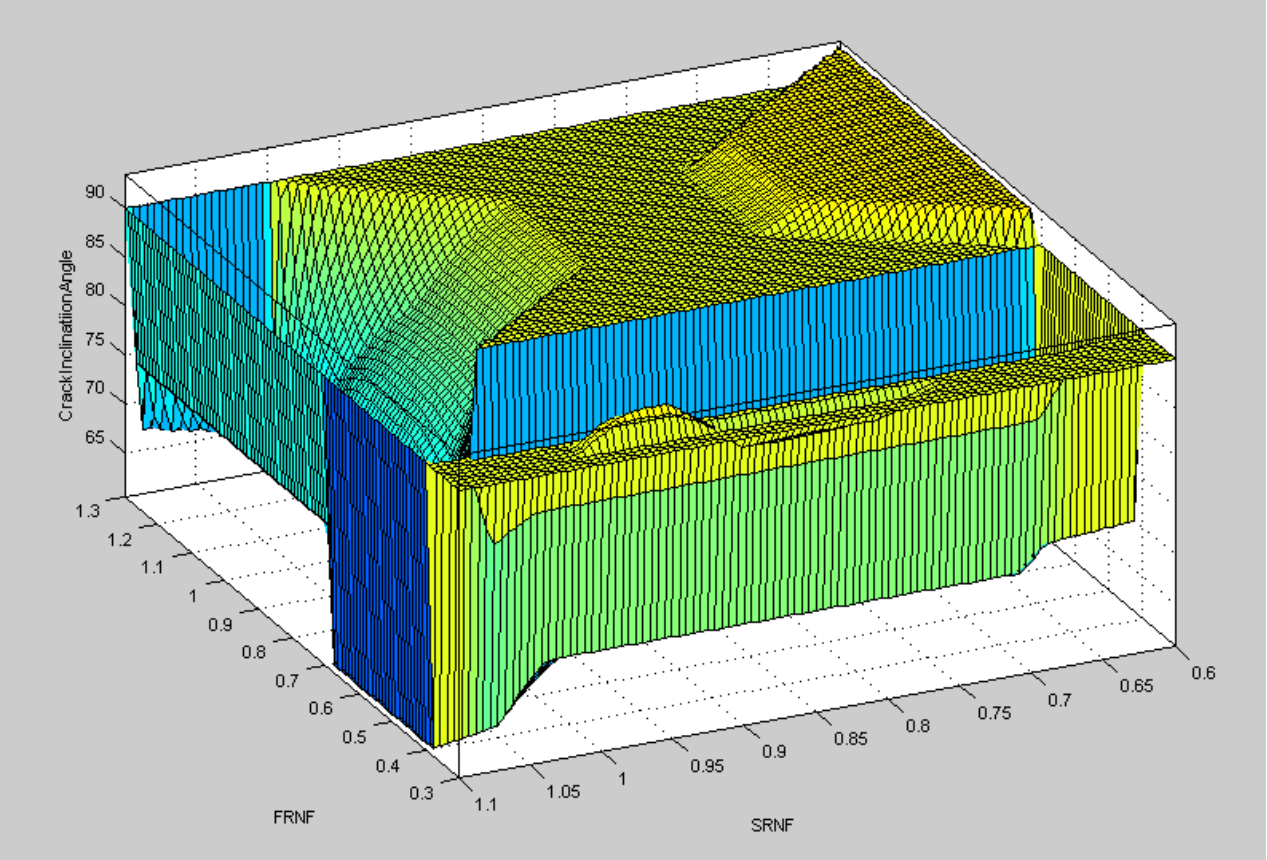


Fig.5.24. Surface plot of rules with SRNF and FRNF as input with crack inclination angle as output

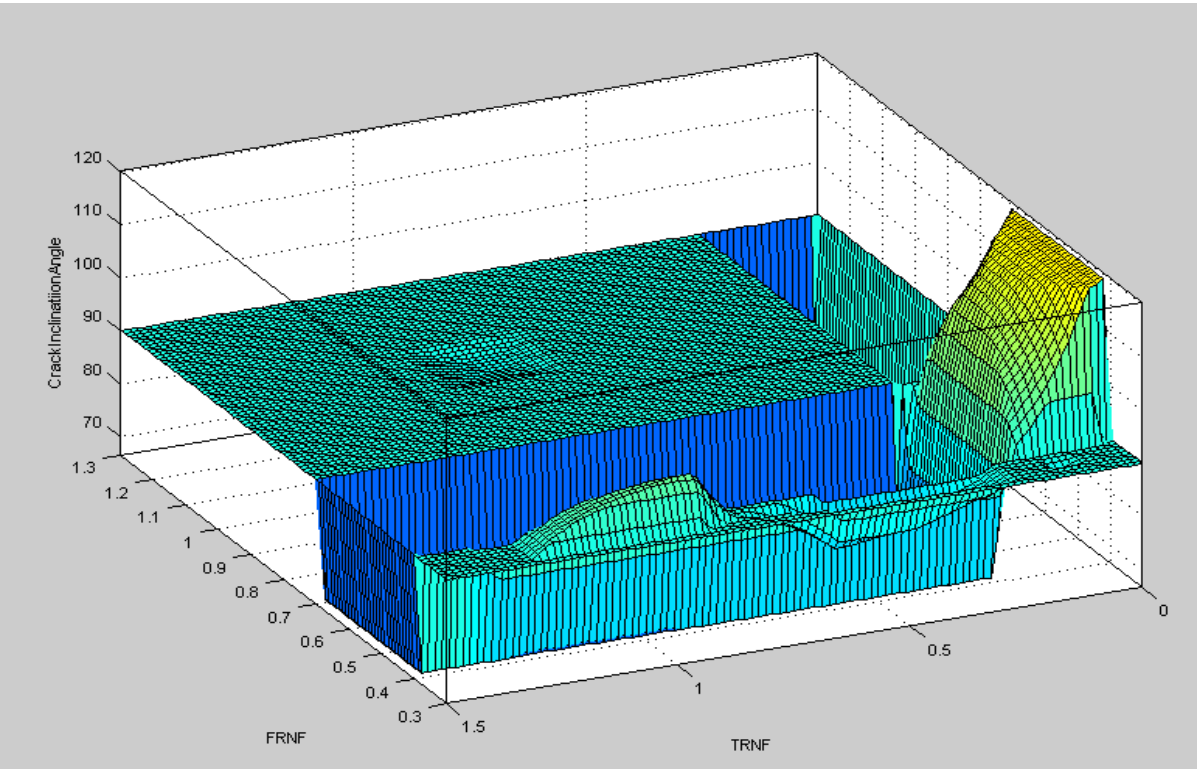


Fig.5.25. Surface plot of rules with TRNF and FRNF as input with crack inclination angle as output

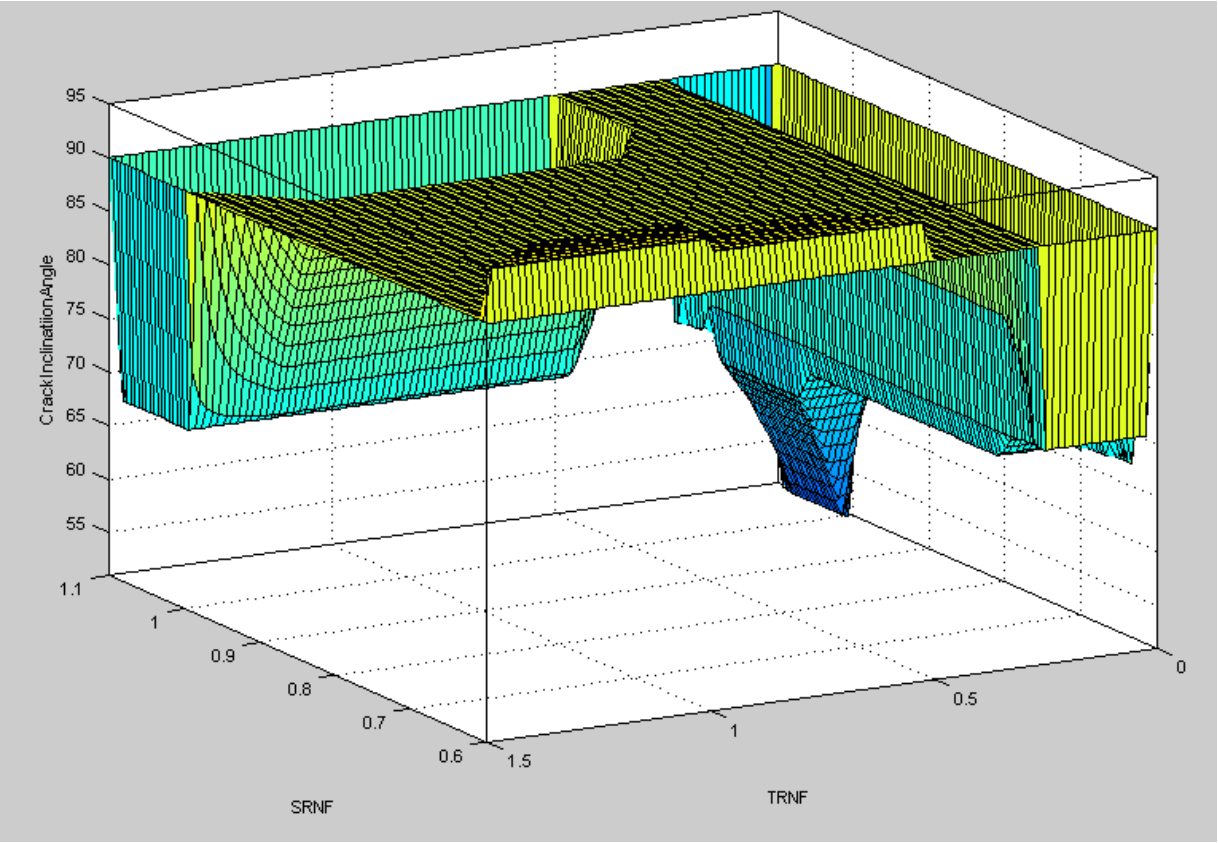


Fig.5.26. Surface plot of rules with TRNF and SRNF as input with crack inclination angle as output

## 5.5. ESTIMATION OF CRACK SEVERITY USING FUZZY LOGIC

In this section, the crack severity will be determined using fuzzy logic using the percentage variation of first, second and third relative natural frequencies. Percentage variation in relative natural frequencies for the first three frequencies will be used as inputs. Total 27 rules have been formulated. The rules are given in Table 5.3. However, it must be remembered that these rules are not universal neither in number of rules nor in its formulation. Reasonable formulation of rules depends on experience and personal expertise in dealing with a particular type of problem. Similarly, the number of rules might vary from person to person along with the membership functions.

Here I have used triangular membership functions. The input being the percentage change in relative natural frequency. For each input, three triangular membership functions

have been used. The input range for each membership function is decided from previously calculated data.

The input and output membership functions are shown in the following figures.

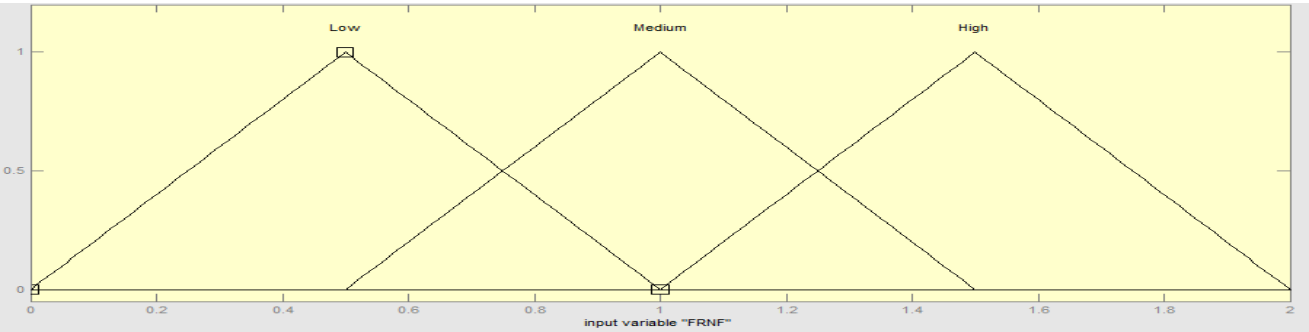


Fig.5.27. Input Variable- Percentage variation in FRNF

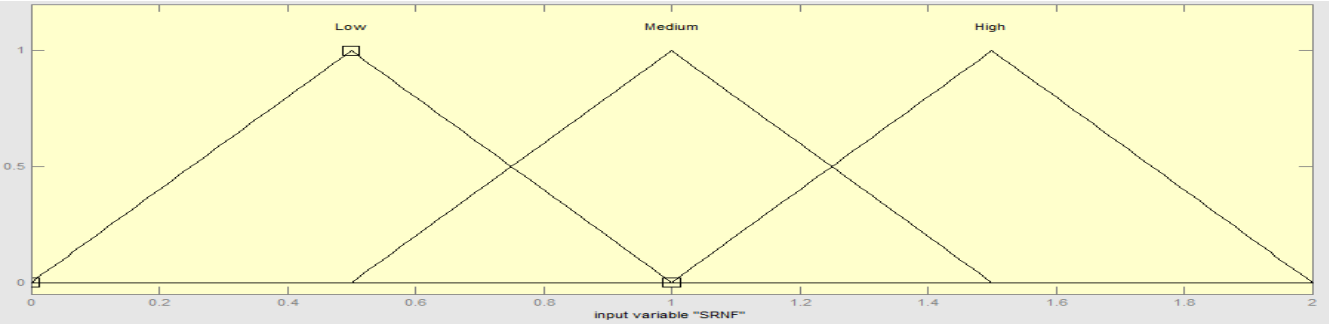


Fig.5.28. Input Variable- Percentage variation in SRNF

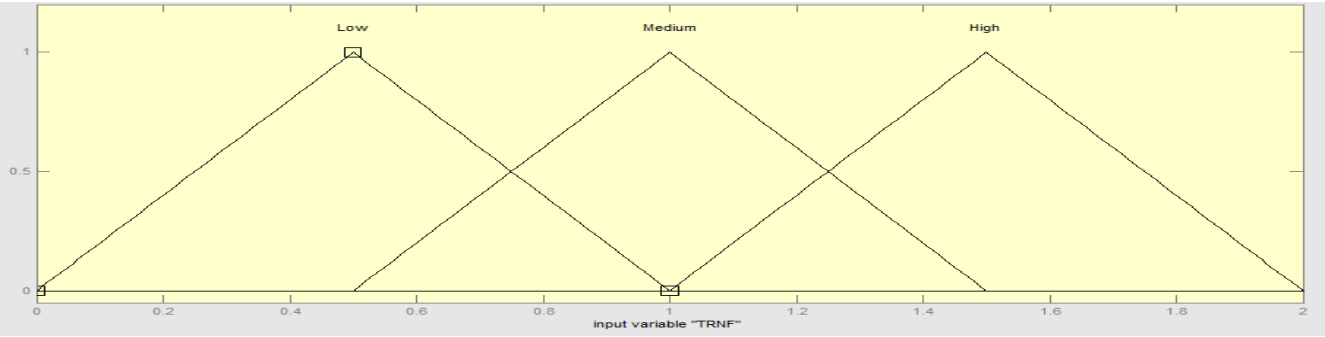


Fig.5.29. Input Variable- Percentage variation in TRNF

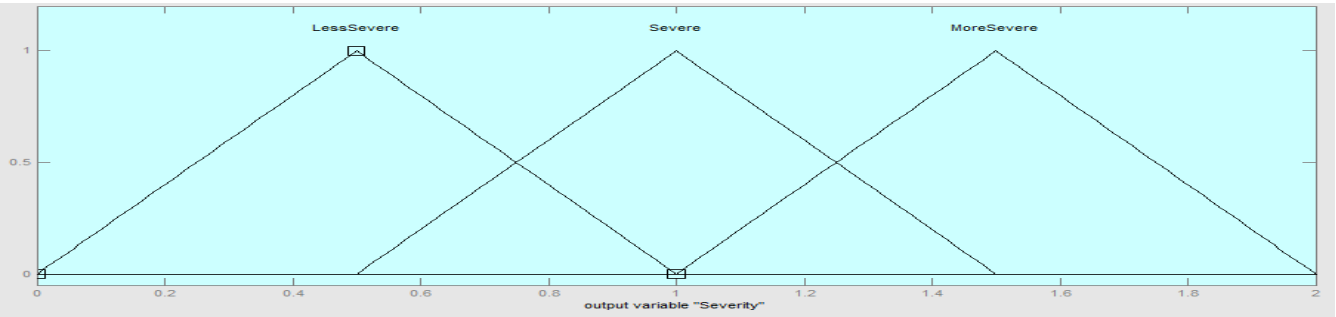


Fig.5.30. Output Variable- Expected Crack Location

Parameters of first input variable, second input variable and third input variable, i.e. Percentage variation in FRNF, SRNF, and TRNF (Transverse) are:

Low = [0 0.5 1]

Medium = [0.5 1 1.5]

High = [1 1.5 2]

Parameters of Output Variable- Crack Severity:

Less Severe = [0 0.5 1]

Severe = [0.5 1 1.5]

More Severe = [1 1.5 2]

### 5.5.1. RULES

**Table 5.4.** Fuzzy Rules for detection of Crack Severity

| Sl. No. | FRNF | SRNF | TRNF | Output |
|---|---|---|---|---|
| 1 | Low | Low | Low | Less Severe |
| 2 | Low | Low | Medium | Severe |
| 3 | Low | Low | High | More Severe |
| 4 | Low | Medium | Low | Severe |
| 5 | Low | Medium | Medium | Severe |
| 6 | Low | Medium | High | More Severe |
| 7 | Low | High | Low | More Severe |
| 8 | Low | High | Medium | More Severe |
| 9 | Low | High | High | More Severe |
| 10 | Medium | Low | Low | Severe |
| 11 | Medium | Low | Medium | Severe |
| 12 | Medium | Low | High | More Severe |
| 13 | Medium | Medium | Low | Severe |
| 14 | Medium | Medium | Medium | Severe |
| 15 | Medium | Medium | High | More Severe |
| 16 | Medium | High | Low | More Severe |
| 17 | Medium | High | Medium | More Severe |
| 18 | Medium | High | High | More Severe |

| | | | | |
|---|---|---|---|---|
| 19 | High | Low | Low | More Severe |
| 20 | High | Low | Medium | More Severe |
| 21 | High | Low | High | More Severe |
| 22 | High | Medium | Low | More Severe |
| 23 | High | Medium | Medium | More Severe |
| 24 | High | Medium | High | More Severe |
| 25 | High | High | Low | More Severe |
| 26 | High | High | Medium | More Severe |
| 27 | High | High | High | More Severe |

All rules are If-Then type rules connected by OR operator.

### 5.5.2. RESULTS

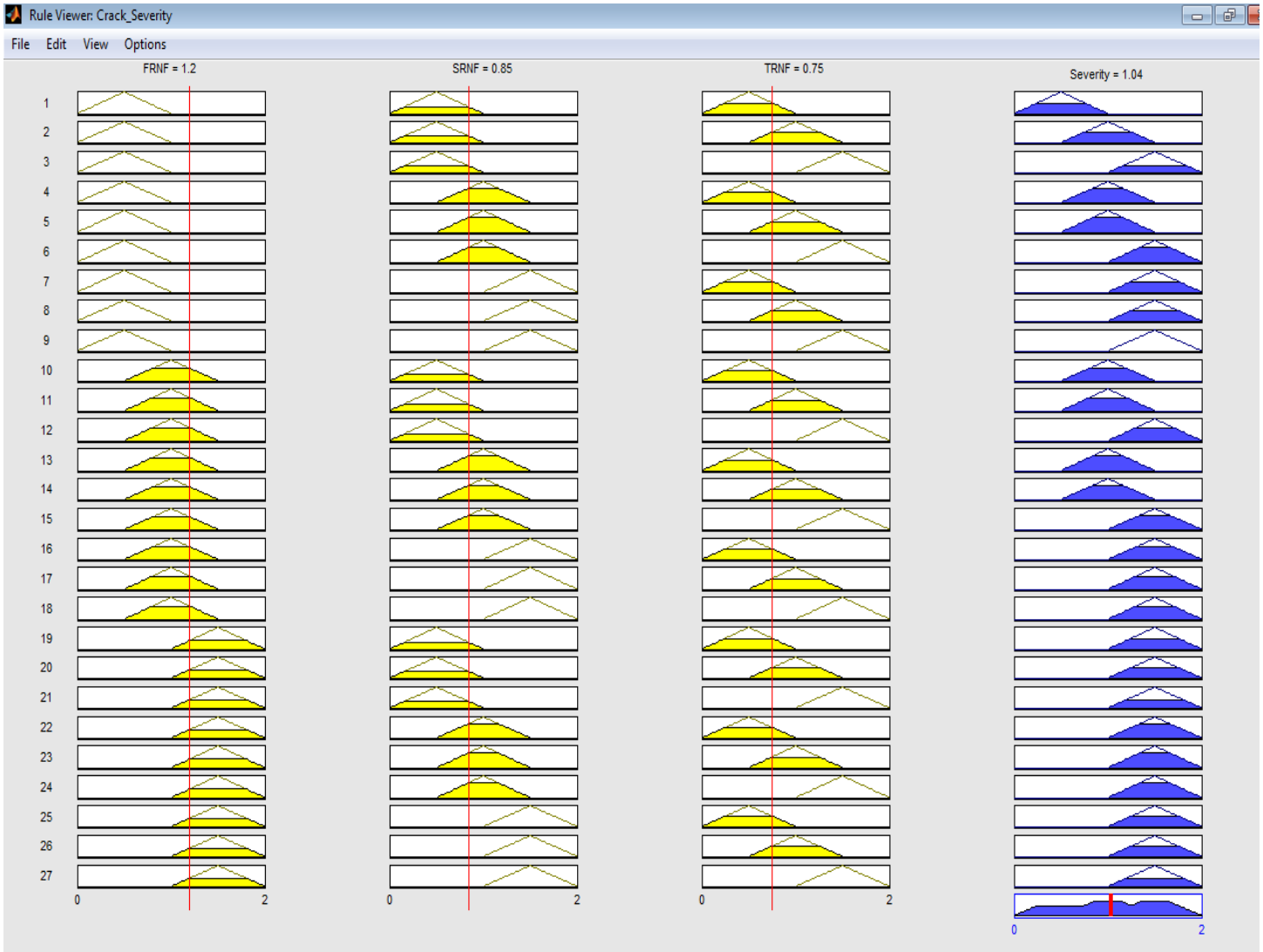


Fig.5.31. Application of Rules for FRNF=1.2, SRNF=0.85, TRNF=0.75 (Severity = 1.04)

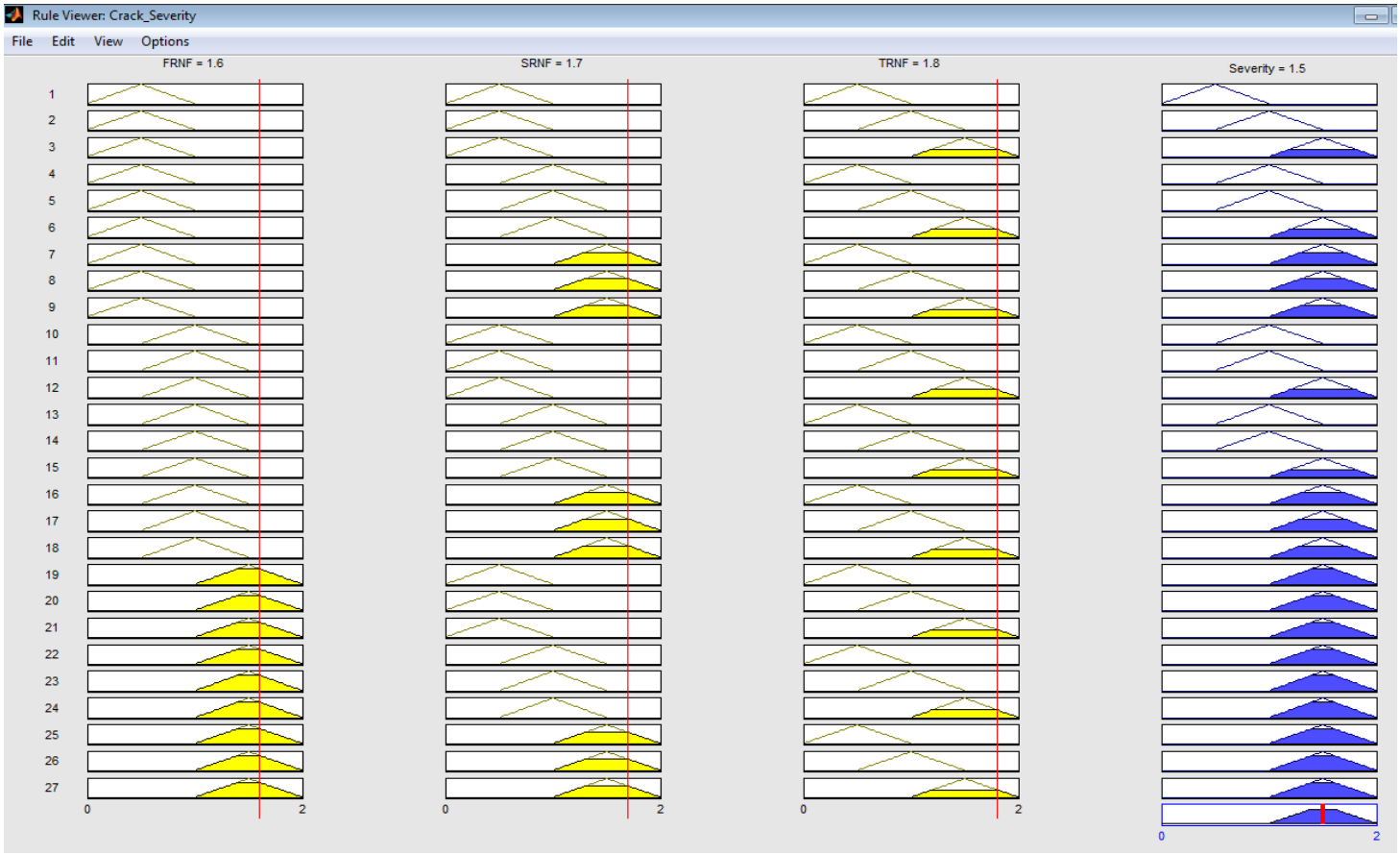


Fig.5.32. Application of Rules for FRNF=1.6, SRNF=1.7, TRNF=1.8 (Severity = 1.5)

When values of percentage variation of FRNF, SRNF and TRNF were chosen to be 1.2, 0.85 and 0.75 respectively, the output was found to be severe (Severity = 1.04) and when the three inputs were chosen 1.6, 1.7, 1.8 respectively, the output was found to be very severe (Severity =1.5). Physically the result may be interpreted as thus: The crack is more severe if it can change the relative natural frequency by a larger percentage value. If a crack is very fine to the extent of nearly non-existent, it will have very little effect on the percentage change in relative natural frequency. This logic has been adopted in the above fuzzy rules to obtain the severity of the crack. The application of the rule has been shown in Fig.5.30 and 5.31 which has been obtained in MATLAB. Better result for other angles can be obtained by modifying the membership functions as well as formulating more number of rules. The surface plots of rules for various input parameters have been shown in Fig.5.32, and 5.33. The surface plot with

SRNF and TRNF as two arguments has been found to be similar in shape to Fig.5.32. Close examination of Fig.5.32 and 5.33 would reveal that they are essentially the same as per rules used in Fuzzy Logic.

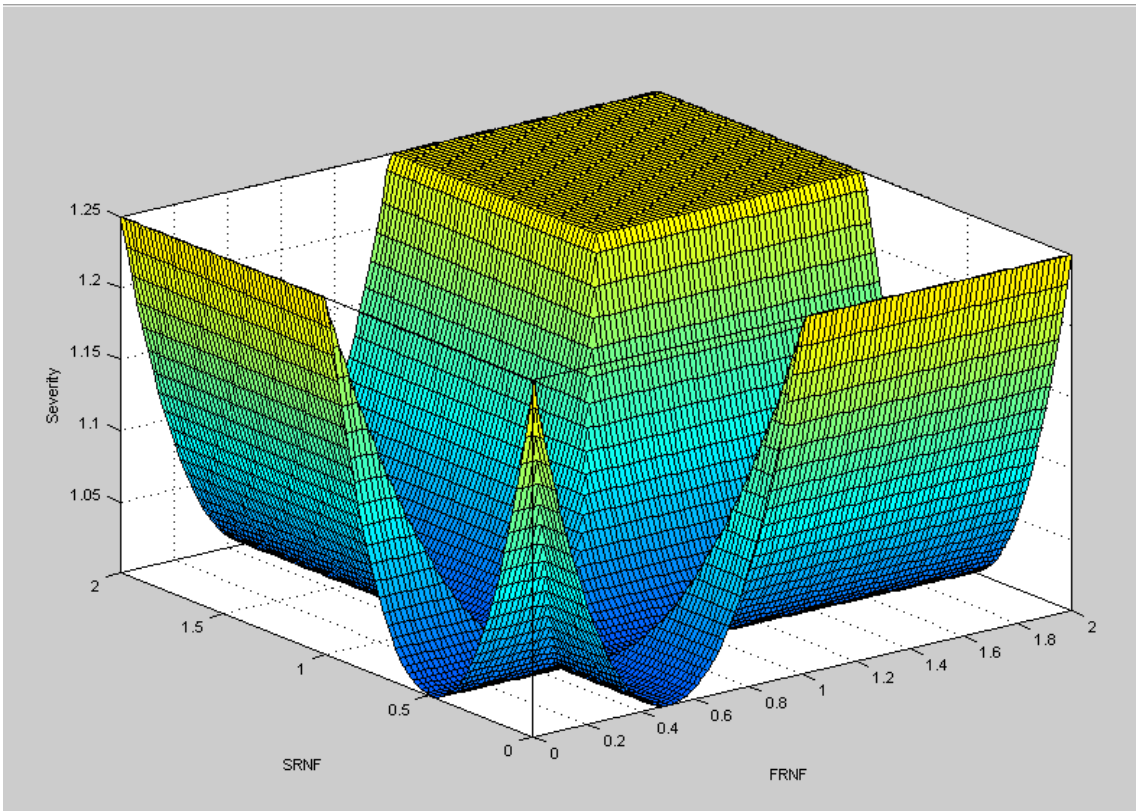


Fig.5.33. Surface plot of rules with SRNF and FRNF as input for crack severity prediction

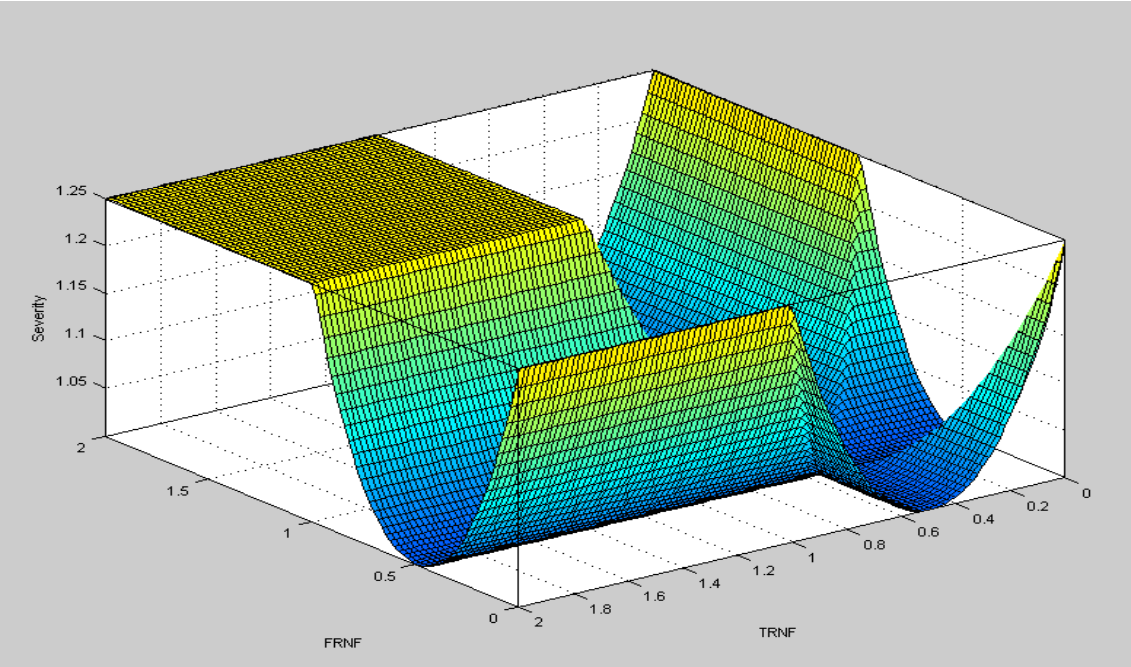


Fig.5.34. Surface plot of rules with TRNF and FRNF as input for crack severity prediction

# CHAPTER 6

## 6. CONCLUSION AND SCOPE FOR FUTURE WORK

In the present research, a database has been prepared considering the change in vibration characteristics of the beam due to the presence of the crack. The natural frequency decreases due to the presence of crack and its variation. As the relative location of crack decreases, its relative natural frequency is observed to increase for the first natural frequency. For second natural frequency, there is no distinct pattern in the change in natural frequency. For third natural frequency, which is a torsional one, the relative natural frequency decreases as crack approaches the fixed end. For fourth natural frequency, the pattern is exactly opposite to that obtained for first natural frequency, i.e. as the relative crack length decreases, the relative natural frequency increases. This change in behaviour might be attributed to the interference of crack tips thereby changing its stiffness matrix. This discrepancy should be further investigated to know the exact cause.

From the plots of variation of relative natural frequency to crack inclination angle, it can be observed that variation with respect to one inclination angle is critical than any other angle. So those critical angles should be taken into account while making any prediction. The critical angle is not fixed for all natural frequencies rather it varies according to particular natural frequency. The critical angle can be easily observed from the plots. Three-dimensional plots of relative natural frequencies have been plotted that can be referred to determine the natural frequency of the beam for any arbitrary angle combination.

It has been found that, the response of a beam to forced vibration changes due to the presence of a crack. The maximum deflection in the case of forced vibration is different from the deflection obtained from the uncracked beam. When the point of excitation changes, the response pattern changes in such a way that looking at the response curve we can get a rough

estimate that whether the point of excitation is within the fixed and first crack or between the cracks.

The mode shapes of cracked beam change slightly with the presence of a crack. The total deformation of the uncracked beam is observed to be smaller than the cracked beam as obtained by ANSYS. But for second, third, fourth and fifth natural frequency, it is observed that the total deformation value for the uncracked beam is larger than that of the uncracked beam.

Implementation of fuzzy rules resulted in a reasonable estimate of relative crack length. In case of crack inclination angle, fuzzy rules gave nearly accurate answers for $90^0$ but for other angles some deviations were observed. The accuracy of Fuzzy System can be improved by considering more number of membership functions as well as more number of fuzzy rules.

### 6.1. SCOPE FOR FUTURE WORK:

In the present study, it has been assumed that the system is undamped. But in real life every system possesses some damping. So the variation of damping characteristics of the beam due to the presence of crack can also be studied and used to make a more robust crack detection mechanism.

All systems are nonlinear in nature. The presence of crack may introduce a certain type of nonlinearity into the system thereby changing its characteristics. So nonlinearity introduced due to crack should be studied properly to explain certain unusual change in vibration characteristics that otherwise cannot be explained.

Implementation of other artificial intelligence techniques such as Neural Network and Genetic Algorithm can be used to predict the crack location, its inclination angle and severity so as to improve upon what has been obtained from Fuzzy Logic.

REFERENCES


[1] Rytter, A., & Kirkegaard, P. H. (1994). *Vibration based inspection of civil engineering structures*. Aalborg Universitetsforlag.

[2] Chati, M., Rand, R., & Mukherjee, S. (1997). Modal analysis of a cracked beam.*Journal of Sound and Vibration*, *207*(2), 249-270.

[3] Viola, E., Federici, L., & Nobile, L. (2001). Detection of crack location using cracked beam element method for structural analysis. *Theoretical and Applied Fracture Mechanics*, *36*(1), 23-35.

[4] Barr, A. D. S. (1966). An extension of the Hu-Washizu variational principle in linear elasticity for dynamic problems. *Journal of Applied Mechanics*, *33*(2), 465-465.

[5] Chatterjee, S., Chatterjee, S., & Doley, B. (2011). Breathing Crack In Beam And Cantilever Using Contact Model Dynamic Analysis–A Study. International Journal of Wisdom Based Computing, 1(3), 39-42.

[6] Nahvi, H., & Jabbari, M. (2005). Crack detection in beams using experimental modal data and finite element model. *International Journal of Mechanical Sciences*, *47*(10), 1477-1497.

[7] Orhan, S. (2007). Analysis of free and forced vibration of a cracked cantilever beam. *Ndt & E International*, *40*(6), 443-450.

[8] Gudmundson, P. (1983). The dynamic behaviour of slender structures with cross-sectional cracks. *Journal of the Mechanics and Physics of Solids*, *31*(4), 329-345.

[9] Narkis, Y. (1994). Identification of crack location in vibrating simply supported beams. *Journal of sound and vibration*, *172*(4), 549-558.

[10] Khiem, N. T., & Lien, T. V. (2001). A simplified method for natural frequency analysis of a multiple cracked beam. *Journal of sound and vibration*, *245*(4), 737-751.

[11] Patil, D. P., & Maiti, S. K. (2003). Detection of multiple cracks using frequency measurements. *Engineering Fracture Mechanics*, *70*(12), 1553-1572.

[12] Carneiro, S. H., & Inman, D. J. (2002). Continuous model for the transverse vibration of cracked Timoshenko beams. *Journal of vibration and acoustics*,*124*(2), 310-320.

[13] Abraham, O. N. L., & Brandon, J. A. (1995). The modelling of the opening and closure of a crack. *Journal of Vibration and Acoustics*, *117*(3A), 370-377.

[14] Pugno, N., Surace, C., & Ruotolo, R. (2000). Evaluation of the non-linear dynamic response to harmonic excitation of a beam with several breathing cracks. *Journal of Sound and Vibration*, *235*(5), 749-762.

[15] Lee, J. (2009). Identification of multiple cracks in a beam using natural frequencies. *Journal of sound and vibration*, *320*(3), 482-490.

[16] Shifrin, E. I., & Ruotolo, R. (1999). Natural frequencies of a beam with an arbitrary number of cracks. *Journal of Sound and Vibration*, *222*(3), 409-423.

[17] Kishen, J. C., & Kumar, A. (2004). Finite element analysis for fracture behavior of cracked beam-columns. *Finite Elements in Analysis and Design*, *40*(13), 1773-1789.

[18] Bouboulas, A. S., & Anifantis, N. K. (2008). Formulation of cracked beam element for analysis of fractured skeletal structures. *Engineering Structures*,*30*(4), 894-901.

[19] Reynders, E., Houbrechts, J., & De Roeck, G. (2012). Fully automated (operational) modal analysis. *Mechanical Systems and Signal Processing*, *29*, 228-250.

[20] Kisa, M., & Gurel, M. A. (2006). Modal analysis of multi-cracked beams with circular cross section. *Engineering Fracture Mechanics*, *73*(8), 963-977.

[21] Zarfam, R., Khaloo, A. R., & Nikkhoo, A. (2013). On the response spectrum of Euler–Bernoulli beams with a moving mass and horizontal support excitation.*Mechanics Research Communications*, *47*, 77-83.

[22] Staszewski, W. J., & Wallace, D. M. (2014). Wavelet-based frequency response function for time-variant systems—an exploratory study. *Mechanical Systems and Signal Processing*, *47*(1), 35-49.

[23] Civalek, Ö., Demir, C., & Akgöz, B. (2010). Free vibration and bending analyses of cantilever microtubules based on nonlocal continuum model. *Math. Comput. Appl*, *15*(2), 289-298.

[24] Zhao, X. W., Hu, Z. D., & van der Heijden, G. H. (2015). Dynamic analysis of a tapered cantilever beam under a travelling mass. *Meccanica*, *50*(6), 1419-1429.

[25] Randall, R. B. (1987). *Frequency analysis*. Brül & Kjor.

[26] Sinha, J. K., & Friswell, M. I. (2002). Simulation of the dynamic response of a cracked beam. Computers & structures, 80(18), 1473-1476.

[27] http://en.wikipedia.org/

[28] Leonard, F., Lanteigne, J., Lalonde, S., & Turcotte, Y. (2001). Free-vibration behaviour of a cracked cantilever beam and crack detection. Mechanical systems and signal processing, 15(3), 529-548.

[29] Ruotolo, R., Surace, C., Crespo, P., & Storer, D. (1996). Harmonic analysis of the vibrations of a cantilevered beam with a closing crack. *Computers & structures*, *61*(6), 1057-1074.

[30] Krawczuk, M., Palacz, M., & Ostachowicz, W. (2003). The dynamic analysis of a cracked Timoshenko beam by the spectral element method. *Journal of Sound and Vibration*, *264*(5), 1139-1153.

[31] Dimarogonas, A. D., Paipetis, S. A., & Chondros, T. G. (2013). *Analytical methods in rotor dynamics* (Vol. 9). Springer Science & Business Media.

[32] Saavedra, P. N., & Cuitino, L. A. (2001). Crack detection and vibration behavior of cracked beams. *Computers & Structures*, *79*(16), 1451-1459.

[33] Gounaris, G., & Dimarogonas, A. (1988). A finite element of a cracked prismatic beam for structural analysis. *Computers & Structures*, *28*(3), 309-313.

[34] Tada, Hiroshi, P. C. Paris, and G. R. Irwin. *The analysis of cracks handbook*. New York: ASME Press, 2000.

[35] Dilena, M., & Morassi, A. (2002). Identification of crack location in vibrating beams from changes in node positions. *Journal of Sound and Vibration*, *255*(5), 915-930.

[36] Sawyer, J. P., & Rao, S. S. (2000). Structural damage detection and identification using fuzzy logic. *AIAA journal*, *38*(12), 2328-2335.

[37] http://in.mathworks.com/help/fuzzy/getting-started-with-fuzzy-logic-toolbox.html

[38] Chondros, T. G., Dimarogonas, A. D., & Yao, J. (1998). A continuous cracked beam vibration theory. *Journal of Sound and Vibration*, *215*(1), 17-34.

[39] Yuen, M. M. F. (1985). A numerical study of the eigenparameters of a damaged cantilever. *Journal of sound and vibration*, *103*(3), 301-310.

[40] Abdo, M. B., & Hori, M. (2002). A numerical study of structural damage detection using changes in the rotation of mode shapes. *Journal of Sound and vibration*, *251*(2), 227-239.

[41] Pandey, A. K., Biswas, M., & Samman, M. M. (1991). Damage detection from changes in curvature mode shapes. *Journal of sound and vibration*, *145*(2), 321-332.

[42] Morassi, A. (1993). Crack-induced changes in eigenparameters of beam structures. *Journal of Engineering Mechanics*, *119*(9), 1798-1803.

[43] Rizos, P. F., Aspragathos, N., & Dimarogonas, A. D. (1990). Identification of crack location and magnitude in a cantilever beam from the vibration modes.*Journal of sound and vibration*, *138*(3), 381-388.

[44] Gounaris, G., & Dimarogonas, A. (1988). A finite element of a cracked prismatic beam for structural analysis. *Computers & Structures*, *28*(3), 309-313.

[45] Weijian, G. G. Y. (2001). A NUMERICAL STUDY ON DAMAGE DIAGNOSIS OF A CONTINUOUS BEAM USING MODAL PARAMETERS [J]. *Journal of Vibration and Shock*, *1*, 021.

[46] Lin, H. P. (2004). Direct and inverse methods on free vibration analysis of simply supported beams with a crack. *Engineering structures*, *26*(4), 427-436.